Xanthine Based Inhibitors for Therapeutics Targeting Phosphodiesterase 9A

A Thesis
Submitted in Partial
Fulfilment of the Requirements for the Degree of

DOCTOR OF PHILOSOPHY

BY

NIVEDITA SINGH

DEPARTMENT OF BIOSCIENCES & BIOENGINEERING
INDIAN INSTITUTE OF TECHNOLOGY GUWAHATI
GUWAHATI-781039, ASSAM, INDIA

NOVEMBER 2016

Xanthine Based Inhibitors for Therapeutics Targeting Phosphodiesterase 9A

A Thesis

Submitted in Partial
Fulfilment of the Requirements for the Degree of

DOCTOR OF PHILOSOPHY

BY

NIVEDITA SINGH

DEPARTMENT OF BIOSCIENCES & BIOENGINEERING
INDIAN INSTITUTE OF TECHNOLOGY GUWAHATI
GUWAHATI-781039, ASSAM, INDIA

NOVEMBER 2016

Dedicated to Almighty God
for making this time period
purposeful…

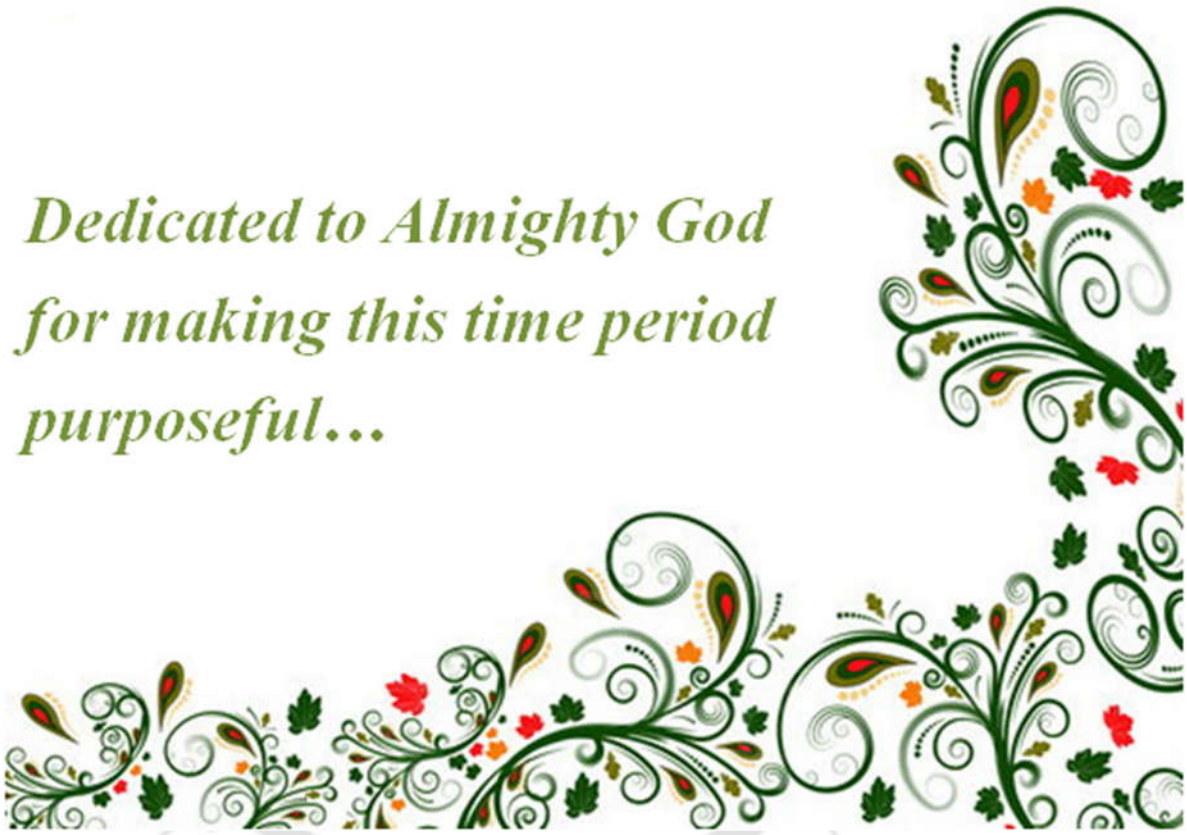

INDIAN INSTITUTE OF TECHNOLOGY GUWAHATI

DEPARTMENT OF BIOSCIENCE & BIOENGINEERING

STATEMENT

I do hereby declare that the matter embodied in this thesis entitled: *"**Xanthine based inhibitors for therapeutics targeting phosphodiesterase 9A***", is the result of investigations carried out by me in the Department of Biosciences & Bioengineering, Indian Institute of Technology Guwahati, India, under the guidance of Dr. Sanjukta Patra and co-supervision of Prof. Parameswar Krishnan Iyer.

In keeping with the general practice of reporting scientific observations, due acknowledgements have been made wherever the work described is based on the findings of other investigators.

November, 2016

Ms. Nivedita Singh
Roll No. 11610615

INDIAN INSTITUTE OF TECHNOLOGY GUWAHATI

DEPARTMENT OF BIOSCIENCE & BIOENGINEERING

CERTIFICATE

It is certified that the work described in this thesis, entitled: *"**Xanthine based inhibitors for therapeutics targeting phosphodiesterase 9A***", done by Ms Nivedita Singh (Roll No: 11610615), for the award of degree of Doctor of Philosophy is an authentic record of the results obtained from the research work carried out under my supervision in the Department of Biosciences & Bioengineering, Indian Institute of Technology Guwahati, India, and this work has not been submitted elsewhere for a degree.

November, 2016

Dr. Sanjukta Patra
Associate Professor
Dept. of Biosciences & Bioengineering
(Thesis supervisor)

INDIAN INSTITUTE OF TECHNOLOGY GUWAHATI

DEPARTMENT OF BIOSCIENCE & BIOENGINEERING

CERTIFICATE

It is certified that the work described in this thesis, entitled: **"*Xanthine based inhibitors for therapeutics targeting phosphodiesterase 9A*"**, done by Ms Nivedita Singh for the award of degree of Doctor of Philosophy is an authentic record of the results obtained from the research work carried out under my co-supervision in the Department of Chemistry, Indian Institute of Technology Guwahati, India, and this work has not been submitted elsewhere for a degree.

November, 2016

Dr. Parameswar Krishnan Iyer
Professor
Dept. of Chemistry
(Thesis Co-supervisor)

ACKNOWLEDGEMENT

This work is an outcome of persistent effort and a great deal of commitment. It has drawn intellectual support and generous help of experts from various fields. The list is endless and also the contributions. I take this as an opportunity to express my sincere thanks to everyone, who has been with me in this entire journey. Firstly, I would like to express my heartfelt gratitude to my supervisor Dr. Sanjukta Patra for her continuous and unconditional support for my Ph.D. research. It can't be expressed in words how grateful I am to her. She gave me opportunity to work in such a nice environment where I could freely nurture my ideas and brought them into reality. I am sincerely grateful for her constant inspirational and encouraging advices both on research as well as on my career throughout these years.

I would also like to express my sincere gratitude to my co-supervisor Prof. Parameswar Krishnan Iyer who gave me opportunity to nurture my chemistry understanding and to work in his lab. He always motivated me and gave valuable guidance. I would like to give sincere thanks to my doctoral committee members; Dr. Vikash Kumar Dubey, Dr. Rakhi Chaturvedi and Dr. A. K. Maurya for evaluating my work progress time to time with critical comments, valuable guidance and inspirational remarks.

I am heavily indebted to my lab members, Dr. P. Saravanan, Dr. Debamitra Chakravarti, Dr. Debasree Kundu, Dr. Bhaskar Das, Preet Sankhyan, Faheem Khan, Sonali Seth, Nitendra Yadav, Hindpur Avinash and Swagata Patra who have provided me constant support, inspiration and enjoyable working environment. I am especially thankful to Akhtar Hussain Malik for helping me in chemistry research, without his support the synthesis work was not possible. I would like to give thanks to the members of Prof. Parameswar Krishnan Iyer's lab. They did not let me feel as an outsider in chemistry department.

I take this opportunity to pay gratitude to all my seniors, friends and batch mates for supporting me throughout Ph.D. time period. I owe my thankfulness to the Department of Bioscience & Bioengineering for providing me all supports and necessary facilities. I would like to give special thanks to Central of Instrument Facility and Department of Chemistry, IIT Guwahati for providing NMR and Mass spectroscopy facilities that were crucial for my chemistry part of research. My sincere gratitude remains for the Department Technical Assistants.

I would like to give big thanks to IIT Guwahati for providing me opportunity to develop myself in such a peaceful campus. I would like to thank Government of India and funding agencies for providing research grant for pursuing Ph.D. work smoothly. I would like to express my sincere thanks to MHRD for providing me research fellowship for maintaining my economic stability.

A special thanks to my family, my parents, my brother and my sisters. It is very difficult to express gratefulness for their unconditional support, love and patience which motivated me to work for my target.

Finally, I would like to give my wholeheartedly gratitude to Almighty God for giving me opportunity to make this time period purposeful, determined and enthusiastic to achieve the set targets.

Nivedita Singh
November, 2016

Abstract

Xanthine is a versatile nitrogenous alkaloid. The pharmaceutical active nature of natural xanthine derivatives such as caffeine, theophylline, theobromine; is widely known for treating various diseases such as respiratory tract disease, neurodegenerative disease, cardiovascular disease, renal disease, etc. Therefore, xanthine can act as structurally rigid scaffold which provides enormous possibility for molecular diversity in drug development process. Both natural and synthetic xanthine derivatives are widely used for the treatment of various diseases caused mainly due to dysfunction of the cell signaling pathway. They primarily act as phosphodiesterase inhibitor, adenosine receptor antagonist and Histone deacetylase activator. In cell signaling pathway, Phosphodiesterase 9A (PDE9A) is one of the most important regulatory enzymes. With highest expression in brain, PDE9A plays prominent role in brain cell signaling. However, in pathophysiological condition normal functioning of PDE9A requires to be regulated to treat various neurodegenerative diseases. The catalytic activity of PDE9A can be regulated by using inhibitors. Despite enormous effort by researchers, till date not a single marketed drug has been achieved which targets PDE9A specifically. Most of the reported PDE9A inhibitors are derivatives of "pyrazolopyrimidinone" scaffold which is a common scaffold for various other proteins. Hence, introduction of new scaffold for inhibitor development is imperative to fetch molecular diversification in PDE9A inhibition research. Xanthine based compounds are reported for their non-specific phosphodiesterase inhibition, however, xanthine based inhibitors have not been reported for PDE9A inhibition. With introduction of "xanthine" as a scaffold, the present study is an attempt to bring molecular diversification in PDE9A

research. This study also emphasizes the importance of xanthine as 'starting material' for synthesizing diverse numbers of xanthine derivatives.

The present thesis has used two approaches - one was virtual screening to identify the existing xanthine based inhibitors for PDE9A and another was manual designing of xanthine based inhibitor for PDE9A. After introduction and literature review in the 1st chapter, chapter-2 concentrates on the screening of existing xanthine based inhibitors from ZINC database targeting PDE9A. Out of 2055 available xanthine derivatives in database only one ZINC compound (ZINC62579975) was proved as potent specific inhibitor for PDE9A over other members of PDE superfamily. Chapter-3 deals with manual designing of xanthine based compounds as per the requirement of the active site pocket of PDE9A. For that, 200 new compounds were designed, out of which 52 compounds were selected based on the lowest free energy of binding cut off of -6.0 kcal/mol. Initial substitutions were carried out at N_1, N_3, N_9 and C_8 positions of xanthine. Among them, N_1, N_3 and C_8 substitution together were proved as the best substitution sites for creating specificity in compounds towards PDE9A. Finally, eight compounds were selected for chemical synthesis. The selection criteria for these eight compounds was their lowest free energy of binding for PDE9A over other PDEs, better interaction affinity towards PDE9A than existing inhibitors and their pharmaceutical active nature. Chapter-4 focuses on the chemical synthesis of eight newly designed compounds. For synthesis of selected compounds, two novel synthesis schemes were developed because the existing synthesis methods were unfavorable for synthesis of diverse number of compounds. The basis for development of new schemes was the use of 'xanthine' molecule as starting material/reaction initiator. Xanthine as 'reaction initiator' has

wide potential to bring maximum diversity because of the presence of three –NH group at N_1, N_3 and N_7 positions and one -CH group at C_8 position for various substitutions. With development of new routes we got clear understanding over the chemical nature of xanthine and its three –NH sites which have been matter of concern for researchers. Due to lack of structural understanding, the use of xanthine has been negligible in synthesizing derivatives. Rather researchers have relied heavily on the ring closure and classical condensation methods. The present study divulged the reactivity pattern of three –NH sites- $N_7>N_3>N_1$. This finding was contrary to the earlier reports but similar to the transmethylation reaction occurring in living system. As N_7 position was highly reactive, its protection was needed for subsequent selective substitutions at N_1, N_3 and C_8 positions for synthesizing eight new selected compounds (C1-C8). Thus, selective protection and selective deprotection were the rational for development of the two novel schemes. Finally, the thesis ends with chapter-5 i.e. the biological studies of compounds obtained from both virtual screening and chemical synthesis. Spectrophotometric inhibition assay was applied to check the inhibitory nature of selected xanthine derivatives. The selected ZINC compound showed better potency for PDE9A (IC_{50}=46.96 ± 1.78) than PDE4D (IC_{50}=61.023 ± 1.71) and PDE5A (IC_{50}=70.04 ± 1.98). Based on the structure activity relationship analysis of eight novel compounds, compound **C6** (IC_{50}= 38.28 ± 1.63) showed highest affinity for PDE9A. The increasing chain length at N_1, N_3 and C_8 positions showed significant impact in increasing the inhibition affinity of compounds towards PDE9A. Substitution with isomeric fragments showed negligible difference in binding affinity towards the target. The substitution at C_8 position has considerable impact in generating the inhibition potential in the newly developed

compounds. Thermal stability of protein-ligand complex was confirmed by thermal shift assay. This study suggested that the chemically synthesized compounds were comparatively more thermally stable towards PDE9A than virtual screened compound. By carrying out extensive combinatorial studies, the present thesis has tried to explore the potential of 'xanthine' both as 'scaffold' and 'reaction initiator' to bring out structural diversification in derivatisation of xanthine based drug development.

TABLE OF CONTENTS

LIST OF TABLES

LIST OF FIGURES

LIST OF ACRONYMS

Acronym	Full Name
AChE	Acetylcholinesterase
AC	Adenylyl Cyclase
AD	Alzheimer Disease
ADMET	Absorption, Distribution, Metabolism, Excretion, Transport
ADT	AutoDock Tool
ANF	Atrial Natriuretic Factor
ANP	Atrial Natriuretic Peptide
ATB	Automated Topology Builder
BBB	Blood Brain Barrier
BLAST	Basic Local Alignment Search Tool
CFTR	Cystic Fibrosis Transmembrane Conductance Regulator
cAMP	Cyclic Adenosine Mono Phosphate
cGMP	Cyclic Guanosine Mono Phosphate
CMC	Chemistry, Manufacturing, and Control
CNP	C-type Natriuretic Peptide
CNG	Cyclic Nucleotide Gate
CNS	Central Nervous System
DNA	Deoxyribo Nucleic Acid

LIST OF ACRONYMS

Acronym	Full Name
DPMX	3,7-dimethyl-1-proparglyxanthine
EST	Expressed Sequence Tag
eNOS	Endothelial nitric oxide
iNOS	inducible nitric oxide
GC	Guanylyl cyclase
GFR	Glomerular Filtration Rate
H-Bond	Hydrogen Bond
H pocket	hydrophobic pocket
HDAC	Histone Deacetylase
HIA	Human Intestinal Absorption.
IBMX	1- methyl 3-isobutyl xanthine
IL	Interleukin
L region	Lid region
LVH	Left Ventricular Hypertrophy
MD	Molecular Dynamics
MDCK	Madin-Darby canine kidney cell
M	Mutagen
NO	Nitric oxide
PDB	Protein Data Bank
PDE	Phosphodiesterase
PDEs	Phosphodiesterases
PDE1B	Phosphodiesterase 1B
PDE2A	Phosphodiesterase 2A
PDE3A	Phosphodiesterase 3A

LIST OF ACRONYMS

Acronym	Full Name
PDE4D	Phosphodiesterase 4D
PDE5A	Phosphodiesterase 5A
PDE6	Phosphodiesterase 6
PDE7A	Phosphodiesterase 7A
PDE8A	Phosphodiesterase 8A
PDE9A	Phosphodiesterase 9A
PDE10A	Phosphodiesterase 10A
PDE11A	Phosphodiesterase 11A
PKA	Protein kinase A
PKG	Protein kinase G
PPB	Plasma Protein Binding
Q pocket	core pocket
RNA	Ribo Nucleic Acid
ROS	Reactive Oxygen Species
SNAP	S-nitroso-N-penicillamine
SPC	Simple Point Charge
T	Transducin
TSM	Tracheal Smooth Muscle
TNF	Tumor Necrosis Factor
WDI	World Drug Index
Ca	Calcium
Mg	Magnesium
Na	Sodium
Zn	Zinc

List of Amino acid residues and codes

Code	Amino acid residues
ALA, A	Alanine
ARG, R	Arginine
ASN, N	Asparagine
ASP, D	Aspartic acid
CYS, C	Cysteine
GLU, E	Glutamic acid
GLN, Q	Glutamine
GLY, G	Glycine
HIS, H	Histidine
ILE, I	Isoleucine
LEU, L	Leucine
LYS, K	Lysine
MET, M	Methionine
PHE, F	Phenylalanine
PRO, P	Proline
SER, S	Serine
THR, T	Threonine
TRP, W	Tryptophan
TYR, Y	Tyrosine
VAL, V	Valine

CHAPTER 1

Introduction and Literature Review

Prologue

Drug development is a multi-step process to develop new therapeutic molecules against specific target diseases. In this process, identification of lead molecule is a very crucial step to proceed towards an effective drug target. Xanthine based molecules are widely regarded as pharmaceutically active molecules against phosphodiesterases which mainly participate in regulation of signal transduction pathways. Thus, due to wider biological implication of these molecules, xanthine can be considered as an effective lead molecule for future drug development. But the complex structural set-up of xanthine has always been a hurdle for diversifying xanthine based research. Clear understanding of the structure of "xanthine" can be a way to solve the existing issues. Most of the known xanthine derivatives are non-specific in nature. PDE9A is one of the most important member of the PDE superfamily. Its catalytic action in pathophysiological condition may lead to various diseases. Thus, inhibiting its catalytic action is imperative to treat various undesirable consequences. With various structural modification, xanthine based molecules can act as good inhibitors of PDE9A. This chapter focuses on the literature review of xanthine based research and its applications towards PDE9A.

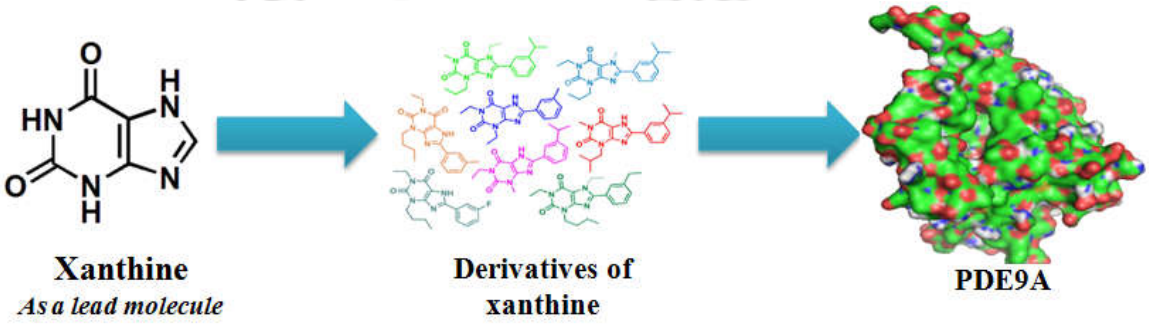

1.1. Introduction

Since ancient time natural products from plants, animals, microbes and minerals have been the repertoire source for drug development. In the recent time, scientific approach has progressed rapidly but still the fundamentals of these developments are rooted in traditional medicines and therapies. According to the World Health Organization (WHO) report, in recent times, about 80% of the population in developing countries depends on traditional and herbal medicines to meet their basic healthcare needs. Due to the wider implication of traditional medicines, the use of these medicines and traditional healing methods have been rapidly adapted by developed and industrialized countries as complementary and alternatives medicines (CAM). Undoubtedly, the healing ability of plants has been established by various ancient Ayurvedic therapies. Ayurvedic medicinal products and therapies are developed over the centuries. In modern era, with extensive research progress in bioinformatics, medicinal chemistry, pharmacology and clinical biology, the key medicinal components and their behaviour are being identified and are being used for treating various diseases. These components provide an attractive basis for the future drug development process. In modern medicine, root of a huge fraction of drugs have been natural sources which are either directly extracted from natural sources or synthetically modified from a lead compound of natural origin.

Alkaloids containing plants have been in wide use since the early era of medicinal development (Amirkia and Heinrich, 2014). Early 19th century was the beginning of isolation and characterization of important plant alkaloid such as xanthine (1817), atropine (1819), quinine (1820), caffeine (1820) etc, (Amirkia and Heinrich, 2014). These discoveries had

created eagerness for search of more and more such type of natural alkaloids and their sources. Alkaloids are known for their diverse roles including self preservation, inhibitors for enzymes of signal communications, feeding deterrents, autoinducer, allelochemicals, sidophore, anti-depressants, antibacterial activities, metabolic activities, quenching activities, etc (Cushnie et al., 2014; Perviz et al., 2016). They are a large and structurally diverse set of natural products. Among these alkaloids, xanthine and its natural derivatives have prominent place in traditional medicine. Natural xanthine derivatives such as caffeine, theophylline and theobromine are purine based nitrogenous compounds which are present in plants such as cocoa, tea and coffee plants (Baraldi et al., 2007). These compounds are usually known as methyl xanthine derivatives. Natural xanthine derivatives are widely known targeting cellular signaling pathways. Cell signaling pathways are required for establishing the cellular communication between various cells and their extracellular environment to coordinate myriad activities which are basis for the growth, development and functioning of any organism.

In mammalian cells, the mechanism of communication is carried out by the complex pathway which is commonly known as signal transduction pathway. Second messengers–cyclic adenosine monophosphate (cAMP) and cyclic guanosine monophosphate (cGMP) act as mediator to transmit wide varieties of external signals coming from extracellular environment through membrane bound receptors to regulate many intracellular metabolic processes (Kim and Park, 2003; Wang et al., 2010). Cyclic nucleotide phosphodiesterases (PDEs) act as a key regulator to regulate the cell signaling process by continuous involvement in breakdown of second messengers, to maintain the consistency of

pathway. PDEs are a superfamily of 11 enzymes encoded by 21 human *pde* genes (Conti and Beavo, 2007; Ke et al., 2011; Maurice et al., 2014; Omori and Kotera, 2007; Shao et al., 2014). Based on the substrate specificity, these phosphodiesterases are further categorized in three parts- cAMP specific PDEs, cGMP specific PDEs and dual specific PDEs. Phosphodiesterase 9A (PDE9A) is one among them which has highest affinity towards cGMP (Francis et al., 2011; Soderling et al., 1998). PDE9A has significant role in regulating the cell signaling pathway of brain cells because of its abundance in brain. In brain, most of the cellular signaling pathways are passed through cGMP (Andreeva et al., 2001; Singh and Patra, 2014). Various pathophysiological conditions lead to lowering the level of cGMP which may affect the normal functioning of signal transduction pathway. In such conditions, normal functioning of PDE9A leads to further decreasing the level of cGMP. It gives a call to researchers to look for the development of drugs for PDE9A regulation. Inhibitors play important role in regulating the catalytic action of PDE9A maintaining the consistency of pathway to some extent by preserving the level of cGMP. Thus, 'inhibition' has always been a key area of consideration in PDE9A research.

Despite enormous effort given by researchers and pharmaceutical companies for more than a decade to develop PDE9A inhibitor, till date, not a single inhibitor has been marketed. Xanthine derivatives are widely known for their non-specific inhibition properties towards phosphodiesterase enzymes (Ogawa et al., 1989). Xanthine derivatives are significant in various other pharmaceutical applications such as adenosine receptor antagonists, inducers of histone deacetylase activity, antitumor drugs, anti asthmatic drug, psycho-stimulant drug, etc. (Allwood et al., 2007; Burbiel et al., 2006; Meskini et al., 1994; Suravajhala et al., 2014).

Due to wider pharmaceutical application of natural xanthine derivatives, it has opened enormous opportunities for synthesis of xanthine based compounds which can target PDE9A specifically. In the last few decades, based on the natural xanthine derivatives, number of xanthine based inhibitors have been synthetically developed and reported (Glennon et al., 1981; Wong and Ooi, 1985). In drug development process, one of the major challenges is deciding the lead molecule which acts as scaffold to provide avenue for achieving maximum diversity. Xanthine with versatile and structurally rigid scaffold provides highest possibility for molecular diversity in constructing xanthine derivatives for combinatorial chemistry (Heizmann and Eberle, 1997).

In this study "xanthine" has been used as a scaffold for the development of potent and selective inhibitors for PDE9A. This thesis is an attempt to explore the potential of 'xanthine' as a scaffold to bring diversification in drug development process for PDE9A.

1.2. Cell signaling pathway- an overview

Cellular communication between various cells and their extracellular environment is imperative to coordinate multitudinous activities which are cornerstone for the growth, development and functioning of any organism (Antoni, 2000; Kim and Park, 2003; Omori and Kotera, 2007; Wang et al., 2010). In mammalian cells, the mechanism of communication is carried out by the complex pathway known as the signal transduction pathway. Most of the cell signaling receptor establishes the communication between extracellular and intracellular environment to stimulate targeted enzyme either by directly linking or indirectly coupling through G-proteins to the target. These intracellular enzymes act as a downstream signaling

element to propagate and stimulate signals coming from extracellular environment through ligand binding. Signal transduction is accomplished by various signaling molecules including first messengers (hormones, neurotransmitters, growth factors, local mediator etc), second messengers (cyclic nucleotides such as cAMP and cGMP, calcium, lipid-derived second messengers) and different types of signaling proteins. Second messengers are key regulators of signal transmission by acting as an intermediate molecule in mammalian cell signaling. **Figure 1.1** illustrates a schematic diagram of signal transduction through the second messengers-cAMP and cGMP along with the metabolic activities associated with these signaling.

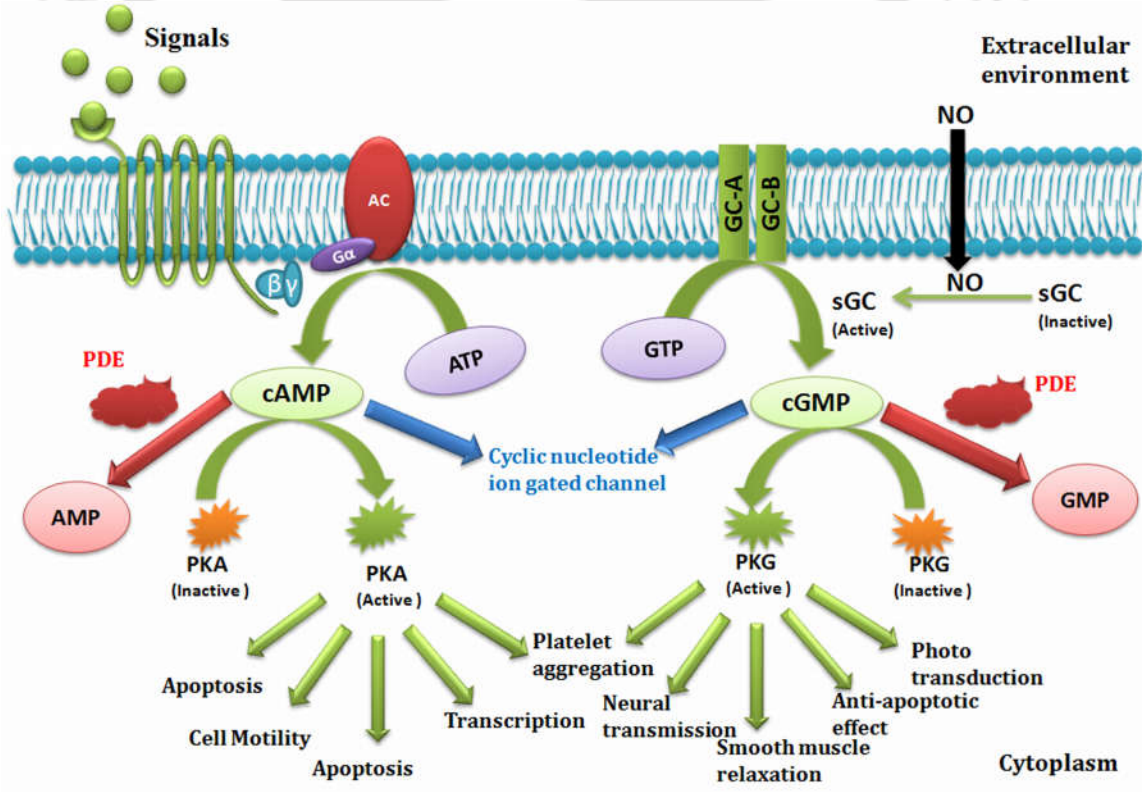

Figure 1.1 Signal Transduction pathway

1.2.1. Role of cGMP in Signal Transduction

cGMP, a second messenger acts as chief intracellular mediator of the vaso-active agents such as nitric oxide, natriuretic peptides, neurotransmitter, hormones etc (Vaandrager and de Jonge, 1996). Synthesis and degradation of cGMP is a cyclic process which involves regulation of many functions in mammalian organs. Synthesis is initiated by activation of guanylyl cyclase. **Figure 1.2** illustrates the cyclic process of synthesis and degradation of cGMP and its role in various cellular functions.

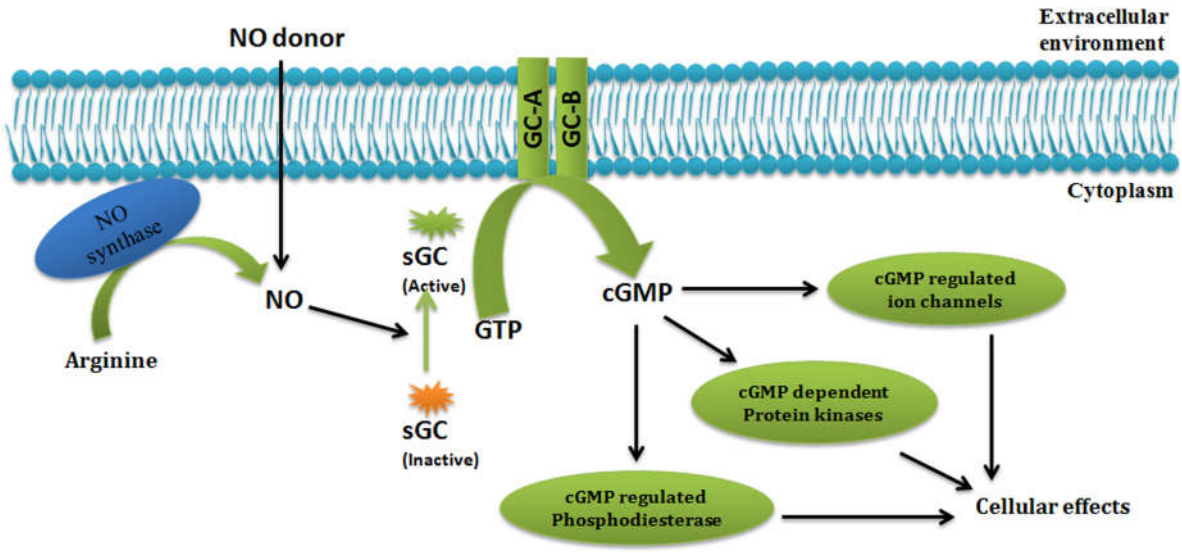

Figure 1.2 Synthesis and breakdown of cGMP in cell signaling pathway

1.2.2. Synthesis of cGMP

Under the influence of signaling molecules i.e. nitric oxide (NO), neuropeptide (e.g. ANF), neurotransmitters, various signaling pathways get activated. In general, cGMP is synthesized from guanosine tri phosphate (GTP) by two broad classes of guanylyl cyclases depending upon their sub-cellular location, the first is soluble guanylyl cyclase and the

second is membrane integrated guanylyl cyclase. Soluble guanylyl cyclase (a dimeric haemoprotein which is found in cytoplasm) is stimulated by inter- and intracellular gaseous second messenger nitric oxide (NO) or S-nitroso-N-penicillamine (SNAP).

The membrane integrated guanylate cyclase is stimulated by peptide agonist such as guanylin, urodilatin (Uro), atrial natriuretic peptide (ANP), or C-type natriuretic peptide (CNP) and fluxes in intracellular Ca^{2+} (Agulló et al., 2005, 2003; Burley et al., 2007; Currie et al., 1992; Hamra et al., 1993; Kim and Park, 2003; Scholz et al., 1996; Su et al., 2005). These membrane integrated guanylate cyclase is comprised in seven isoform named as GC-A to GC-G which share a well conserved unique topological characteristics such as an extracellular binding domain at the N-terminus which involves in binding of specific ligands, a single transmembrane domain, a cytoplasmic juxtamembrane domain, a regulatory domain that is homologous with protein kinases, a hinge region and a C-terminal catalytic domain (Currie et al., 1992; Kuhn, 2003; Lucas et al., 2000).

1.2.3. Molecular targets of cGMP

Three major molecular targets of cGMP are cGMP dependent protein kinase (PKG), cGMP dependent phosphodiesterase (PDE) and cyclic nucleotide gated ion channel (CNG) (de Vente, 2004; Friebe and Koesling, 2003; Lucas et al., 2000; Mullershausen et al., 2004). cGMP involves in myriad of cellular function including relaxation of smooth muscle, inhibition of platelet aggregation, blunting of cardiac hypertrophy, protection against ischemia/reperfusion damage of the heart, improvement in cognitive functions etc (Francis,

2010). In mammalian cell, cGMP is well-known for activating protein kinase G (PKG) which involves in various intracellular cGMP dependent cellular functions (Wall et al., 2003).

(a) Activation of Protein Kinase G by cGMP

cGMP/PKG is important pathway in cell signaling which depends on the distribution of PKG in various tissues. PKG is an abundantly found protein in smooth muscles, platelets, cerebellum, hippocampus, dorsal root ganglia, neuromuscular junction end plate and kidney. But its concentration is low in cardiac muscle, vascular endothelium, granulocytes, chondrocytes, osteoclasts, and diverse brain nuclei (Hofmann et al., 2006). In mammals, cGMP dependent protein kinase is classified as PKG-1 and PKG-2 which are encoded by two separate gene *pkg-1* and *pkg-2* on chromosome 10 (Francis, 2010; Hofmann et al., 2009, 2000). PKG-I with an acetylated N-terminus is preponderantly localized in the cytoplasm but in case of the platelets it is anchored at membrane whereas PKG-II with N-terminal myristoylation is generally integrated at the plasma membrane (Wall et al., 2003). PKG has two functional domains- regulatory domain which contains two binding sites for cGMP and catalytic domain (Hofmann et al., 2000). When cGMP allosterically interacts and binds to R-domain- two in each site, then catalytic center releases which further involves in phosphorylation of serine/threonine residues in target proteins and in the N-terminal autophosphorylation site (Francis, 2010; Hofmann et al., 2009, 2000). Thus, cGMP is solely responsible for activation of PKG in biological system. PKG takes part in a plethora of cellular function such as smooth muscle relaxation, regulation of smooth muscle proliferation, platelet aggregation, cardiac protection (i.e. by reducing cardiac contractility, protection against ischemia/reperfusion injury, reversal of cardiac hypertrophy), endothelial

permeability, neuronal plasticity, lower urinary tract function, regulation of gene expression, induction of apoptosis, intestinal secretion, renin release and bone growth (Deguchi et al., 2004; Francis, 2010; Hofmann et al., 2000; Wang et al., 2006). These PKGs are cross-activated by cAMP in various tissues (Jiang et al., 1996; Lucas et al., 2000).

(b) Ion channel opening through cGMP binding

Cyclic nucleotide gated (CNG) channels are non-selective cation channels. The opening of these channels is directly dependent on binding of cyclic nucleotides cGMP or cAMP. cGMP plays important role in the vision by activating the ion channel (Na^+-Ca^{2+} channel) in rod and cone cells in retina. In dark, cGMP initiate the opening of Na^+-Ca^{2+} channel which augments the level of Ca^{2+}. Thus, the level of Ca^{2+} is balanced by Na^+-Ca^{2+} exchanger. But as the light falls on the rhodopsin, its 11-cis-retinal is converted to all-trans-retinal which triggers the activation of rhodopsin. Activated rhodopsin catalyzes replacement of GDP by GTP on transducin (T), which then dissociates into T_α-GTP and $T_{\beta\gamma}$. T_α-GTP then activates cGMP dependent phosphodiesterase which reduces the level of cGMP by hydrolyzing cGMP into 5'-GMP. Thus, the level of cGMP decrease leads to the hyperpolarisation in the retinal cells.

(c) Degradation of cGMP by phosphodiesterases

Phosphodiesterases are important enzymes involved in the regulation of cell signalling by regulating the level of cGMP which acts as mediator in processing the signals coming from extracellular environment through the membrane receptors. This will be discussed in detail in the upcoming sections.

1.3. Cyclic nucleotide phosphodiesterase enzyme - an overview

Phosphodiesterases (PDEs) are the most prominent superfamily of enzymes involved in the degradation of second messengers - cAMP and cGMP into 5'-AMP and 5'-GMP, respectively by process of hydrolysis as shown in **figure 1.3** (Braumann et al., 1986; Trong et al., 1990). **Figure 1.3** represents the phosphodiester bond cleavage by phosphodiesterase enzyme, resulting in disruption in cell signaling.

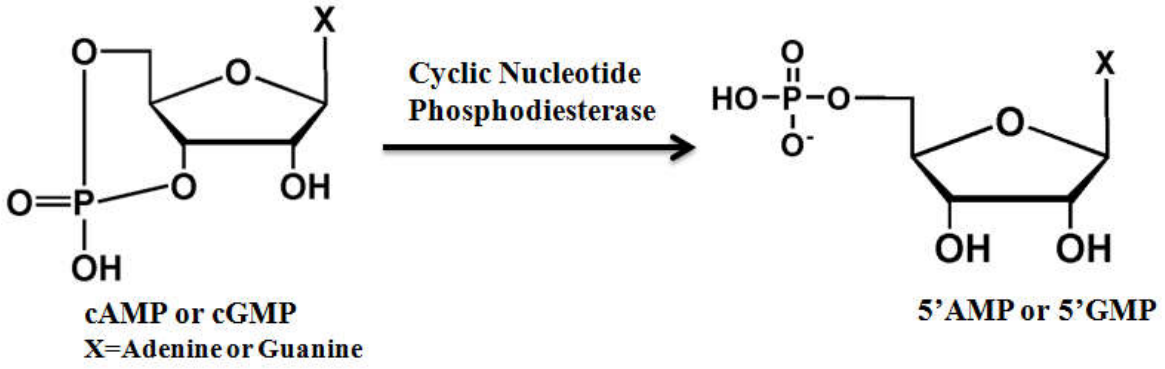

Figure 1.3 Hydrolysis reaction carried out by cyclic nucleotide phosphodiesterase

PDEs can be classified into three classes- class I, class II and class III. Mammalian PDEs belong to class III (Omori and Kotera, 2007). PDEs are encoded by 21 genes in the human genome that are classified into 11 different families (1-11). This classification is based on amino acid sequence, conserved C-terminal catalytic domain of ~270-300 amino acids and regulatory domain which presents between N-terminal splicing region and C-terminal catalytic domain. Each family consists of several isoforms and different variants that are formed using various transcriptional start site and alternative mRNA splicing of their genes (Bender, 2006; Ke and Wang, 2007; Lugnier, 2006). The regulatory domain contains

most diverse region of the phosphodiesterase enzyme structure, based on which the superfamily can also be classified in different groups, as shown in **figure 1.4**.

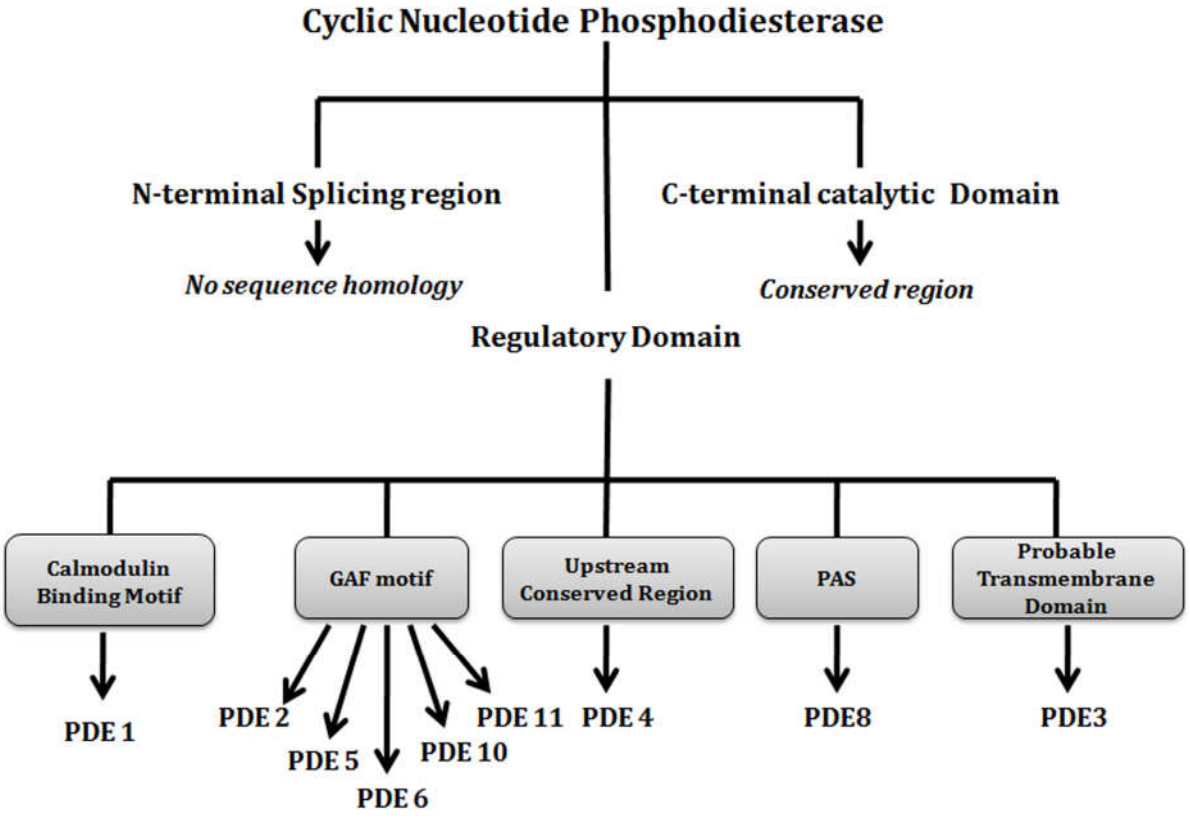

Figure 1.4 Structure based classification of PDEs based on regulatory domain

Phosphodiesterase members also differ in terms of substrate specificity and subcellular localization. These differences can be exploited for development of specific inhibitors (Russell et al., 1973). **Table 1.1** provides complete details of various members of PDE superfamily. The table talks about various subtypes of PDE superfamily, their reported K_m values for cGMP/cAMP, sites of expression, available inhibitors and the cellular activities influenced by inhibition of PDE.

Based on the substrate specificity, phosphodiesterases are divided into three groups (1) cAMP specific - PDE 4, 7 and 8 (2) cGMP specific - PDE 5, 6 and 9 and (3) dual specific (both cAMP and cGMP specific)- PDE 1, 2, 3, 10 and 11 (Conti and Beavo, 2007; Mehats et al., 2002). These specificity are determined by the catalytic domain but mechanism of specific recognition of substrate by phosphodiesterases is still a question [Ke et al., 2011; Hou et al., 2011] (Hou et al., 2011; Ke et al., 2011). According to Zhang et al (2004), "Glutamine switch mechanism" might be an important reason behind such selectivity. This is because γ-amino group of conserved invariant glutamine in the active site of PDEs can alternatively adopt two different orientations. In one orientation the hydrogen bond network supports guanine binding, resulting in cGMP selectivity, and in the second orientation the network supports adenine binding, leading to selectivity towards cAMP. Whereas in case of dual-specificity, the side chain of glutamine can switch over between the two orientations, resulting in specificity towards both the cyclic nucleotides (Jeon et al., 2005; Zhang et al., 2004). Binding patterns of invariant glutamine of different phosphodiesterases have been represented in **figure 1.5.**

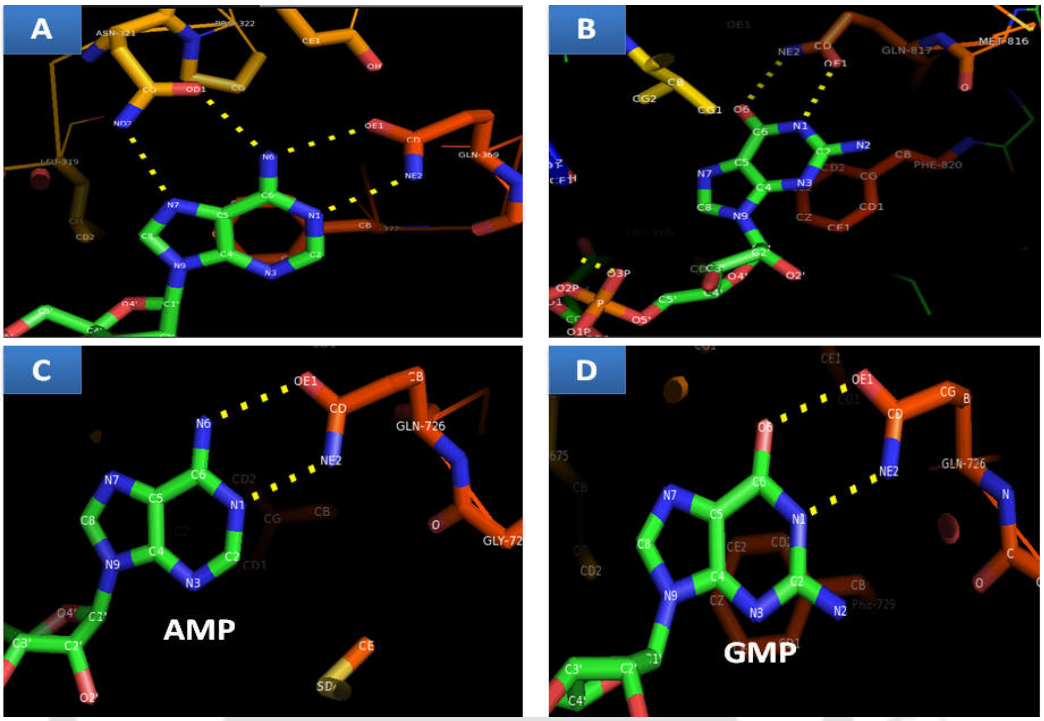

Figure 1.5 Comparative binding patterns of invariant glutamine: (A) interaction of AMP with cAMP specific PDE4D by making two H-bonds between adenine moiety of AMP and invarient Q369; (B) interaction of GMP with cGMP specific PDE5A by two H-bonds between guanine base of GMP and invariant Q817, this interaction is in the opposite orientation of glutamine side chain as shown in AMP-PDE4D interaction; (C) Interaction pattern of dual specific PDE10A with AMP; (D) Interaction pattern of dual specific PDE10A with GMP

Phosphodiesterase 9A (PDE9A) is one of the most prominent phosphodiesterases among all PDEs due to its highest expression in brain and has highest affinity for cGMP. But complexity in structure and side effects associated with other PDEs makes the development of specific inhibitors targeting PDE9A a challenging task.

Table 1.1 Overview of cyclic nucleotide phosphodiesterase superfamily

PDE	Sub-types	Properties	Km Value	Tissue expression	Therapeutic target	Inhibitors	Cellular function associated with PDE inhibition	References
PDE1	3	Ca^{++}/ calmoduline-stimulated	PDE1A=112.7⁄ 5.0μM [cAMP⁄cGMP] PDE1B= 24.3⁄2.7μM [cAMP⁄cGMP] PDE1C=1.7⁄1.3 μM [cAMP⁄cGMP]	Brain, lung, Heart, smooth muscle	Neurodegenerative diseases such as Neuronal ischemia, epilepsy, Parkinson's & Alzheimer's disease (AD)	Calimidazolium, Dioclein, Phenethiazines, SCH51866, Vinpocetine, Zaprinast	Apoptosis, phosphorylation of AMPA receptors, enhancement of pulmonary vasodilation	(Bender, 2006; Dunkern and Hatzelmann, 2007; Evgenov et al., 2006; Gonçalves et al., 2009; Jiang et al., 1996; Medina, 2011)
PDE2	1	cGMP stimulated	PDE2=10/30μ M [cAMP⁄cGMP]	Adrenal gland, heart, lung, liver, platelets	Acute respiratory Distress Syndrome (ARDS), sepsis	EHNA, Bay 60-7550, MPB–forskolin, PDP	Endothelial cell permeability, presynaptic inhibition	(Boess et al., 2004; Hu et al., 2012; Michie et al., 1996; Surapisitchat et al., 2007; Witzenrath et al., 2009; Wunder et al., 2009)
PDE3	2	cGMP-inhibited, cAMP-selective	PDE3=0.2/0.1μ M [cAMP⁄cGMP]	Adipose tissue, heart, lung, liver, inflammatory cells, platelets	Asthma , chronic heart disease, cardiovascular disease, intermittent caudation, vascular smooth muscle relaxation	Amrinone, Bucladesine, Cilostazol, Cilostamide Enoximone, , Milrinone, Org 9935, Olprinone, SK&F 95654, Siguazodan, Saterinone	Induction of insulin secretion	(Ahmad et al., 2000; Kieback and Baumann, 2006; Surapisitchat et al., 2007)
PDE4	4	cGMP-insensitive, cAMP-specific	2–4 μM for cAMP	Sertoli cells, kidney, brain,liver, lung, inflammatory cells	Autoimmune disease, inflammatory disease, neurodegenarative disease, cancer, allergic disorder.	Apremilast, NCS 613, Rolipram, Roflumilast	Long-term potentiation	(Mackenzie and Houslay, 2000; Rabe, 2011; Schett et al., 2010; Yougbare et al., 2011)
PDE5	1	cGMP specific	2.9±0.8μM for cGMP (full length PDE5A) 5.1 μM for	Cardiomyocyte s Lung, platelets, vascular,	Coronary heart disease, cardiovascular disease, pulmonary	Dipyridamole, SK&F 96231, Tadalafil, Vardenafil, , Sildenafil, Zaprinast	Antihypertrophic effects, inflammatory immune response, apoptosis etc	(Das et al., 2005; Kass et al., 2007; Rao and Xi, 2009; Tedford et al., 2008;

			cGMP (catalytic domain PDE5A)	smooth muscle,	hypertension, renal failure, sexual dysfunction, stroke			Wang et al., 2006; Westermann et al., 2012; Zoraghi et al., 2007)
PDE6	3	Transducin-activated, cGMP specific	2.5 µM for cGMP	Photoreceptors, pineal gland	Sometime adverse effect on vision	Dipyridamole, Sildenafil, Vardenafil, Zaprinast	N/A	(Cahill et al., 2012; Lugnier, 2006)
PDE7	2	cAMP specific, Rolipram-insensitive	0.03-0.2 µM for cAMP	Lung, hematopoietic cells, placenta, pancreas, brain, heart, thyroid, skeletal muscle, immune cells	Immune and inflammatory disorders, neurological disease such as spinal cord injury	ASB16165, BAY 73-6691, PF-04447943, S14, VP1.15	Lessen inflammatory response, regulation of pro-inflammatory and immune T-cell functions, reduction in tissue injury, reduction in TNF-α, IL-6, COX-2 and iNOS expression	(Bender, 2006; Castaño et al., 2009; Paterniti et al., 2011)
PDE8	2	cAMP specific, Rolipram-insensitive IBMX-insensitive	0.04–0.15 µM for cAMP	Testes, eye, liver, skeletal muscle, heart, kidney, ovary, brain, T lymphocytes	Polycystic ovary syndrome (PCOS)	Dipyridamole	Suppression of Teff cell functions, lipid accumulation	(Lugnier, 2006; Shimizu-Albergine et al., 2008; Vang et al., 2010)
PDE9	1	cGMP specific, IBMX-insensitive	0.070-0.25 µM for cGMP 230 µM for cAMP	Brain, kidney, spleen, small intestine.	cardiovascular diseases, Insulin-resistance syndrome and diabetes, obesity, neurodegenerative disorders	BAY73-6691, PF-04447943	Synaptic plasticity, LTP(long term potentiation)	(Fisher et al., 1998; Huai et al., 2004; Soderling et al., 1998; Wang et al., 2010)
PDE10	1	Dual specific	0.05–0.26 µM for cAMP 3–7.2 µM for cGMP	Testes, striatum (brain)	Anxiety, cognition deficiency disorder, neurodegenerative disease	MP10	Long-term potentiation	(Abdel-Magid, 2013)
PDE11	1	Dual specific	0.52 µM for cAMP 1.04 µM for cGMP	Skeletal muscle, prostate, testis, salivary glands.	Asthma, adrenal, testicular, bipolar disorder, depression, prostatic cancers	Tadalafil	Spermatogenesis	(Makhlouf et al., 2006)

1.4. cGMP specific Phosphodiesterase 9A

Phosphodiesterase 9 (PDE9) is cGMP specific enzyme and has highest affinity for cGMP among all PDEs. Till date only one gene of PDE9 has been reported and hence, it is commonly known as 'PDE9A'. It comprises of 20 variants based on N-terminal alternative splicing. In PDE9A, the conserved catalytic domain contains three subdomains- (i) an N-terminal cyclin-fold region, (ii) a linker region and (iii) a C-terminal helical bundle. A deep hydrophobic pocket exists at the interface of the three subdomains. **Figure 1.6** illustrates the distribution pattern of amino acid residues in the active site pocket of PDE9A containing IBMX (1- methyl 3-isobutyl xanthine) as ligand.

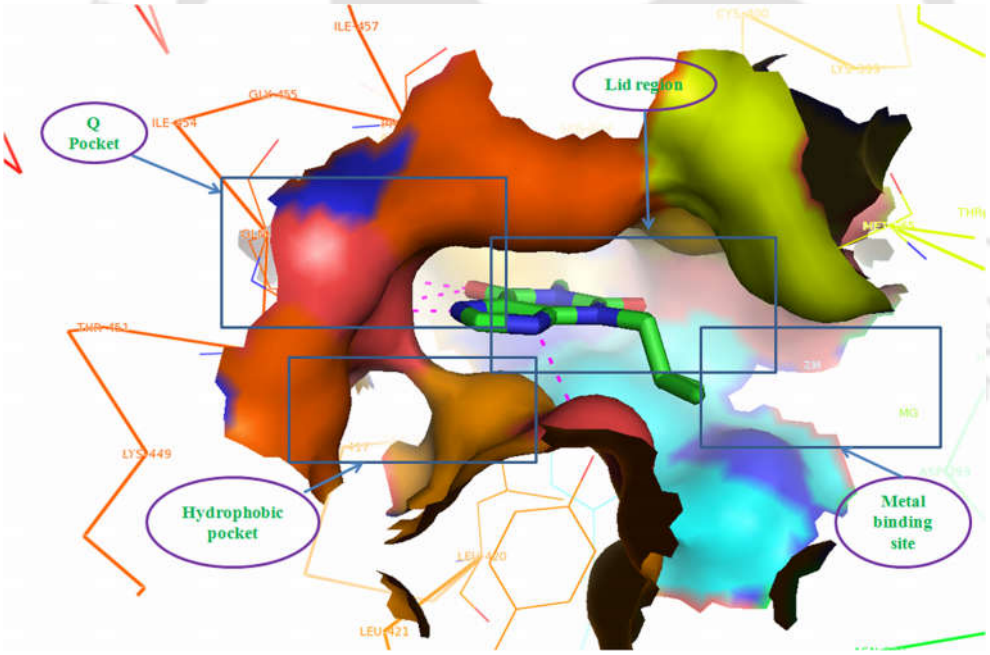

Figure 1.6 Surface view of IBMX bound to PDE9A

The active site pocket of PDE9A is composed of four subsites: a metal-binding site (M site), a core pocket (Q pocket), a hydrophobic pocket (H pocket) and the lid region (L

region) (Jeon et al., 2005). Zinc (Zn) and Magnesium (Mg) are present at the metal binding site. Zn and Mg participate in the interaction with inhibitors as well as with histidine rich site in the active site. The hydrophobic pocket is mainly composed of TRP416, LEU420, LEU421, PHE251 and VAL417. The Q pocket of PDE9A contains conserved catalytic residue GLN453 which is involved in the substrate/inhibitor selectivity by making hydrogen bond interaction.

1.4.1. Catalytic mechanism of PDE9A

On the basis of crystal structure of PDE9A, Liu et al. captured the enzymatic reaction of hydrolysis, using freeze trapping method (Huai et al., 2004; Liu et al., 2008). **Figure 1.7** presents the catalytic mechanism of PDE9A which breaks cyclic phosphodiester bond in the presence of metal ions and cGMP. Hydrolytic center of PDE9A contains two metal cations M1 and M2 and three water molecules W0, W1, W2. In the absence of ligand (substrate or inhibitor), these metal ions form co-ordination bonds with side chains of protein and water molecules. M1 forms four co-ordination bonds with ASP293, ASP402, HIS292 and HIS256 residues of the active site of PDE9A whereas, two co-ordination bonds with water molecules W1 and W0. M2 makes co-ordination bond with ASP293 and four water molecules W0, W2, W3, W4 and W5. Substrate cGMP comes in the catalytic center by displacing W1 and W2, and then involves in interaction with M1 and M2 through the formation of coordination bond with axial and equatorial phosphate oxygen of cGMP respectively. W0 acts as a nucleophile in the hydrolytic reaction that becomes integral part of 5'- GMP by breaking O3'-P bond of cGMP and finally the reaction shifts from ES (enzyme-substrate) to EP (enzyme-product). Thus, this is the rate limiting phenomenon in which metal ions act as Lewis acid involving in

catalyzing the hydrolytic reaction, alternatively HIS252 acts as general acid. This study reveals that the specificity of PDE9A towards cGMP could be due to hydrogen bond formation between guanine base and side chain of GLN453 whose orientation is fixed by the interaction between Nε atom of GLN453 and Oε of GLU406. Here, GLU406 assists polarization of amide side chain of GLN453. This interaction gives a unique feature to PDE9A (Liu et al., 2008).

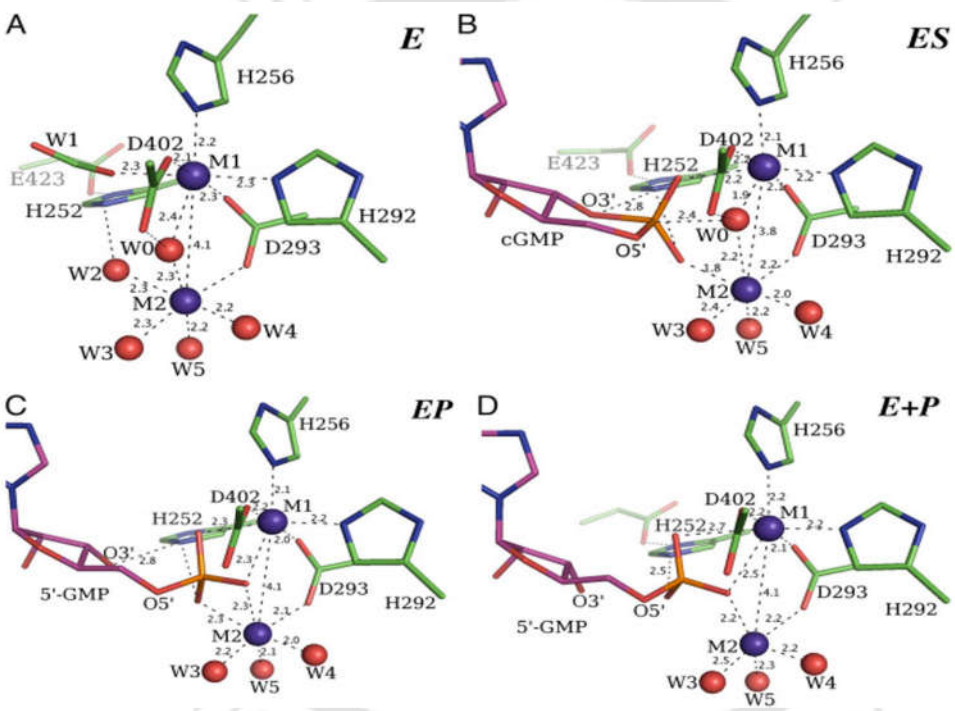

Figure 1.7 Structural representation of PDE9A hydrolytic center (A) Active site with two metal ions M1 and M2 (can be Mn^{2+}- Mn^{2+} or Mn^{2+}-Mg^{2+} or Mg^{2+}- Mg^{2+} or Mg^{2+}-Zn^{2+}etc) in absence of ligand (B) Substrate cGMP interacting with PDE9A hydrolytic centre leads to the formation of ES complex (C) Transition from ES to EP complex after the breaking at 3'-5' cyclic bond but 5'-GMP is still interacting with PDE9A hydrolytic center (D) partial interaction of 5'-GMP in PDE9A active center as E+P complex

1.4.2. Distribution and localization of PDE9A in mammals

In mammals, PDE9A is expressed in all tissues except in blood (Guipponi et al., 1998; Rentero et al., 2003). Highest level of expression of PDE9A is in brain, spleen, small intestine and kidneys (Fisher et al., 1998; Rentero et al., 2003). In brain, PDE9A is the highest expressed protein amongst all PDEs (Andreeva et al., 2001). In the brain, almost all cellular signalling pathways is via cGMP. Regulation of the synthesis and degradation of cGMP fluctuates in different regions of the brain depending on physiological and pathological state. cGMP signaling is important for numerous functions in the brain such as synaptic plasticity, phototransduction, learning, memory and stem cell differentiation. Differentiation of stem cells to neuron is promoted by high level of cGMP whereas, low level of cGMP promotes differentiation to non-neuronal cells (i.e. glial cells) (Erceg et al., 2005; Gómez-Pinedo et al., 2011; Kleppisch, 2009). PDE9A is highly expressed in the basal forebrain, cerebellum and olfactory bulb (Andreeva et al., 2001). Hence, PDE9A inhibition can deal with number of psychiatric and neurodegenerative disease associated with the lowering of cGMP level (Kleiman et al., 2012). Though a very few inhibitors have been developed targeting PDE9A, all of them lack specificity.

1.4.3. Cloning, expression and characterization of PDE9A

In the year 1998, Fisher et al. for the first time recognized an EST (expressed sequence tag) clone of PDE9A from EST database (Incyte Pharmaceuti-cals Inc., Palo Alto, CA) by BLAST (Basic Local Alignment Search Tool). The BLAST search was based on the sequence homology with catalytic domain of PDE4B. However, the query clone was not identical to any of the already known PDE family member clones. Then, they isolated the

identified clone from prostate cDNA library and extended its 5' end with nested PCR from a testis cDNA library. Finally, they achieved cDNA of PDE9A, encoding a full-length protein of 593 amino acid residues (Fisher et al., 1998). PDE9A was reported to have the highest affinity for cGMP amongst all PDEs (Soderling et al., 1998). In the same year, four splice variants (PDE9A1, PDE9A2, PDE9A3 and PDE9A4) were reported by Guipponi et al. These variants were also confirmed as new sub-families of PDE9A (Guipponi et al., 1998). The full length of PDE9A1 has been cloned and characterized from mouse. After a few years, a new variant PDE9A5 was reported by Wang et al (Wang et al., 2003). In terms of the length of amino acid residues, it was found that PDE9A5 was smaller than PDE9A1 and PDE9A2, but longer than PDE9A3 and PDE9A4. PDE9A5 is similar in enzymatic properties to PDE9A1 but has different tissue distribution and subcellular localization. PDE9A1 is located exclusively in nucleus because of the presence of pat7 motif which acts as nuclear localization signal while other PDEs are located in the cytosol (Wang et al., 2003). In the same year, another group reported separately 16 other variants including PDE9A5 from the same PDE9A mRNA transcript through alternative splicing (Rentero et al., 2003). In 2006, one more variant was introduced in PDE9A. Hence, more than 20 variants of PDE9A have been reported so far (Rentero et al., 2006).

1.4.4. Architecture of PDE9A gene

Phosphodiesterase 9A enzyme is encoded by *pde9A* gene. It is 122kb in length consisting of 22 exons and is located on chromosome 21q22.3 between TFF1 and D21S360 genes in human genome. It is located on chromosome 17 in mouse genome (Guipponi et al., 1998; Rentero et al., 2003). On the basis of PCR amplification and EST sequences analysis,

20 different PDE9A mRNA transcripts have been identified so far. These variants are produced as a result of alternative splicing at 5' mRNA region. However, the C-terminal part of mRNA consists of 12 exons that are involved in formation of conserved catalytic domain. Rest of the first 10 exons participates in multiple splicing. The occurrence of these splice variant can be tissue dependent because majority of variants are relatively found in all tissues, but only some PDE9 mRNAs are restricted to a few tissues (i.e. PDE9A11 in peripheral blood leukocytes, PDE9A12 in prostate, PDE9A14 in ovary, and PDE9A15 in thymus). Most abundant variant PDE9A1 is present in prostate, colon, rectum, foetal brain, foetal kidney, and intestine. It is also moderately expressed in the cerebellum and forebrain (Rentero et al., 2003). According to Rentero et al, translation of *pde9A* gene is performed by more than one start codons (ATG) (Rentero et al., 2006). The first start codon is present in exon 1 whereas, the second one is located 52 bases downstream of the first start codon of exon 1. Other two start codons might be present at exon 7 and 8 as shown in **figure 1.8**. Some splice variants are involved in the production of protein that is targeted to cell membrane and cellular vesicles whereas the rest are targeted to cytoplasm (Rentero et al., 2006). **Figure 1.8** illustrates the detail of Phosphodiesterase 9A gene and their alternating splice variants along with their start codon variation.

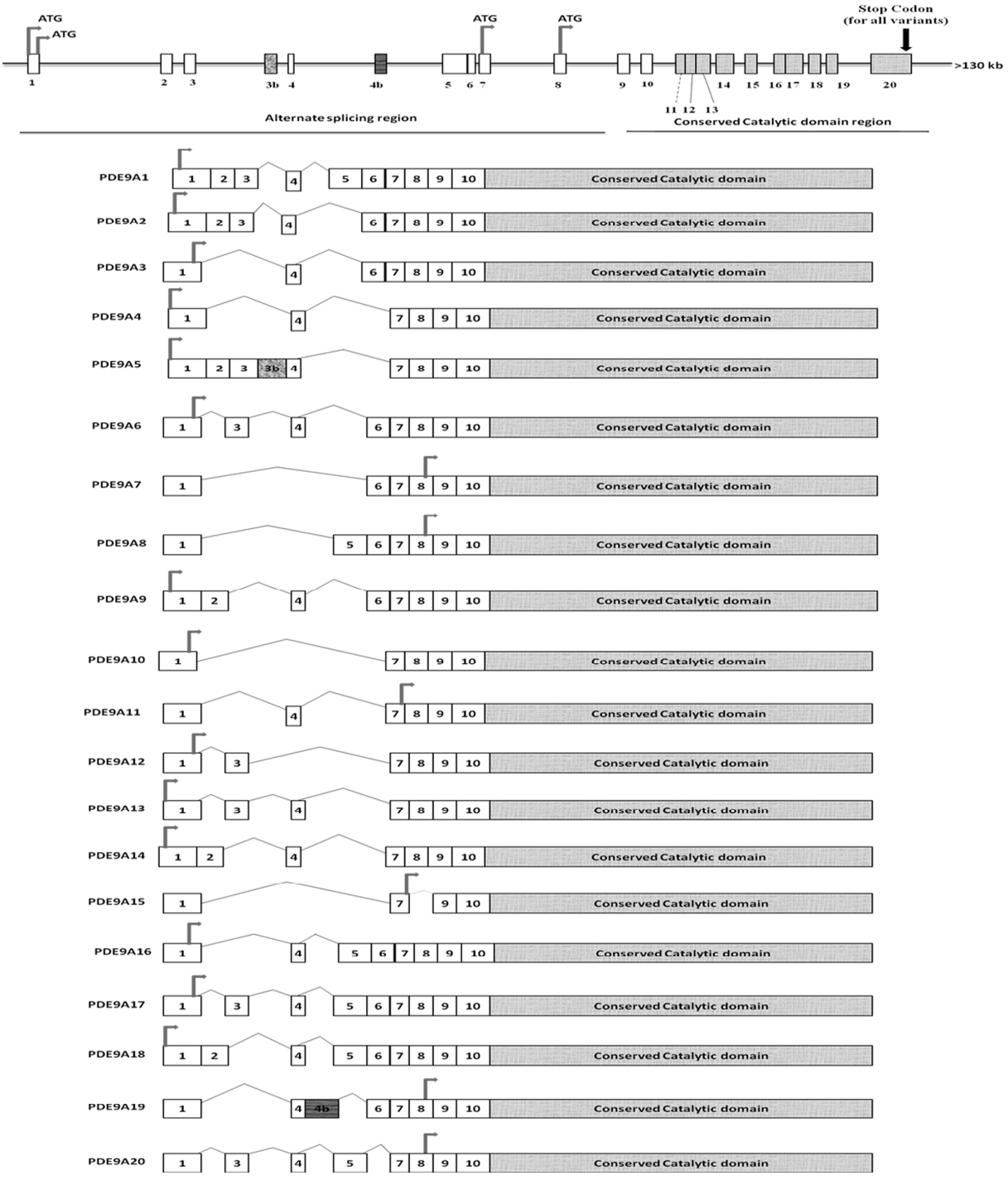

Figure 1.8 Schematic diagram of human *pde9A* gene and its mRNA transcripts

1.4.5. Importance of catalytic domain of PDE9A

All PDE9A transcripts have conserved catalytic domain at the C-terminus. The C-terminus constitutes the active site containing a nucleotide recognition pocket having the hydrophobic clamp created by side chain of PHE456 and LEU420 along with the hydrolysis center (Liu et al., 2008; Zhang et al., 2004). The crystal structure of PDE9A2 catalytic domain complexed with IBMX was reported by Huai et al and has been presented in **figure 1.9** (Huai et al., 2004).

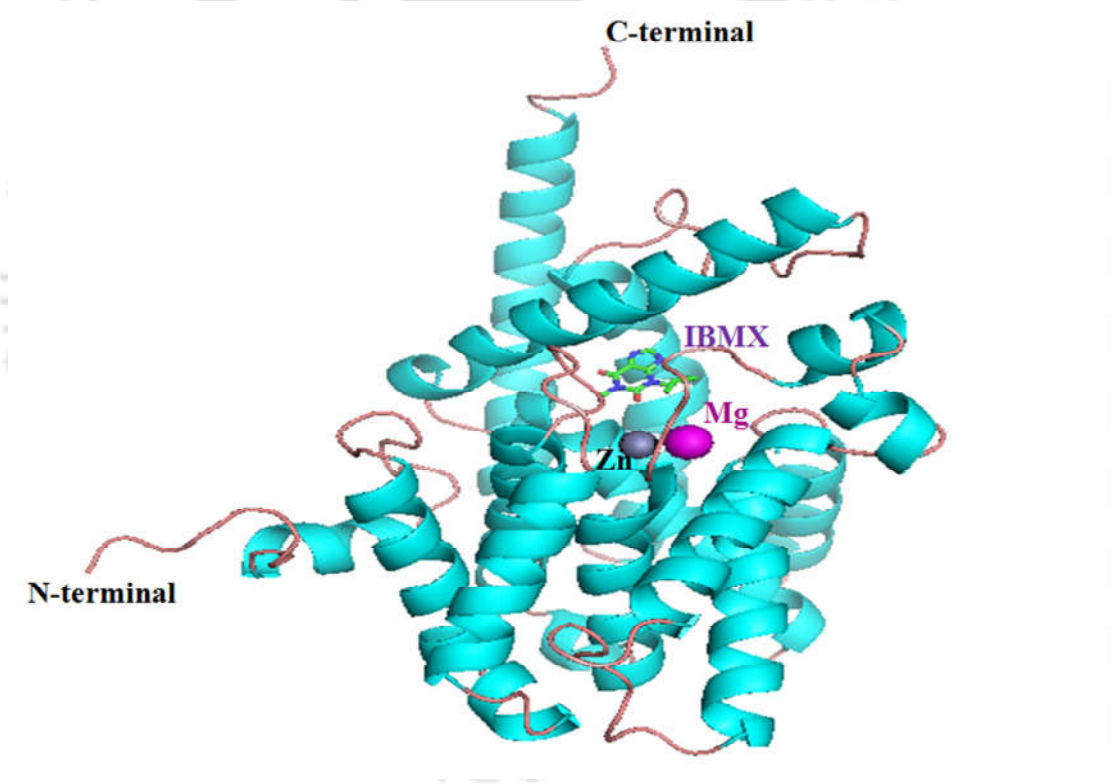

Figure 1.9 Catalytic domain of PDE9A showing 16 α-helices.

It has been observed that the N-terminal regulatory domain does not participate in altering the catalytic activity of the protein. Catalytic domain contains 16 α-helices present between 181-506 amino acid residues. The catalytic domain of PDE9A is similar to catalytic

domain of PDE4D2 but drastically different from PDE5A1. This has been demonstrated by superimposition of catalytic domain of PDE9A2 over PDE5A1 and PDE4D2. RMS deviation of 1.5 Å was observed between Cα atom of 207-495 residues in PDE9A2 and residues 115-411 in PDE4D2 showing structural similarity (Huai et al., 2004). It has also been brought out that catalytic domain of PDE9A2 forms a dimer in the similar pattern as PDE4D2 does. The residues involved in dimerization are TYR315, ASN316, ASP317, ASN323, and ARG353. Dimerization takes place by formation of hydrogen bond between two subunits that provide major force for dimer formation. Unlike PDE4D2, PDE9A is not involved in further tetramerization.

1.4.6. Therapeutic disease targets of PDE9A

Diminished cGMP signaling results in various therapeutic disorders that can be cured by inhibition of cGMP specific PDE9A which leads to signal enhancement. Presence of PDE9A at mapping position of 21q22.3 might be a reason for a number of human chromosome 21 mapped genetic diseases such as Down syndrome and bipolar affective disorder (Guipponi et al., 1998). Diseases targeted by inhibition of PDE9A are hyperglycemia, dyslipidemia, type 1 and type 2 diabetes, insulin resistance syndrome, obesity and several neurodegenerative diseases such as Alzheimer's disease, Schizophrenia, age-based cognitive decline (Bell et al., 2004; Black, Shawn et al., 2005; Fryburg and Gibbs, 2004; Joshua D. Vardigan et al., 2011). In brain, inhibition of PDE9A is required to improve synaptic transmission and alleviate vulnerable synapses resulting in an improvement in cognitive deficit in Alzheimer disease (Verhoest et al., 2009). In 2005, first potent and selective inhibitor of PDE9A, BAY 73-6691 came into picture (Wunder et al., 2005). Studies

on BAY 73-6691 showed its multiple role to improve learning and memory, basal synaptic transmission and long-term potentiation, decrease in the stimulation of cytokines by neutrophil adhesion and induction of apoptosis (Kroker et al., 2012; Miguel et al., 2011; Saravani et al., 2012; van der Staay et al., 2008; Wunder et al., 2005). BAY 73-9961 has been used for the treatment of Alzheimer's disease, corpus cavernous relaxation in mice model (da Silva et al., 2013). There is no report confirming the completion of clinical trial of BAY 73-9961. Another potent and selective inhibitor PF-04447943 has been used to increase cGMP in cerebrospinal fluid for the treatment of Alzheimer disease and other cognitive diseases (Hutson et al., 2011; Nicholas et al., 2011; Joshua D Vardigan et al., 2011; Verhoest et al., 2012; Wunder et al., 2005). To date PF-04447943 has completed six clinical trials and some more are on track (Nicholas et al., 2011; Schwam et al., 2011). Researchers are making constant progress towards the development of specific and potent inhibitors with improved inhibition capacity than the existing ones (DeNinno et al., 2009; Meng et al., 2012; Wang et al., 2010). **Figure 1.10** provides the details of PDE9A selective inhibitors reported so far (Claffey et al., 2012; Verhoest et al., 2012, 2009; Wang et al., 2010; Wunder et al., 2005).

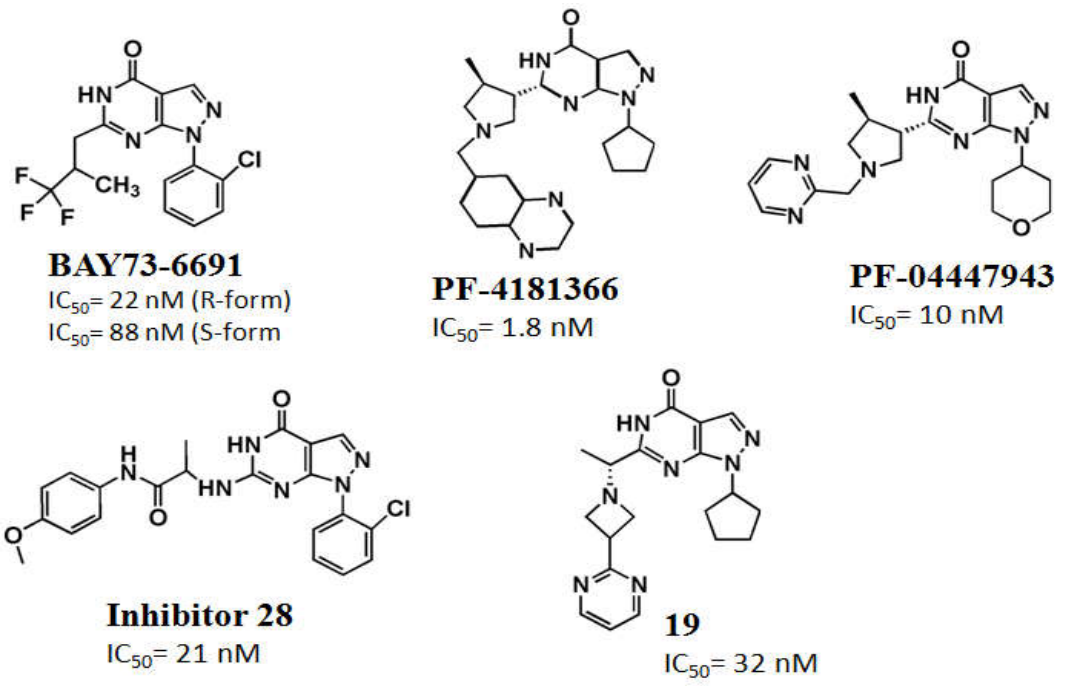

Figure 1.10 Known potent non-xanthine inhibitors of PDE9A

1.4.7. Importance of uniqueness of PDE9A structure in drug development

Inhibitor design and development is a key area that is in consideration towards a successful inhibitor search. Therefore, various inhibitors have been synthesized and tested with PDE9A but most of them have shown moderate selectivity towards PDE9A. One main reason behind lacking in potency and selectivity of inhibitors for PDE9A is reactivity of the inhibitors with other members of PDE superfamily. Researchers are facing problems in achieving a specific drug for PDE9A due to its structural similarity with PDE1 and PDE8. PDE9A inhibitors should be developed by considering PDE1 with comparative computational as well as experimental studies. This is needed because of PDE1 side effect has always been a key concern during the treatment of various brain diseases because of

abundance of PDE1 in brain (Meng et al., 2012). Thus, to find out selective inhibitors for PDE9A, it is necessary to understand the active site pocket thoroughly. With the objective of finding out the nuances of the protein structures, we carried out a comparative analysis of catalytic domain of various PDEs. **Table 1.2** illustrates the information of residues present in the 5 Å region around cGMP in all PDEs. This was obtained by the superimposition of PDE9A-cGMP complex over other PDE-cGMP complexes based on sequence alignment method in PyMol.

Table 1.2 Comparative study of amino acid residues present in the 5 Å region around cGMP bound to various PDEs brought out by sequence alignment

PDE Type	PDB ID	Residues in contact with cGMP within 5Å region in active site pocket																	
PDE9A	3DYL	F	H	H	H	D	H	T	M	D	I	N	E	V	L	Y	A	Q	F
		251	252	256	292	293	296	363	365	402	403	405	406	417	420	424	452	453	456
PDE5A	1T9R	Y	H	H	H	D	H	T	L	D	L	A	I	A	V	F	M	Q	F
		612	613	617	653	654	657	723	725	764	765	767	768	779	782	786	816	817	820
PDE6C	3DBA	-	-	-	-	-		S	-	-	-	E	T	V	H	F	T	-	-
								121				133	134	146	148	152	176		
PDE4B	1XLZ	Y	H	H	H	D	H	T	M	D	L	N	P	T	I	F	S	Q	F
		233	234	238	274	275	278	345	347	392	393	395	396	407	410	414	442	443	446
PDE7A	3G3N	Y	H	H	H	D	H	T	I	D	I	N	P	S	V	F	I	Q	F
		211	212	216	252	253	256	321	323	362	363	365	366	377	380	384	412	413	416
PDE8A	3ECM	Y	H	H	H	D	H	T	M	D	V	N	P	A	I	Y	S	Q	F
		555	556	560	596	597	600	668	670	726	727	729	730	741	744	748	777	778	781
PDE1B	1TAZ	Y	H	H	H	D	H	T	M	D	I	H	P	T	L	F	S	Q	F
		222	223	227	263	264	267	334	336	370	371	373	374	385	388	392	420	421	424
PDE2A	1Z1L	Y	H	H	H	D	H	T	L	D	L	D	Q	A	I	F	L	Q	F
		655	656	660	696	697	700	768	770	808	809	811	812	823	826	830	858	859	862
PDE3B	1SOJ	Y	H	H	H	D	H	T	L	D	I	G	P	T	I	F	L	Q	F
		736	737	741	821	822	825	893	895	937	938	940	941	952	955	959	987	988	991
PDE10A	4DFF	Y	H	H	H	D	H	T	L	D	L	S	V	A	I	F	G	Q	F
		524	525	529	563	564	567	633	635	674	675	677	678	689	692	696	725	726	729

Most unique feature of PDE9A is the presence of GLU406 which involves in fixing the orientation of the side chain of invariant GLN453 by making intra-molecular H-bond. GLU406 forms hydrogen bond of 2.8 Å length between side chain Nε2 of Gln453 and Oε1 of

Glu406. This bond formation enhances the selectivity towards cGMP as well as inhibitors. Consequently, if GLU406 is targeted by inhibitors, it can give better specificity towards PDE9A. TYR424 is the other unique residue present at the entrance of the active site pocket of both PDE9A and PDE8A (TYR748) while phenylalanine is present in the corresponding position of other PDEs. TYR424 further increases the polarity of the active site and can act as active residue for inhibitor selectivity (Huai et al., 2004). Therefore, TYR424 in PDE9A can be targeted for inhibitor designing because the polar hydroxyl group of tyrosine may be involved in hydrophilic interaction with inhibitors, giving good selectivity over PDE1 (Meng et al., 2012; Wang et al., 2010). From the table, we conclude that F251 is a crucial residue that is present only in PDE9A which may contribute towards substrate selectivity. As described above, GLU406 has specific role in substrate selectivity of PDE9A. Hence, by analyzing the active site pocket of various members of PDE superfamily thoroughly we can say targeting these residues might give some idea about the active site network of PDE9A to be exploited further.

1.5. Molecular diversification of ligands in PDE9A drug development process

Existing status:

Till date, several PDE9A inhibitors have been developed for the treatment of diabetes, insulin-resistance syndrome, cardiovascular diseases, and CNS diseases such as Alzheimer disease. Interestingly, most of the inhibitors have been constructed over "pyrazolopyrimidinone'' scaffold as shown in **Figure 1.10.** Sildenafil (Viagra and Revatio),

a most successful PDE5 inhibitor, has also used the same scaffold. The use of common scaffold by various PDEs could be responsible for various side effects. Thus, moderate inhibition potential of existing common "pyrazolopyrimidinone" scaffold has incentivized the researchers to search for other scaffolds to bring out structural diversification in the PDE9A drug development process (Li et al., 2015). To bring out such diversification, 'xanthine' can be a potential target because derivatives constructed over xanthine scaffold have been widely known for their non-specific PDE inhibition properties. Xanthine as a scaffold provides maximum possibility for structural diversification because of the presence of all possible sites (three –NH sites and one –CH site) for substitution. With appropriate substitution over xanthine scaffold according to the requirement as per the active site composition and size of PDE9A, specific designed inhibitor can be achieved.

1.6. Xanthine- as potential scaffold in drug development

Organic substances containing nitrogen are widespread throughout the natural world. Natural xanthine derivatives such as caffeine, theobromine and theophylline occupy prominent place in the world of natural compounds. Structurally these are very closely related and are present in different plants such as tea, coffee, and cocoa. Because of their pharmacological effect, which is fundamentally of stimulative nature, these compounds have been significant since time immemorial as luxurious non-essential foodstuffs and as in various medication purposes. These xanthine derivatives are commonly known as methylxanthines– a chemically defined group of substances within the alkaloids. The amount of these alkaloids present in plants depends on various factors, such as their natural processing procedures, genotype and their geographical origin (Matissek, 1997). The

presence of common xanthine scaffold gives a call to look towards 'xanthine' as potential candidate for future drug development.

1.6.1. Insight to molecular structure of Xanthine

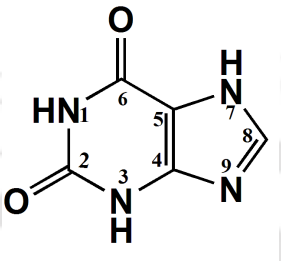

Structure of xanthine

Xanthine is heterocyclic, aromatic, nitrogen based alkaloid. Xanthine was first discovered in 1817 by German chemist Emil Fisher and later the name 'xanthine' was coined in 1899 (Suravajhala et al., 2014). Xanthine contains similar skeleton as that of purines which form the building blocks of unit of life i.e. ribonucleotides (RNA) and deoxyribonucleotides (DNA). The structural resemblance with two important purine derivatives- Adenine and Guanine; make xanthine a better therapeutic molecule. The structure of xanthine consists of two fused rings-one is of six members and another is of five members. Theoretically, two types of tautomerism are displayed in xanthine molecule. First is annular i.e. migration of proton of imidazole ring between N_7 and N_9 positions. Second is lactim-lactam i.e. migration of proton between N_1 and N_3 and oxygen of carbonyl group at C_2 position. Despite annular tautomerism in xanthine, 7H form predominates over 9H form (Gulevskaya and Pozharskii, 1991). Xanthine provides maximum possibility of substitutions. Till date, xanthine derivatives with five types of mono substitutions (1-, 3-, 7-, 8- and 9-),

eight di-substitutions (1,3-, 1,7-, 1,8-, 1,9-, 3,7-, 3,8-, 3,9- and 7,8-), three types of tri-substitutions (1,3,7-, 1,3,8-, 1,3,9-) are reported (Allwood et al., 2007; Bandyopadhyay et al., 2012; Bansal et al., 2010; Gulevskaya and Pozharskii, 1991; Hayallah et al., 2002; Miyamoto et al., 1993; Müller et al., 1998; Sakai et al., 1992). Most of these substitutions are readily obtainable, but substitution at N_9 position become difficult because the substituent at N_9 position does not get stability because of the retro-orientation of double bonds between N_7 and N_9 positions of imidazole ring of xanthine. Thus, the structural understanding has utmost importance to utilize the full potential of xanthine ring in development of xanthine based compounds.

Biological implication of the basic structure of xanthine ring

The basic structure of xanthine consists two rings - one ring is of six membered pyrimidinedione ring and second ring is of five membered imidazole ring. The basic structure of xanthine itself has significance in rendering it pharmaceutical activity. It was evident by studies on alternation of basic structure of xanthine ring including enlargement of xanthine ring, insertion of additional benzene ring, hybridization of xanthine with adenosine and synthesizing mesoionic derivatives of xanthine (Daly et al., 1988; Glennon et al., 1981; Schneller et al., 1989; van Galen et al., 1992). Alternation in xanthine basic structure leads to decrease in biological potency. Enlargement of six-membered pyrimidinedione ring of xanthine to a seven-membered diazepinedione ring leads to weaker interaction with adenosine receptor. This was mainly because the enlarged ring system loss planarity (Daly et al., 1990; van Galen et al., 1992). Thus, along with different substitution site basic structure of xanthine itself has significant role in generating biological potency towards the target.

Biological implication of different substitution sites of xanthine ring

From various *in vitro* analysis of natural xanthine derivatives such as theophylline, theobromine and caffeine, it was found that N_3 substitution has important role in generating bronchodilator properties of the developed compounds (Takagi et al., 1988). N_1 substitution at xanthine generates adenosine antagonism properties (Takagi et al., 1988). N_7 substitution shows mixed impact. N_7 substitution increases bronchoselectivity whereas, it decreases the adenosine receptor affinity (Miyamoto et al., 1994; van Galen et al., 1992). Due to presence of methyl group at N_7 position of caffeine, it is threefold less potent than theophylline towards adenosine receptor. Therefore, in most cases, bulkiness of N_7-substituents considerably decreases the affinity towards adenosine receptor. (Schwabe et al., 1985; van Galen et al., 1992). The C_8 substitution has significant impact in increasing the pharmaceutical properties of compounds. N_1, N_3 and C_8 substitutions together are most promising sites of substitution on xanthine scaffold for generating compounds with selective potency towards subtypes of adenosine receptors as well as generating inhibition potential towards PDEs (Laddha et al., 2009). Along with adenosine antagonist, xanthine derivatives with C_8 substitution are also reported as PDE inhibitor, Topo II inhibitor, dipeptidyl peptidase 4 and acetylcholinesterase (AChE) inhibitor (Kadi et al., 2015; Liou et al., 2013). Aryl substitution at C_8 position shows immense affinity for increasing the inhibition potential of compounds towards PDEs as well as adenosine receptors. As compared to theophylline, 8-phenyl theophylline shows 100- and 30-fold more potency towards A1 and A2 receptors, respectively (van Galen et al., 1992). Increasing chain length at N_1 and N_3 site of xanthine increases the potency of compounds towards adenosine receptor and PDEs (van Galen et al.,

1992). Substitution with alkyl groups at N_1, N_3 and N_7 positions of xanthine are crucial for activation of Cystic Fibrosis Transmembrane Conductance Regulator (CFTR). However, substitution at C_8 and N_9 positions does not activate CFTR. Thus, by manipulating C_8 position of compounds, they can be made selective towards adenosine receptor. N_7 position may activate CFTR except when N_1 and N_3 positions are occupied with methyl group (Chappe et al., 1998). **Figure 1.11** illustrates the pharmacological consequences of different substitution sites of xanthine scaffold.

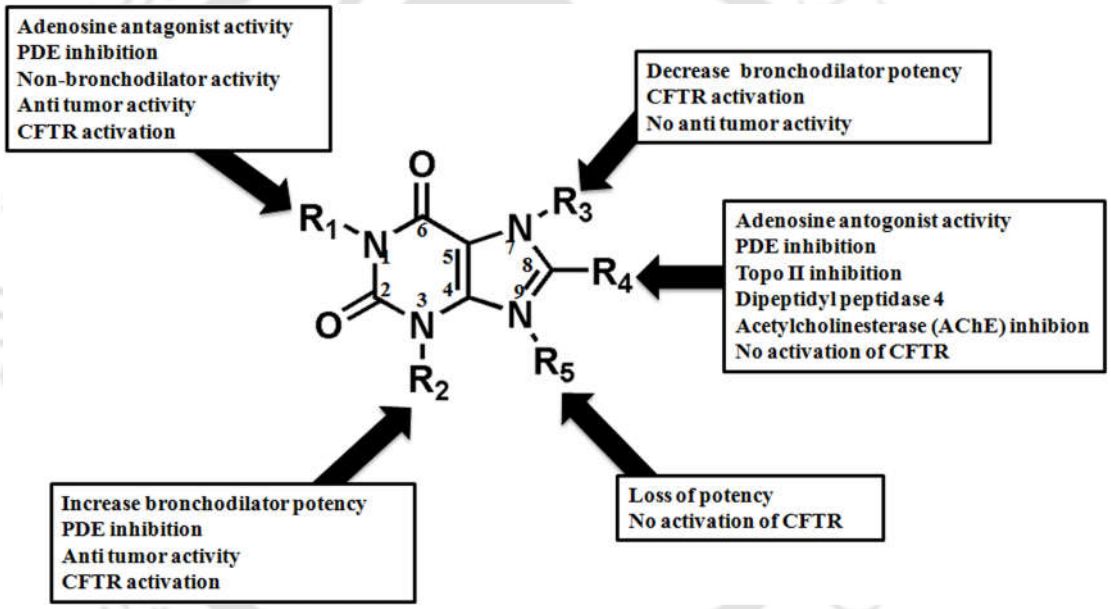

Figure 1.11 Pharmaceutical potential of different substitution sites on xanthine

1.6.2. Overview of existing xanthine derivatives

Natural xanthine analogs are known for their pharmaceutical activities such as inhibition of phosphodiesterases, adenosine antagonizing activity, antimicrobial activities, antioxidant activities (Ogawa et al., 1989; Suravajhala et al., 2014). Many xanthine based plant alkaloids such as caffeine, theophylline, theobromine and paraxanthine are most often

used psycho-stimulant and anti-asthmatic drugs (Burbiel et al., 2006). Natural xanthine derivatives are commonly present in cocoa, tea and coffee plants (Baraldi et al., 2007). Xanthine derivatives are used as a target for various pharmaceutical applications. Targeted diseases of these molecules are Alzheimer's disease, asthma, behavioral targets, cancer, Diabetes, analgesic, Parkinson disease, respiratory disease, renal disease, etc. Caffeine is well known natural xanthine derivative present in tea which is associated with reducing the risk of various brain diseases (Joghataie et al., 2004). In last few decades, based on the natural xanthine derivatives large number of inhibitors have been designed, developed and used worldwide for pharmaceutical applications. Most common reported synthetic xanthine derivatives are IBMX, DMPX (3, 7-dimethyl-1-proparglyxanthine), pentoxifylline, enprofylline, propentofylline, aminophylline, KMUP, proxifylline and so on (Ruttikorn et al., 1988; Semmler et al., 1993). But most of the xanthine inhibitors non-specifically target PDEs. Xanthine scaffold is considered as one of the most significant drug target as far as the drug likeness properties are concerned. **Figure 1.12** illustrates the structural details of natural and synthetic xanthine derivatives. **Table 1.3** represents the details of reported key xanthine derivatives in terms of their biological source, mode of action and therapeutic disease targets.

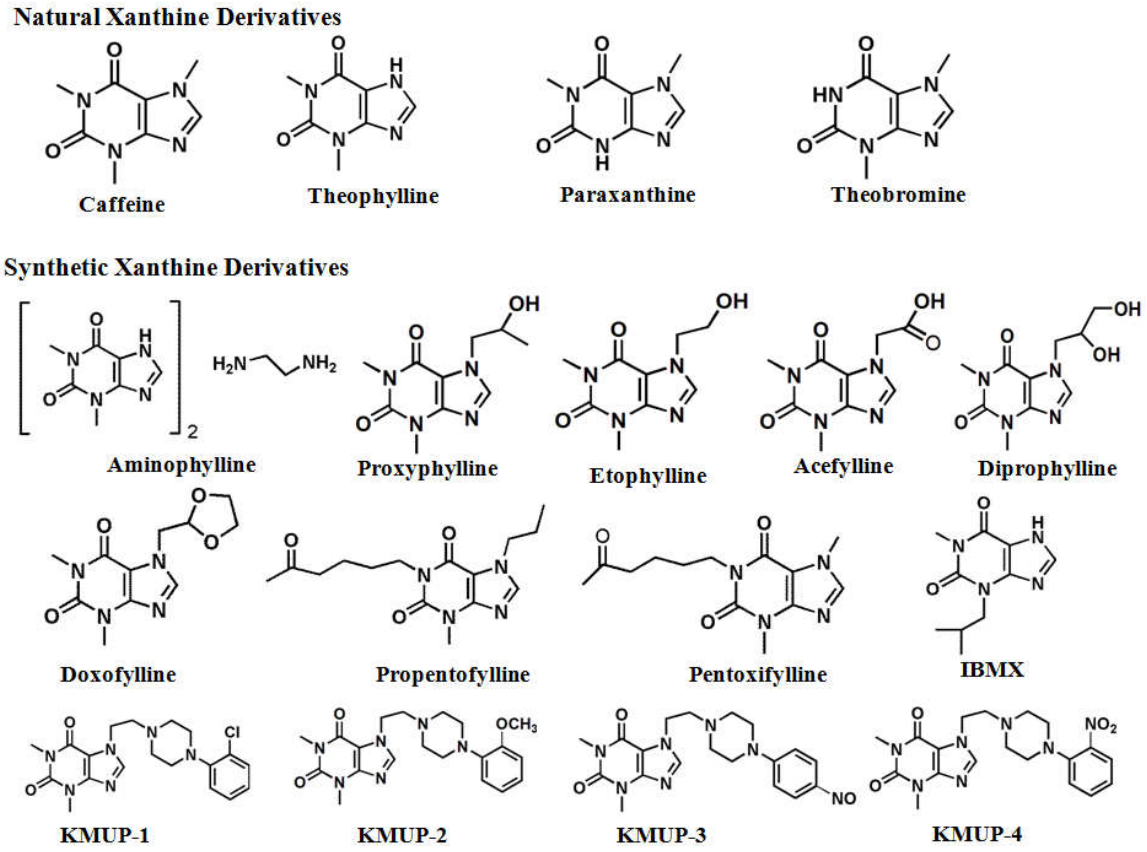

Figure 1.12 Chemical structure of existing xanthine derivatives: natural and synthetic.

Table 1.3 Mode of action and therapeutic details of existing xanthine derivatives

Sl. No.	Xanthine derivatives	Mode of Action	Therapeutic use	References
1.	Caffeine (1,3,7–trimethyl xanthine) **Source-** coffee, tea, chocolate, soft drinks and energy drinks	antagonism of adenosine receptors; inhibition of PDE; intensifies and prolongs the effects of epinephrine, antimicrobial activities; anti-inflammatory activity	bronchodilator; treatment of neurodegenerative disease; treatment of apnea in premature infants, respiratory stimulant effect	(Graham et al., 1994; Joghataie et al., 2004; Pennella and Vittoria Mattioli, 2015)
2.	Theophylline (1,3-dimethyl xanthine) **Source-** tea, cacao bean (chocolate), Ye rba mate, Kola	PDE inhibition, antagonism of adenosine receptor, histone deacetylase activity, alkaline phosphatase inhibition activity, increasing of catecholamine release, inhibition of calcium ion influx, increasing blood pressure	diuretic, cardiac stimulation, smooth muscle relaxation, CNS stimulator, treatment of COPD and asthma, infant apnea treatment, increasing renal blood flow, antiviral, anti cancerous, antitumor activity	(Boswell-Smith et al., 2006; Foukas et al., 2002; Rabe et al., 1995; Sugimura and Mizutani, 1979)
3.	Theobromine (3,7- dimethyl xanthine) **Source**-cacao, chocolate	antagonizing adenosine receptors, PDE inhibition, reduces inflammation and innate immunity, activates PKA, inhibits TNF-alpha,	treatment of neurodegenerative diseases and prostate cancer, antiangiogenic properties, antitussive effect	(Barcz et al., 2000; Kakuyama (nee Iwazaki) and Sadzuka, 2001; Slattery and West, 1993; Usmani et al., 2005)
4.	Paraxanthine (1,7-dimethyl xanthine) **Source-** Animals that have consumed caffeine	non-selective PDE inhibitor, inhibits TNF-alpha and leukotriene synthesis, adenosine receptor antagonist, stimulation of thermogenesis, increase in plasma epinephrine	treatment of intermittent claudication, treatment of psychoactive central nervous system (CNS) stimulant, elevated diastolic blood pressure, reduces inflammation and innate immunity	(Müller et al., 1998)

5.	Aminophylline (Derivative of Theophylline)	phosphodiesterase inhibition, inhibits TNF-alpha, adenosine receptor antagonist	antioxidant, treatment of asthma or COPD, anaphylactic shock and cardiac arrest, anti-inflammatory	(Roy et al., 2015; Rutherford et al., 1981; Skinhøj and Paulson, 1970)
6.	IBMX	phosphodiesterase inhibition, inhibits TNF-α and leukotriene synthesis, induced elevation of Ca^{2+}	reduces inflammation and innate immunity, sensitizes cardiac myocytes to anoxia	(Geisbuhler et al., 2002; Huai et al., 2004; Usachev and Verkhratsky, 1995)
7.	Pentoxifylline	altering peritoneal fibrinolytic activity, inhibitor of primary post-traumatic adhesion formation	peripheral vascular disease and cerebrovascular disease	(Steinleitner et al., 1990; Tarhan et al., 2006; Ward and Clissold, 1987)
8.	Propentofylline	inhibitor of both adenosine transporter and phosphodiesterases, neuroprotective, antioxidant and anti-inflammatory	treatment of brain tumor, Vascular dementia (VaD) and Alzheimer's disease (AD)	(Bondan et al., 2015; Gwak et al., 2008; Stefanovich, 1985; Vukadinovi?a et al., 1986)
9.	KMUP (1,2,3,4) (xanthine and piperazine derivative)	activation of PKA, PKG and K+ channels, eNOS/cGMP-enhancer, inhibition of PDEs, antagonization of adenosine receptor	anti-inflammatory, anti-proliferation, neuroprotective, cardioprotective, anti-osteoclastogenic, anti-resorptive activities, inhibiting pulmonary hypertension	(Chung et al., 2010; Dai et al., 2015; Hong et al., 2014; Liou et al., 2013; Liu et al., 2011; Wu et al., 2005)
10.	Doxofylline (7-(1,3-dioxalan-2-ylmethyl) theophylline)	inhibition of PDEs, reduce various side effects such as gastric acid secretion	anti-inflammatory and bronchodilator activities	(Dini and Cogo, 2000; Gupta et al., 2011; van Mastbergen et al., 2012)

1.6.3. Xanthine derivatives in therapeutics

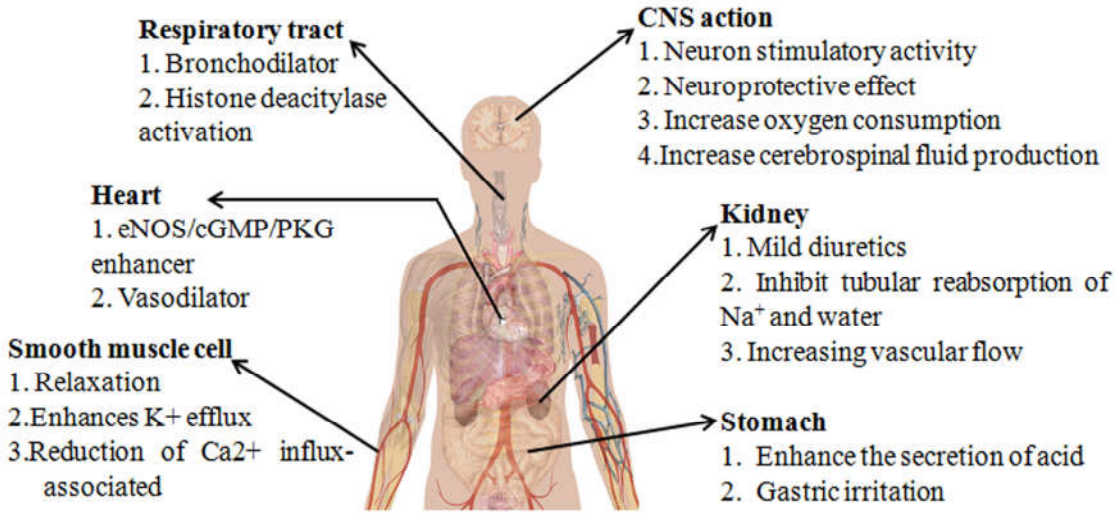

Figure 1.13 Therapeutic targets of xanthine derivatives.

Treatment of Respiratory Tract diseases

Over a decade xanthine derivatives have been widely used for the treatment of respiratory diseases. They are best known for their bronchodilator action. Earlier in 20th century, Theophylline was particularly used as bronchodilator but years later, the aminophylline (combination of Theophylline and ethylenediamine) and glycine theophyllinate were started to be used as effective bronchodilator to treat acute asthma (Cushley and Holgate, 1985). Since then several bronchodilators have been developed, most of them were constructed with N_7 substitution at xanthine scaffold. They are diprophylline, acephylline piperazine, etophylline and proxyphylline (Hasegawa et al., 1991; Zuidema and Merkus, 1981). Despite various N_7 substituted theophylline have been developed but N_7 substitution shows comparatively lower potency as bronchodilator (Hasegawa et al., 1991). However, C_8 substitution at xanthine with N_1 and N_3 substitution has been reported with

better potency of anti allergic properties (Abdulrahman et al., 2012). Substitution at N_9 position generally losses the bronchodilator potency of xanthine derivatives.

Treatment of Neurodegenerative diseases

Adenosine acts as modulator in various physiological and pathophysiological processes in central nervous system (CNS). The structural similarity of xanthine derivatives play imperative role in the blockade of adenosine receptors and thus act as neuroprotective with increasing the concentration of extracellular adenosine. Propentofylline and KMUP-1 (7-[2-[4-(2-chlorophenyl) piperazinyl]ethyl]-1,3-dimethylxanthine) are widely used as neuro-protecting xanthine derivatives (Grome et al., 1996; Mielke et al., 1996). Likewise various other xanthine derivatives show neuroprotective effect because of their course of action as phosphodiesterase inhibitor, blocker of adenosine uptake in neuron and glial cells and antagonist of adenosine receptors (Grome et al., 1996; HAGHGOO et al., 1995; Mielke et al., 1996). The neuroactive effect of xanthine derivatives increases the life of brain cells by maintaining the consistency in cell signaling pathway by inhibition of PDEs. Higher neural activity may lead to increase in oxygen consumption and cerebrospinal fluid production in brain. Because of these reasons xanthine derivatives have been used for the treatment of various neurodegenerative disease including Alzheimer disease, Parkinson disease, ischemia, etc (Franco et al., 2013).

Treatment of Hypertension and Cardiovascular diseases

Conventional xanthine derivatives such as caffeine, theophylline, theobromine and aminophylline are reported as vasodilators. Endothelial nitric oxide synthase (eNOS) (eNOS) and inducible NOS (iNOS) are important enzymes which play important role in

production of nitric oxide (NO) and cyclic guanosine monophosphate (cGMP). Both nitric oxide (NO) and cGMP are second messenger in signal transduction pathway. Xanthine derivative, KMUP-1 has been reported as eNOS/cGMP/PKG enhancer to increase eNOS expression that leads to improve the hypertension to treat left ventricular hypertrophy (LVH) which develop due to cardiac stress (Yeh et al., 2012). Xanthine derivatives act as therapeutics on the heart and vessels by acting on the cell signaling of these organs. For instance, caffeine acutely increases blood pressure, peripheral vascular resistance, arterial stiffness, circulating catecholamine, and endothelial dependent vasodilation (Zainab and Djafarian, 2016).

Treatment of Renal diseases

Natural xanthine derivatives such as caffeine and theophylline have been reported for the treatment of renal disease since 1864. It is widely known that natural xanthine derivative have been used to increase urine output until the development of more potent diuretic (Osswald and Schnermann, 2011). The diuretic potency of natural xanthine derivatives are reported as theophylline>caffeine>paraxanthine>theobromine (Osswald and Schnermann, 2011). Though diuretic and natriuretic effect of natural xanthine derivatives are well established but the mechanism behind this activity is still not clear. A_1 receptor blockade by xanthine derivatives could be most probable reason for diuretic effect of these derivatives because they act as antagonist of adenosine which is key regulator of kidney function by regulating the level of glomerular filtration rate (GFR), medullary blood flow, and renal water and electrolyte transport. Here, xanthine derivatives act as A_1 receptor antagonists which increase renal fluid and Na^+ excretion by blocking the receptor (Rieg et al., 2005).

Relaxation of Smooth muscle cells

The phosphodiesterase inhibition properties of xanthine derivatives have been related to their tracheal relaxant activities (Ogawa et al., 1989). Smooth muscle relaxation is carried out through the activation of Adenylyl cyclase (AC) and soluble Guanylyl cyclase (GC) which leads to synthesis of second messengers - cAMP and cGMP respectively. The level of these second messengers is regulated by cyclic nucleotide phosphodiesterases. The phosphodiesterase inhibitory action of xanthine derivatives leads to accumulation of cAMP/cGMP which further activates PKA/PKG and enhances K^+ efflux. It leads to reduction of Ca^{2+} influx-associated contractility in tracheal smooth muscle (TSM) [Lin et al, 2006]. KMUP-1, KMUP-3 and KMUP-4 are well studied smooth muscle relaxant (Lin et al., 2002; Wu et al., 2005, 2001).

Secretion of Gastric acid as a side effect

In course of treatment with xanthine derivatives, gastric distress is one of the most frequent side effects. It has been reported that the xanthine derivative which are antagonist of adenosine are mostly responsible for gastric acid and pepsin secretion. Theophylline, aminophylline, caffeine etc come under this category. However, xanthine derivatives such as doxofylline and enprofylline, are poor antagonist of adenosine and does not stimulate gastric acid and pepsin secretion (Lazzaroni et al., 2007). Here also, A_1 receptor blockade by antagonist of adenosine might be the responsible factor for gastric secretion.

1.6.4. Role of xanthine derivatives in pharmacology

Anti-inflammatory activity of xanthine derivatives

Xanthine derivatives such as caffeine, theophylline, pentoxifylline, KMUP-1, etc. show anti-inflammatory effect (Dai et al., 2015). Anti-inflammatory responses of these derivatives are the result of their non-selective phosphodiesterase inhibition and/or their non-selective adenosine receptor antagonist properties. PDE inhibition and/or adenosine antagonist role of xanthine derivatives leads to increase in cAMP concentration, activation of protein kinase A, inhibition of tumor necrosis factor (TNF-α) and leukotriene synthesis. With inhibition of leukotrienes synthesis, inflammation reduces. Leukotrienes enhance inflammation by increasing leukocyte infiltration, phagocyte microbial ingestion, and generation of pro-inflammatory cytokines (including IL-5, TNFα, and macrophage inflammatory protein-1β). Xanthine derivatives such as caffeine, theophylline, etc are reported for their effective role in reduction of leukotrienes synthesis (Lee et al., 2014).

Antimicrobial activity of xanthine derivatives

In drug development process, antimicrobial effect of drugs becomes important to effectively combat microbial resistance. The compounds with antimicrobial activity could be effective to deal such situations. Xanthine derivatives such as caffeine, theophylline, aminophylline, and pentoxifylline are reported for their antimicrobial effects such as bactericide, fungicide and nematocide (Allwood et al., 2007; Hosseinzadeh et al., 2006). Caffeine is reported for enhancing the inhibitory effect of existing antibacterial agents such as penicillin and tetracycline against *Staphylococcus aureus* (Hosseinzadeh et al., 2006).

Besides that, antimicrobial properties of caffeine have been reported against human pathogens like *Klebsiella pneumonia*, and *Pseudomonas aeruginosa* (Sledz et al., 2015).

Anti-oxidant activity of xanthine derivatives

There are various reports which say pathological changes may occur due to excessive accumulation of oxygen and nitrogen reaction product in body fluids including free radicals such as reactive oxygen species (ROS) and nitric oxide (NO). These changes may cause premature aging and numerous diseases. ROS act as mediator in various cellular signaling pathways. The hyperproduction of ROS is limited by the both enzymatic mechanisms and natural antioxidants such as uric acid, glutathione, vitamin C and E. In lack of appropriate regulation the level of ROS increases and leads to oxidative and nitrosative stress. Xanthine derivatives such as caffeine, theophylline, theobromine, etc., have been reported for their antioxidant activities (Aleksandrova Katherine et al., 2014; Vignoli et al., 2011; Yashin et al., 2013).

Antitumor activity of xanthine derivatives

Several xanthine derivatives are reported for their inhibitory affinity of cell transformation. In lower eukaryotes and bacteria, these compounds induce gene mutations. They act as an antagonist of adenosine receptor and exert antiangiogenic properties in many types of tumors including ovarian cancer cells, prostate cancer (Barcz et al., 2000; Slattery and West, 1993). Xanthine derivatives such as caffeine, theophylline, pentoxifylline, theobromine, etc, are reported for inhibition of adriamycin and doxorubicin efflux from tumor cells. This inhibition leads to increase in concentration of doxorubicin in tumor. Thus,

anti-tumor activity of doxorubicin enhances (Kakuyama and Sadzuka, 2001; Sadzuka et al., 1995).

1.6.5. Mechanism of action of xanthine derivatives in mammals

Histone deacetylase activation

Histone deacetylase (HDAC) is an important enzyme that regulates the chromatin structure and thus, affects inflammatory gene expression (Cosio et al., 2004). Acetylation and deacetylation of histone is important phenomenon for transcriptional activation and repression, respectively of inflammatory gene expression. HDAC acts as repressor for activation of inflammatory genes. The activation of histone deacetylase depends on the level of glucocorticoids which is received by glucocorticoid receptor (GR). In cigarette smokers, due to oxidative stress, the glucocorticoids level reduces which leads to reduction in HDAC activity. Thus, in absence of HDAC activity, expression of inflammatory gene increases. Theophylline and other xanthine derivatives act as stimulator of HDAC activation (Cosio et al., 2004; Ito et al., 2002).

Xanthine derivatives as antagonist of Adenosine receptor

Adenosine is an endogenous nucleoside, an essential component for life dispersed in various mammalian tissues. It acts as a physiological regulator in variety of cellular signaling pathways and synaptic processes. It involves in multitudinous physiological functions including synthesis of nucleic acids, reduces tissue injury and promotes repair, controls the level of neurotransmitters in the central nervous system (CNS), etc (Sachdeva and Gupta, 2013). Multiple actions carried out by adenosine depend on the activation of adenosine

receptors. In mammals, four types of adenosine receptors such as A_1, A_3, A_{2A} and A_{2B} are reported. Adenosine and its agonist regulate the activity of adenylate cyclase by activation of all four adenosine receptor in which activation of A_1 and A_3 lead to G_i mediated inhibition of adenylate cyclase while activation of A_{2A} and A_{2B} lead to G_s mediated activation of adenylate cyclase. The activation of adenylate cyclase further leads to increase the concentration of cAMP, a second messenger play vital role in various cellular functions. In pathophysiological condition, the activation of A_1 and A_3 receptors are detrimental for normal cellular functioning and can cause various diseases. The role of antagonist of adenosine becomes essential to regulate the catalytic action of A_1 and A_3. Generally normal functioning of A_{2A} and A_{2B} receptor are important for various cellular functioning via activation of adenylate cyclase. But over expression of these receptor causes various dysfunctions such as vasodilation, mast cell degranulation, chloride secretion in epithelial cells, smooth muscle contraction, increase cytokines, increase of glucose production, etc (Hayallah et al., 2002). Hence, to treat such situation, antagonist of A_{2A} and A_{2B} receptors is required. Due to structural similarity with adenosine, xanthine derivatives act as both agonist and antagonist of adenosine receptors (Franchetti et al., 1994; Hayallah et al., 2002). **Figure 1.14** illustrates the mechanism of action of xanthine derivatives in cell signaling by antagonizing activity on adenosine receptors. Both natural and synthetic xanthine derivatives are reported for their adenosine antagonist properties (Jacobson and Gao, 2006). Among natural xanthine derivatives caffeine has shown profound biological effect as adenosine receptor antagonist (Franco et al., 2013; Jacobson and Gao, 2006).

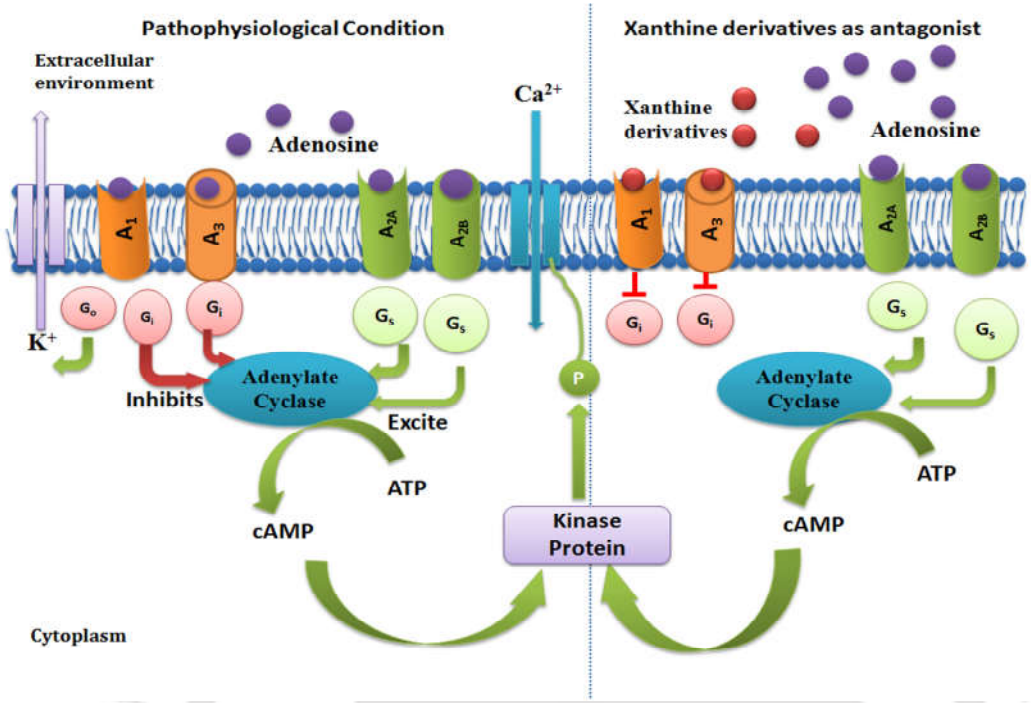

Figure 1.14 Activation of adenosine receptors in normal physiological condition and role xanthine as antagonist of adenosine receptor in pathophysiological condition

Xanthine derivatives as inhibitor of Phosphodiesterase catalytic activity

Xanthine derivative are known for their phosphodiesterase inhibition. Most of the natural derivatives are non-specific inhibitor for PDEs (Tanaka et al., 1991; Wong and Ooi, 1985). **Figure 1.15** depicts the role of xanthine derivatives targeting PDEs. Most of the natural derivatives are non-specific inhibitor for PDEs (Boswell-Smith et al., 2006; Huai et al., 2004; Rabe et al., 1995).

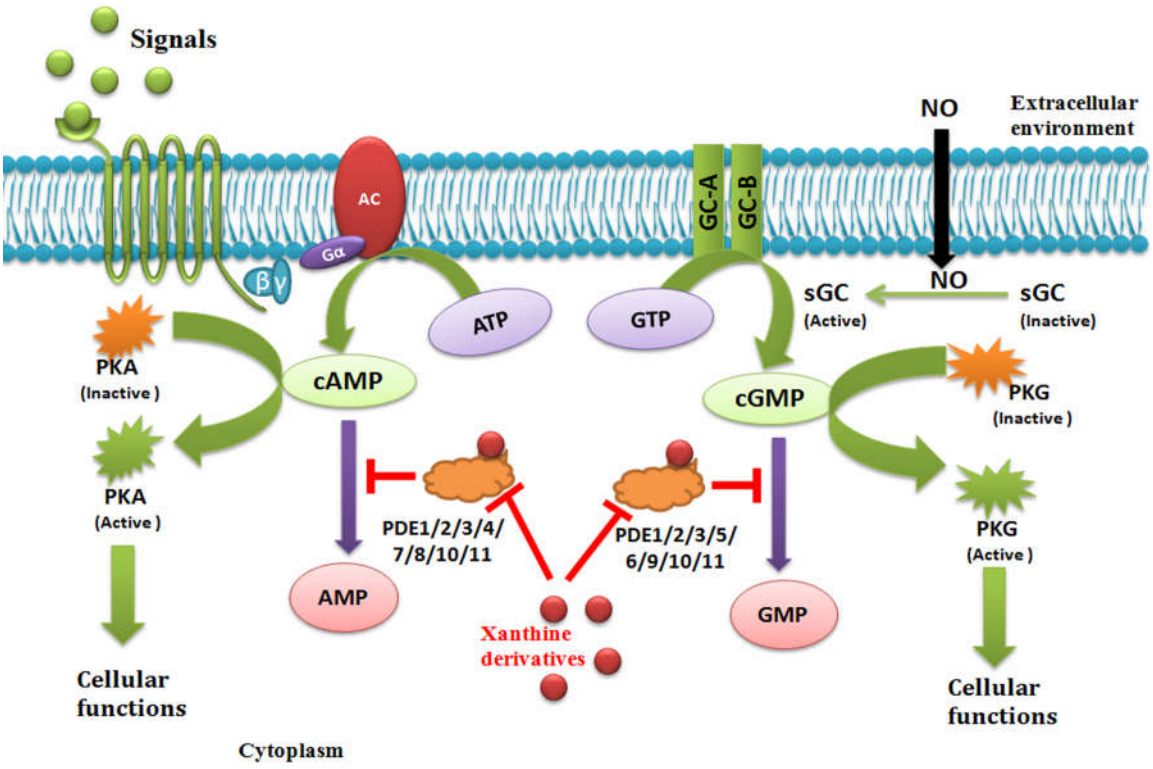

Figure 1.15 Action of xanthine derivatives as inhibitor for regulating the catalytic action of PDEs in cell signaling pathway

1.7. Potential of xanthine derivatives to regulate the PDE9A regulated signal transduction pathway

Xanthine derivatives are widely known for their inhibiting properties of PDEs in general. Very few research has been carried out with xanthine based compounds for inhibiting PDE9A (Huai et al., 2004). However, as xanthine provides maximum ground for substitution, it can act as better drug scaffold for bringing diversity in drug designing and development based on the active site requirement of PDE9A. These inhibitors can be used to control the pathophysiological conditions that may arise either due to dysfunction of

receptors that receive signals or due to lowering the level of signals. In such conditions further processing of signals may get hampered due to further lowering the level of cGMP by normal functioning of PDE9A. All these in turn may affect the normal functioning of pathway (Andreeva et al., 2001; Singh and Patra, 2014). Here xanthine derivatives as inhibitor play imperative role in regulating the catalytic action of PDE9A (Singh and Patra, 2014). **Figure 1.16** depicts the role of xanthine as regulator of catalytic action of PDE9A in pathophysiological condition.

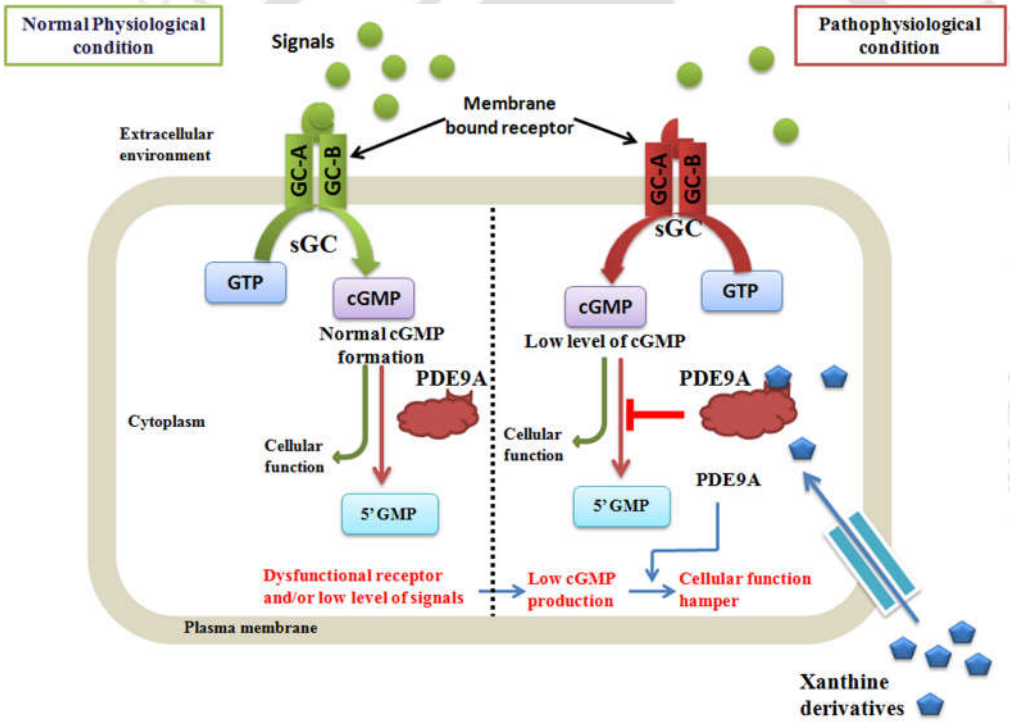

Figure 1.16 Action of PDE9A in normal and pathophysiological conditions. Role of xanthine derivatives as inhibitor to control the catalytic action of PDE9A in pathophysiological condition

1.8. Scope of xanthine derivatives as potential scaffold for PDE9A inhibitor

With the availability of three –NH groups at N_1, N_3 and N_7 positions and one –CH group at C_8 position, xanthine provides maximum possibility for derivatisation. Despite enormous ground available for substitution/modification still use of xanthine is limited in the drug development process. Till date, no research has been carried out using xanthine as starting material for synthesis of xanthine derivatives. This is mainly because of the lack of proper understanding of the structural nature of xanthine. According to reports available till date on xanthine, N_3 position has been considered as most reactive in xanthine because of highest acidity of –NH group at N_3 position and substitution follows the –NH group of N_3>N_7¬>N_1 positions (Gulevskaya and Pozharskii, 1991). This analysis was contradictory to the transmethylation process of xanthine in living organism. The transmethylation of xanthine occurs in sequence of xanthine→7-methylxanthine→ 3,7-dimethylxanthine (theobromine) →1,3,7-trimethyl xanthine (caffeine). The lack of understanding of the reactivity of different substitution sites of xanthine could be the most probable reason for not using xanthine as reaction initiator. Due to this, worldwide researchers have relied heavily on various unfavorable synthesis methods such as ring closure mechanism, classical condensation method for synthesis. Heavy reliance on these mechanisms does not satisfy the basic principle of drug development i.e. accessibility, availability and affordability. Therefore, lack of proper understanding of xanthine is the biggest reason for absence of standard synthesis procedure for xanthine derivatives. The present thesis has made an effort to fill this lacuna.

1.9. Research Approach for the present study

Xanthine explores tremendous potential to act as potential scaffold for future drug development. In PDE9A drug development, xanthine based inhibitors can be a new drug candidates. This will bring out structural diversification in drug development process. With understanding the huge potential of xanthine as scaffold the present study used two approaches for development of potent drug candidates for PDE9A. First approach was screening of existing xanthine derivatives targeting PDE9A using virtual screening, molecular docking, molecular dynamics, and pharmaceutical properties analysis. Second approach was designing of novel xanthine derivatives using manual designing, molecular docking, pharmaceutical properties analysis and chemical synthesis. By using these two approaches we landed with some potent PDE9A selective xanthine derivatives. The potency of selected compounds obtained from *in silico* studies were further confirmed by *in vitro* biological studies such as inhibition studies and stability studies. Thus, by this study we came to known the active site requirement of PDE9A by thorough analysis of PDE9A active site and found the importance of some unique amino acid residue in deciding the substrate/inhibitor selectivity. It helped in modification of xanthine derivatives according to the active site requirement of the protein. This study also uses xanthine as starting material for synthesis of xanthine derivatives which can bring diversification in derivatisation of xanthine. The present study has attempted to explore the immense potential of xanthine not only as 'scaffold' for future drug development with maximum sites available for substitution but also as 'reaction initiator' for synthesis of these derivative by safe, time saving, high

yield and cost effective manner. **Figure 1.16** depicts the research approach followed in the present study.

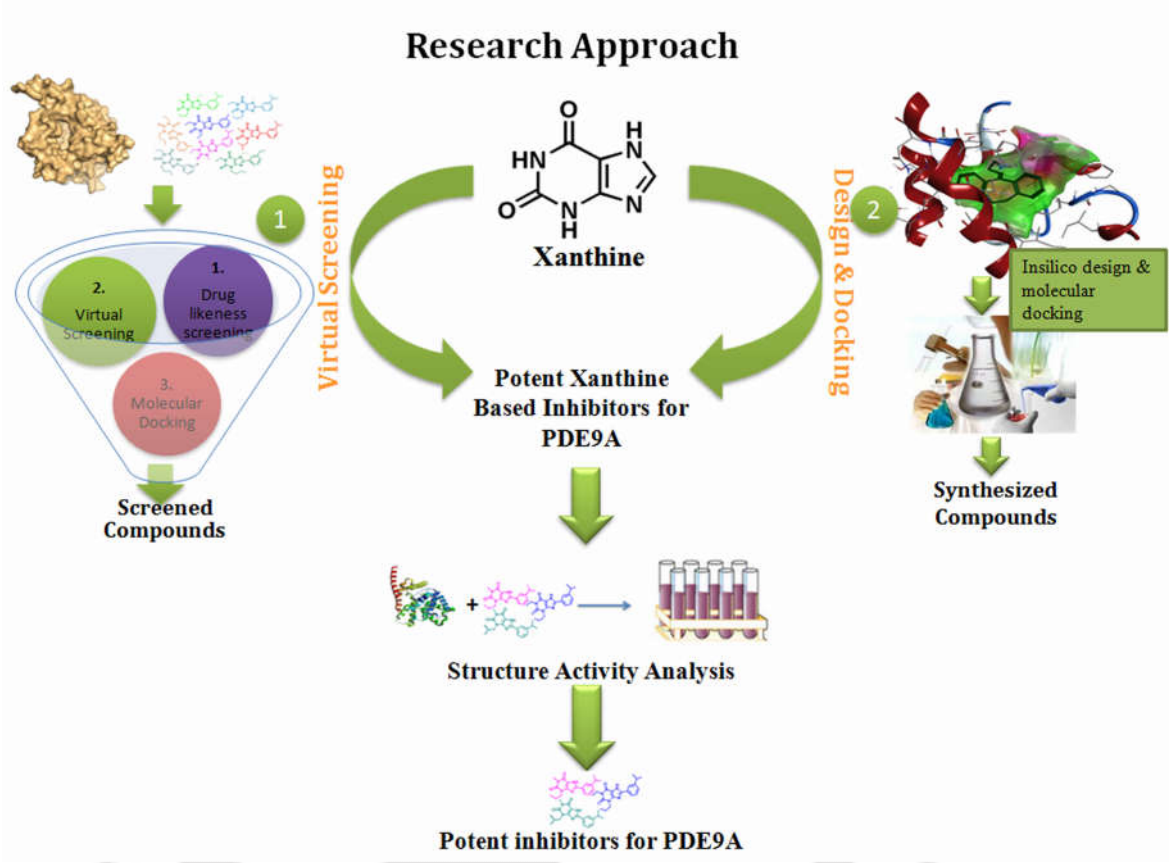

Figure 1.17 Research approach used for the present study

1.10. Conclusion

The second messenger - cAMP and cGMP are substrates for a large superfamily of phosphodiesterases which regulate cell signaling pathway in mammalian cells. PDE9A has the highest affinity for cGMP among all PDEs. Absence of marketed drug makes PDE9A an attractive target in arena of drug development. In pathophysiological conditions, most of the cellular functions associated with cGMP signaling are hampered by the consistent lowering

of cGMP levels by normal functioning of PDE9A. Hence, inhibition of PDE9A is needed to maintain the consistency of cGMP-dependent cell signaling pathway. Various inhibitors developed so far have been failed in generating specificity towards PDE9A. Most of the PDE9A inhibitors are constructed over the common "pyrazolopyrimidinone" scaffold. The same scaffold has been used for inhibitor designing for other PDEs that might be reason for showing non-specificity most time. Introduction of other scaffolds in PDE9A drug development process is need of the hour. It would bring structural diversification in drug development process. Present study is one step towards the realization of structural diversification. The present chapter covers the overview of signal transduction process in general and details of the structure, function, mode of action, tissue distribution, genetics, therapeutic role, and current status of drugs developed for PDE9A in particular. This chapter further explores the huge potential of 'xanthine' in drug development process both as 'reaction initiator' for synthesis of xanthine derivatives in general and as 'scaffold' for generating numbers of PDE9A inhibitors in particular. Thus, the present study has attempted to open a new page in the xanthine based research.

CHAPTER 2

Identification of Potent Xanthine Based Inhibitors Targeting Phosphodiesterase 9A

Prologue

Cellular communication via signal transduction is imperative for normal physiological functioning of an organism. cGMP plays prominent role as a mediator in signal transduction pathway. Lowering the level of cGMP by the function of PDE9A leads to various pathophysiological conditions. Therefore, to administer this situation effectively, signal transduction pathway needs regulators in the form of inhibitors to regulate the level of PDE9A. Bottlenecks in the development of specific inhibitors targeting PDE9A are due to its structure resemblance with other PDEs. Therefore, very few specific inhibitors have been developed for PDE9A till date and most have been reported with moderate specificity. Thus, development of potent inhibitors is a need. Interestingly, compounds of xanthine derivatives have been reported to have wide implications on the inhibition of PDEs, but they are non specific in nature though their drug-like properties are significant due to presence of xanthine as a scaffold. Making these non specific inhibitors to potent specific inhibitors targeting PDE9A is what the present chapter aims at. In this direction, this chapter focuses on the computational studies for screening of xanthine derivatives from ZINC database targeting PDE9A. Thus, existing xanthine derivatives can be further explored as promising candidates by combinatorial approach of both in silico and in vitro studies.

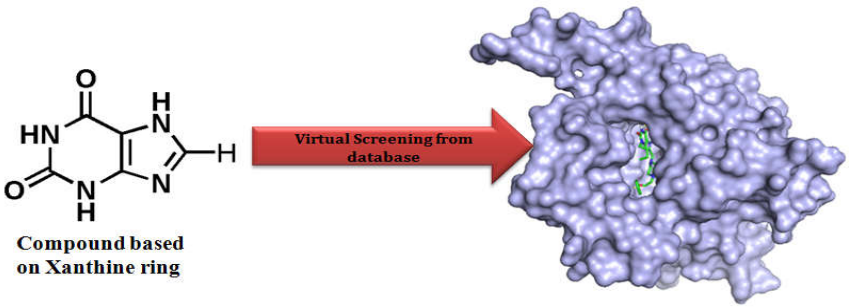

2.1. Introduction

In the last few decades, ample research has been carried out on phosphodiesterase 9A. Inhibition has always been a key area of consideration. Though the structure and mechanism of action of the enzyme has been divulged by researchers but its structural uniqueness in terms of substrate selectivity, is yet to be explored (Huai et al., 2004; Liu et al., 2008). The presence of some unique amino acid residues such as GLU406 and TYR424; playing a pivotal role in inhibitor selectivity is yet to be exploited (Hou et al., 2011; Huai et al., 2004). Several inhibitors have been reported for PDE9A. The well studied inhibitors for PDE9A are BAY 73-6691 and PF-04447943 (Hutson et al., 2011; Nicholas et al., 2011; Vardigan et al., 2011; Verhoest et al., 2012; Wunder et al., 2009). Their moderate inhibition potential and substrate acceptance by other members of PDE superfamily has made selective inhibition a daunting task. This is a prominent reason for not having a single specific marketed drug against PDE9A. Earlier studies on drug development targeting phosphodiesterases have brought out xanthine derivatives as nonspecific inhibitors of PDEs (Glennon et al., 1981; Maurice et al., 2014; Tanaka et al., 1991; Wong and Ooi, 1985). One of the well known xanthine derivative IBMX has been co-crystalised with PDE9A and submitted to the protein data bank (Huai et al., 2004). The co-crystallized structure can be used for docking studies. The structural resemblance of the substrate cGMP with xanthine molecule makes the xanthine based derivatives a prompting molecule as inhibitor candidates for PDE9A. There are large numbers of xanthine derivatives available in databases. Therefore, this chapter focuses on screening of selective inhibitors for PDE9A using *v*irtual screening.

Virtual screening is an emerging high throughput screening procedure to screen most suitable candidates intending their introduction into further drug development stages. These methods save time and direct the arduous and expensive test to focus on

top suitable compounds that come from screening. The compound chosen for the present work has been xanthine derivatives. There are a huge number of synthesized xanthine derivative that have been submitted to ZINC database. Thus, present research work screens potent and selective inhibitors for PDE9A using xanthine as a scaffold from ZINC database through virtual screening and docking. This chapter integrates virtual screening, molecular docking, molecular dynamics and ADMET drug-likeness studies for selection of potent inhibitors of PDE9A. The potency of screened compounds was intended to further validate by *in vitro* biological test. The selection of potent compounds from database gives incentives for further drug development based on the obtained potent inhibitors.

2.2. Materials and Methods

In silico approach is the best way to screen drug-like candidate from the huge dataset. In this study, xanthine based compounds were screened from ZINC database for PDE9A inhibition. **Figure 2.1** illustrates the methodology used for screening best compounds from existing ones.

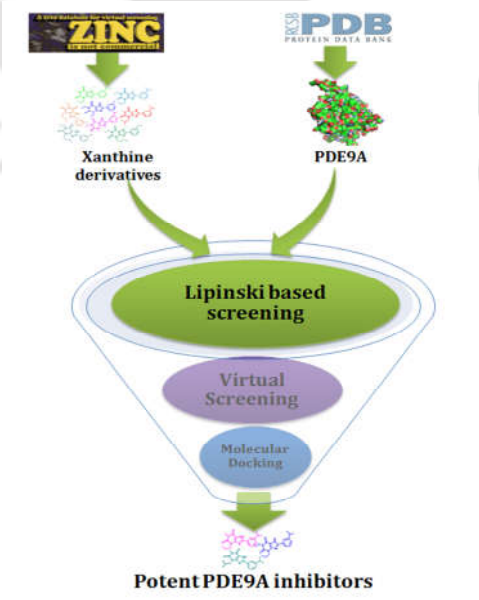

Figure 2.1 Methodology used for the selection of potent inhibitors for PDE9A

2.2.1. Structural analysis of active site of PDE9A for *in silico* studies

The structure of PDE9A catalytic domain (2HD1) was extracted from protein data bank (PDB) and its active site composition was analyzed. The structure based pharmacophore analysis was performed using PyMol and Discovery Studio Visualizer to understand the amino acid residues within 5 Å regions of substrate (cGMP) in cGMP-PDE9A complex. 5 Å regions around substrate were selected as this range covered all active site residues. This study was carried out by superimposition of all PDEs over PDE9A to understand the role of corresponding amino acid residues in the active site pocket of various members of PDE superfamily (Singh and Patra, 2014).

2.2.2. Initial screening of xanthine based derivatives from ZINC database using Lipinski rule of five

Xanthine derivatives belong to a class of nitrogen based alkaloids. Derivatives such as Caffeine, Theophylline, IBMX etc. are known for their non-selective inhibition of PDEs (Hatzelmann et al., 1995). The structural resemblance of xanthine with substrate cGMP makes xanthine ring a suitable target for PDEs. Hence, in this study "xanthine ring" was taken as scaffold to search specific inhibitors for PDE9A from non commercial ZINC database [http://zinc.docking.org/]. A total of 2055 xanthine derivatives available in the ZINC database were extracted for initial pharmacophore screening. The files for virtual screening were generated with the help of raccoon, a graphical interface for processing ligand libraries in different formats (PDB, multi-structure MOL2 and PDBQT), multiple receptor conformations (e.g. relaxed complex experiments) and flexible residues. These molecules were then prepared in Raccoon using Lipinski filter. The shortlisted compounds were subjected to virtual screening. **Figure 2.2** illustrates the structure of xanthine ring.

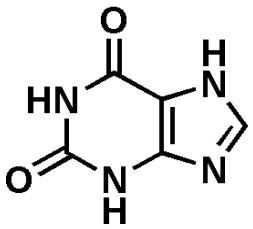

Figure 2.2 Structure of 'Xanthine ring'

2.2.3. Macromolecule files preparation for virtual screening and other *in silico* studies

Upon consideration of entireness and resolution of structures available in RCSB protein data bank, three dimensional crystal structures of coding domain of PDE1B, PDE2A, PDE3B, PDE4D, PDE5A, PDE7A, PDE8A, PDE9A and PDE10A were extracted from the data bank (http://www.rcsb.org; PDB ID are 1TAZ, 1Z1L, 1SOJ, 1ZKN, 1RKP, 3DBA, 3G3N, 3ECM, 2HD1, 4DFF respectively). The water molecules were initially removed and hydrogen molecules were added. The protein 'pdb' files were prepared in Swiss-pdb Viewer which helped in analyzing the protein thoroughly and preparing the macromolecule file for virtual screening and docking by removing hetero atom including ligands and water molecules. For virtual screening, protein pdbqt file was prepared in raccoon. For docking, protein pdbqt file was prepared in AutoDock Tool (ADT) by removing polar hydrogen followed by addition of non-polar hydrogen, computation of Gasteiger charges and merging of non-polar hydrogen.

2.2.4. Virtual Screening for selection of specific inhibitors for PDE9A

Virtual screening of shortlisted 1480 compounds was carried in Autodock 4.2. The preparation of grid file was required to understand the shape and property of the receptor under different sets of fields. Grid files were generated by covering all residues under 5Å region in the active site of protein. The residues in 5Å region of active sites have been analyzed by extracting ligand-protein complex file from protein data bank.

The parameter used for generation of grid file in ADT was in x, y and z direction with resolution of 0.253Å. The docking files were 90×90×90 points generated in ADT. The parameters for docking file generation was 20 GA run, 150 population sizes, 27000 maximum numbers of generation and 25000000 maximum numbers of evaluations. Finally, separate folder for each compound having macromolecule (pdbqt) files, ligand (pdbqt) files, grid (gpf) files and docking (dpf) files were generated. The virtual screening was carried out in CentOS Linux system with the help of scripts for generating grid .glg file and docking .dlg file.

2.2.5. Molecular docking of screened compounds obtained from virtual screening

Molecular docking was used to check the interaction pattern and further computational validation of compounds shortlisted with lowest free energy of binding. Out of 1480 compounds, the 10 top hits were selected for molecular docking. The parameters used were 100 GA run, 300 population size, 27000 maximum numbers of generation and 25000000 maximum numbers of evaluations. Docking was carried out in Autodock 4.2 and ADT. Molecular docking of all ten compounds was carried out in CentOS Linux system. The interaction patterns were studied in PyMol software and Discovery Studio 3.1.

2.2.6. Comparative studies of top four screened compounds with other PDEs

PDE9A has certain unique features in its structure which makes this enzyme more specific towards cGMP. But it also has certain structural similarity with some of the other members of the PDE super family which is a major bottleneck in the path of

drug discovery targeting PDE9A specific inhibitor. The comparative docking studies of selected compounds with other members of PDE superfamily were important to determine the potency and selectivity of screened inhibitors towards PDE9A. These comparative studies were performed by molecular docking in Autodock 4.2. with the same parameters as mentioned in the above section.

2.2.7. Molecular Dynamic Simulation of the best compound obtained from screening against ZINC database

After performing docking based virtual screening, MD simulation was carried out to equilibrate the protein structure and to understand the stability and compactness of the protein-ligand complex. Selected compounds obtained from docking and comparative studies were used as initial structures for MD simulation. MD simulation was carried out using GROMACS 4.5 software (Pronk et al., 2013) and GROMOS 53a6 force-field (Oostenbrink et al., 2004). Automated Topology Builder (ATB) server was used to generate topology and force field parameters of the ligand (Malde et al., 2011). The protein-ligand complex was solvated with simple point charge (SPC) water molecules in a 0.9 nm cubic box and chlorine ions were used to neutralize the whole system. Energy minimization of protein-ligand complex was carried out using the steepest descent algorithm until it converged with a force tolerance of 100 kJ mol^{-1} nm^{-1}. After minimization, the protein-ligand complex was equilibrated at 300K through a stepwise heating protocol in the NVT ensemble using 2.0 fs integration time and 500 ps. Equilibration step followed 500 ps in the NPT ensemble with 1 bar pressure by restraining the position of protein and ligand molecule. Finally, MD simulation of protein-ligand complex was performed for a timescale of 6 ns under periodic boundary conditions. Velocity-rescale thermostat (Bussi et al., 2006) and Parrinello−Rahman

barostat (Parrinello, 1981) were used to control the temperature and pressure with a temperature and pressure coupling time constant of 1.0 ps. Particle-mesh Ewald method was used to calculate non-bonded interactions with a cut-off of 0.9 nm (Essmann et al., 1995). During simulation all bonds with hydrogen atom was constrained by using the LINCS algorithm (Hess et al., 1997).

2.2.8. Drug likeness and ADMET properties of screened inhibitors

Drug likeness is a required property for any inhibitor on certain decided parameters to qualify for being taken up as future drug. The best compound obtained from *in silico* studies was subjected to study drug-likeness properties. These properties includes rule of 5, leadlike rule, CMC like rule, MDDR like rule, WDI (World Drug Index) and blood brain barrier (BBB) permeability. PreADMET software was used to calculate the drug likeness, ADMET (adsorption, distribution, metabolism, excretion and transport) and toxicity properties of the selected compound [preadmet.bmdrc.kr].

2.3. Results and Discussion

Multi fold screening method has been applied for determining potent selective inhibitors of PDE9A. The workflow has been shown in **figure 2.3.** *In silico* studies such as initial Lipinski based screening, virtual screening, molecular docking and molecular dynamics gave a selective compound. The resultant compound was selected to continue for enzyme inhibition study in drug development process.

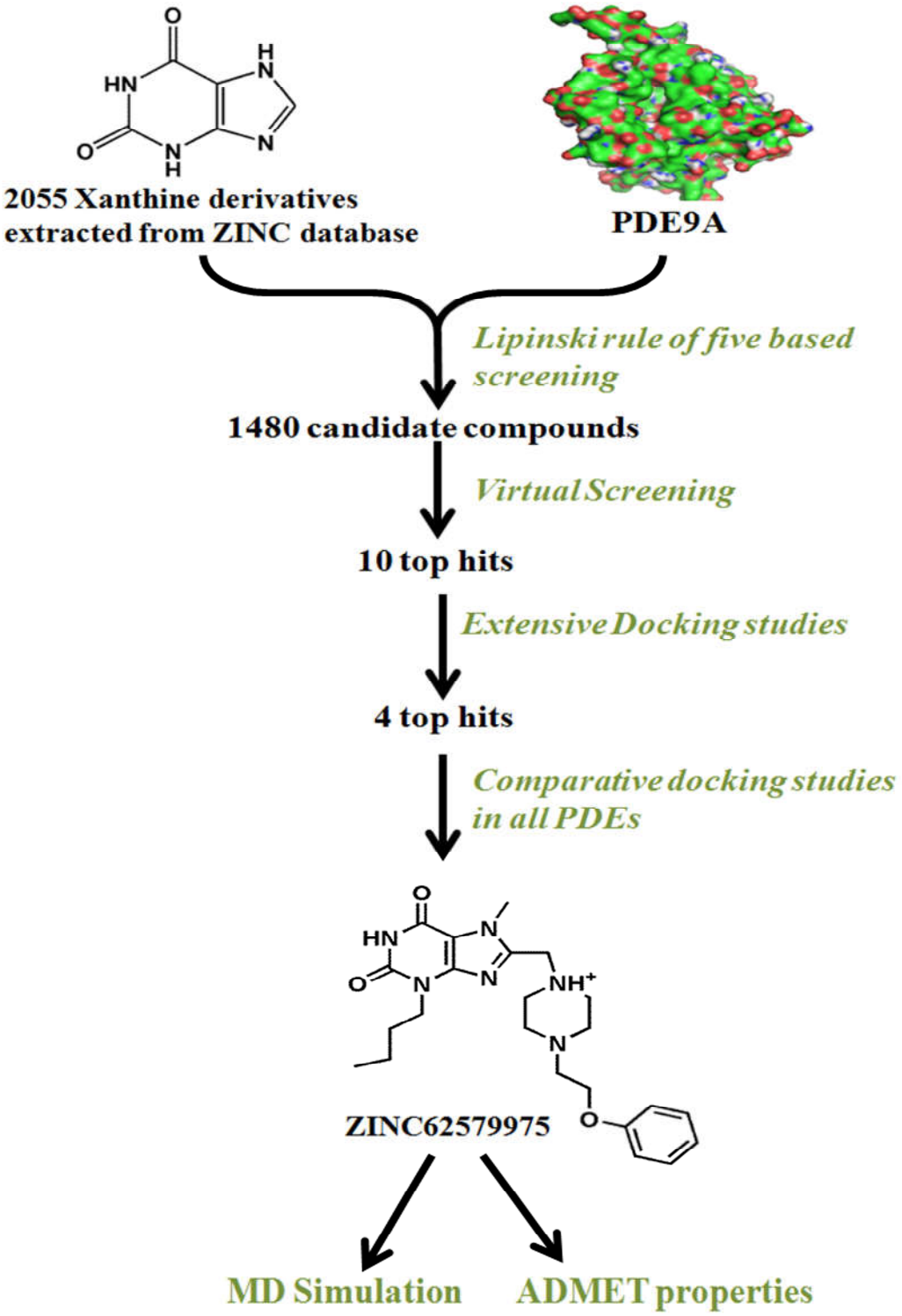

Figure 2.3 Work flow for screening of xanthine derivatives from ZINC database

2.3.1. Structure analysis of Phosphodiesterase 9A

The three dimensional crystal structure of PDE9A was extracted from PDB and analyzed. The active site pocket in the 5 Å regions around the ligand bound protein was

considered for study. IBMX-bound PDB file (2HD1) was used as a reference complex. The residues present within the 5Å region of IBMX in PDE9A were F251, H252, H256, H292, D293, H296, T363, M365, D402, I403, N405, E406, V417, L420, Y424, A252, Q453 and F456. Some of the residues which contributed to unique functional properties of PDE9A were F251, E406 and Y424 (Hou et al., 2011; Singh and Patra, 2014). However, PDE9A bears structural similarity with other PDEs as well. This has been a bottleneck in achieving specific inhibitor targeting PDE9A. Comparative structural analysis of the 5Å region of all PDE superfamily members gave structural insight to understand the active site pocket of PDE9A and its role in development of a specific inhibitor (Singh and Patra, 2014). A common conserved residue present in all PDEs was "glutamine" which corresponded to GLN453 in PDE9A. It has been reported that GLN453 plays an imperative role in substrate selectivity of PDE9A (Huai et al., 2004; Wang et al., 2010). GLU406 was another unique residue in the active site of PDE9A because of its involvement in formation of intermolecular hydrogen bond with GLN453 side chain (Hou et al., 2011). In PDE9A the presence of GLU406 fixes the orientation of GLN453 (Singh and Patra, 2014). This uniqueness might have significance on substrate or inhibitor selectivity of PDE9A (Hou et al., 2011). The structural analysis of PDE9A was important to understand and analyze protein-inhibitor interaction studies.

2.3.2. Pre-docking screening of extracted compounds from ZINC database

Xanthine is a nitrogenous purine base natural compound which has been well known for its biological implication especially on phosphodiesterase inhibition. The structure of xanthine contains three –NH group at N_1, N_3 and N_7 positions and one -CH group at C_8 position. These positions have been targeted for substitution of the xanthine scaffold (Allwood et al., 2007; Erickson et al., 1991; Sebastido and Ribeiro, 1989). The

modification at these positions might have some implications on the binding affinity of respective molecules towards PDE9A. Hence, in the present study, "xanthine ring" was used as a scaffold to extract compounds from the ZINC database. Virtual screening was used to identify suitable inhibitors for PDE9A from database for further studies. Among 2055 xanthine derivatives extracted from ZINC database, 1480 compounds were retrieved in first phase under pharmacophore screening based on "Lipinski rule of five". This pharmacophore screening was based on five factors such as H-bond donor, H-bond acceptor, molecular weight, number of atoms and rotatable bonds. This screening was important to extract compounds based on their drug-likeness properties.

2.3.3. Docking based virtual screening of xanthine derivatives

The pharmacophore screened 1480 compounds were subjected to virtual screening by molecular docking in Autodock 4.2. The virtual screening parameters were optimized by docking study of IBMX with PDE9A. For the purpose of virtual screening, the crystal structure (2HD1) of PDE9A bound with IBMX was extracted from protein data bank. IBMX was extracted from PDE9A and then redocked back to the structure. The optimized parameters obtained from this analysis were 20 conformations, resolution of 0.253Å and grid file of 90×90×90 points while other parameters were set at default values. In docking procedure, the average RMSD in IBMX-PDE9A docked complex for top 20 conformations was 2.11 Å. This showed a difference of 0.11 Å with the original x-ray pose. This suggested that the approach of using Autodock 4.2 for virtual screening of large number of compounds were suitable for the PDE9A system. Thus, identical parameters were used for further virtual screening and molecular docking studies. Based on the best interaction result in terms of lowest free energy of binding and number of conformation in largest cluster in PDE9A active site, 10 best hits were selected. **Figure**

2.4 illustrates the structure of the top 10 hits. These top ten hits showed different modifications at N_1, N_3, N_7 and C_8 positions. **Table 2.1** presents the virtual screening result of top ten hits in terms of lowest free energy of binding, number of conformation in largest cluster, and occurrence in number of clusters. These top 10 xanthine derivatives were further subjected for extensive docking studies with 100 GA run.

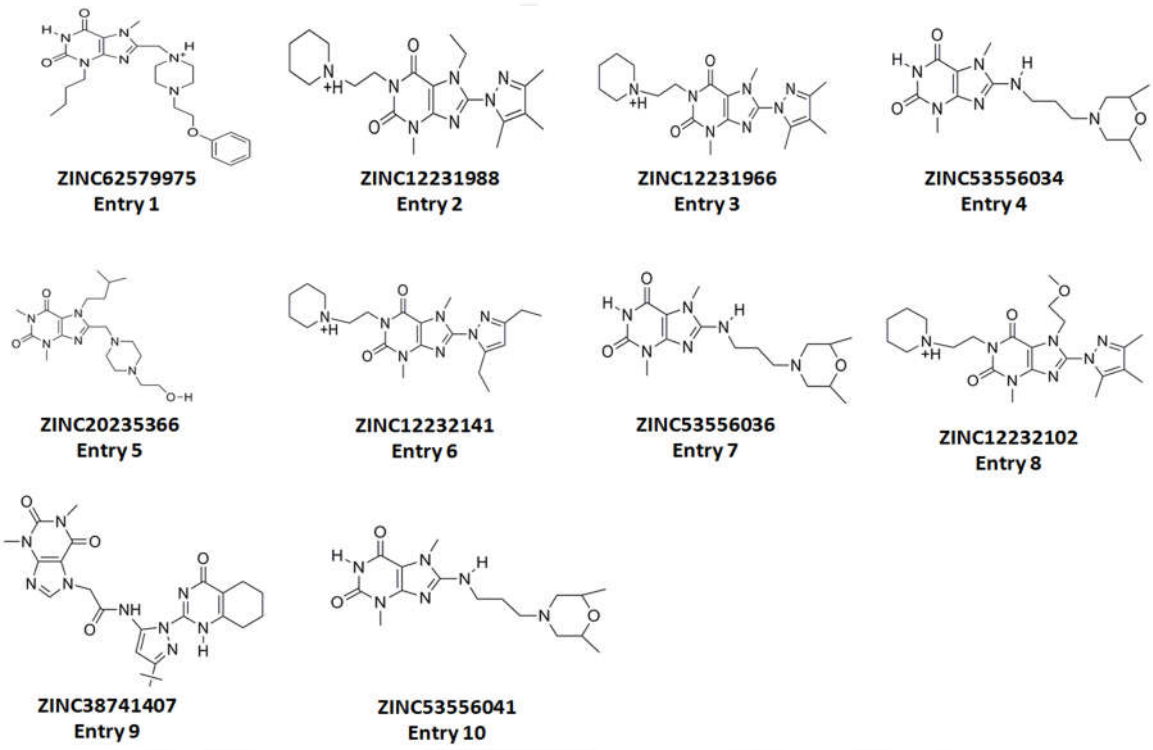

Figure 2.4 Structure of top 10 hits with their corresponding ZINC IDs obtained after docking based virtual screening

Table 2.1 Result of docking based virtual screening of top 10 hits

Entry	Zinc ID	Formula	LFBE (kcal/ mol)	NCLC	No of cluster
1	ZINC62579975	*3-butyl-7-methyl-8-[[4-(2-phenoxyethyl)piperazin-1-yl]methyl]purine-2,6-dione*	-12.72	14	4
2	ZINC12231988	*7-ethyl-3-methyl-1-[2-(1-piperidyl)ethyl]-8-(3,4,5-trimethylpyrazol-1-yl)purine-2,6-dione*	-12.32	19	2
3	ZINC12231966	*3,7-dimethyl-1-[2-(1-piperidyl) ethyl]-8-(3,4,5-trimethylpyrazol-1-yl)purine-2,6-dione*	-12.29	20	1
4	ZINC53556034	*8-[3-[(2S,6R)-2,6-dimethyl morpholin-4-yl]propylamino]-3,7-dimethyl-purine-2,6-dione*	-12.22	19	2
5	ZINC20235366	*8-[[4-(2-hydroxyethyl)piperazin-1-yl]methyl]-7-isopentyl-1,3-dimethyl-purine-2,6-dione*	-12.18	20	1
6	ZINC12232141	*8-(3,5-diethylpyrazol-1-yl)-3,7-dimethyl-1-[2-(1-piperidyl) ethyl]purine-2,6-dione*	-12.11	20	1
7	ZINC53556036	*8-[3-[(2S,6S)-2,6-dimethyl morpholin-4-yl]propylamino]-3,7-dimethyl-purine-2,6-dione*	-12.06	14	3
8	ZINC12232102	*7-(2-methoxyethyl)-3-methyl-1-[2-(1-piperidyl)ethyl]-8-(3,4,5-trimethylpyrazol-1-yl)purine-2,6-dione*	-12.01	16	3
9	ZINC38741407	*N-[5-tert-butyl-2-(4-oxo-5,6,7,8-tetrahydro-3H-quinazolin-2-yl)pyrazol-3-yl]-2-(1,3-dimethyl-2,6-dio*	-11.97	20	1
10	ZINC53556041	*8-[3-[(2R,6R)-2,6-dimethylmorpholin-4-yl]propylamino]-3,7-dimethyl-purine-2,6-dione*	-11.9	20	1

NCLC= Number of conformations in largest cluster, LFEB= Lowest free energy of binding, H-bond=Hydrogen bond

2.3.4. Docking studies of top 10 hits with PDE9A

Initial virtual screening of 1480 compounds was carried out with 20 GA run. By this study 10 top hits were screened based on their lowest free energy of binding. These compounds were further subjected to stringent docking study with 100 GA run for further validation. This study showed the interaction pattern of the best conformation of the inhibitors in the active site pocket of PDE9A. From this study, top four compounds were selected based on their lowest free energy of binding. **Table 2.2** shows the docking result of top four compounds in terms of their lowest free energy of binding, inhibition constant and number of hydrogen bonds involved in binding. **Figure 2.5** illustrates the structures of top four hits. ZINC62579975 showed best binding result with lowest free energy of binding -12.59 kcal/mol with PDE9A by forming four hydrogen bonds in the active site. The residues involved in the H-bond interaction in the active site pocket of PDE9A were MET365, ASP402 and GLN453. ZINC62579975 formed two hydrogen bonds with GLN453. In the binding site pocket of PDE9A, GLN453 acts as invariant conserved catalytic residue which plays extremely important role in substrate/ligand selectivity. The other three hits - ZINC12231988, ZINC12231966 and ZINC12232141 were closely related in terms of structure and their interaction patterns. Presence of substituent at N_1 position of ZINC12231988, ZINC12231966 and ZINC12232141 leads to change in orientation of the compounds when they interact in the active site pocket of PDE9A. The change in orientation is with comparison to the interacting position of ZINC62579975 with PDE9A. This change may be attributed to the fact that ZINC62579975 has no N_1 substitution. N_1 substitution of the three above mentioned ZINC compounds forms one H-bond with ASP402. This change in orientation leads to placing of the C_8 substituent towards the invariant GLN453. However, no interaction was observed with GLN453 residue. On the other hand, in ZINC62579975-PDE9A

complex, the N_1 position is not substituted and thus, the –NH group at N_1 position along with carbonyl group at C_6 position established a strong H-bond interaction with invariant GLN453. Thus, the presence of unsubstituted –NH group in ZINC62579975 acted as a deciding factor for selectivity against PDE9A among all four hits. The difference in the orientation of ZINC62579975 in the active site was also the result of the presence of unsubstituted -NH group. In ZINC62579975, C_8 substituent placed towards the histidine rich site of the PDE9A formed two additional H-bonds- one with ASP402 and second with ILE403. ZINC62579975 with four H-bonds formed more contacts with PDE9A. The potency and selectivity of ZINC62579975 towards PDE9A was further validated by comparative docking studies with other PDEs. **Figure 2.6** illustrates the comparative interaction pattern of top 4 hits with PDE9A. The interaction pattern of ZINC62579975 in the active site pocket of PDE9A has been broadly illustrated by **figure 2.7**, **figure 2.8** and **figure 2.9**.

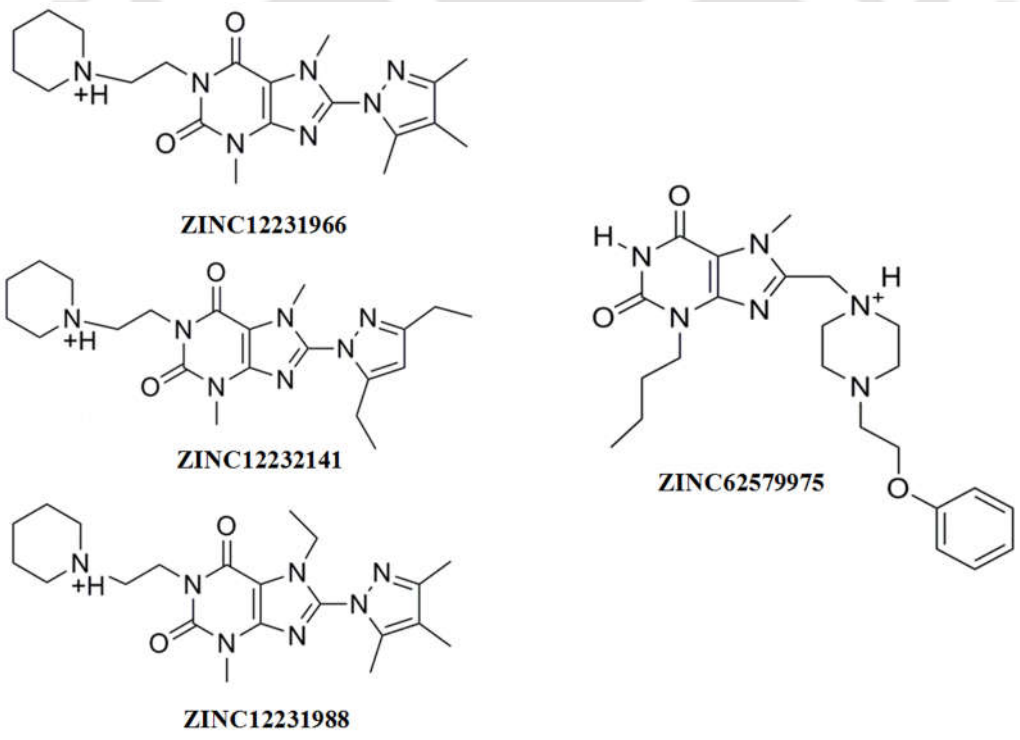

Figure 2.5 Structure of top four hits obtained after stringent docking studies with PDE9A

Table 2.2 Result of docking studies of the four screened compounds

Top hits	ZINC compounds	LFEB (kcal/mol)	NCLC	K_i (nm)	Residues	H bonds
1	ZINC62579975	-12.59	81	0.59	MET365, ASP402, GLN453	4
2	ZINC12231988	-12.55	100	0.65	ASP402	1
3	ZINC12231966	-12.52	100	0.66	ASP402, ILE403	1
4	ZINC12232141	-12.41	100	1.29	ASP402, ILE403	2

LFEB = Lowest free energy of binding, NCLC = Number of conformations in largest cluster, K_i = Inhibition constant

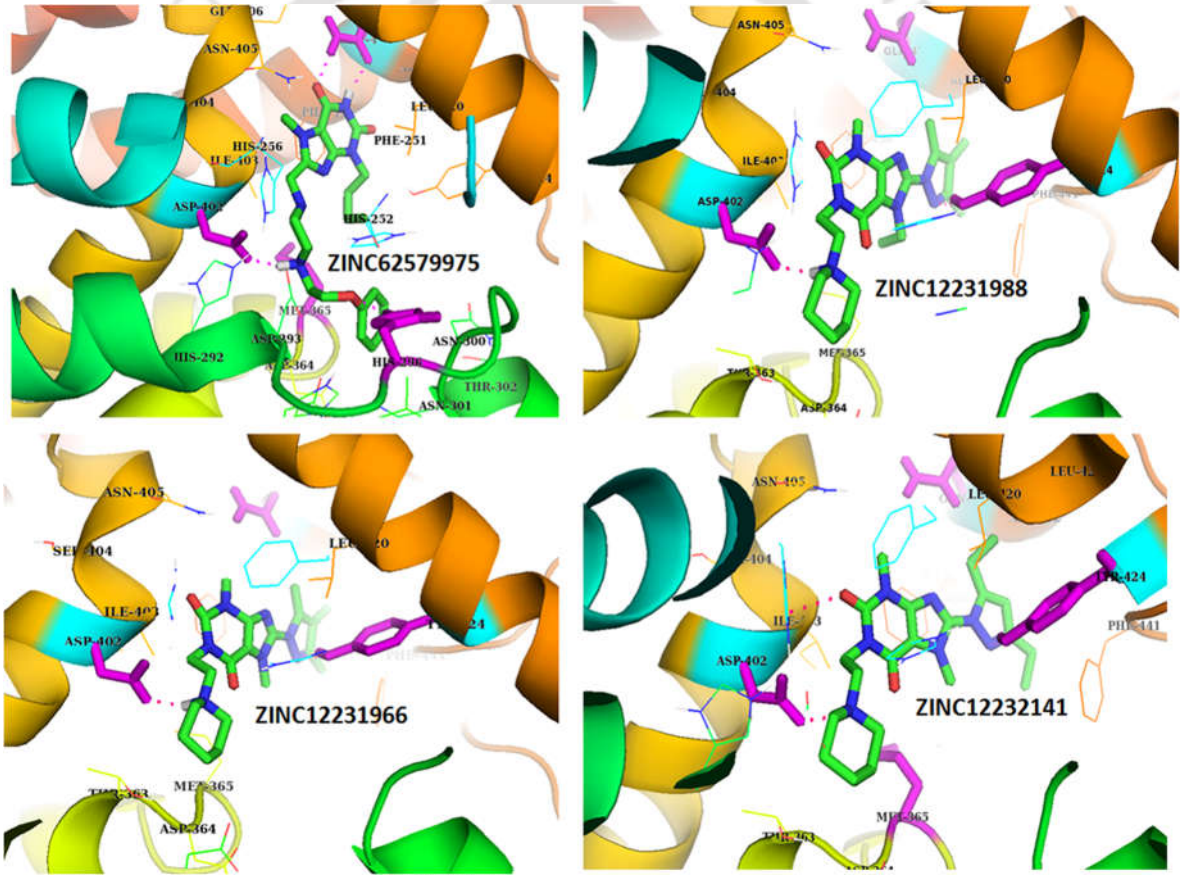

Figure 2.6 Interaction pattern of top four hits with PDE9A

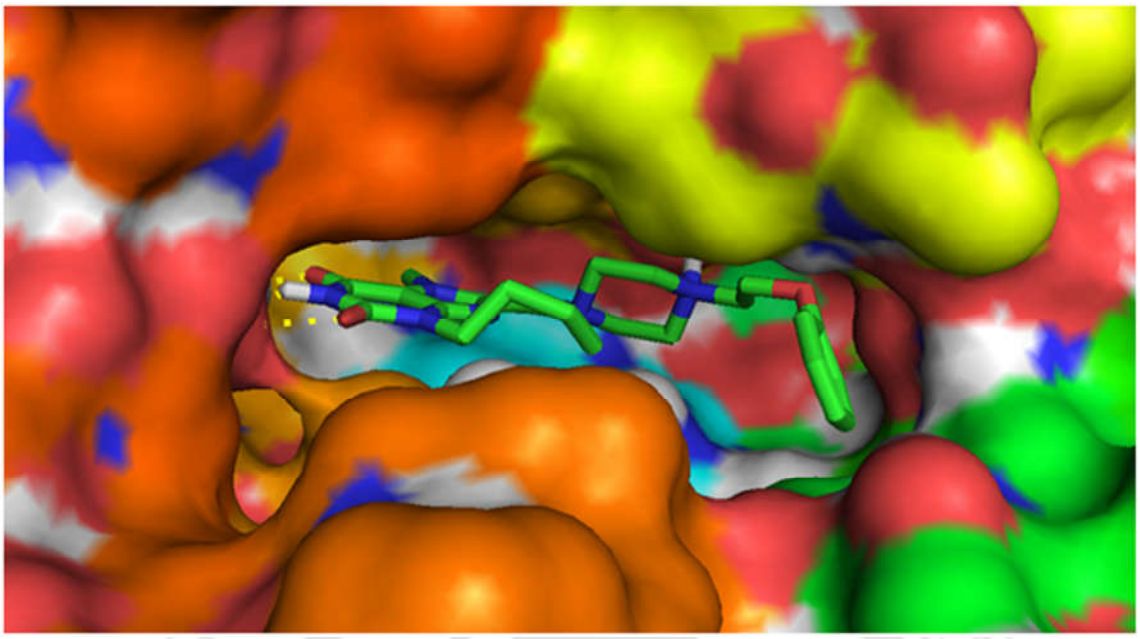

Figure 2.7 Depiction of surface view interaction of ZINC62579975 in the active site pocket of PDE9A

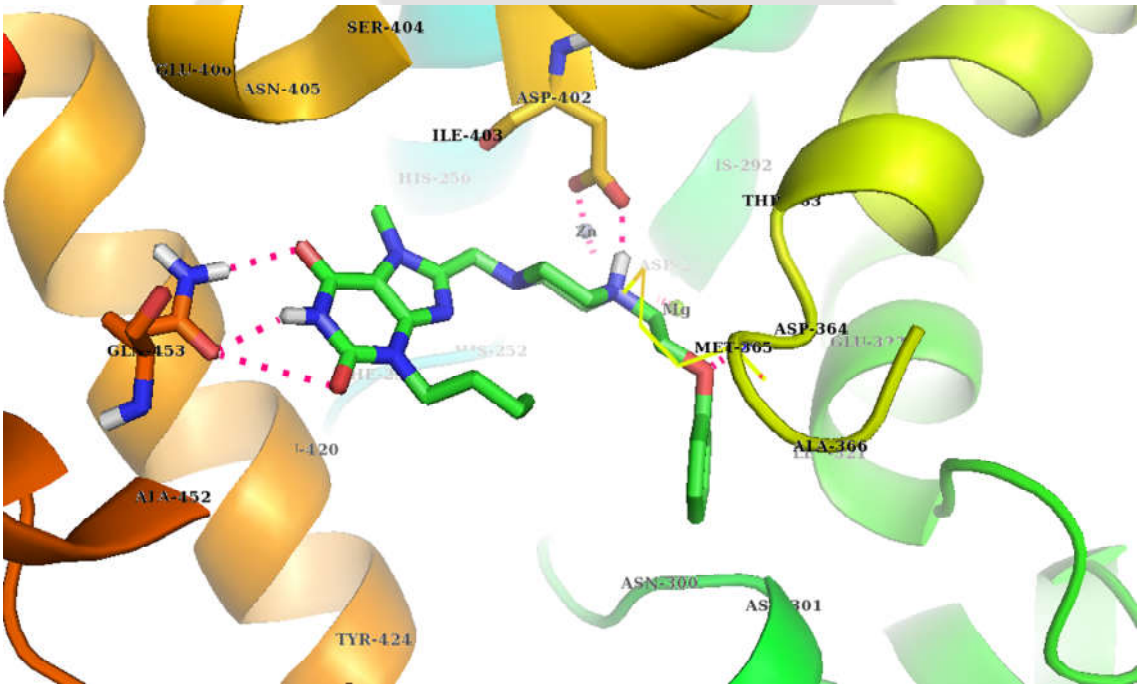

Figure 2.8 Interaction pattern of ZINC62579975 in the active site of PDE9A

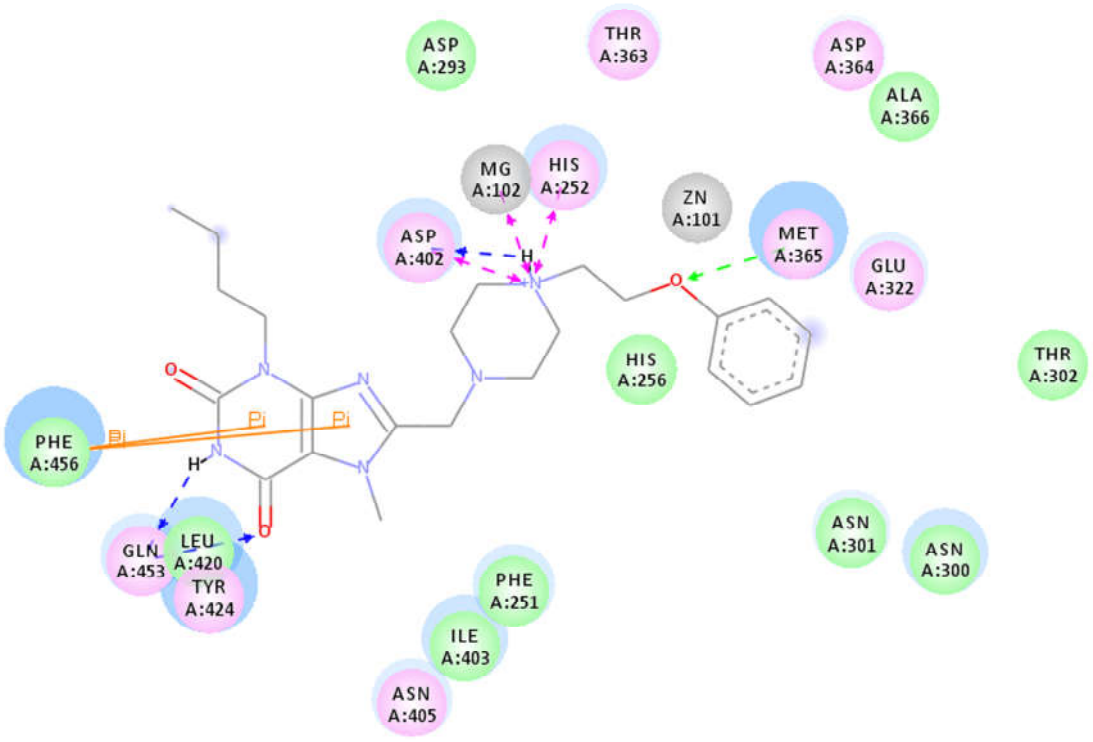

Figure 2.9 Interaction of ZINC62579975 with PDE9A in Discovery Studio Visualizer

2.3.5. Comparative binding studies of ZINC62579975 with various members of PDE superfamily

Phosphodiesterase 9A is one among the 11 members of phosphodiesterase superfamily. It has certain structural similarity with other PDEs which creates impediments in the development of specific inhibitor. For instance, PDE1 has ample presence in the brain cells and may be moderately inhibited by the ligands of PDE9A. This has been one of the major reasons for failure of most of the drugs to achieve specificity while developing inhibitors of PDE9A (Meng et al., 2012). In this study, the potency of ZINC62579975 towards PDE9A was determined by docking studies of all four top hits with other PDEs. Based on the comparative docking studies, ZINC62579975 established best interaction towards PDE9A among all PDEs. **Table 2.3** shows the docking result of ZINC62579975 with various members of PDE superfamily

in terms of lowest free energy of binding, inhibition constant, number of hydrogen bonds and number of residues involved in binding.

Table 2.3 Comparative binding pattern of ZINC62579975 with various members of PDE superfamily

PDEs	Specificity	LFBE (kcal/mol)	NCLC	Ki (nM)	Interacting Residues	H bonds
PDE9A	cGMP specific	-12.59	81	0.59	MET365, ASP402, GLN453	4
PDE5A	cGMP specific	-8.92	49	289.8	ASP764	1
PDE4D	cAMP specific	-7.7	13	2260	ASN281, GLU504	2
PDE7A	cAMP specific	-11.69	78	2.70	ASP362, GLN413	2
PDE8A	cAMP specific	-12.19	47	1.16	ASP726, GLN778	2
PDE1B	Dual specific	-10.68	92	14.8	HIS267, ASP370	2
PDE2A	Dual specific	-11.82	62	2.17	ASP808, GLN859	2
PDE3B	Dual specific	-8.77	10	370.2	ASN830, LEU895	2
PDE10A	Dual specific	-11.03	51	8.21	LEU635, ASP674	2

LFBE= Lowest Free energy of Binding, NCLC= Number of conformation in the largest cluster, Inhibition Constant (Ki), H-bond= Hydrogen bond

ZINC62579975 showed significant difference in free energy of binding between two cGMP specific phosphodiesterases - PDE5A (-8.92 kcal/mol) and PDE9A (-12.59 kcal/mol). The difference in lowest free energy of binding of ZINC62579975 with PDE9A and PDE5A is -3.67 kcal/mol. The compound formed only one H-bond with ASP764 at the entrance of the active site of PDE5A. It was unable to enter into the active site pocket of PDE5A and was restricted at the entrance of the active site pocket. It might be due to the large size of the compound as compared to the active site size of PDE5A. **Figure 2.10** illustrates the surface view of ZINC62579975 bound to PDE5A.

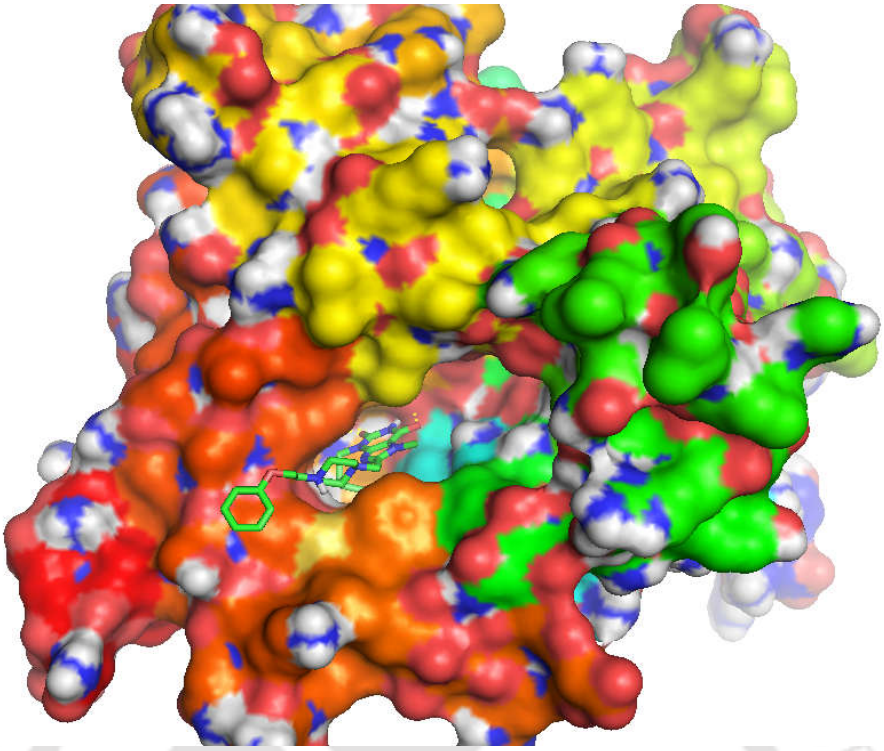

Figure 2.10 Surface view of ZINC62579975 in the active site of PDE5A

With cAMP specific phosphodiesterases (such as PDE4D, PDE7A and PDE8A), ZINC62579975 showed highest affinity towards PDE8A (-12.19 kcal/mol). One reason for the higher affinity of the compound towards PDE8A is the structural similarity between PDE9A and PDE8A due to presence of TYR (TYR424 in PDE9A and TYR748 in PDE8A) at the corresponding position in the active sites of both PDEs; whereas in other PDEs, the corresponding position is occupied by phenylalanine (Huai et al., 2004; Singh and Patra, 2014). PDE9A has abundance in brain whereas PDE8A has negligible presence in brain. Hence, the inhibition potential of PDE8A will probably not be able to affect the specificity of the inhibitor towards PDE9A. **Figure 2.11** illustrates the binding pattern of ZINC62579975 with PDE8A. ZINC62579975 showed significant difference in binding scores between PDE4D and PDE9A. In PDE4D the compound showed weak binding affinity with free energy of binding of -7.7 kcal/mol.

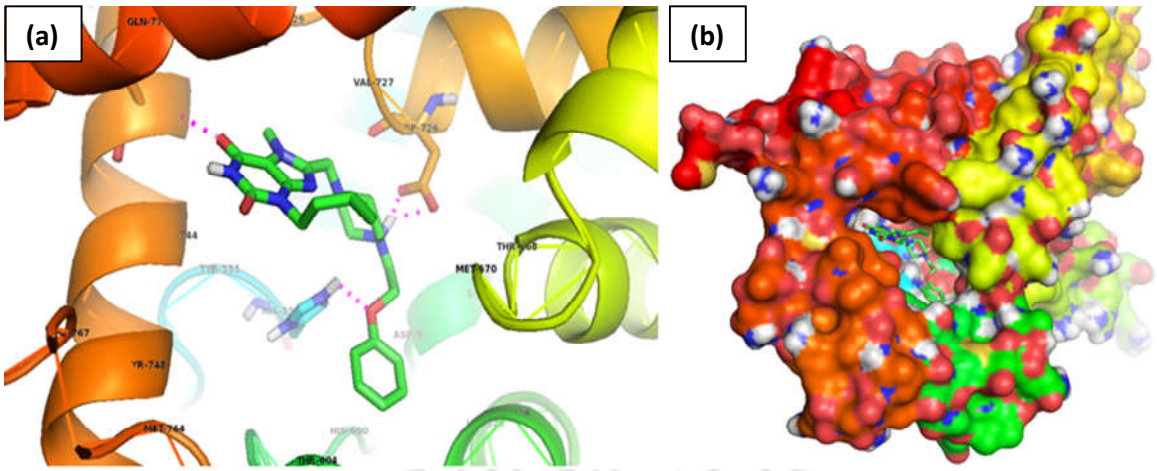

Figure 2.11 Interaction pattern of ZINC62579975 with PDE8A (a) active site view (b) surface view

Amongst the dual specific PDEs (PDE1, PDE2, PDE3 and PDE11), PDE1 is also expressed in the brain whereas PDE2 and PDE3 have negligible presence in brain. Hence, presence of PDE1 in brain may create selectivity issue during development of inhibitors for PDE9A. However, in the present study, ZINC62579975 showed comparatively higher potency with PDE9A (-12.19 kcal/mol) as compared to PDE1B (-10.68 kcal/mol).

Thus, ZINC62579975 showed highest binding affinity towards PDE9A. Present finding of the structure and interaction pattern of the screened ZINC62579975 molecule in the active site pocket of PDE9A, may be helpful in further drug development studies.

2.3.6. Comparative binding studies of ZINC62579975 with existing xanthine derivative

It was imperative to understand the binding affinity of screened compounds using known xanthine derivative as a reference molecule. In this study, IBMX was chosen as a reference molecule because of its non-inhibitory property towards PDE9A in *invitro* studies (Huai et al., 2004). This serves as a negative control. IBMX has been reported as

a non-inhibiting xanthine derivative. However, its interaction pattern in the active site of PDE9A may suggest some guidelines on what type of interaction pattern may suggest a compound to be inhibitory/non inhibitory. This may be helpful to analyze the improvement in binding affinity of xanthine derivative obtained from virtual screening. In docking study, IBMX formed two H-bonds with invariant GLN453 in PDE9A active site. **Figure 2.12** illustrates the comparative interaction pattern of ZINC62579975 and IBMX in the active site of PDE9A.

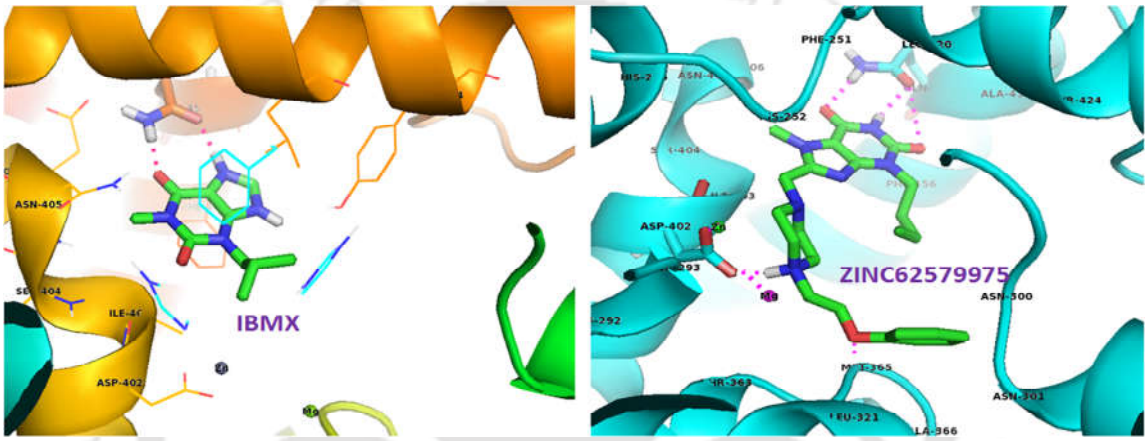

Figure 2.12 Comparative Interaction pattern of (a) IBMX with PDE9A (b) ZINC62579975 with PDE9A

Figure 2.12 depicts that the orientation of IBMX is exactly opposite to that of ZINC62579975 in the active site pocket of PDE9A. Further, ZINC62579975 formed four H-bonds with PDE9A whereas IBMX formed only two H-bonds. In ZINC62579975-PDE9A complex, amino acid residues involved in interaction were MET365, ASP402 and GLN453. ZINC62579975 formed two H-bonds with invariant GLN453. The stronger interaction might be due to its larger size of compound which helped in occupying larger area of the active site pocket and presence of more number of polar groups in ZINC62579975 which contributed to the firm interaction with the active site residues. ZINC62579975 with lowest free energy of binding of -12.59 kcal/mol showed

better specificity than non specific IBMX with lowest free energy of binding of -5.71 kcal/mol. ZINC62579975 showed better binding affinity with difference in free energy of binding of -6.88 kcal/mol over IBMX. Based on this difference of free energy of binding and binding interaction pattern, ZINC62579975 may be considered as candidate for development of potent specific inhibitor of PDE9A.

2.3.7. Comparative binding studies of ZINC62579975 with known inhibitors of PDE9A

BAY73-6691 and PF04447943 are well known inhibitors reported for their specificity towards PDE9A (Huai et al., 2004; Verhoest et al., 2012). They were used as positive control. These are non xanthine inhibitors of PDE9A which is constructed over pyrazolopyrimidinone scaffold. The study of interaction of these inhibitors was important to understand their binding pattern with PDE9A. This helped in comparing the affinity of ZINC62579975 with PDE9A. The comparative studies were carried out by molecular docking. **Figure 2.13** shows the interaction pattern of BAY73-6691 and PF04447943 with PDE9A. It was observed that ZINC62579975 formed more contacts with PDE9A as compared to BAY73-6691 and PF04447943. The binding affinity of BAY73-6691 and PF04447943 were represented in terms of lowest free energy of binding of -7.34 kcal/mol and -10.10 kcal/mol respectively. BAY73-6691 formed only two H-bonds with its –NH at N_1 and C=O at C_6 positions with side chain of GLN456 in the active site pocket of PDE9A. This might be due to the small size of BAY73-6691. Another reason could be the presence of less polar groups in BAY73-6691 than ZINC62579975. The other inhibitor PF04447943 formed three H-bonds in the active site of PDE9A where GLN453, THR363 and ASP364 were involved in H-bond interaction. Therefore, ZINC62579975 can be predicted as a good inhibitor for PDE9A.

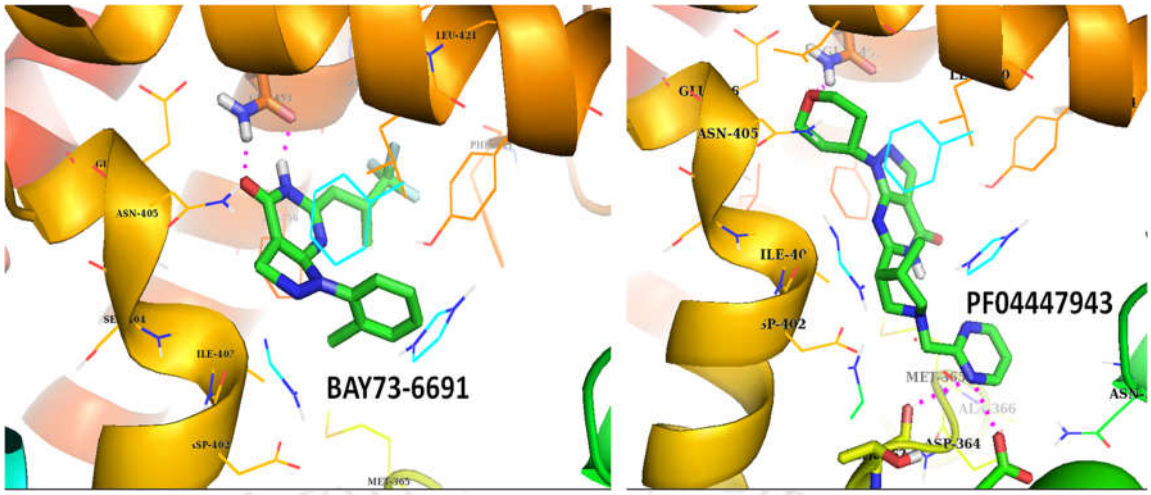

Figure 2.13 Interaction pattern of BAY73-6691 and PF04447943 with PDE9A

2.3.8. Molecular dynamics simulations of ZINC62579975

Molecular dynamics (MD) simulations is a time dependent physical behaviour of atoms and molecules in the biological system. It is one of the best ways to understand the stability and compactness of the protein-ligand complex (Ganoth et al., 2006). In the present study the MD simulation of the screened compound (ZINC62579975) was carried out to analyze physical behaviour of that compound with PDE9A. MD simulation of 6 ns was performed for the PDE9A- ZINC62579975 complex. The reliability of the MD simulation method and selected parameters were evaluated by using the crystal structure of PDE9A (2HD1) as the reference. In order to check the stability of protein-ligand complex, the RMSD of the backbone atoms was calculated from MD run and was plotted as time dependent function in **figure 2.14**. As seen from this figure, the RMSD curve became stable after 3.8 ns and the PDE9A-ligand complex achieved equilibrium. After 3.8 ns, the protein reaches an average value of 0.23 Å and got stabilized thereafter.

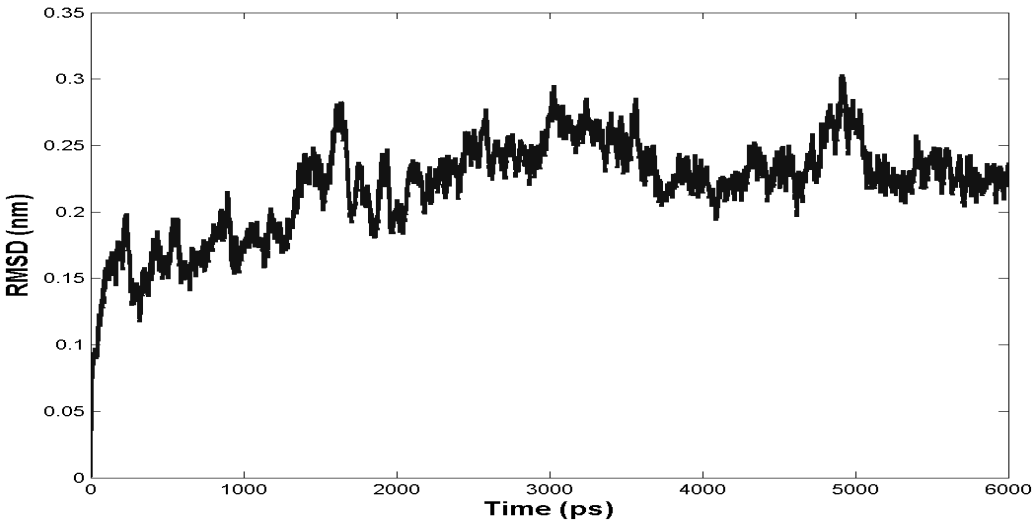

Figure 2.14 The RMSD curve of the PDE9A crystal structure (PDB ID: 2HD1) which was used for MD- augmented virtual screening

2.3.9. Drug likeness properties of ZINC62579975

To take the screened inhibitor for further studies, the drug-likeness properties, ADMET properties and toxicity prediction were carried out using PreADMET online server [https://preadmet.bmdrc.kr/]. The compound ZINC62579975 follows the Lipinski rule of five and other drug-likeness properties such as MDDR rule. **Table 2.4** shows the Drug likeness and ADMET properties of ZINC62579975. ZINC62579975 possessed molecular weight of less than 500 Da, hydrogen-bond donor atoms are less than five and hydrogen-bond acceptors are less than 10, cLogP value is less than 5 and the molar refractivity is in the range of 40−130 (https://ilab.acdlabs.com/iLab2/). The blood-brain (C.brain/ C.blood) permeability of ZINC62579975 is 0.210766 which is less than the required value. However, we feel further improvement in the screened molecule may enhance the same making it acceptable for further drug development studies. Also, experimental validation of such results may help in taking a firm decision.

Table 2.4 Drug likeness and ADMET properties of screened ZINC62579975

Properties	**ZINC62579975**
Molecular Weight	440.54
No. of Hydrogen Bond Donors	1
No. of Hydrogen Bond Acceptors	9
Calculated partition co-efficient (cLogP)	0.84
Topological polar surface area (TPSA)	123.00 ± 0.5 cm^3
Molar Refractivity	82.94
logs	-4.24
MDDR like_Rule	Drug-like
BBB(Blood Brain Barrier) permeability	0.210766
HIA (Human intestinal absorption (HIA, %))	89.668024
Plasma Protein Binding	40.640795
Skin Permeability (logKp, cm/hour)	-4.62261

2.4. Xanthine scaffold for future PDE9A drug development

Most of the reported inhibitors for PDE9A have been constructed on a pyrazolopyrimidinone scaffold. The introduction of new scaffolds is important to diversify the drug development studies for PDE9A. This diversification could lead to increase the potential of drug development. Since long, xanthine based compounds have been target molecules for various diseases, but there has been diminutive effort by researchers to take up xanthine derivatives as target molecule for PDE9A inhibition. The present study has tried to reveal the potential of xanthine based molecule towards specific inhibition of PDE9A. In the next chapter we will try to see the possibilities of exploring xanthine as a scaffold for development of new compounds.

2.5. Conclusion

In the present study, 2055 compounds were extracted using xanthine ring as scaffold from the ZINC database and were subjected to Lipinski rule of five filter. Among them 1480 compounds were selected for molecular docking based virtual screening based on lowest free energy of binding cut off. The top ten hits were selected for further stringent docking studies with 100 GA run. Four top hits obtained from this study were subjected to comparative binding studies with various members of PDE superfamily. Among them, ZINC62579975 showed comparatively higher potency towards PDE9A as compared to other PDEs. The active site residues involved in interaction with ZINC62579975 were MET365, ASP402 and GLN453. The stability of ZINC62579975 was determined by MD simulation using timescale of 6 ns. It was observed that ZINC62579975 follows Lipinski rule of five and have drug-like properties. Though its blood brain barrier permeability is low, final validation through *in vitro* studies will provide the correct possibilities. In addition, the structure of ZINC62579975 can be used for further structure based drug development. Till date, most of reported inhibitors targeting PDE9A have common pyrazolopyrimidinone scaffold. Therefore, entry of new scaffolds is an urgent need in PDE9A research to bring out structural diversification. Xanthine can be one such scaffold to achieve this target. The current chapter has tried to focus on these aspects and the next chapter will explore the wide potential of xanthine as scaffold by manual designing of novel xanthine derivatives based on the active site requirement of PDE9A.

CHAPTER 3

Development of Xanthine Based Inhibitors Targeting Phosphodiesterase 9A

Prologue

In Chapter 2, after virtual screening of large number of existing xanthine based derivatives extracted from ZINC database, only one compound (ZINC62579975) which was found to be potent specific inhibitor for PDE9A. Structure based drug designing approach was employed to add more compounds to the repertoire. Here also "xanthine" was used as a scaffold in structure based manual designing. The selection of xanthine as a scaffold was due to its various existing pharmaceutical applications. Structural similarity among PDEs is the major path-blocker in the selection of specific inhibitors for a particular member of the PDE superfamily. Hence, through extensive literature review we tried to understand the structure of PDEs in general and PDE9A in particular. Through these studies, it has been found that some amino acid residues play significant role in creating uniqueness in the active site of PDE9A. While treating neurodegenerative disease targeting PDE9A, major setback in drug development process is received due to the presence of PDE1 in brain. Thus, there was a need to seriously think on the structural set-up of protein and the desirability of compounds in such set-up. By keeping all these factors in mind, structure-based drug design approach was employed for the development of specific xanthine based inhibitors for PDE9A. This chapter focuses on using parallel approach of manual designing and molecular docking studies to generate compounds specific for PDE9A. This has been instrumental in further modifications of the lead compounds moving a step closer in designing specific drugs for PDE9A.

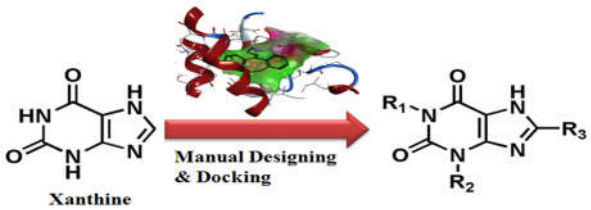

3.1. Introduction

In recent years, several researchers have been working towards specific inhibitor development of PDE9A. BAY73-6691 and PF04447943 are two such inhibitors of PDE9A which have been reported and used in various pathophysiological conditions such as Alzheimer disease, cognitive disease and corpus cavernosum relaxation (da Silva et al., 2013; Hutson et al., 2011; Nicholas et al., 2011; Verhoest et al., 2009; Wunder et al., 2005). However, most of the reported inhibitors show moderate specificity towards their target. Also, there have been reports of various side effects as these molecules also respond as substrates of PDE1. These factors have been a bottleneck in the progress of specific drug development targeting PDE9A (Meng et al., 2012). Therefore, a specific inhibitor for PDE9A is need of the hour. Desirably, the inhibitor should have capability to bind specifically with PDE9A as well as have drug-likeness properties. Most of the reported inhibitors for PDE9A are pyrazolopyrimidinone group of compounds. They are constructed over "pyrazolopyrimidinone" scaffold. The use of limited available scaffold has been a major constraint in the development of specific PDE9A inhibitor. Hence, there is a need to have more molecules to the available repertoire of scaffold to bring out structural diversification in the PDE9A drug development process. Xanthine derivatives are group of compounds well-known for their phosphodiesterase inhibition property in mammalian cells. Though most of the derivatives target PDEs non-specifically, these derivatives provide wide possibilities for the development of more specific inhibitors for the particular PDE. Because of its structural similarity with substrates (cAMP or cGMP) and availability of all possible sites (three –NH sites and one –CH site) for substitution; "Xanthine" can have potential to act as new scaffold in the drug development process for PDE9A.

Xanthine based compounds are well known for their drug-like properties. Many xanthine based plant alkaloids have been used as psycho-stimulant and anti-asthmatic drugs (Baraldi et al., 2007; Burbiel et al., 2006; Nehlig et al., 1992). They show activity towards PDEs due to their structural resemblance with substrates (cAMP or cGMP) of PDEs. In the last few decades, a number of xanthine based inhibitors have been designed, developed and used by various researchers for pharmaceutical applications. Xanthine derivatives such as caffeine, theophylline, IBMX, pentoxifylline etc. nonspecifically inhibit most phosphodiesterases. However, IBMX does not show inhibition towards PDE9A (Huai et al., 2004). This may be attributed to the bigger size of PDE9A active site. The ligand is not able to fit compactly leading to fluctuation in the interactive conformation of the conserved residue, GLN453 (which plays a pivotal role in deciding the substrate specificity in PDE9A) due to inter amino acid interaction. Hence, it creates weak interaction with IBMX. Another possible reason for showing non inhibition could be the small size of IBMX molecule which is unable to cover the entire active site pocket of the target protein. Hence, substitutions and modifications of the xanthine scaffold leading to increase in size of the molecule could play significant role in designing novel inhibitors fitting appropriately in the active site pocket of PDE9A and show specific inhibition. Computer based drug development can be an aid to this purpose. **Figure 3.1** illustrates the computer based drug development methodology used in this work.

Computer aided drug designing and use of various *in silico* approaches like manual designing, molecular docking, drug-likeness property prediction, etc. are some of the key steps in the long sojourn of drug development. It helps in prior prediction of interaction pattern of new molecules with enzymes before synthesis and experimental validation. This reduces the time span of the entire drug development process. The

current study represents the design and development of potent and selective inhibitors targeting PDE9A using xanthine scaffold. Designing of compounds and their prior prediction by docking reduces the load of synthesis and provide a directional approach towards drug development. Only the pre-screened compounds will be in the final list of compounds to be synthesised.

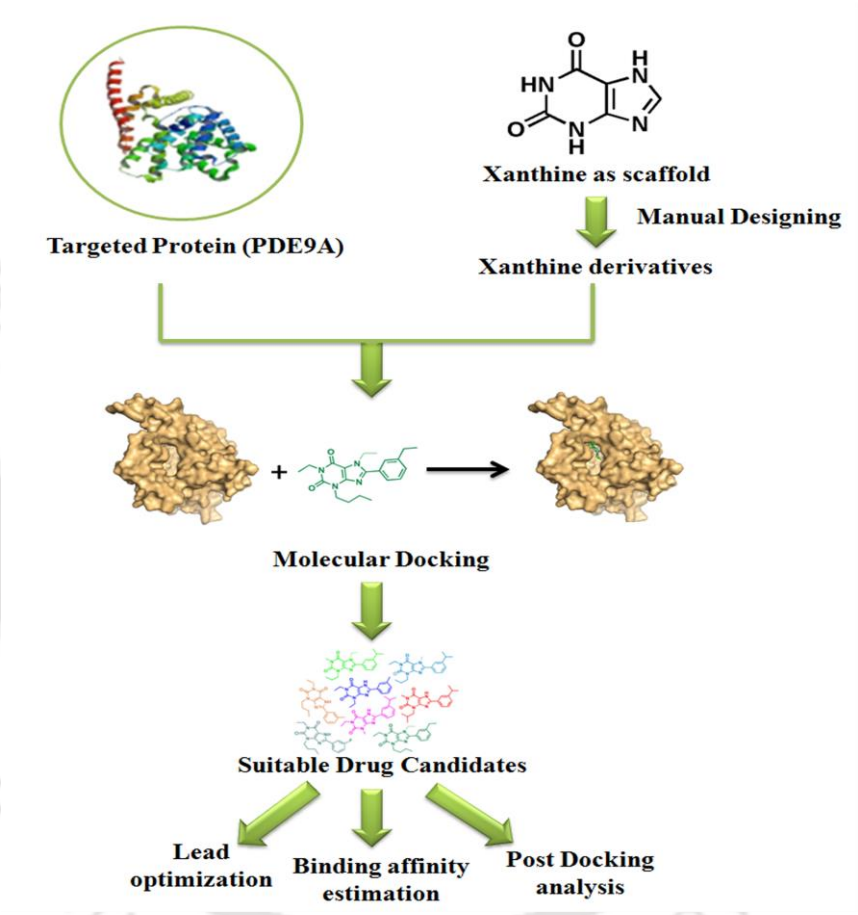

Figure 3.1 Method for drug design and development using molecular docking approach followed by post docking analysis (drug likeness, ADMET properties)

3.2. Materials and methods

3.2.1. Manual designing of xanthine based ligands

Xanthine derivatives are known for their phosphodiesterase inhibition property in mammals. But most of the derivatives target PDEs non-specifically. This might be due to

their small size that could be responsible for their not fitting properly in the active site pocket of PDEs. Substitution of xanthine derivatives with fragments according to the active site amino acid composition of the targeted protein can lead to formation of compounds having higher affinity for PDE9A. These derivatives need to be constructed over 'xanthine' scaffold. Therefore, modification of xanthine at different positions can give specific compounds targeting PDE9A. It has been reported that substitution at N_1 and N_3 positions with increasing chain length increases the affinity towards phosphodiesterases and adenosine receptors (Miyamoto et al., 1994; van Galen et al., 1992). Substitution at C_8 position of xanthine with aromatic ring (aryl/cycloaryl/ heteroaryl group) also increases the potency towards adenosine receptors (Bandyopadhyay et al., 2012; Chappe et al., 1998). It has also been reported that substitution at N_7 position is not favorable while in some cases N_9 substitution shows negative effect (Azam et al., 2009). Therefore, in this study, N_1, N_3, C_8 and N_9 positions were chosen for the initial phase of modifications of the xanthine scaffold. Here, "xanthine" was used as a scaffold to construct various derivatives by manual designing approach. Fragments R_1, R_2, R_3 and R_4 were chosen for substitution/modification at N_1, N_3, C_8 and N_9 positions of the xanthine scaffold, respectively. Ligands with different substituents were manually designed in ChemDraw Ultra 8.0. **Figure 3.2** is an illustration of the selected positions where modifications/substitutions at xanthine were carried out in order to construct potent and specific inhibitors for PDE9A.

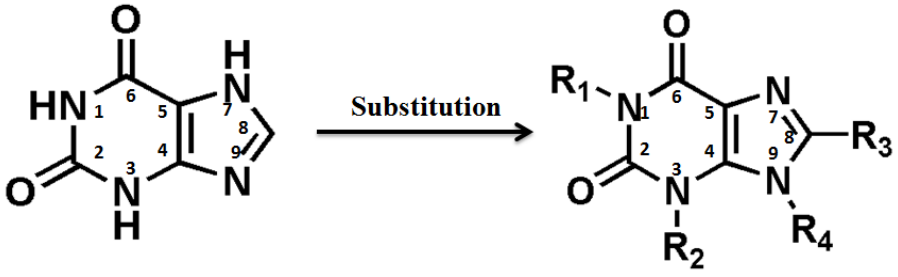

Figure 3.2 Structure of Xanthine and its modification sites at N_1, N_3, C_8 and N_9 positions

3.2.2. Molecular docking of manually designed xanthine derivatives with PDE9A

Molecular docking is an *in silico* approach to predict binding affinity of ligands (substrate or inhibitor) in the active site pocket of enzymes by various interactions such as hydrogen bond interaction, hydrophobic interaction, van der Waals interaction and electrostatic interactions. AutoDock is an important docking tool to identify small molecules which have the possibility to be a future drug by studying their mode of action, interaction pattern and affinity towards a particular enzyme. It shows the interaction between partially flexible macromolecule (i.e. side chains in macromolecules are flexible) and flexible ligands (http://autodock.scripps.edu/). It estimates the free energy of binding by using scoring function based on the AMBER force field (Kumar et al., 2014). In this study, docking was carried out by AutoDock 4.2 using Lamarckian Genetic Algorithm (LGA).

Protein-ligand docking studies were initiated by extracting crystal structure of coding domain of phosphodiesterase proteins - PDE1B, PDE2A, PDE3B, PDE4D, PDE5A, PDE7A, PDE8A, PDE9A and PDE10A from RCSB Protein Data Bank (http://www.rcsb.org; PDB IDs were 1TAZ, 1Z1L, 1SOJ, 1ZKN, 1RKP, 3DBA, 3G3N, 3ECM, 2HD1, 4DFF respectively). Prior to docking, all heteroatoms including ligands and water molecules were removed from the crystal structure using Swiss PDB Viewer. Two metal ions zinc and magnesium were assigned with charge +2. Macromolecule file for docking was prepared in Auto Dock Tool (ADT) by removing polar hydrogen followed by addition of non-polar hydrogen, computation of gasteiger charges and merging of non-polar hydrogen. Each ligand file was prepared separately by using PRODRG server and ChemDraw Ultra 8.0. Energy minimization of newly designed ligands was carried out by using PRODRG online server. Since, most of the PDEs

extracted from PDB were in the form of 3D co-crystallized structure with inhibitor or substrate, their site of interaction was chosen as the binding site for making grid file. Parameters for making grid file comprised of 90 points in x, y and z directions with equal spacing of 0.253Å. Each protein was used as rigid model with flexible side chains. Flexible ligand models were used for docking and further optimization. Manually designed ligands were docked with PDEs by keeping common parameters such as 100 GA run, 300 population sizes, 27000 maximum numbers of generation and 25000000 maximum numbers of evaluations. Clustering of docked complexes was created with 2Å root-mean-square deviation tolerance. Molecular docking was carried out in CentOS Linux system. Docking result was analyzed with the help of AutoDock Tool, PyMol, and Discovery Studio Visualizer which provided information about hydrogen bond interactions and π - π interactions. Hydrophobic interaction, electrostatic interaction and van der Waals interaction were analyzed by pose-view (http://poseview.zbh.uni-hamburg.de/) and Lig Plot (Wallace et al., 1995).

3.2.3. Comparative analysis of pharmaceutical properties of selected compounds

Pharmaceutical properties are among the most important parameters for a compound to be suitable drug candidate. Prediction of drug likeness properties is the final deciding factors for *in silico* study of inhibitors to qualify for being taken up as future drug candidate. The best compounds obtained from *in silico* studies, were subjected to study drug-likeness properties. These properties include rule of 5, leadlike rule, CMC like rule, MDDR like rule and BBB permeability. PreADMET software was used to calculate the drug likeness, ADMET and toxicity properties of the selected compounds.

3.2.4. Comparative binding study of selected compounds with existing xanthine derivatives

Numerous natural and synthetic xanthine derivatives have been reported with their nonspecific PDE inhibitory activity. Comparative interaction study with existing xanthine based inhibitors was required to ensure the potency of selected compounds towards PDE9A. IBMX is the most common xanthine derivative for most of the phosphodiesterase inhibition. But in case of PDE9A, IBMX does not show any inhibition (Huai et al., 2004). Among xanthine derivatives, only IBMX co-crystal structure with PDE9A has been submitted in Protein Data Bank. This co-crystal structure was extracted from data bank and redocked. The binding affinity of selected compounds for PDE9A from manual designing was compared with the docking result of IBMX-PDE9A complex. Hence, in the present study IBMX was used as a reference molecule (negative control) to analyze the potency of selected molecules towards PDE9A. The docking parameters used for these comparative analyses were 100 GA run, 300 population size, 27000 maximum number of generation and 25000000 maximum number of evaluations.

3.2.5. Comparative inhibition study of selected compounds and known PDE9A inhibitor

In last two decades, extensive work has been carried out in development of potent inhibitors for PDE9A to treat different diseases associated with lowering the level of cGMP (da Silva et al., 2013; Hutson et al., 2011; Nicholas et al., 2011; Singh and Patra, 2014; Verhoest et al., 2012; Wunder et al., 2005). Surprisingly, none of them belong to the xanthine class of compounds. Most of the reported PDE9A inhibitors have been constructed over “pyrazolopyrimidinone” scaffold. Amongst them, BAY73-9961 is an experimentally validated PDE9A inhibitor. In this study, docking of this inhibitor was

carried to get the binding pattern inside the active site pocket of PDE9A. A comparative study of the reported inhibitor with selected compounds for PDE9A was carried out by comparative analysis. This was helpful to understand the binding pattern and the role of various active site residues in ligand binding.

3.3. Results and Discussion

Manual designing has been a successful method in structure based drug development process. The workflow of the present study has been illustrated in **figure 3.3**.

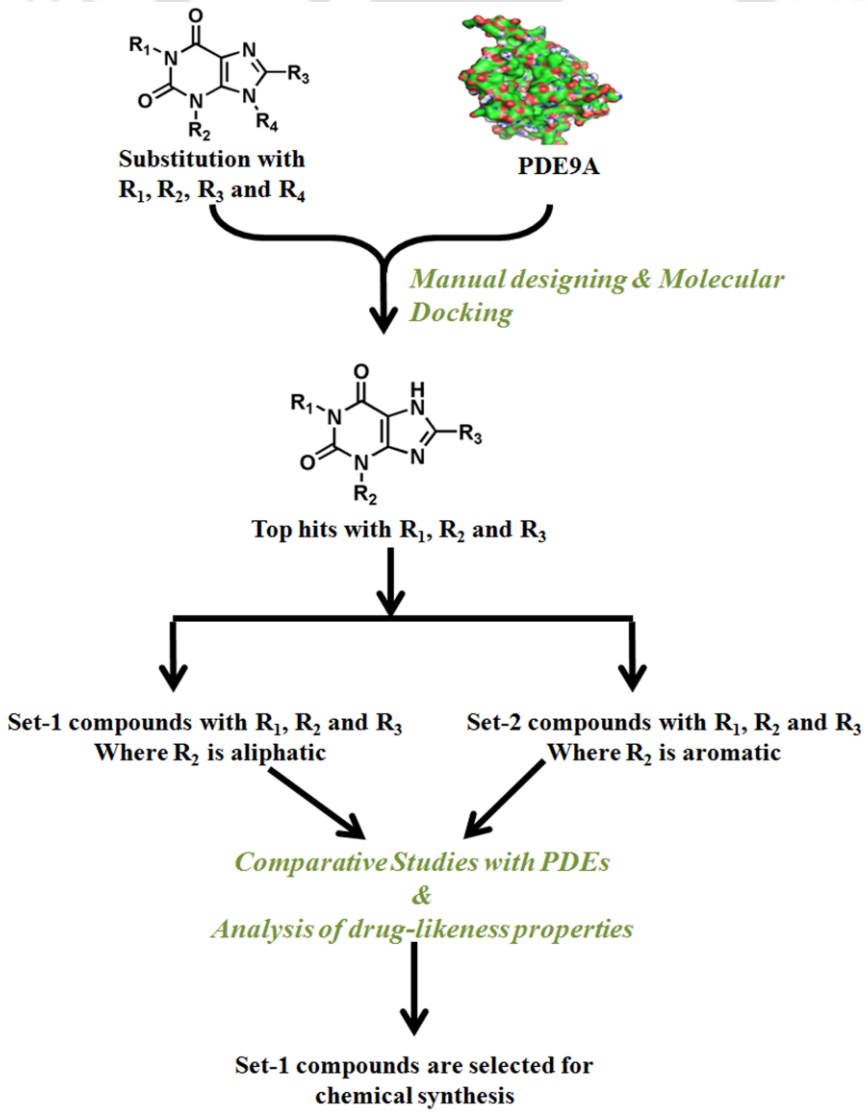

Figure 3.3 Workflow for designing novel potent inhibitors of PDE9A

In silico studies such as manual designing and subsequent molecular docking studies gave some specific compounds for PDE9A. The pharmaceutical properties and comparative binding studies established final assurance for suitability of these compounds in further drug development process. Therefore, the compounds obtained from the *in silico* studies were subjected to chemical synthesis.

3.3.1. Manual designing of xanthine based ligands targeting PDE9A

By substitution or modification at N_1, N_3, N_9 and C_8 positions on xanthine scaffold, 200 compounds were designed. Molecular docking study was carried out to analyze the selectivity and further improve the ligand structure to target PDE9A. The structures of initial phase of designed compounds with different substitution at N_1, N_3 and N_9 are presented in **Table 3.1(A-D)**. Initially, substitution (compound 1-5) was carried out at N_1 and N_3 position of xanthine with fragments R_1 and R_2, respectively (R_1 was kept constant with methyl group). Then modifications (compound 6-8) were carried out with substitution at N_1, N_3 and N_9 positions with R_1, R_2 and R_4 fragments, respectively by keeping R_1 and R_4 constant. With these three modifications (compound 6-8), it was observed that switching from aliphatic to aromatic fragments at N_3 position (of compound 8) improved the binding affinity of compounds. Hence, further modifications were carried out by keeping the best interaction (in compound 8) fragment (x) as constant at N_3 position whereas, different modifications (compound 9-14) were performed at N_1 and N_9 positions. Amongst compound 9 to 13, compound 12 showed better inhibition with lowest free energy of binding of -11.54 kcal/mol (lowest amongst the six designed compounds). Thereafter, further modifications (compound 15-22) were continued with substitution at N_1, N_3 and N_9 positions by keeping a different aromatic

fragment (y) at N_3 position constant with varying aliphatic fragments at both N_3 and N_9 positions.

Unfortunately, all these modifications examined so far, were unable to produce specific compounds for PDE9A. This might be due to the retro-orientation of double bond between N_7 and N_9 in the imidazole ring of xanthine. Hence, in place of N_9 modification, C_8 position was selected for further modifications. Modification at C_8 position was carried out with R_3 fragments (mainly aromatic in nature) along with N_1 and N_3 substitutions. With the substitution of various aromatic fragments at C_8 position, it was seen that the resulting compounds (compound 23 to 52) had higher occupancy in the active site of PDE9A. Therefore, based on these modifications, selective compounds for PDE9A were developed.

3.3.2. Interaction studies of manually designed xanthine derivatives to find out specific inhibitors for PDE9A

Docking of 200 newly designed compounds with PDE9A had shown various interaction patterns. These results provided a path towards designing of specific molecules. Among 200 compounds, 52 compounds were selected based on free energy of binding (ΔG°) cut off of -6.0 kcal/mol. The compounds having free energy of binding less than -6.0 kcal/mol with PDE9A possessed low inhibition constant (Ki) value. Thus, other compounds were rejected for further validation on account of their less inhibitory activity. **Table 3.1** (A-D) shows fragments composition and their effect in terms of the lowest free energy of binding (LFEB), residues involved in interaction, number of conformations in the largest cluster, number of interactive H- bond formed between PDE9A and ligand.

Table 3.1 Initial interaction studies of manually designed compounds with PDE9A by using N_1, N_3 and N_9 position of xanthine for substitution

(A) Substitution at N_1 and N_3 positions of xanthine

Sl no.	R_1 (N_1 Substitution)	R_2 (N_3 Substitution)	LFEB (kcal/mol)	Interacting Residues	NCLC	H bond
1	$-CH_3$	$-CH_2(CH_3)_2$	-6.78	ASN405	71	1
2	$-CH_3$	$-CH_2(CH_3)CH_2CH_3$	-6.35	GLN453	54	2
3	$-CH_3$	$-CH_2CH_2COCH_3$	-6.31	TYR424, ASN405, GLN453	36	4
4	$-CH_3$	$-CH_2CH_2CH_2COCH_3$	-6.76	TYR424, ASN405, GLN453	35	4
5	$-CH_3$	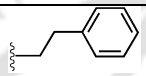	-7.96	ASN405, GLN453	28	2

(B) Substitution at N_3 and N_9 positions of xanthine keeping R_1 fragment (methyl) constant

Sl no.	R_1 (N_1 Substitution)	R_2 (N_3 Substitution)	R_4 (N_9 Substitution)	LBFE (kcal/ mol)	Interacting Residues	NCLC	H bond
6	$-CH_3$	$-CH_2$ CH_2COCH_3	$-CH_2OCH_2CH_2OH$	-6.96	HIS252, TYR424, ASP402, GLU406	70	4
7	$-CH_3$	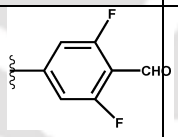	$-CH_2OCH_2CH_2OH$	-6.37	GLN453	39	2
8	$-CH_3$	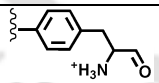	$-CH_2OCH_2CH_2OH$	-11.1	ASP402, ILU403, GLU406	45	3

(C) Substitution at N_1 and N_9 positions of xanthine by keeping R_2 fragment (x) constant

Sl no.	R_1 (N_1 Substitution)	R_2 (N_3 Substitution)	R_4 (N_9 Substitution)	LBFE (kcal/ mol)	Interacting Residues	NCLC	H bond
9	$-CH_3$	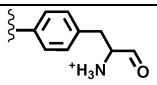	$-CH_2OCH_2CH_2F$	-10.23	ASP293, ASP402	45	2
10	$-C_2H_5$	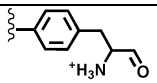	$-CH_2OCH_2CH_2F$	-10.64	ASP293, ASP402	54	2

11	- $CH_2CH_2CH_3$	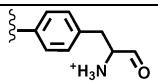	-$CH_2OCH_2CH_2OH$	-11.21	ASP293, ASP402, ILU403, GLU406	41	4
12	- CH_2CH_2CHO	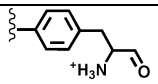	-$CH_2OCH_2CH_2OH$	-11.54	ASP293, ASP402, ILU403, GLU406, TYR424	58	5
13	- CH_2CH_2CHO	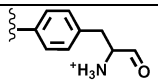	-OCH_2CH_2OH	-11.08	ASP293, ASP402, ILU403, GLU406	64	4
14	- CH_2CH_2CHO	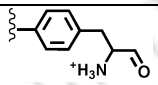	-$OCH_2CH_2CHF_2$	-10.55	ASP293, ASP402	53	2

(D) Substitution at N_1 and N_9 positions of xanthine by keeping R_2 fragment (y) constant

Sl no.	**R_1 (N_1 Substitution)**	**R_2 (N_3 Substitution)**	**R_4 (N_9 Substitution)**	**LFEB (kcal/ mol)**	**Interacting Residues**	**NCLC**	**H bond**
15	- CH_2CH_2CHO	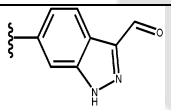	- $CH_2OCH_2CH_2OH$	-8.12	GLU406, TYR424	71	3
16	- $CH_2CH_2CH_3$	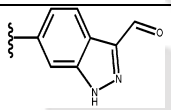	- $CH_2OCH_2CH_2OH$	-8.14	HIS252, ILU403, ASN405, YR424, GLN453	68	5
17	- $CH_2CH_2CH_3$	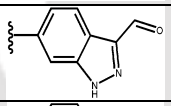	-CH_2CH_2CHO	-7.79	TYR424	50	1
18	- $CH_2CH_2CH_3$	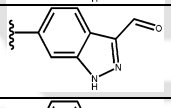	-$CH_2CH_2COCH_3$	-8.14	HIS252, ILU403, ASN405,TYR42, GLN453	68	5
19	- $CH_2CH_2CH_3$	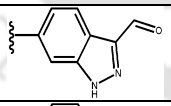	-CH_2OCOCH_3	-8.05	TYR424	53	1
20	- $CH_2CH_2CH_3$	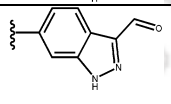	-$CH_2CH_2NH_2^+$ CH_3	-10.13	HIS296, ASP402	68	2
21	- $CH_2CH_2CH_3$	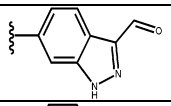	-$OCH_2CH(NH_3^+)$ CHO	-10.81	ASP293, HIS296, ASN301, ASP402	29	4
22	- $CH_2CH_2CH_3$	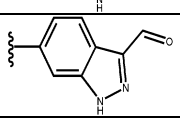	- $OCOCH_2CH_2NH_3^+$	-11.74	ASP293, HIS296, ASP402	34	4

LFEB= Lowest free energy of binding, NCLC=Number of conformations in the largest cluster, H-bond= Hydrogen bond

Based on the above analysis it was found that simultaneous substitution at N_1, N_3 and N_9 sites were not suitable to construct stable compounds for PDE9A. It was analyzed that compounds having R_4 substitution at N_9 site allowed the retro-orientation of double bond from N_9 to N_7 position in imidazole ring of xanthine due to resonance effect of the imidazole ring. This led to loss of interaction between ligand and nearby active site residues in 5Å region of the active site. It further led to unstability of compounds in the active site pocket of PDE9A. N_9 substituted compounds entered into the active site pocket by maintaining the position of xanthine scaffold at the entrance of active site, while the positions of R_2 and R_4 substituent were oriented toward the histidine rich site in the pocket. Histidine rich site is conserved site in all members of PDE superfamily, therefore, N_9 substitution in compounds was responsible in making the compounds non-specific. This might be a probable reason for compounds with N_9 substitution showed parallel interaction with (PDE1B, PDE5A, PDE2A, PDE7A) as well.

By analyzing docked conformations of each of the 52 newly designed compounds with PDE9A, it was observed that the substitution at N_1 and N_3 positions with aliphatic fragments showed lesser number of interactions with PDE9A. This might be due to more tortional angles present in the ligand structure which were responsible for the flexibility of compounds in the active site pocket of PDE9A. This resulted in the unstable protein-ligand interaction. Switching from aliphatic to aromatic fragment at N_3 position contributed rigidity to the compound. Thus, due to rigidity and increased size of compounds, they fit appropriately in the active site pocket of PDE9A. This change brought reduction in the interacting conformations in different clusters. Substitution with aromatic fragments at C_8 position provided appropriate platform intended to make potent and specific inhibitors for PDE9A. Compounds having substitution at C_8 along with N_1 and N_3 positions occupied the complete active site pocket that was essential to fetch

majority of conformations in one cluster. It was also required to maintain the stability of interactions between protein and ligand. Thus, the substitution with R_1, R_2 and R_3 fragments at N_1, N_3 and C_8 positions of xanthine, respectively, showed promising docking result. It was further confirmed by comparative docking study with other members of PDE superfamily. Literature indicates the stability of compounds with modification at N_1, N_3 and C_8 positions (Hayallah et al., 2002; Weyler et al., 2006). This was also confirmed by the present docking analysis. Thus, N_1, N_3 and C_8 were suitable positions at xanthine scaffold where substitution can be carried out to make the compound selective inhibitor for PDE9A. But the modification needs rational. The active site pocket of PDE9A has uniqueness in PDE family due to presence of specific amino acid residues such as PHE251, GLU406 and TYR424. The substitution at N_1 position with alkyl group and at C_8 position with phenyl ring having aliphatic chain at meta-position resulted in designing of many novel compounds. All these compounds showed appropriate occupancy in the active site of PDE9A in a similar mode. Thus, substitution at N_1 position with aliphatic and C_8 position with aromatic fragment were the deciding factor for the orientation of the compounds inside the active site pocket of PDE9A. After substitution at N_1 and C_8 position, modification at N_3 position was carried out to understand the effect of this substitution on binding affinity of compounds. Substitution with either aliphatic or aromatic fragment at N_3 position did not make any significant change in the orientation of compound in the active site pocket. However, substitution at N_3 position determined the binding strength of compounds towards the target protein. Hence, substitutions at N_3 position were studied separately (with N_1 having aliphatic fragment and C_8 having aromatic fragment substitution). Substitution with aromatic fragment at N_3 position gave better interaction with the enzyme than aliphatic fragment substitution at the same position. **Figure 3.4** illustrates the analysis of the effect of

changes at N_1, N_3 and C_8 positions of xanthine scaffold. In this study, the compounds with modification at N_1, N_3 and C_8 positions were categorized into two sets- set-1 and set-2. Both sets consisted of compounds with aliphatic chain at N_1 position and aromatic fragments at C_8 position, but they differ with N_3 substitution. In set-1, N_3 position was substituted with aliphatic side chain whereas, in set-2, aromatic fragment was substituted at N_3 position. The selected compounds from these two sets were separately studied for comparative *in silico* studies with various members of PDE superfamily.

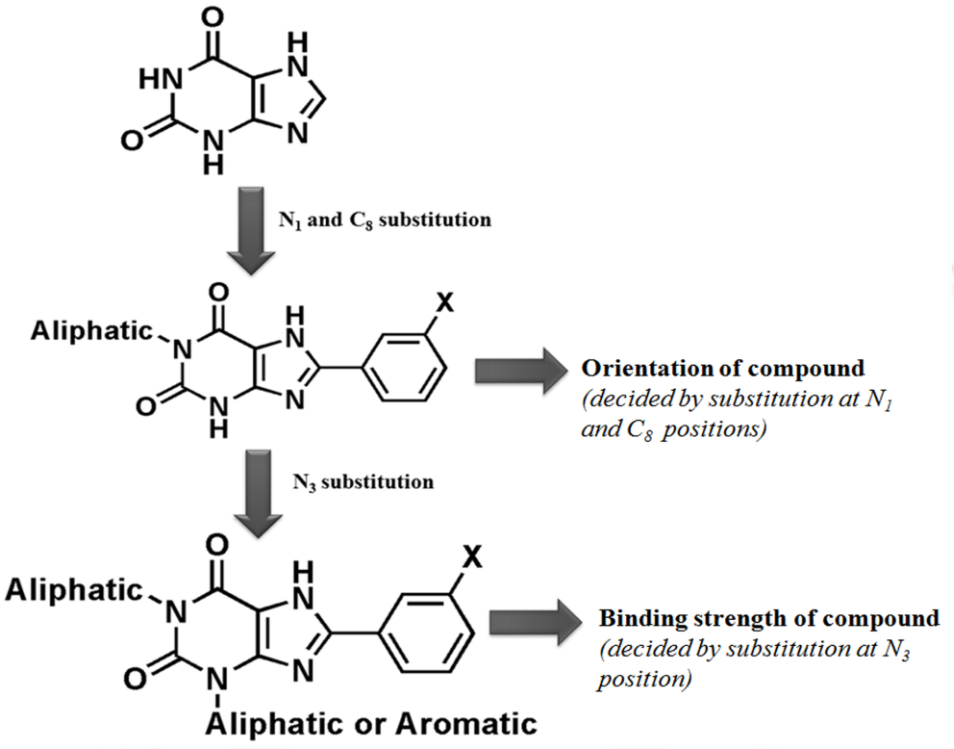

Figure 3.4 Interaction pattern analysis of compounds with substitution at N_1, N_3 and C_8 positions of xanthine within active site pocket of PDE9A

3.3.3. Interaction study of set-1 compounds with PDE9A

Till designing of compound 22, we came across some important finding regarding the importance of specific fragments on the particular site of the xanthine. All the compounds (23-37) of set-1 showed interaction with PDE9A in a similar pattern. In this pattern, the compounds interacted with GLN453 residue of PDE9A by forming two

hydrogen bonds. This pattern showed the positioning of these compounds in PDE9A active site, determined mainly by the substitution at N_1 with alkyl groups and C_8 position substitution with phenyl substituent. Aliphatic chains (at N_1 position) in these compounds were positioned towards the GLN406 residue site which determines the specificity of compound towards PDE9A whereas the phenyl substituent (phenyl ring with alkyl or halide group at meta-position) positioned towards the hydrophobic region in PDE9A active site. In substitution at N_1 position, modification from methyl to ethyl to propyl was carried out. It was found that with increasing the carbon chain length the binding strength of the compounds increased. With propyl group, the lowest free energy of binding was less than with ethyl group, but the number of conformation in lowest binding energy cluster was only 39. Thus, ethyl substituted compounds were most stable. At C_8 position, the binding with phenyl ring with different modifications at meta-position gave orientation of compounds towards hydrophobic site in PDE9A active site where the residues LEU421, PHE441, VAL447 and ALA452 were placed. These residues formed strong hydrophobic interaction between ligand and protein. In this way, the modification at N_1 and C_8 positions appropriately fitted the compound in the active site pocket of PDE9A. Though substitution at N_3 position was also important for the positioning of these compounds, but modification from aliphatic to aromatic group does not change the orientation of compounds. Modification of the N_3 position determined the binding strength of compounds with PDE9A. Most interesting information obtained from the substitution at N_1, N_3 and C_8 positions was the effect of increasing chain length that increased the binding strength of compounds. **Table 3.2** provides the details of set-1 compounds in terms of different substituent (R_1, R_2 and R_3), lowest free energy of binding, interacting residues, confirmations in largest cluster and number of H-bonds between ligand and protein.

Table 3.2: Set-1 Substitution with aliphatic groups at N_1 and N_3 positions and with aromatic fragment at C_8 position of xanthine scaffold

Sl no.	R_1 (N_1 Substitution)	R_2 (N_3 Substitution)	R_3 (C_8 Substitution)	LFEB (kcal/ mol)	Interacting Residues	NCLC	H bond
23	-H	$-CH_3$	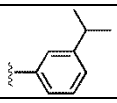	-8.25	ASP402, ASN405	100	2
24	$-CH_3$	$-CH_3$	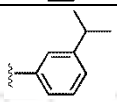	-8.66	GLN453	100	2
25	- CH_3	$-CH_2CH_2CH_3$	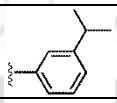	-8.92	GLN453	100	2
26	- CH_2CH_3	$-CH_2CH_2CH_3$	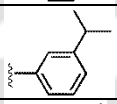	-9.16	GLN453	99	2
27	- CH_2CH_3	$-CH_2CH_2CH_3$	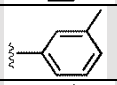	-8.40	GLN453	100	2
28	- CH_2CH_3	$-CH_2CH_2$ CH_2CH_3	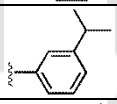	-9.21	GLN453	79	2
29	- CH_2CH_3	$-CH_2CH_2$ CH_2CH_3	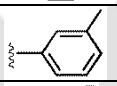	-8.72	GLN453	93	2
30	- CH_2CH_3	$-CH_2CH_2$ CH_2CH_3	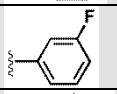	-8.30	GLN453	100	2
31	$-CH_2CH_2CH_3$	$-CH_2CH_2$ CH_2CH_3	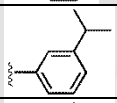	-9.53	GLN453	39	2
32	$-CH_3$	$-CH_2CH_2(CH_3)_2$	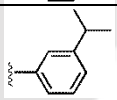	-9.16	GLN453	95	2
33	$-CH_3$	$-CH_2CH_2(CH_3)_2$	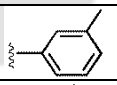	-8.66	GLN453	100	2
34	- CH_2CH_3	$-CH_2CH_2(CH_3)_2$	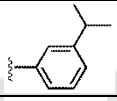	-9.40	GLN453	88	2
35	- CH_2CH_3	$-CH_2CH_2(CH_3)_2$	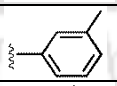	-8.93	GLN453	98	2
36	$-CH_2CH_2CH_3$	$-CH_2CH_2(CH_3)_2$	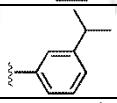	-9.14	GLN453	41	2
37	$-CH_2CH_2CH_3$	$-CH_2CH_2(CH_3)_2$	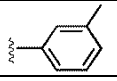	-8.88	GLN453	67	2

LFEB= Lowest free energy of binding, NCLC=Number of conformations in the largest cluster, H-bond= Hydrogen bond

In set-1, compound **34** showed strongest binding with lowest free energy of binding of -9.40 kcal/mol. Compound **28** was the second most potent compound for PDE9A in set-1 which consisted the isomeric fragment of Compound **34** at N_3 position. At N_3 position, compound **28** consisted of n-butyl group whereas, isobutyl group in compound **34**. **Figure 3.5** shows interaction of compound **28** and compound **34** in the active site of PDE9A. Both the compounds formed two H-bonds with GLN453 showing similar interaction pattern in the active site pocket of PDE9A. Likewise, all set-1 compounds from compound **23-37** showed similar binding pattern. Most of these compounds formed two hydrogen bonds with the conserved amino acid residue, GLN453 in the active site of PDE9A. Though compound **34** and compound **28** showed differences in both binding energy and interaction pattern between PDE9A and other members of PDE superfamily, but these differences were quite low mainly because they share similar structure with isomeric fragment at N_3 position as depicted in **figure 3.5** and **figure 3.6**. Thus, we went for another round of modification in which the substitution was carried out at N_3 position with aromatic fragments.

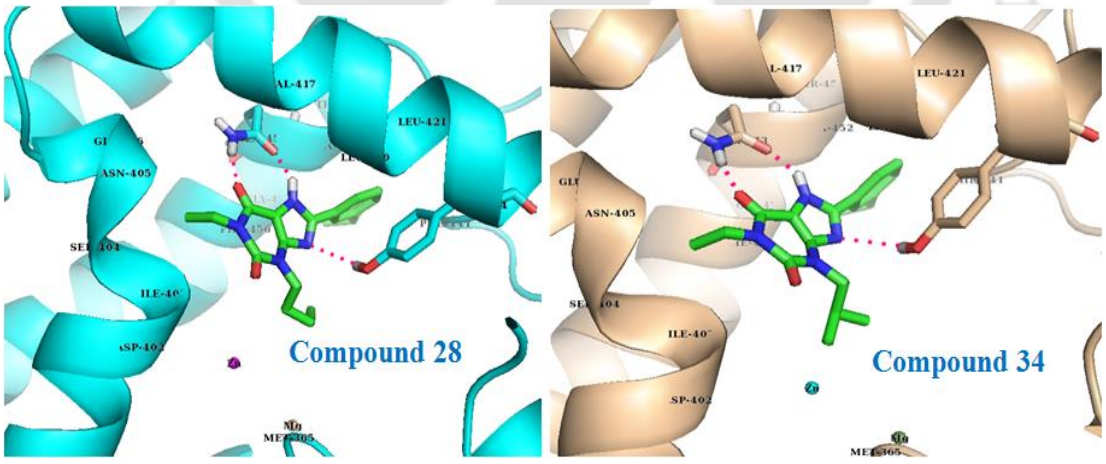

Figure 3.5 Interaction patterns of compound **28** and **34** with PDE9A as seen in PyMol

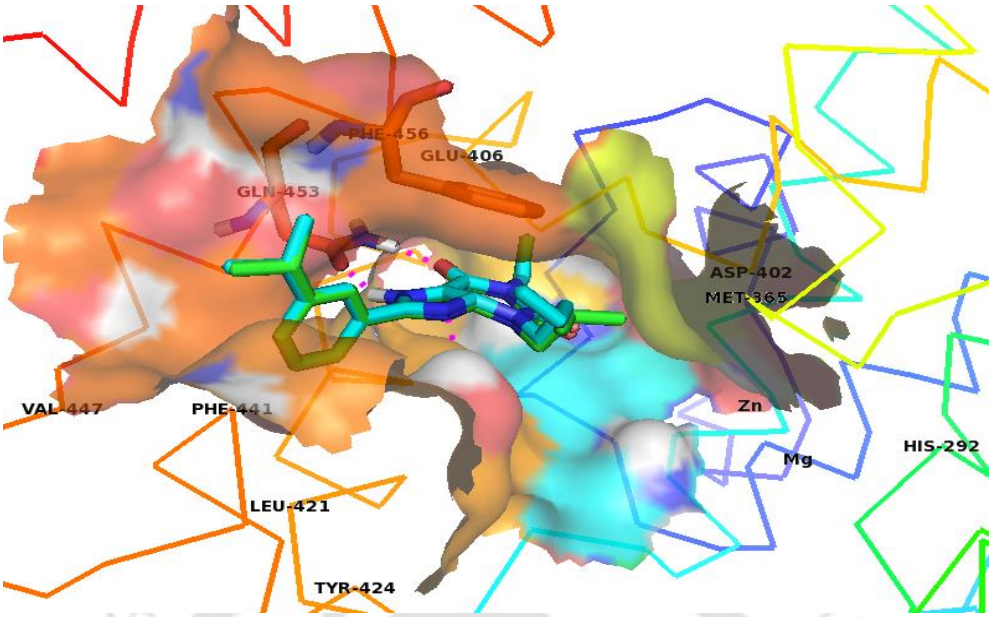

Figure 3.6 Interaction pattern of Superimposed compound **28** and **34** with PDE9A

3.3.4. Interaction study of set-2 compounds with PDE9A

Compound **23-37** showed that substitution at both N_1 and C_8 positions had significant role in the occupancy of compound in the active site pocket of PDE9A. But at the same point, the role of N_3 position cannot be ignored in the selectivity of compound. Modification at N_3 position determined the binding strength of the compound. Moving from substitution of alkyl group to aromatic fragments at N_3 position showed significant impact on decreasing of free energy of binding. Aromatic fragment at N_3 position interacted with higher strength and was positioned towards the histidine rich site of PDE9A of the active site pocket containing HIS252, HIS256, HIS292, ASP293, HIS296, and ASP364. This positioning provides space for electrostatic and van der Waals interaction between ligand and protein. Aliphatic fragment substitution at N_1 position interacted in similar manner like compounds of set-1. Aliphatic fragment at N_1 position positioned towards the GLU406, a key residue in PDE9A which is responsible for stabilizing the side chain of invariant GLN453. With increasing the carbon atom in the aliphatic chain at N_1 position of compound, the interaction stability of the compound

increased with PDE9A. Compounds (**38-52**) showed significant decrease in lowest free energy of binding in the active site of pocket of PDE9A due to the presence of aromatic fragment at N_3 position. **Table 3.3** provides the details of set-2 compounds (**38-52**). The presence of aromatic fragment at N_3 position increased the binding strength of the formed compounds. Compound **38-42** showed good interaction towards PDE9A over other PDEs on account of the difference in lowest free energy of binding. The interaction pattern of these compounds was similar. With increasing carbon chain length of aliphatic fragment at N_1 position from methyl to ethyl to propyl, the interaction strength increased.

Table 3.3: Set-2 List of compounds with substitution with aliphatic groups at N_1 position and aromatic fragment at N_3 and C_8 positions of the xanthine scaffold

Sl no.	R_1 (N_1 Substitution)	R_2 (N_3 Substitution)	R_3 (C_8 Substitution)	LFEB (kcal/ mol)	Interacting Residues	NCLC	H bond
38	-CH_3	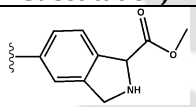	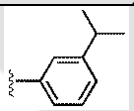	-11.12	GLN453	52	2
39	-CH_2CH_3	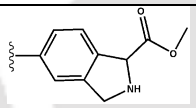	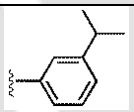	-11.67	HIS252, ASP364, GLN453	66	3
40	-$CH_2CH_2CH_3$	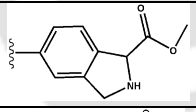	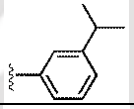	-12.03	HIS252, ASP364, GLN453	90	3
41	-CH_3	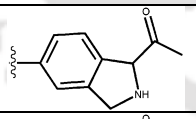	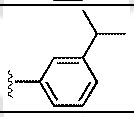	-11.29	GLN453, HIS252,	52	2
42	-CH_2CH_3	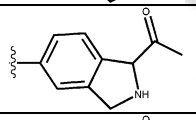	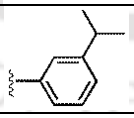	-11.62	GLN453	66	2
43	- $CH_2CH_2CH_3$	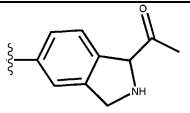	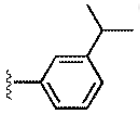	-12.23	GLN453	92	1
44	- CH_2CHO	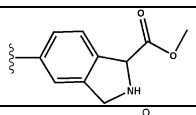	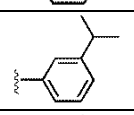	-12.25	MET365, GLU406, GLN453, PHE456	92	4
45	- CH_2CHO	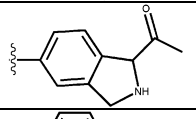	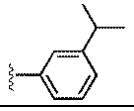	-12.53	MET365, GLU406, GLN453, PHE456	97	4
46	- CH_2CHO	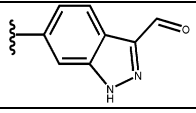	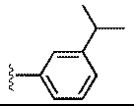	-11.41	MET365, GLU406, GLN453, PHE456	68	4

47	- $CH_2CH_2CH_3$	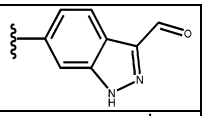	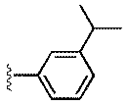	-12.23	GLN453	92	1
48	- CH_2CHO	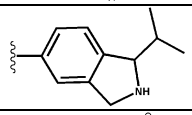	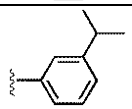	-12.43	THR363, ASN405, GLN453	83	2
49	- CH_2CHO	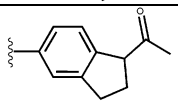	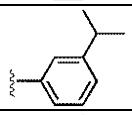	-10.74	MET365	42	1
50	- CH_2CHO	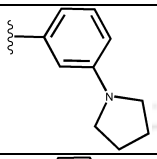	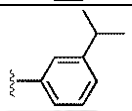	-12.31	GLU406, GLN453	100	3
51	- CH_2CHO	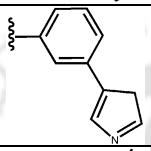	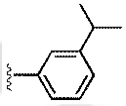	-11.45	ASP402, GLU406	100	2
52	- CH_2CHO	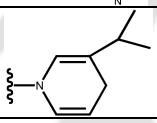	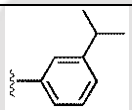	-12.43	THR363, ASN405, GLN453	99	3

LFEB= Lowest free energy of binding, NCLC=Number of conformations in the largest cluster, H-bond= Hydrogen bond

Among these four compounds, compound **40** showed the highest specificity for PDE9A over other PDEs. The lowest free energy of binding of compound **40** in PDE9A was -12.03 kcal/mol. Top conformations showed difference in RMSD in the range of 0.06-1.78 Å as compared to the crystal structure of PDE9A. In compound **40**-PDE9A complex, interacting residues were HIS252, ASP364, GLN453 and PHE456**.** PHE456 formed π-π interaction with selective compounds, whereas, HIS252, ASP364 and GLN453 were involved in hydrogen bond interaction with the respective compounds. C_8 substitution with phenyl substituent positioned towards the hydrophobic region of active site pocket of PDE9A and established strong hydrophobic-hydrophobic interaction with protein. **Figure 3.7** shows interaction pattern of Compound **40** with PDE9A in terms of hydrogen bond formation. **Figure 3.8** illustrates the surface view compound **40** -PDE9A

complex. Surface view gives the idea about the orientation of positioning of compounds in active site pocket.

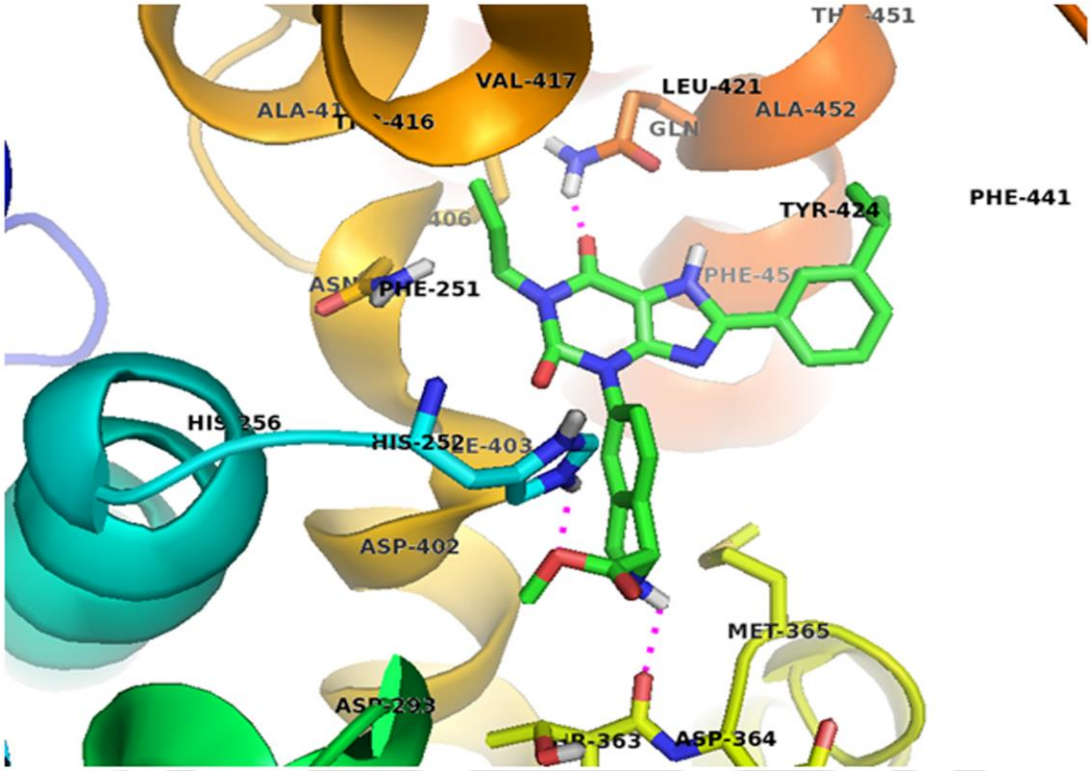

Figure 3.7 Interaction pattern depiction of compound **40** with PDE9A as seen in PyMol

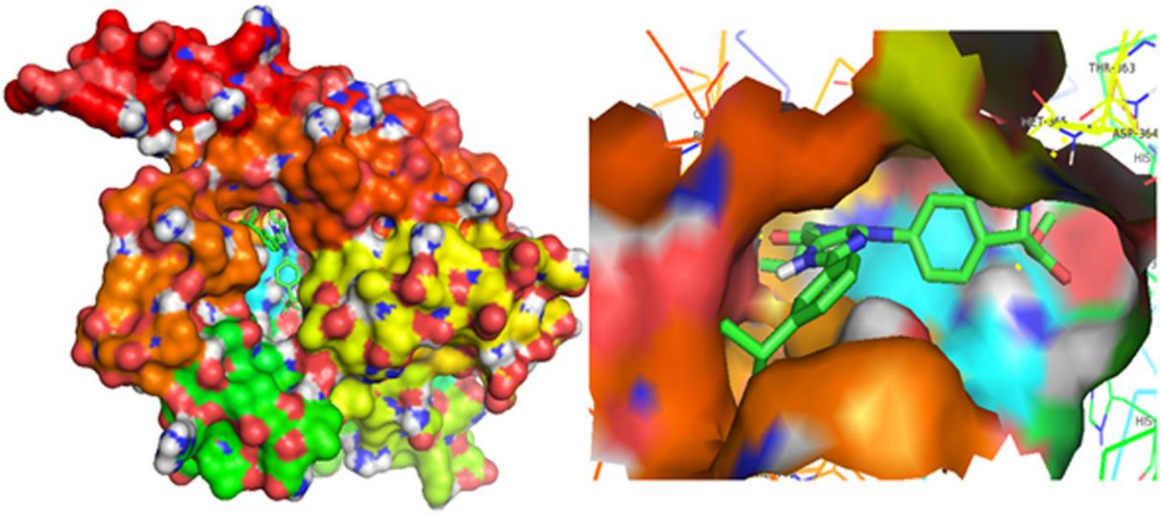

Figure 3.8 Depiction of the surface view of compound **40** when it interacts with PDE9A

3.3.5. Comparative interaction study of the best compounds from set-1 and set-2 with various members of PDE superfamily

Compound **34** and compound **40** were the best compounds obtained from set-1 and set-2, respectively. These two compounds were taken for comparative interaction studies to decide the suitability of compounds for next step of drug development process. **Table 3.4** presents the results of comparative docking study of Compound **34** and compound **40** in various members of PDE superfamily in terms of their lowest free energy of binding in largest cluster, inhibition constant, number of clusters, interacting residues and number of hydrogen bonds. Interaction pattern of compound **34** was similar to that of compound **40**. But in terms of lowest free energy of binding, compound **40** showed better binding strength than Compound **34**. Both compound **34** and compound **40** showed better potency towards PDE9A among all PDEs. Based on the docking data, set-1 compounds interacted with PDE9A by forming two hydrogen bonds whereas selected set-2 compound formed three hydrogen bonds in the active site of PDE9A. Compound **40** showed better binding strength towards PDE9A than compound **34** due to presence of aromatic fragment at N_3 position. In terms of hydrogen bond interaction, compound **34** formed two hydrogen bonds with GLN453 while Compound **40** formed three hydrogen bonds with HIS252, THR363 and GLN453. GLN453 is a conserved residue in all PDEs which plays significant role in substrate/inhibitor selectivity because of orientation of the side chain of GLN453. In PDE9A the orientation of GLN453 is decided by the intermolecular H-bond interaction with neighboring residue GLU406. In compound **34**-PDE9A complex GLN453 formed two H-bonds with compound whereas in compound **40**-PDE9A complex GLN453 formed only one H-bond. Thus, in terms of inhibitor selectivity by GLN453, set-1 compounds formed firm interaction with PDE9A.

Whereas selected set-2 compound formed only one H-bond with GLN453. The second H bond (which was formed in case of set-1 compounds) broke as the compound was pulled away. As seen from **figure 3.7**, the –NH group of N_7 position was pulled away from the GLN453 side chain. This condition arose due to strong interaction established by polar aromatic fragment at N_3 position of compound **40** in the histidine rich site of PDE9A active site. Hence, due to presence of aromatic fragments, set-2 compounds formed better overall interaction than set-1 compounds. However, in terms of better selectivity of the compound/inhibitor by interaction with GLN453 (the specificity deciding amino acid), set-1 compounds showed better interaction with PDE9A (they formed two hydrogen bond as seen from **figure 3.5**).

Comparative interaction analysis with cGMP specific phosphodiesterase - PDE5A

Both PDE9A and PDE5A are cGMP specific proteins but their structures are very different from each other. PDE9A forms dimer in natural state whereas, PDE5A does not form dimer. Because both have specificity towards cGMP, it was very important to modify inhibitors in such a way that the inhibitor will be specific towards PDE9A. The best compounds from both set-1 (compound **34**) and set-2 (compound **40**) showed significant difference in the interaction pattern with PDE9A and PDE5A. To inhibit the protein, the compound should be able to enter into the active site. Both compound **34** and compound **40** completely entered into the active site pocket of PDE9A whereas, in case of PDE5A, they restricted at the mouth of the active site pocket of PDE5A as seen from **figure 3.9.** The reason behind this might be either its bigger size than the active site pocket or repulsion towards the compound in the active site of PDE5A. The compound was restricted at the entrance of the active site though, the compound interacted by one hydrogen bond at the outer surface. This limited interaction made excellent difference in

binding pattern of compound between two cGMP specific PDEs (PDE9A and PDE5A) which led to confirm the specificity of compounds towards PDE9A. **Figure 3.9** depicts the surface view and binding patterns of compound **34** and compound **40** bound PDE5A.

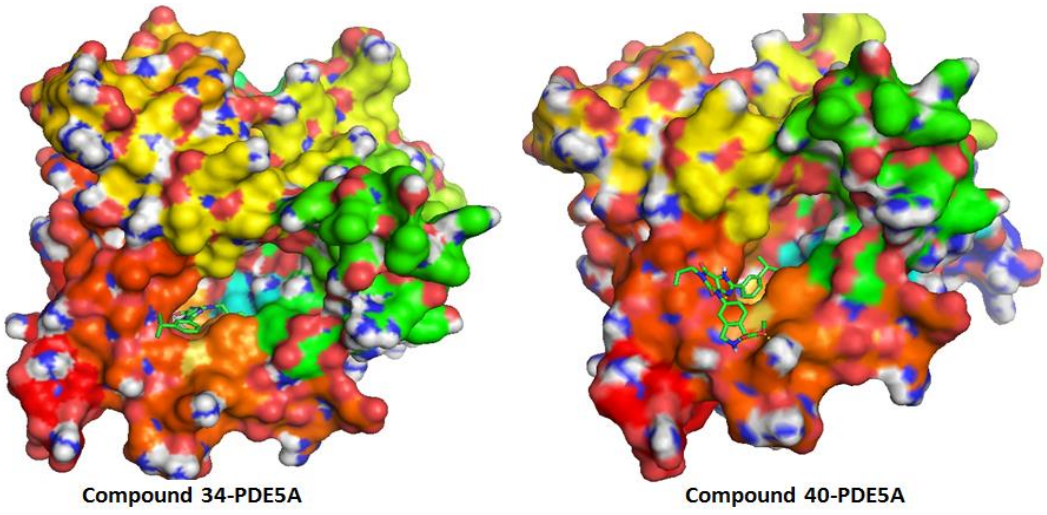

Figure 3.9 Surface view of PDE5A-compound **34** complex (left) and compound **40** complex (right) in PDE5A

Table 3.4 Comparative analysis of docking of compound **34** and **40** with various members of PDE superfamily

Type	Specificity	Best compound (compound 34) from set-1					Best compound (Compound 40) from set-2				
		LFEB (kcal/mol)	NCLC	No. of clusters	Interacting Residues	H bonds	LFEB (kcal/mol)	No. of clusters	NCLC	Interacting Residues	H-bonds
PDE 9A	cGMP	-9.40	88	3	GLN453, TYR424, PHE456	3	-12.03	90	2	HIS252, THR363, GLN453	3
PDE5A	cGMP	-8.43	84	2	LYS812	1	-7.18	40	8	LYS812	1
PDE4D	cAMP	+13.46	-	-	No H-bond	0	+19.96	-	-	No H-bond	0
PDE7A	cAMP	-8.87	98	2	GLN413	1	-10.98			GLN413, HIS212	2
PDE8A	cAMP	-5.22	*Not entered into the active site*			0	-6.98	*Not entered into the active site*			0
PDE1B	dual specific	-7.16	40	9	GLN421		-9.04	61	10	HIS223, GLU293	2
PDE3B	dual specific	+23.21	-	-	No H-bonding	0	+43.09	-	-	No H-bonding	0
PDE2A	dual specific	-8.61	42	3	GLN859	1	-10.27	22	9	ASP808	
PDE10A	dual specific	-7.55	79	3	TYR524	1	-10.17	22	11	GLU592	1

NCLC=Number of conformation in largest cluster, LFEB=Lowest free energy of binding, H-bond=Hydrogen bond

Comparative interaction analysis with cAMP specific phosphodiesterase PDE4D, PDE7A and PDE8A

The phosphodiesterase enzymes which show specificity toward the substrate cAMP are commonly known as cAMP specific phosphodiesterase. PDE4D, PDE7A and PDE8A fall into this category. Among all these, PDE8A active site is very similar to PDE9A due to the presence of TYR748. TYR is present at the entrance of active site pocket of both PDE9A (TYR424) and PDE8A (TYR748), whereas, in other PDEs, the corresponding position is occupied by phenylalanine (Huai et al., 2004; Singh and Patra, 2014). Therefore, the binding pattern of most of the compounds was similar in both PDE9A and PDE8A. Interestingly, presence of GLU406 in PDE9A fixed the orientation of amide of GLN453 side chain by the formation of intermolecular hydrogen bond. GLU406 also created difference in the binding pattern in both PDE8A and PDE9A. However, compound **38-42** showed significant difference in the binding pattern of ligands in the active site of PDE9A and PDE8A. In case of PDE8A, compound **38-42** was unable to enter into the active site pocket of the enzyme and was binding somewhere else on the surface of the protein as shown in **figure 3.10**. The main reason behind this significant difference in the binding pattern between PDE8A and PDE9A was the substitution with alkyl group at the N_1 position of compounds **38-42** of set-2. The compounds having carbonylated aliphatic fragment were unable to make such difference in the interaction pattern in the active site of PDE8A and PDE9A. In Compounds **38-42**, interesting difference was encountered in the binding pattern of PDE8A and PDE9A because of the presence of alkyl group at N_1 position. But only substitution with alkyl group at N_1 position was not sufficient to determine the difference in binding pattern between PDE9A and PDE8A. The positioning of alkyl group at N_1 position and phenyl

substituent (phenyl ring with alkyl substitution at meta-position) at C_8 position were together responsible for creating such difference in the binding pattern of the compound **38-42** of set-2 with PDE9A and PDE8A. Among all selected compounds, compound **40** showed best interaction towards PDE9A maintaining the difference in lowest free energy of binding of 5.05 kcal/mol between PDE9A (-12.03 kcal/mol) and PDE8A (-6.98 kcal/mol). **Figure 3.10** illustrates the surface view of compound **40**-PDE8A complex. Surprisingly, compound **34** and other derivatives of set-1 also showed similar significant difference in binding pattern of PDE9A and PDE8A. This affirmed the fact that N_3 modification created little impact in selectivity between PDE9A and PDE8A.

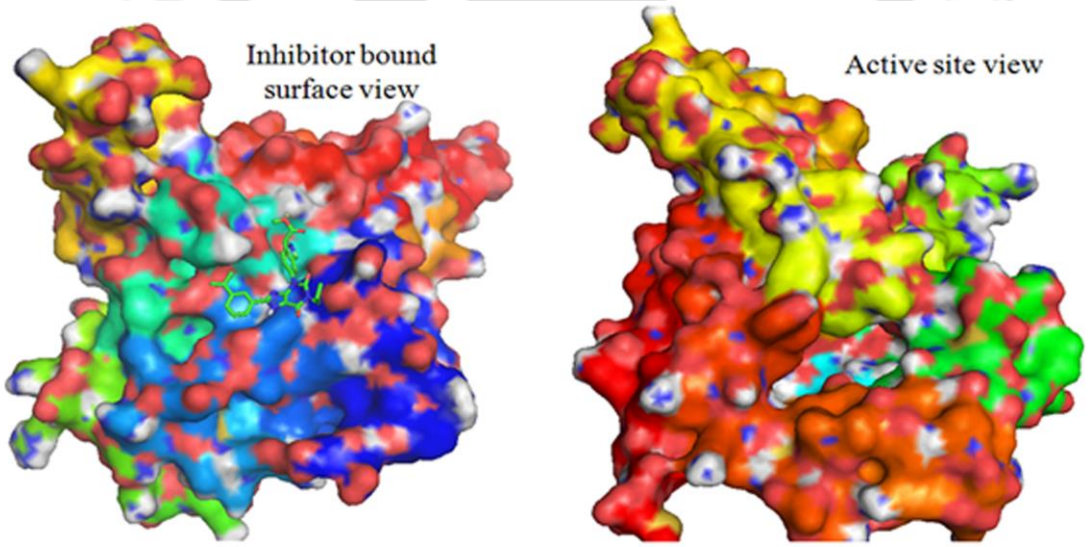

Figure 3.10 Interaction of Compound **40** with PDE8A - inhibitor bound surface view (left) and empty active site view (right)

With PDE4D, most of set-1 compounds and compound **38-42** from set-2 were unable to interact. In PDE7A, compound **34** and compound **40** interacted with lowest free energy of binding -8.87 and -10.98 kcal/mol, respectively. In PDE7A, compound **34** formed one hydrogen bond with GLN413 whereas, compound **40** formed two H-bonds with GLN413

and HIS212. These compounds were interacting with PDE7A but the strength of interaction was comparatively lower than with PDE9A.

Comparative interaction analysis with dual-specific phosphodiesterases - PDE1B, PDE2A, PDE3B and PDE10A

Some phosphodiesterases such as PDE1B, PDE2A, PDE3B and PDE10A show affinity for both substrates-cAMP and cGMP. As per many reports, PDE1B has adverse side effects on PDE9A inhibition. This is because of its abundance in the brain (Andreeva et al., 2001). To improve selectivity towards PDE9A, it was necessary to make difference in the binding pattern and binding energy between PDE9A and PDE1B. Thus, along with higher specificity towards PDE9A it was important to reduce the side effects of PDE1B. Reducing side effects of PDE1B during inhibitor designing for PDE9A will be an important improvement while developing specific inhibitors for treatment of neurodegenerative diseases (Meng et al., 2012). Hence, compounds were modified in such a way that observable difference would be created. Both Compound **34** and Compound **40** showed noteworthy differences in free energy of binding, H-bond interaction, hydrophobic interaction and van der Waals interactions between PDE9A and PDE1B. In comparison to PDE9A, PDE1B formed lesser contacts with selected compounds of both sets. Compound **34** formed one hydrogen bond with GLN421 with lowest free energy of binding -7.16 kcal/mol whereas, compound **40** formed two H-bonds with HIS223 and GLU293 with lowest free energy of binding of -9.04 kcal/mol. Hence, with significant difference in the level of interaction with both PDE9A and PDE1, compound **34** and compound **40** might be able to reduce the side effects of PDE1B.

3.3.6 Analysis of predicted pharmaceutical properties of set-1 and set-2 compounds

Though compounds from both sets showed significant potency towards PDE9A over other PDEs, pharmaceutical activity determination was critical to make crucial decision for taking the designed compounds for further studies. Final validation and comparison between set-1 and set-2 compounds were performed by the analysis of their drug-likeness and pharmaceutical properties. Therefore, to pursue with inhibitors for further studies, it was necessary to find out the possibilities of these compounds to be pharmaceutically active. For this, the drug-likeness properties, ADMET properties and toxicity prediction were performed using PreADMET online server [https://preadmet.bmdrc.kr/]. Eight most potent compounds from set-1 and four most potent and selective compounds from set-2 were selected for comparative studies. Among them, set-1 compounds were proved to be better pharmaceutically active compounds, whereas, set-2 compounds were found to be poor in pharmaceutical properties. The details of their drug-likeness and ADMET properties have been shown in **Table 3.5** and **Table 3.6**. PDE9A has abundance in brain; hence, preferably the compound should be CNS active in nature. To be a suitable drug candidate, compounds should have standard blood brain barrier (BBB) permeability. Based on the earlier studies, standard BBB permeability for compound should be above 2. By the comparative analysis of compounds from both sets, it was found that set-1 compounds were better in their BBB permeability. However, set-2 compounds were poor in BBB permeability and other pharmaceutical properties such as MDDR rule, WDI rule, CMC like rule, etc. In set-1 compounds, compound **28** and compound **34** were the most pharmaceutically active compounds. The BBB permeability of compound **28** and **34** were 4.52008 and 4.25033, respectively. The higher BBB permeability supported the

suitability of these compounds to target PDE9A in brain to treat neurodegenerative diseases. Set-1 compounds also fulfilled the Lipinski rule of five along with other drug-likeness properties such as MDDR rule, WDI rule, CMC like rule etc. The result of drug-likeness properties of set-1 compounds are summarized as: (i) molecular weight is less than 500 Da, (ii) hydrogen-bond donor atoms are less than five (iii) hydrogen-bond acceptors are less than 10, and (iv) cLogP value is less than 5 and the molar refractivity is in the range of 40−130. Based on the pharmaceutical properties values obtained from the PreADMET web tool, it was assumed that the set-1 compounds could have potential to be better drug candidates for PDE9A. Compound **28** was the only compound of set-1 which possessed "drug-like" MDDR properties. From the pharmaceutical property analysis, compound **28** was found to be most active compound amongst all selected compounds. Hence, compound **28** was selected for further comparative study with existing inhibitors.

Table 3.5 Drug-likeness, ADMET properties and toxicity properties of selected set-1 compounds

Ligand	CMC like rule	MDDR rule	Rule of 5	WDI rule	HIA %	C2C Permeability (nm/sec)	MDCK (nm/sec)	LOG kP (cm/hr)	PPB %	BBB	AMES Test
Compound 25	Qualified	Mid-structure	Suitable	In 90% cutoff	91.9	22.6956	16.8414	-3.58301	88.473	2.91	M
Compound 26	Qualified	Mid-structure	Suitable	In 90% cutoff	92.2	25.1965	0.83886	-3.46886	87.872	3.59	M
Compound 27	Qualified	Mid-structure	Suitable	In 90% cutoff	91.59	22.5532	31.0647	-3.69949	87.6285	2.308	M
Compound 28	Qualified	Drug-like	Suitable	in 90 of cutoff	92.5	26.5615	0.83169	-3.32096	88.0310	4.52008	M
Compound 29	Qualified	Mid-structure	Suitable	In 90% cutoff	91.92	23.5057	10.3494	-3.55643	88.0761	3.10388	M
Compound 31	Qualified	Mid-structure	Suitable	In 90% cutoff	91.62	33.9384	6.56881	-3.87227	86.8493	2.52511	M
Compound 33	Qualified	Mid-structure	Suitable	In 90% cutoff	92.22	24.2156	0.536568	-3.4678	88.4337	3.53723	M
Compound 34	Qualified	Mid-structure	Suitable	in 90 of cutoff	92.51	27.0553	0.084916	-3.35269	87.8646	4.25033	M

MDDR-like rule: nondrug-like / drug-like / mid-structure, MDCK (MDCK = Madin-Darby canine kidney cell,) cell permeability (nm/sec), Skin permeability (logKp, cm/hour), BBB- blood-brain barrier penetration, WDI = World Drug Index, PPB = Plasma Protein Binding, BBB = Blood Brain Barrier, C2C = $CaCo_2$ Cell, M = Mutagen, HIA = Human Intestinal Absorption.

Table 3.6 Drug-likeness, ADMET properties and toxicity properties of selected set-2 compounds

Ligand	CMC like rule	MDDR rule	Rule of 5	WDI rule	HIA%	C2C Permeability (nm/sec)	MDCK (nm/sec)	Log Kp (cm/hr)	PPB %	BBB	AMES Test
Compound 38	Qualified	Mid-structure	Suitable	Out of 90% cutoff	91.66	19.15	0.056	-4.00	77.06	0.25	M
Compound 39	Not-Qualified	Mid-structure	Suitable	Out of 90% cutoff	91.96	19.77	0.045	-3.82	79.78	0.37	M
Compound 40	Not-Qualified	Drug-like	Suitable	Out of 90% cutoff	92.26	20.55	0.044	-3.62	83.84	0.64	M
Compound 41	Qualified	Mid-structure	Suitable	Out of 90% cutoff	92.12	17.57	0.071	-4.02	74.94	0.32	M
Compound 42	Qualified	Mid-structure	Suitable	Out of 90% cutoff	92.42	18.64	0.045	-3.81	78.00	0.47	M

MDDR-like rule: nondrug-like / drug-like / mid-structure, MDCK (MDCK = Madin-Darby canine kidney cell,) cell permeability (nm/sec), Skin permeability (logKp, cm/hour), BBB- blood-brain barrier penetration, WDI = World Drug Index, PPB = Plasma Protein Binding, BBB = Blood Brain Barrier, C2C = $CaCo_2$ Cell, M = Mutagen, HIA = Human Intestinal Absorption.

3.3.7. Comparative binding study of set-1 compounds and existing xanthine derivative

The comparative interaction study with known xanthine inhibitors was needed to understand the impact of change carried out during the manual designing process. In this study, IBMX was used as reference molecule to understand the interaction pattern of newly designed compounds. It bound with PDEs mostly at the invariant glutamine. Since glutamine is conserved in active site of all PDEs, hence, the interaction has been mostly non-selective. **Figure 3.11** illustrates the comparative interaction pattern of compound **28** and IBMX in the active site of PDE9A.

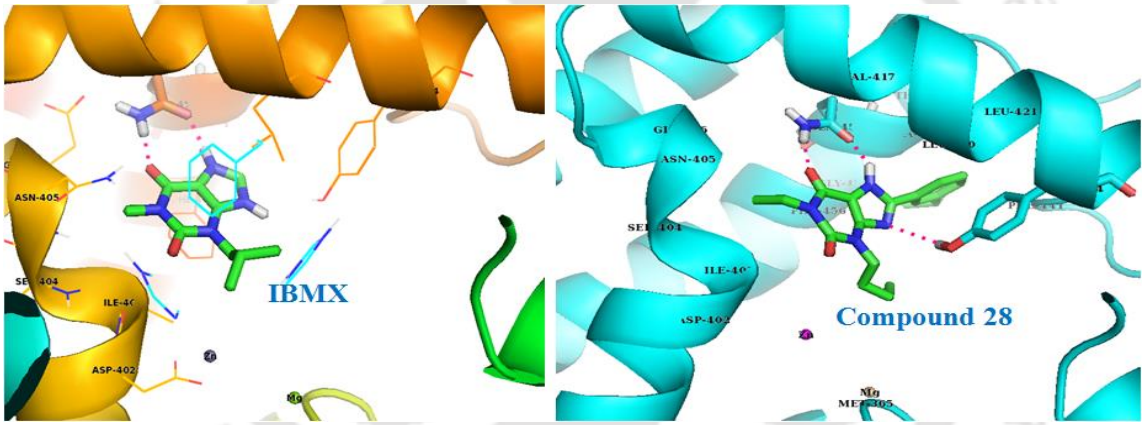

Figure 3.11 Comparative interaction pattern of IBMX (left) and compound **28** (right) with PDE9A

The interaction of compound **28** showed similar interaction pattern as shown by IBMX in PDE9A active site. IBMX formed two H-bonds with invariant GLN453 of PDE9A active site. The set-1 compounds developed from the manual designing interacted with GLN453 by forming two hydrogen bonds. Compound **28** was bound in similar orientation as IBMX was bound in the active site PDE9A as illustrated in **figure 3.11**. Like IBMX, Compound **28** formed two H-bonds with GLN453. The phenyl substituent with isopropyl group at meta-position positioned towards the hydrophobic

region of the PDE9A active site. This led to strong hydrophobic-hydrophobic interaction between the protein and ligand. C_8 substitution with aromatic fragment increased the binding strength of the compound and also stabilized the position of compound in PDE9A active site. Therefore, the bigger size of Compound **28** was responsible for establishing better interactions with PDE9A as compared to IBMX. Compound **28** with free energy of binding of -9.21 kcal/mol showed better specificity than non-selective IBMX with lowest free energy of binding of -5.71 kcal/mol towards PDE9A. As per the difference in interaction between IBMX and compound **28**, the later might have better potential as an inhibitor of PDE9A. As most of the set-1 compounds have similar binding pattern, they can be considered as good inhibitors for PDE9A.

3.3.8 Comparative binding study of set-1 compounds and known PDE9A inhibitor

The interaction pattern of known PDE9A inhibitors (BAY73-6391) in the active site of PDE9A further confirmed the significance of GLN453 in inhibitor selectivity towards PDE9A. BAY73-6691 formed two H-bonds with the side chain of GLN453 in the active site pocket of PDE9A. In PDE9A-BAY73-6691 complex, the C=O of C_6 site and NH of N_1 site of BAY73-6691 involved in interaction with GLN453 of PDE9A, whereas, in PDE9A-compound **28** complex, the C=O of C_6 site and NH of N_7 site of compound **28**, was involved in H-bond interaction with GLN453 of PDE9A. Hence, compound **28** and BAY73-6691 interacted in opposite orientation with GLN453 in PDE9A active site. **Figure 3.12** illustrates the comparative interaction study of BAY73-6691 and compound **28** with PDE9A.

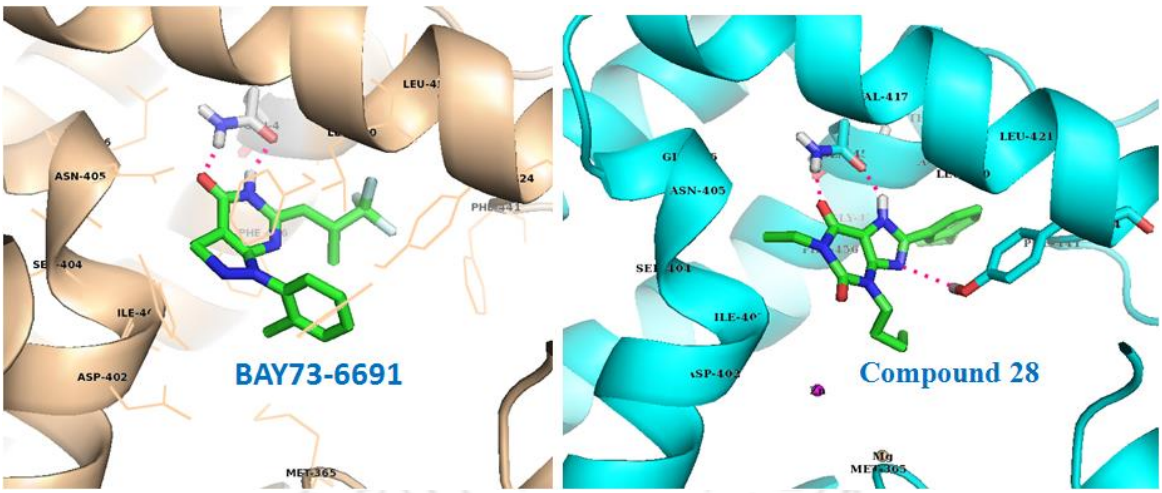

Figure 3.12 Comparative interaction pattern of BAY73-6691 and compound **28** with PDE9A

This comparative interaction studies suggested the affinity of GLN453 in inhibitor selectivity was dependent on the compound either with unsubstituted N_1 position or with unsubstituted N_7 position. Since pyrazolopyrimidinone and xanthine scaffolds share structural similarity, hence compounds based on both scaffolds shared similarity in their interaction pattern with PDE9A. For targeting invariant residue GLN453, carbonyl group at C_6 along with unsubstituted –NH at N_1 position of pyrazolopyrimidinone or N_1 and/or N_7 position of xanthine were required to establish hydrogen bond interaction between ligand and protein. This study gave idea about the structural details of inhibitors required for making them desirable specific inhibitors of PDE9A.

3.4. Conclusion

By utilizing the uniqueness of PDE9A structure among all PDEs, this study tried to construct potent inhibitor for PDE9A. From the present chapter eight compounds were selected for chemical synthesis and further biological studies. To achieve at the same, nearly 200 compounds were manually designed by selecting four different sites - N_1, N_3, N_9 or/and C_8 for substitution at xanthine scaffold. Molecular docking was carried out to

analyze the binding efficiency of these compounds with PDE9A. Based on the lowest free energy of binding, 52 compounds were selected for comparative study in all PDEs by keeping lowest free energy of binding cut off of -6.0 kcal/mol. N_9 substitution was not suitable for PDE9A because of the retro-orientation of double bond between N_7 and N_9 in imidazole ring of xanthine. Substitutions at N_1, N_3 and C_8 positions showed best sites for selective interaction with PDE9A. Two sets of compounds were discovered with substitutions at N_1, N_3 and C_8 positions. Both sets were differentiated mainly on the N_3 substitution. Set-1 compounds substituted with aliphatic fragment at N_3 site, whereas, in set-2 compounds N_3 position was substituted with aromatic fragments. Due to the presence of aromatic fragment at N_3 position, set-2 compounds showed better binding strength with PDE9A than set-1 compounds. However, the presence of aromatic fragment at N_3 position in set-2 compounds gave polarity as well as rigidness to the compounds that might be a major reason behind their poor pharmaceutically active nature. Interestingly, most of the set-1 compounds possessed pharmaceutically active properties.

Side effect with PDE1 has been the major bottleneck in making the existing inhibitors successful towards PDE9A. Best compounds from both the sets showed significant specificity for PDE9A over PDE1B. Most of the designed compounds showed similar binding pattern in both PDE9A and PDE8A due to presence of TYR424 at the corresponding positions of both PDE9A and PDE8A. This similarity could create diminutive effect while treating neurodegenerative diseases as PDE8A is negligibly present in brain. Most of compounds of set-1 and compound **38-42** of set-2 showed significant difference in binding pattern in PDE9A and PDE8A. These compounds were unable to enter into the active site pocket of PDE8A. This difference was important to construct inhibitors specific for PDE9A. Hence, present study resulted in two types of

compounds- eight compounds (25, 26, 27, 28, 29, 31, 33 and 34) from set-1 and five compounds (38, 39, 40, 41 and 42) from set-2.

Though compounds from set-2 showed better interaction than compounds from set-1, but less pharmaceutical activeness of later appealed to choose eight compounds from set-1 for further studies. From this chapter it can be concluded that (i) substitution with aliphatic fragment at N_1 position was deciding factor for making difference between PDE9A and PDE8A, (ii) substitution at C_8 position determined the stability of compounds because of the presence of aromatic fragment with aliphatic chain at meta-position, and (iii) substitution at N_3 position with aliphatic chain rendered pharmaceutically active nature to the compounds. Thus, with these concluding remarks, eight set-1 compounds were selected for chemical synthesis and further biological studies.

CHAPTER 4

Chemical Synthesis of Selected Xanthine Derivatives

Prologue

Structure based drug designing approach used in chapter 3 gave some promising results for PDE9A. Among the two sets of compounds which established potency for PDE9A, eight compounds from set-1 were chosen for their chemical synthesis because of their better interaction affinity for PDE9A and drug-likeness properties. Therefore, using computational approach the unnecessary burden of random chemical synthesis was reduced. Only those compounds were to be synthesized which showed promising in silico results towards PDE9A among all PDEs, but synthesis of xanthine derivative was not an easy task. Most of the earlier researchers have relied on the ring-closure synthesis and classical condensation procedures for the synthesis of xanthine derivative. But these procedures suffer from major bottlenecks that directly challenges the basic principles required to be followed by any drug viz. affordability, accessibility and availability. Hence, the quest for new synthesis approach is need of the hour. This chapter focuses on designing innovative approach for the synthesis of selected novel compounds. The schemes used xanthine as a starting material, were cost effective, time saving, affordable and accessible. Synthesizing xanthine derivatives from xanthine was a novel initiative in the field of xanthine based drug development. Thus, by chemical synthesis, we obtained selected compounds for their final validation by biological studies.

4.1. Introduction

Xanthine derivatives are significant in various pharmaceutical applications. One of the most validated targets of these derivatives is the phosphodiesterase superfamily (Allwood et al., 2007). Most of the xanthine derivatives are reported as non-specific inhibitors of various PDEs. In recent years, modification on existing well known drugs have been targeted in drug development process for enhancing the suitability of compounds towards their targets to lessen the toxicity and increasing the efficiency of the compound. *In silico* studies in previous chapter suggested the uniqueness of N_1, N_3 and C_8 positions for selective inhibitor development for PDE9A. Based on the *in silico* studies, it was found that N_1 site is the selectivity determining factor, N_3 site determines the binding strength of ligand and protein based on the lowest free energy of binding energy while C_8 site determines the hydrophobic-hydrophobic interaction between ligand and protein. Above all, the binding/inhibition affinity of the compound is decided by the carbonyl group at C_6 position and –NH group at N_7 position. **Figure 4.1** depicts the biological implication of different substitution sites of the xanthine molecule.

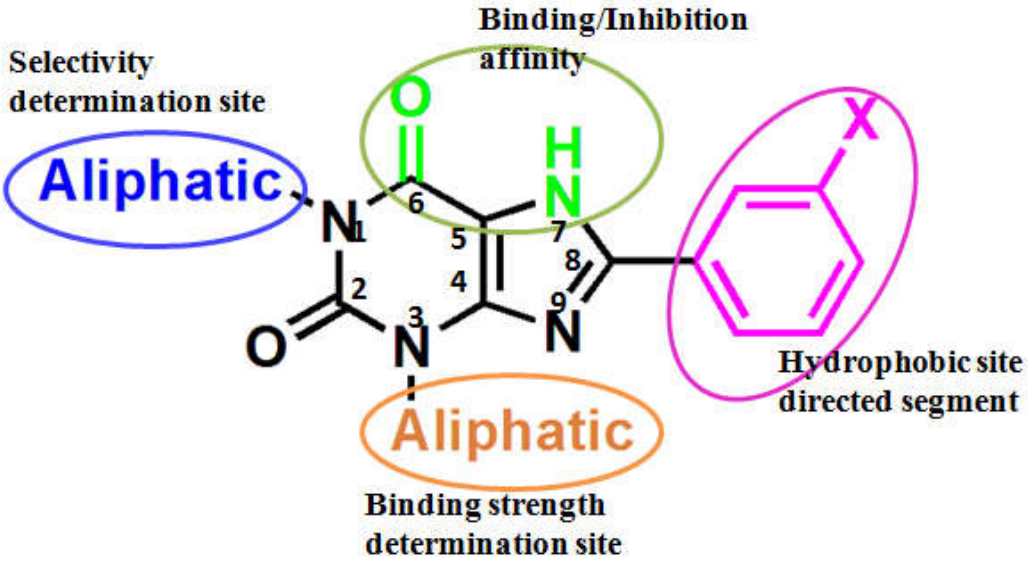

Figure 4.1 Biological importance of different substitution sites of xanthine

Due to wider pharmaceutical application of natural xanthine derivatives, it has opened enormous opportunities for synthesis of xanthine based compounds. In last few decades, based on the natural xanthine derivatives, number of xanthine based inhibitors have been synthetically developed and reported as therapeutic molecule (Glennon et al., 1981; Wong and Ooi, 1985). In drug development process, one of the major challenges is deciding the lead molecule which acts as scaffold to provide avenue for achieving maximum diversity. Xanthine with versatile and structurally rigid scaffold provides scope for molecular diversity in constructing xanthine derivatives for combinatorial chemistry (Heizmann and Eberle, 1997).

Despite of wider pharmaceutical applications, xanthine based research has not taken up full pace as it ought to have. This resulted in very few xanthine based molecules synthesized so far. The most probable reason for this 'lacking' has been the use of unfavorable synthetic process available till date. Most of the previous research has proposed the ring closure synthetic route and classical condensation route for the synthesis of the xanthine derivatives (Allwood et al., 2007; Bandyopadhyay et al., 2012; Bussi et al., 2006). These schemes suffer from numerous bottlenecks, such as the use of acid/base or external oxidant, isolation of imine intermediate, use of toxic and expensive reagents/catalysts, high temperature, hazardous solvents lengthened reaction time, tiresome workup, formation of by-products, low yields, expensive chemicals, etc. (Bandyopadhyay et al., 2012; Ivanov et al., 1992). Thus, classical condensation and ring closure methods are not suitable for the synthesis of diverse derivatives because these synthesis methods require multiple steps and inaccessible chemicals to initiate reaction and yet the end result is low yield product formation (Bandyopadhyay et al., 2012; Kim et al., 2010; Lee et al., 2016). Another approach for the synthesis of new xanthine derivatives have been the use of existing xanthine based molecules such as Theophylline,

Caffeine, Theobromine, etc. (Chen et al., 2014; Kim et al., 2010; Sakai et al., 1992). The problem with using these compounds as starting material is their limited available sites for substitution. For instance, in case of Theophylline, N_1 and N_3 sites are already occupied by methyl groups. Thus, only N_7 and C_8 positions are available for the substitution (Kim et al., 2010).

Considering the above limitations, there was an urgent need to find out a viable alternative to overcome the existing issues. The quest for new synthesis route has been the most challenging task for researchers working with xanthine derivatives (Bandyopadhyay et al., 2012; Hayallah et al., 2002). Abundance of xanthine both biologically and synthetically, makes xanthine an ideal choice as reaction initiator for synthesis of its derivatives. Additionally, using xanthine as a starting material to synthesize its derivatives has several benefits including its easy availability, cost effectiveness, reduced time and possibility of large scale synthesis. With this initiative only modification at different positions of xanthine was required without disturbing the ring of xanthine. The present study proposes new synthesis routes for xanthine derivatives. It provides insight to understand the structure of 'xanthine' as a 'scaffold' and as 'reaction initiator' for synthesizing xanthine derivatives. Understanding the nature of xanthine molecule would probably aid to sort out the existing hurdles faced by researchers in this field. It would smoothen the synthesis path and make 'xanthine' a better choice both as 'scaffold' and 'reaction initiator' to bring out diversification in derivatisation of xanthine based drug development process.

4.2. Material and Methods

4.2.1. Chemicals

The chemicals used for chemical synthesis were purchased from Sigma Aldrich, Merck Private Ltd, Spectrochem Private Ltd and HiMedia.

4.2.2. Selection of compounds for chemical synthesis

In silico studies established N_1, N_3 and C_8 sites on xanthine scaffold as potential binding sites for inhibitor development targeting PDE9A (Bandyopadhyay et al., 2012; Chappe et al., 1998; Miyamoto et al., 1993). The aim of the synthesis described here was to construct specific compounds for PDE9A. Eight compounds were selected from set-1 because of their suitability with drug-likeness properties and ADMET properties. PDE9A is a brain expressing protein hence, the compounds should have CNS active properties. The selected compounds from set-1 showed excellent BBB permeability along with other drug-likeness properties. To simplify the understanding of further synthesis processes, selected compounds from set-1 were renamed as depicted in **Table 4.1.**

Table 4.1 Renaming of the eight selected compounds

Entry	Selected Compounds of Set-1	Chemical Structure	Renamed Compounds
1	**Compound 25**	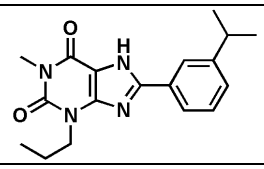	Compound **C1**
2	**Compound 26**	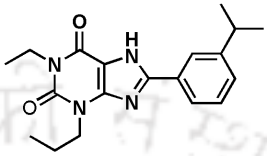	Compound **C2**
3	**Compound 27**	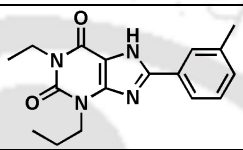	Compound **C3**
4	**Compound 32**	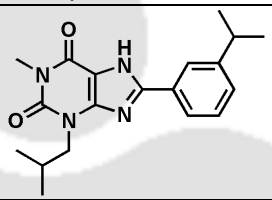	Compound **C4**
5	**Compound 34**	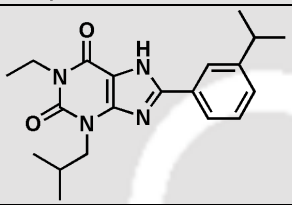	Compound **C5**
6	**Compound 28**	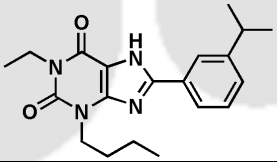	Compound **C6**
7	**Compound 29**	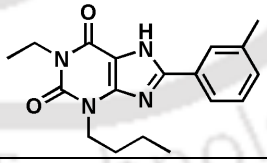	Compound **C7**
8	**Compound 30**	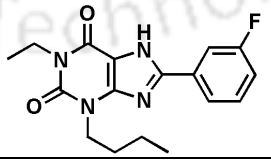	Compound **C8**

4.2.3. Chemical synthesis of xanthine derivatives

^{1}H NMR and ^{13}C NMR spectra were recorded using 600 MHz NMR spectrophotometer in DMSO-d_6 using Tetra Methyl Silane (TMS) as internal standard. Chemical shift are denoted in ppm (δ) relative to TMS (^{1}H). Routine mass spectra

(HRMS) were performed on Agilent Mass Spectroscopy using ESI positive mode. NMR and Mass spectra of synthesized compounds have been provided in Appendix-I and Appendix-II.

General procedure for synthesis of 8-bromo-1H-purine-2, 6 (3H, 7H)-dione) (**1**)**:** To a mixture of Xanthine (1 g, 657 mmol) in 6.5 mL water in a glass tube, 711 µL (13.7 mmol) of concentrated bromine (Br_2) solution was added and capped tightly. The reaction was allowed to stir at 100°C for 2h. After completion of the reaction, product mixture was allowed to cool at room temperature and filtered. The yellowish solid was washed with water 2-3 times which followed washing with diethyl ether (Et_2O) under vacuum. The product was dried under oven at 40°C. Light yellowish powdered compound (**1**) was obtained with yield of 71 % (1.08 g). ^{1}H NMR (600 MHz, DMSO-d_6) δ: 14.003(s, 1H), 11.667(s, 1H), 10.924(s, 1H); ^{13}C NMR (150 MHz, DMSO-d_6) δ: 154.54, 151.06, 148.83, 124.00, 109.47; MS (+ESI) m/z: 231.01, 232.0058(MH^+).

Synthesis of 7-benzyl-8-bromo-1H-purine-2,6(3H,7H)-dione (**2**)**:** To a mixture of 8-Bromo xanthine (8-bromo-1H-purine-2, 6 (3H,7H)-dione) (0.3g, 1.298 mmol) in 3 mL anhydrous DMF, 1.298 mmol K_2CO_3 and 80.6 µL benzyl chloride (0.7 mmol) were added in a 25 mL round bottom flask. Reaction was allowed to run at 70°C for 2.5h on silica bath. After the completion of reaction, product mixture was kept on ice. To neutralize the product mixture, 10% HCl was added. White color precipitate was formed which was filtered and washed 2-3 times with water and allowed to vacuum dry. White powderd product (**2**) was obtained with 67 % yield (0.28 g). ^{1}H NMR (600 MHz, DMSO-d_6) δ: 11.804 (s, 1H), 11.061 (s, 1H), 7.35 (t, *J*=7.41, 7.41 Hz, 2H), 7.30 (t, *J*=7.22, 7.22 Hz, 1H), 7.23 (d, *J*=7.77 Hz, 2H), 5.442 (s, 2H); ^{13}C NMR (150 MHz, DMSO-d_6) δ: 155.20, 151.15, 149.13, 136.05, 129.12, 128.82, 128.27, 127.43, 108.86, 49.57; MS (+ESI) m/z: 321.94, 322.94 (MH^+).

Synthesis of 7-benzyl-8-bromo-3-propyl-1H-purine-2, 6 (3H, 7H)-dione) **(3a1):** To a mixture of compound **2** (7-benzyl-8-bromo-1H-purine-2, 6 (3H,7H)-dione) (307 mg, 0.956 mmol) and anhydrous K_2CO_3 (132 mg, 0.956 mmol) in a 2 mL anhydrous DMF, 47.36 µL propyl iodide (0.487 mmol) was added and stirred at 70°C for 6 h. After the completion of reaction, the reaction flask was kept on ice for 10 minutes. Hydrochloric acid (10%) was added drop-wise to neutralize the product mixture followed by addition of water. With addition of water white color precipitate was formed which was filtered and washed 3-4 times with water followed by drying in oven at 40°C. The resultant solid powder was the mixture of two compounds-7-benzyl-8-bromo-3-propyl-1H-purine-2, 6 (3H,7H)-dione and 7-benzyl-8-bromo-1,3-dipropyl-1H-purine-2,6(3H,7H)-dione. The products were purified by column chromatography. The major product was 7-benzyl-8-bromo-3-propyl-1H-purine-2, 6 (3H,7H)-dione (Compound **3a1**) in white powdered form. The final yield of the compound **3a1** (7-benzyl 8-bromo 3-propyl xanthine) was 78 % (270 mg). ^{1}H NMR (600 MHz, DMSO-d_6)δ: 11.33(s, 1H), 7.36 (t, *J*=7.57, 7.57 Hz, 2H), 7.31(t, *J*=7.31, 7.31 Hz, 1H), 7.264 (d, *J*=7.17, 1H), 5.48 (s, 2H), 3.83 (t, 2H), 1.65 (sext, 2H), 0.874 (t, 3H); ^{13}C NMR (150 MHz, DMSO-d_6) δ: 154.06, 150.27, 149.10, 135.58, 128.76, 128.47, 127.95, 127.18, 108.81, 49.34, 43.41, 20.81, 10.94; MS (+ESI) m/z: 363.0453, 364.0453 (MH^+).

Synthesis of 7-benzyl-8-bromo-3-isobutyl-1H-purine-2, 6 (3H, 7H)-dione) **(3a2):** To a mixture of Compound **2** (385 mg, 0.12 mmol) and anhydrous K_2CO_3 (0.33 mg, 0.239 mmol) in a 1 mL anhydrous DMF, 137.96 µL isobutyl iodide (0.12 mmol) was added. The reaction mixture was then stirred at 70°C for 6 h. The post-reaction processing followed the same procedure used for **3a1**. The resultant powder was the mixture of two compounds- 7-benzyl-8-bromo-3-isobutyl-1H-purine-2,6 (3H,7H)-dione and 7-benzyl-8-bromo-1,3-diisobutyl-1H-purine-2,6(3H,7H)-dione. Column chromatography was

carried out to separate two products. 7-benzyl-8-bromo-3-isobutyl-1H-purine-2,6 (3H,7H)-dione (compound **3a2**) was the major product in white powdered form with final yield of 83 % (373 mg). ^{1}H NMR (600 MHz, DMSO-d_6) δ: 11.33(s, 1H), 7.36 (t, *J*=7.42,7.42 Hz, 2H), 7.31(dd, J=5.44, 9.10 Hz, 1H), 7.26 (d, *J*=7.34 Hz, 2H,), 5.47 (s, 2H), 3.7 (d, J= 7.48 Hz, 2H), 2.15 (m, 1H), 0.87(d, 6H); ^{13}C NMR (150 MHz, DMSO-d_6) δ: 154.06, 150.34, 149.32, 128.75, 127.93, 127.15, 108.86, 49.48, 48.81, 26.75, 19.72; MS (+ESI) m/z: 377.0609.

Synthesis of 7-benzyl-8-bromo-3-butyl-1H-purine-2, 6 (3H,7H)-dione) **(3a3):** To a mixture of 7-benzyl 8-bromo xanthine (7-benzyl-8-bromo-1H-purine-2, 6 (3H,7H)-dione) (90 mg, 0.28 mmol) and anhydrous K_2CO_3 (0.39 mg, 0.280 mmol) in 1 mL anhydrous DMF, 22.6 µL propyl iodide (0.199 mmol) was added. The reaction then stirred at 70°C for 6h. The post-reaction processing and work-up followed the same procedure used for **3a1**. The powder obtained was a mixture of two compounds- 7-benzyl-8-bromo-3-butyl-1H-purine-2, 6 (3H,7H)-dione and 7-benzyl-8-bromo-1,3-dibutyl-1H-purine-2,6(3H,7H)-dione. The product mixture was purified by column chromatography. 7-benzyl-8-bromo-3-butyl-1H-purine-2, 6 (3H,7H)-dione (compound **3a3**) was the major product in white powdered form with a final yield of 85 % (96 mg). ^{1}H NMR (600 MHz, DMSO-d_6) δ: 11.32(s, 1H), 7.34 (t, *J*=7.36, 7.36 Hz, 2H), 7.29 (t, *J*=7.05, 7.05 Hz, 1H), 7.23 (d, *J*=7.87, 2H), 5.46 (s, 2H), 3.85 (t, *J*= 7.30, 2H), 1.59 (quint, 2H), 1.28 (sext, 2H), 0.88 (t, *J*=7.4, 7.4 Hz, 3H); ^{13}C NMR (150 MHz, DMSO-d_6) δ: 154.05, 150.23, 149.07, 135.57, 128.76, 128.07, 127.95, 127.19, 108.82, 49.34, 41.65, 29.60, 19.36, 13.60; MS (+ESI) m/z: 377.0629.

Synthesis of 7-benzyl-8-bromo-1-methyl-3-propyl-1H-purine-2, 6(3H,7H)-dione)**(4a1):** To a mixture of compound **3a1** (630 mg, 1.73 mmol) and anhydrous K_2CO_3 (480 mg,

3.47 mmol) in 8 mL anhydrous DMF, 216 µL methyl iodide (3.47 mmol) was added. The reaction mixture was then stirred at 70°C for 12 h. After completion of the reaction, flask was allowed to cool at room temperature. The product mixture was diluted with ethyl acetate. Organic part was separated from the aqueous part by using water and brine alternatively. At the end of extraction, the organic part was isolated and dried with sodium sulfate. The yellowish solution obtained was vacuum dried in rotary evaporator. The yellowish mixture obtained was purified by column chromatography with ethyl-hexane (10:90) solvent. Purified whitish powder product (4a1) was obtained with a yield of 92 % (604 mg). ^{1}H NMR (600 MHz, DMSO-d_6) δ: 7.36 (dd, *J*=4.57, 10.13, 2H), 7.31(t, *J*=1.81, 9.03, 1H), 7.26 (m, 2H,), 5.48 (s, *J*=3.76, 2H), 3.9 (dd, *J*=6.80, 7.91, 2H), 3.22 (s, *J*= 3.03, 3H), 1.67 (sext, 2H), 0.88 (t, *J*=7.45, 7.45 Hz, 3H); ^{13}C NMR (150 MHz, DMSO-d_6) δ: 153.73, 150.34, 147.56, 135.56, 128.74, 128.22, 127.91, 127.12, 108.36, 49.35, 44.43, 27.76, 10.95; MS (+ESI) m/z: 377.0603

***Synthesis of 7-benzyl-8-bromo-1-ethyl-3-propyl-1H-purine-2,6 (3H,7H)-dione)*(4a2):** To a mixture of compound **3a1** (500 mg, 1.38 mmol) and anhydrous K_2CO_3 (381 mg, 2.75 mmol) in 5 mL anhydrous DMF, 220 µL ethyl iodide (2.75 mmol) was added. The reaction was allowed to stir at 70°C for 12 h. After completion of the reaction, reaction mixture was allowed to cool on ice for 10 minutes. The product mixture was neutralized with 10% HCl. As white precipitate began to appear, water was added to the neutralized mixture. After addition of water the product was accumulated in a white precipitated form. The whitish precipitate was filtered and washed with water 3-4 times. Product was allowed to dry at 40°C in a hot air oven to obtain white powder (compound **4a2**). The final yield of the compound **4a2** (7-benzyl-8-bromo-1-ethyl-3-propyl-1H-purine-2,6(3H,7H)-dione) was 95% (510 mg). ^{1}H NMR (600 MHz, DMSO-d_6) δ: 7.35 (t, J=7.40, 7.40, 2H), 7.29 (t, J=7.35, 7.35, 1H), 7.246 (d, J= 7.31, 2H), 5.551 (s, 2H), 3.888

(q, J=6.99, 6.99, 6.81, 4H), 1.662 (m, 2H), 1.095 (t, J= 7.00, 7.00, 3H), 0.868 (t, J=7.44, 7.44, 3H); ^{13}C NMR (150 MHz, DMSO-d_6) δ: 153.33, 149.88, 147.57, 135.55, 128.33, 127.89, 127.09, 108.36, 49.32, 44.32, 35.75, 20.75, 12.96, 10.93; MS (+ESI) m/z: 391.0778

***Synthesis of 7-benzyl-8-bromo-3-isobutyl-1-methyl-1H-purine-2,6 (3H,7H)-dione)* (4a3):** To a mixture of compound **3a2** (812 mg, 2.15 mmol) and anhydrous K_2CO_3 (595 mg, 4.3 mmol) in 10 mL anhydrous DMF, 268 µL methyl iodide (3.47 mmol) was added. The reaction was then stirred at 70°C for 12 h. After completion of the reaction, flask was allowed to cool at room temperature. The product mixture was diluted with ethyl acetate and transferred to a separating funnel. The organic part was extracted from the aqueous part by washing with water and brine alternatively and dried with sodium sulfate. The product mixture was vacuum dried in a rotary evaporator. Dark yellowish product mixture was obtained. The product mixture was purified by column chromatography using ethyl-hexane (10:90). The white powder (compound **4a3**) was obtained. The final yield of the product was 93 % (780 mg). ^{1}H NMR (600 MHz, DMSO-d_6) δ: 7.36 (t, *J*=7.41, 7.41 Hz, 2H), 7.31(t, *J*=7.31, 7.31, 1H), 7.26 (d, *J*=7.31 Hz, 2H), 5.52 (s, 2H), 3.85 (d, *J*= 7.48 Hz, 2H), 3.23 (s, 3H), 2.17 (sept, 1H), 0.88 (d, 6H); ^{13}C NMR (150 MHz, DMSO-d_6) δ: 153.33, 149.88, 147.57, 135.55, 128.33, 127.89, 127.09, 108.36, 49.32, 44.32, 35.75, 20.75, 12.96, 10.93; MS (+ESI) m/z: 391.0763.

***Synthesis of 7-benzyl-8-bromo-1-ethyl-3-isobutyl-1H-purine-2,6(3H,7H)-dione* (4a4):** To a mixture of compound **3a2** (0.224g, 0.646 mmol) in 3 mL anhydrous DMF, 0.178 mmol anhydrous K_2CO_3 and 104 µL (0.129 mmol) of ethyl iodide was added. Reaction was allowed to run at 70°C for 12 h on silica bath. After completion of the reaction, product was extracted with ethyl acetate and water sequentially. The extracted organic part was dried with sodium sulphate. Yellowish reaction mixture was obtained after

vacuum evaporation. Reaction mixture was purified by column chromatography. White powdered compound **4a4** was obtained with final yield of 90 %. ^{1}H NMR (600 MHz, DMSO-d_6) δ: 7.36 (t, J=7.41, 2H), 7.31(t, *J*=7.31, 1H), 7.26 (d, *J*=7.31, 2H), 5.51 (s, 2H), 3.90 (q, 2H), 3.77 (d, 2H), 3.23 (s, 3H), 2.15 (sept, 1H), 0.86 (d, 6H); ^{13}C NMR (150 MHz, DMSO-d_6) δ: 153.37, 150.16, 147.82, 135.59, 128.78, 128.50, 127.92, 127.12, 108.36, 49.36, 42.23, 37.72, 35.81, 26.82, 19.78, 12.98. MS (+ESI) m/z: 405.0931.

Synthesis of 7-benzyl-8-bromo-3-butyl-1-ethyl-1H-purine-2,6 (3H,7H)-dione **(4a5):** To a mixture of compound **3a3** (525 mg, 1.39 mmol) and anhydrous K_2CO_3 (385 mg, 2.78 mmol) in 6 mL anhydrous DMF, 224 µL ethyl iodide (2.78 mmol) was added. The reaction was allowed to stir at 70°C for 12 h. After completion, reaction mixture was allowed to cool on ice for 10 minutes. The product mixture was neutralized with 10% HCl followed by addition of water to the neutralized mixture. After addition of water the product was accumulated in white precipitated form. The precipitated product was filtered and washed 3-4 times with water. Product was then allowed to dry at 40°C in the hot air oven overnight. White powdered compound **4a5** was obtained with final yield of 92.6 % (522 mg). ^{1}H NMR (600 MHz, DMSO-d_6) δ: 7.36 (t, *J*=7.43, 2H), 7.30 (t, *J*=7.31, 1H), 7.23 (d, *J*=7.33, 2H), 5.52 (s, 2H), 3.94 (dd, *J*=7.08, 14.45 Hz, 2H) 3.89 (t, *J*= 7.01, 7.01 Hz, 2H), 1.62 (quint, 2H,), 1.28 (sext, 2H), 1.106 (t, *J*=6.99, 6.99 Hz, 3H), 0.899 (t, *J*=7.36, 7.36 Hz, 3H); ^{13}C NMR (150 MHz, DMSO-d_6) δ: 153.86, 150.37, 148.07, 136.08, 129.26, 128.87, 128.42, 127.62, 108.91, 49.85, 42.92, 36.28, 30.05, 19.88, 14.09, 13.50; MS (+ESI) m/z: 405.0941.

Synthesis of 7-benzyl-8-(3-isopropylphenyl)-1-methyl-3-propyl-1H-purine-2,6(3H,7H)-dione **(5a1):** A mixture of compound **4a1** (226 mg, 0.599 mmol), 3-isopropyl phenyl boronic acid (196 mg, 1.2 mmol), anhydrous K_2CO_3 (166 mg, 1.2 mmol) was taken in 25

mL round bottom flask. Then tertakis (triphenylphosphine) palladium (36 mg, 0.03 mmol) was added under argon atmosphere in the flask. The reaction was then stirred at 110°C for 2 days. After completion of the reaction, product mixture was allowed to cool at room temperature, 10 mL water was added and stirred for 10 minutes. Upon cooling, the reaction mixture darkened and black emulsion appeared on the upper layer of the solution. The reaction mixture was then diluted with ethyl acetate and transferred to a separating funnel. Two layers were formed, the organic layer was extracted with ethyl acetate. Organic extract was washed with 5% sodium carbonate solution and brine sequentially. After extraction, the organic phase was transferred to a 250 mL Erlenmeyer flask equipped with a magnetic stir bar. Activated charcoal (0.50 g) and sodium sulfate (2g) were added to the flask. This mixture was stirred for 10 min. The solution was then filtered through 1 cm celite bed. The resulting pale yellow solution was concentrated under reduced pressure to yield the crude product in oil form. The product was purified by column chromatography (10% ethyl acetate: 90% Hexane). The product **5a1** formed was yellowish oily in nature with yield of 88 % (220 mg). ^{1}H NMR (600 MHz, DMSO-d_6): 7.456 (d, *J*=5.71 Hz, 1H), 7.416 (d, *J*=7.74 Hz, 1H), 7.35 (t, *J*=7.69, 7.69 Hz, 2H), 7.30 (s, 1H), 7.26 (d, *J*=7.33 Hz, 2H), 7.014 (d, *J*=7.50 Hz, 1H), 5.63 (s, 2H), 4.02 (t, *J*=7.18, 7.18 Hz, 2H), 3.24 (s, 3H), 2.85 (dt, *J*= 6.30, 6.30, 12.43 Hz, 1H), 1.75 (m, 2H), 1.097 (s, 3H), 1.086 (s, 3H), 0.916 (t, *J*=7.39, 7.39 Hz, 3H); ^{13}C NMR (150 MHz, DMSO-d_6) δ: 154.54, 151.87, 150.67, 148.97, 147.69, 137.15, 128.94, 128.78, 127.48, 126.70, 126.41, 125.98, 107.44, 48.75, 44.31, 33.19, 27.62, 23.53, 20.88, 11.07.

Synthesis of 7-benzyl-1-ethyl-8-(3-isopropylphenyl)-3-propyl-1H-purine-2,6(3H,7H)-dione **(5a2):** A mixture of compound **4a2** (283 mg, 0.7233 mmol), 3-isopropyl phenyl boronic acid (237 mg, 1.45 mmol), anhydrous K_2CO_3 (200 mg, 1.45 mmol) was taken in 25 mL round bottom flask. Then, Tertakis (triphenylphosphine) palladium (45 mg) was

added under argon atmosphere in the flask. The reaction was carried out in 5 mL DMF, stirred at 110°C for 2 days. The post-reaction processing for obtaining pure product followed the same procedure used for **5a1**. The product formed was whitish semisolid in nature (compound **5a2**) with a yield of 85 % (265 mg). ^{1}H NMR (600 MHz, DMSO-d_6): 7.44 (t, *J*=6.74, 6.74 Hz, 1H), 7.416 (d, *J*=8.29 Hz, 1H), 7.34(s, 1H), 7.30 (t, *J*=7.31, 7.31 Hz, 2H), 7.25 (t, *J*=7.24 Hz, 1H), 7.008 (d, 2H), 5.63 (s, 2H), 4.02 (t, *J*=7.18 Hz, 2H), 3.92 (q, *J*=6.83 Hz, 2H), 2.85 (sept, 1H), 1.75 (sext, 2H), 1.14 (s, 3H),1.092 (d, *J*= 6.89 Hz, 6H), 0.912 (t, *J*=7.42,7.42 Hz, 3H); ^{13}C NMR (150 MHz, DMSO-d_6) δ: 154.13, 151.71, 150.36, 148.79, 147.72, 137.06, 128.93, 128.74, 128.61, 127.49, 126.71, 126.42, 125.92, 107.45, 48.78, 44.22, 35.65, 3319, 23.54, 20.89, 13.11, 11.07; MS (+ESI) m/z: 431.2457.

Synthesis of 7-benzyl-1-ethyl-3-propyl-8-m-tolyl-1H-purine-2,6(3H,7H)-dione **(5a3):** A mixture of compound **4a2** (218 mg, 0.557 mmol), 3-methyl phenyl boronic acid (151 mg, 1.14 mmol), anhydrous K_2CO_3 (73.5 mg, 1.14 mmol) was taken in 25 mL round bottom flask. Tertakis (triphenylphosphine) palladium (34 mg, 0.003 mmol) was added in the presence of argon atmosphere. The reaction was carried out in 5 mL DMF, stirred at 110°C for 2 days. The post-reaction processing for obtaining pure product followed the same procedure used for **5a1**. The product **5a3** obtained was light yellow semisolid with yield of 68% (152 mg). ^{1}H NMR (600 MHz, DMSO-d_6) δ: 7.35 (d, *J*=6.92 Hz, 2H), 7.288 (m, 2H), 7.24(d, *J*=8.55 Hz, 2H), 7.06 (d, *J*=5.79 Hz, 1H), 7.002 (m, 2H), 5.63 (s, 2H), 4.02 (t, *J*=7.18 Hz, 2H), 3.92 (q, *J*=6.83 Hz, 2H) 2.85 (sept, 1H), 2.29 (s, 3H), 1.75 (sext, 2H), 1.14 (s, 3H); ^{13}C NMR (150 MHz, DMSO-d_6) δ: 154.59, 152.06, 151.73, 150.97, 149.03, 148.04, 137.15, 128.99, 128.78, 127.51, 126.76, 126.39, 125.97, 107.39, 49.77, 48.77, 33.21, 27.71, 26.90, 23.55, 19.93, 19.23; MS (+ESI) m/z: 431.2465

Synthesis of 7-benzyl-3-isobutyl-8-(3-isopropylphenyl)-1-methyl-1H-purine-2,6(3H,7H)dione **(5a4):** A mixture of compound **4a3** (417 mg, 1.07 mmol), 3-isopropyl phenyl boronic acid (350 mg, 2.13 mmol) and anhydrous K_2CO_3 (295 mg, 2.13 mmol) was taken in 50 mL round bottom flask. Tertakis (triphenylphosphine) palladium (64 mg, 0.006 mmol) was added under argon atmosphere in the flask. The reaction was carried out in 10 mL DMF at 110°C for 48 h. The post-reaction processing for obtaining pure product followed the same procedure used for **5a1**. The product formed was semisolid and yellowish in color (compound **5a4**) with yield of 66 % (301 mg). ^{1}H NMR (600 MHz, DMSO-d_6): 7.538(s, 1H), 7.43 (m, 2H), 7.39 (d, *J*=2.18, 1H), 7.319 (s, 1H), 7.29 (t, *J*=7.40, 7.40, 2H), 7.239 (t, *J*=7.25,7.25, 1H), 6.997 (d, 2H), 5.62 (s, 2H), 3.8 (d, *J*= 7.48, 2H), 3.23 (s, 3H), 2.88 (hept, 1H), 2.23 (ddq, 1H), 0.90 (d, 6H).; ^{13}C NMR (150 MHz, DMSO-d_6): 154.59, 152.06, 151.73, 150.97, 149.03, 148.04, 137.15, 128.99, 128.78, 127.51, 126.76, 126.39, 125.97, 107.39, 49.77, 48.77, 33.21, 27.71, 26.90, 23.55, 19.93, 19.23.; MS (+ESI) m/z: 431.2465.

Synthesis of 7-benzyl-1-ethyl-3-isobutyl-8-(3-isopropylphenyl)-1H-purine-2,6(3H,7H)-dione **(5a5):** A mixture of compound **4a4** (315 mg, 0.778 mmol), 3-isopropyl phenyl boronic acid (268 mg, 1.63 mmol), anhydrous K_2CO_3 (225 mg, 1.63 mmol) was taken in 50 mL round bottom flask. Tertakis (triphenylphosphine) palladium (60 mg, 0.005 mmol) was added under argon atmosphere in the flask. The reaction was carried out in 6 mL DMF at 110°C for 48 h. The post-reaction processing for obtaining pure product followed the same procedure of **5a1**. The product formed was semisolid and yellowish in color (compound **5a5**) with a yield of 71%. ^{1}H NMR (600 MHz, DMSO-d_6) δ: 7.538(s, 1H), 7.43 (m, 2H), 7.39 (t, *J*=7.31 Hz, 1H), 7.32 (s, 1H), 7.29(t, *J*=7.40 Hz, 1H), 6.99 (d, *J*=7.31 Hz, 2H), 5.63 (s, 2H), 3.92 (q, J=7.10, 7.10, 6.99 Hz, 2H), 3.88 (d, *J*= 7.44 Hz, 2H), 2.99 (hept, 1H), 2.24 (ddq, 1H), 1.15 (d, 6H), 1.11(t, 3H), 1.08 (d, 6H); ^{13}C NMR

(150 MHz, DMSO-d_6) δ: 154.70, 152.47, 151.13, 150.45, 149.63, 148.69, 137.83, 129.80, 129.61, 129.40, 128.37, 128.15, 128.15, 127.37, 127.01, 126.56, 107.76, 50.24, 49.40, 36.34, 34.00, 27.58, 24.52, 24.52, 24.19, 20.59, 13.76.**;** MS (+ESI) m/z: 445.2631.

Synthesis of 7-benzyl-3-butyl-1-ethyl-8-m-tolyl-1H-purine-2,6 (3H,7H)-dione **(5a6):** To a mixture of compound **4a5** (183 mg, 0.452 mmol), 3-methyl phenyl boronic acid (129 mg, 0.903 mmol), anhydrous K_2CO_3 (125 mg, 0.903 mmol) was taken in 25 mL round bottom flask, Tertakis (triphenylphosphine) palladium (35 mg, 0.003 mmol) was added under argon atmosphere in the flask. The reaction was carried out in 4 mL DMF at 110°C for 48 h. The post-reaction processing for obtaining pure product followed the same procedure used for **5a1**. The product formed was light yellow semisolid (compound **5a6**) with yield of 85% (159 mg).^{1}H NMR (600 MHz, DMSO-d_6) δ: 7.403 (s, 1H), 7.376 (m, 2H), 7.341 (t, *J*=7.53, 7.53 Hz, 1H), 7.27 (t, *J*=7.43, 7.43 Hz, 2H), 7.226 (t, J=7.31, 7.31 Hz, 1H), 5.6 (s, 2H), 4.03 (t, 2H) 3.89 (q, *J*= 6.93, 6.93, 6.99, 2H), 2.3 (s, 3H), 2.15 (quint, 2H), 1.3 (dq, *J*= 7.32, 7.32, 7.19, 14.63 Hz, 2H), 1.10(t, *J*=6.98 Hz, 3H), 0.903 (t, *J*=7.36 Hz, 3H); ^{13}C NMR (150 MHz, DMSO-d_6) δ: 157.07, 154.42, 151.85, 150.10, 147.54, 138.29, 129.58, 129.37, 128.87, 128.68, 128.29, 126.13, 125.89, 126.13, 125.89, 107.44, 48.13, 42.06, 35.56, 29.56, 20.76, 19.53, 13.40, 13.40, 12.98; MS (+ESI) m/z: 417.2288.

Synthesis of 7-benzyl-3-butyl-1-ethyl-8-(3-fluorophenyl)-1H-purine-2,6(3H,7H)-dione **(5a7):** A mixture of compound **4a5** (130 mg, 0.321 mmol), 3-floro phenyl boronic acid (94 mg, 0.674 mmol), anhydrous K_2CO_3 (93 mg, 0.674 mmol) was taken in 25 mL round bottom flask. Tertakis (triphenylphosphine) palladium (25 mg, 0.002 mmol) was added under argon atmosphere in the flask. The reaction was carried out in 3 mL DMF at 110°C for 48 h. The post-reaction processing for obtaining pure product followed the same procedure of **5a1**.The product **5a7** formed was semisolid in nature and light green

in color with yield of 75% (100 mg).^{1}H NMR (600 MHz, , DMSO-d_6) δ: 7.536 (dd, *J*=8.06, 13.95, 1H), 7.445 (dd, 4.74, 13.85 Hz, 2H), 7.378 (td, *J*=2.39, 8.75, 8.75 Hz, 1H), 7.272 (t, J=7.37, 7.37 Hz, 2H), 7.223 (t, *J*=7.26, 7.26 Hz, 1H), 6.982 (d, *J*=7.35, 2H), 5.691 (s, 2H), 4.03 (t, *J*=7.26, 7.26, 2H), 3.906 (q, J= 6.96, 6.96, 6.98, 2H), 1.69 (m, 2H), 1.32 (m, 2H), 1.101 (t, J=7.00, 7.00 Hz, 3H), 0.906 (t, *J*=7.36, 7.36, 3H); ^{13}C NMR (150 MHz, DMSO-d_6) δ: 163.33, 161.70, 154.68, 150.81, 149.00, 137.40, 131.86, 131.04, 129.45, 128.29, 126.79, 125.80, 118.22, 116.48, 107.77, 49.29, 43.14, 36.38, 30.31, 20.08, 14.29, 13.76; MS (+ESI) m/z: 421.213.

***Synthesis of 8-(3-isopropylphenyl)-1-methyl-3-propyl-1H-purine-2,6(3H,7H)-dione* (6a1 or C1):** Deprotection of 7-benzyl-8-(3-isopropylphenyl)-1-methyl-3-propyl-1H-purine-2,6(3H,7H)–dione (220 mg) was carried out in a 25 mL flask equipped with magnetic bead. 3 mL methanol was added into the flask. Then the solution was degassed and backfilled with argon alternatively for three times. 10% Pd/H (100 mg) was taken into 2nd round bottom flask and dissolved with 5 mL methanol. The flask mixture was degassed three times by evacuation and backfilled with argon. The content of 1st flask was poured into the 2nd flask while stirring via syringe. The 2nd flask was then purged with H_2 gas. Then the reaction was allowed to stir at room temperature for 48 h. The resultant product mixture was passed through celite (1 cm). The solution obtained was concentrated under reduced pressure. Product formed was yellowish powder which was washed with 1 mL diethyl ether and filtered. The final product **6a1** formed was pure white in color with yield of 93% (160 mg). ^{1}H NMR (600 MHz, DMSO-d_6):13.78 (s, 1H), 8.033 (s, 1H), 7.924 (d, *J*=7.69 Hz, 1H), 7.396(m, 1H), 7.35 (d, *J*=7.68 Hz, 1H), 4.018 (m, 2H), 3.26 (s, 1H), 2.945 (ddd, *J*=5.19, 8.58, 10.31 Hz, 1H), 1.739 (m, 2H), 1.245 (d, *J*= 3.57 Hz, 3H), 1.234 (d, *J*= 3.34 Hz, 3H), 0.900 (t, *J*=7.43, 7.43 Hz, 3H); ^{13}C NMR (150 MHz, DMSO-d_6) δ: 154.88, 151.55, 150.75, 149.82, 148.91, 129.59, 129.33,

129.08, 128.37, 128.00, 124.84, 108.27, 45.14, 34.11, 28.45, 24.41, 21.51, 11.72; MS (+ESI) m/z: 327.18.

Compounds **6a2-6a7** were prepared by catalytic deprotection as described above.

1-ethyl-8-(3-isopropylphenyl)-3-propyl-1H-purine-2,6(3H,7H)-dione **(6a2 or C2):** Yield, 76%, ^{1}H NMR (600 MHz, DMSO-d_6) δ:13.82 (s, 1H), 8.04 (s, 1H), 7.9 (, d, *J*=7.56 Hz, 1H), 7.42(t, *J*=7.67 Hz, 1H), 7.37 (d, *J*=7.64, 1H), 4.03 (t, *J*=7.18 Hz, 2H), 2.96 (m, 1H), 1.75 (sext, 2H), 1.26 (d, *J*= 6.70 Hz, 6H), 1.14 (t, 3H) 0.906 (t, 3H); ^{13}C NMR (150 MHz, DMSO-d_6) δ: 154.50, 151.12, 149.81, 148.56, 129.58, 129.35, 129.08, 124.89, 124.85, 108.24, 45.04, 38.68, 36.41, 34.11, 24.41, 21.41, 21.52, 13.85, 11.70**;** MS (+ESI) m/z: 341.2002.

1-ethyl-3-propyl-8-m-tolyl-1H-purine-2,6(3H,7H)-dione **(6a3 or C3):** Yield, 77%, ^{1}H NMR (600 MHz, DMSO-d_6) δ: 13.76 (s, 1H), 7.945 (d, *J*=5.12 Hz, 1H), 7.899 (d, *J*=7.6 Hz, 1H), 7.37 (t, *J*=7.66, 7.66 Hz, 1H), 7.279 (d, *J*=7.52, 1H), 4.001 (m, 2H), 3.93(q, J= 7.00, 7.00, 7.02 Hz, 2H), 2.356 (s, 3H), 1.727 (m, 2H), 1.123 (td , J=2.39, 6.95, 7.02, 3H), 0.891 (t, *J*=7.43,7.43 Hz, 3H); ^{13}C NMR (150 MHz, DMSO-d_6) δ: 154.47, 151.11, 150.83, 150.57, 148.92, 138.87, 131.54, 129.50, 129.27, 127.57, 124.25, 108.27, 45.05, 36.41, 21.64, 21.53, 13.87, 13.85, 11.71; MS (+ESI) m/z: 313.1684.

3-isobutyl-8-(3-isopropylphenyl)-1-methyl-1H-purine-2,6(3H,7H)-dione **(6a4 or C4):** Yield, 81 %, ^{1}H NMR (600 MHz, DMSO-d_6) δ: 8.046 (s, 1H), 7.9 (d, J=2.64, 1H), 3.891 (d, J= 7.37 Hz, 2H), 3.274 (s, 3H), 2.954 (dt, *J*=6.87, 6.87, 13.78 Hz, 1H), 2.23 (dt, *J*= 7.01, 7.01, 13.71 Hz, 1H), 1.250 (d, *J*= 6.89 Hz, 6H), 0.908 (d, *J*= 6.66 Hz, 6H). Note [A broader peak came it may probably submerged NH peak, two aryl peaks]; ^{13}C NMR (150

MHz, DMSO-d_6) δ: 154.78, 151.76, 150.68, 149.81, 149.06, 129.60, 129.36, 129.10, 124.85, 108.22, 50.61, 34.10, 28.51, 27.51, 24.42, 20.56; MS (+ESI) m/z: 341. 1999.

***Synthesis of 1-ethyl-3-isobutyl-8-(3-isopropylphenyl)-1H-purine-2,6(3H,7H)-dione* (6a5 or C5):** Yield, 76 %, ^{1}H NMR (600 MHz, DMSO-d_6) δ: 13.80 (s, 1H), 8.024 (s, 1H), 7.911 (d, J=7.62, 1H), 7.407 (t, *J*=7.68, 7.68, 1H), 7.347 (d, *J*=7.67, 1H), 3.941 (q, J=6.95, 6.95, 6.97, 2H), 3.876 (d, *J*= 7.45, 2H), 2.94 (m, 1H), 2.244 (dp, *J*= 6.88, 6.88, 6.87, 6.87, 13.76 Hz, 1H), 1.237 (d, *J*=6.92, 6H), 1.125(t, *J*= 7.00, 7,00 Hz, 3H), 0.892 (d, *J*=6.71, 6H); ^{13}C NMR (150 MHz, DMSO-d_6) δ: 154.51, 151.34, 150.69, 149.81, 149.21, 129.60, 129.10, 128.21, 128.08, 124.87, 108.24, 50.49, 36.43, 34.11, 27.55, 24.42, 20.56, 13.85; MS (+ESI) m/z: 354.2182.

***3-butyl-1-ethyl-8-m-tolyl-1H-purine-2,6(3H,7H)-dione* (6a6 or C7):** Yield, 50 %, ^{1}H NMR (600 MHz, DMSO-d_6): 7.930 (s, 1H), 7.889 (d, *J*=7.65 Hz, 1H), 7.336 (t, *J*=7.57, 7.57 Hz, 1H), 7.220 (d, *J*=7.33 Hz, 1H), 4.030 (t, *J*=6.95, 6.95 Hz, 2H), 3.929 (q, *J*= 6.58, 6.58, 6.62 Hz, 2H), 3.15 (s, 1H), 2.348 (s, 3H), 1.682 (m, 2H), 1.315 (dq, *J*=7.22, 7.22, 7.46, 14.29 Hz, 2H), 1.107 (t, *J*=6.91, 6.91 Hz, 3H), 0.909 (t, *J*= 7.29, 7.29 Hz, 3H); ^{13}C NMR (150 MHz, DMSO-d_6):154.22, 151.10, 149.93, 148.17, 138.85, 131.52, 129.50, 127.57, 124.27, 108.24, 43.23, 36.40, 30.30, 21.65, 20.03, 14.27, 13.85. MS (+ESI) m/z: 327.1841.

***3-butyl-1-ethyl-8-(3-fluorophenyl)-1H-purine-2,6(3H,7H)-dione* (6a7 or C8):** Yield, 56%, ^{1}H NMR (600 MHz, DMSO-d_6) δ: 7.981 (d, *J*= 7.75 Hz, 1H), 7.925 (d, *J*=10.07 Hz, 1H), 7.567 (dd, *J*=7.70, 14.21 Hz, 1H), 7.331 (t, *J*=8.30, 8.30 Hz, 1H), 4.05 (t, *J*=7.02, 7.02 Hz, 2H), 3.944 (q, *J*= 6.83, 6.83, 6.84 Hz, 2H), 1.699 (m, 2H), 1.324 (m, 2H), 1.134 (, t, *J*=6.93, 6.93, 3H), 0.926 (t, *J*= 7.32, 7.32 Hz, 3H); ^{13}C NMR (150 MHz, DMSO-d_6) δ: 163.78, 162.16, 154.63, 151.05, 131.91, 131.85, 127.08, 123.24, 117.63,

117.52, 113.62, 113.46, 43.27, 36.46, 30.26, 20.02, 14.38, 14.38, 14.27, 13.84; MS (+ESI) m/z: 331.1575.

Synthesis of 3-(4-methoxybenzyl)-7-benzyl-8-bromo-1H-purine-2,6(3H,7H)-dione **(3b1):** To a mixture of 7-benzyl 8-Bromo xanthine (7-benzyl-8-bromo-1H-purine-2,6 (3H,7H)-dione) (1.07 g, 3.33 mmol) in 10 mL anhydrous DMF, 6.66 mmol of K_2CO_3 and 40.65 µL of 4-methoxybenzyl chloride (0.9 mmol) were added in a 50 mL round bottom flask. Reaction was allowed to run at 70°C for 2.5 h on silica bath. After the completion of the reaction, the product mixture was kept on ice. Hydrochloric acid (10%) was added drop-wise to neutralise the product mixture. White colored precipitate was formed. Product was filtered and washed 2-3 times with water. The product was allowed to vacuum dry. White powder product **3b1** was formed with 70.06 % (1.03 g) yield. ^{1}H NMR (600 MHz, DMSO-d_6) δ: 11.421 (s, 1H), 7.343(t, *J*= 7.26, 7.26 Hz, 2H), 7.296 (d, *J*=6.19 Hz, 1H), 7.259 (t, *J*=8.26, 8.26 Hz, 4H), 6.863 (d, *J*=8.43 Hz, 2H), 5.455 (s, 2H), 4.976 (s, 2H), 3.693 (s, 3H); ^{13}C NMR (150 MHz, DMSO-d_6) δ: 159.44, 154.23, 150.97, 149.46, 136.19, 129.78, 129.44, 128.64, 127.89, 114.53, 109.65, 55.72, 50.09, 45.12; MS (+ESI) m/z: 441.0397.

***Synthesis of 3-(4-methoxybenzyl)-7-benzyl-8-bromo-1-ethyl-1H-purine-2,6(3H,7H)-dione*) (4b1):** To a mixture of compound **3b1** obtained in step-3b (0.98 g, 2.22 mmol) and anhydrous K_2CO_3 (0.644 g, 4.66 mmol) in 10 mL anhydrous DMF, 0.3749 µL ethyl iodide (4.66 mmol) was added. The reaction then stirred at 70°C for 12 h. After completion of the reaction, reaction mixture was allowed to cool at room temperature. The product mixture was diluted with ethyl acetate. The organic part was separated from aqueous part by washing with water and brine alternatively. After extraction, the organic part was isolated and dried with sodium sulfate. The yellowish solution obtained was dried under vacuum in a rotary evaporator. Whitish product mixture was obtained. The

product mixture was purified by column chromatography with ethyl-hexane (10:90) solvent. Product **4b1** was obtained in the form of white powder with final yield of 88 % (915 mg). ^{1}H NMR (600 MHz, DMSO-d_6) δ: 7.338 (t, *J*= 7.40, 7.40 Hz, 2H), 7.286 (d, *J*=7.286 Hz, 3H), 7.248 (d, *J*=7.53 Hz, 2H), 6.861 (d, *J*=8.45 Hz, 2H), 5.498 (s, 2H), 5.042 (s, 2H), 3.885 (q, *J*=6.77, 6.77, 6.86 Hz, 3H) (s, 2H), 3.686 (s, 3H Ar), 1.089 (t, *J*= 6.94, 6.94 Hz, 3H).**;** ^{13}C NMR (150 MHz, DMSO-d_6) δ: 159.34, 153.98, 150.68, 148.13, 136.19, 136.19, 129.92, 129.44, 129.11, 129.08, 128.62, 127.85, 114.52, 114.31, 109.15, 55.69, 50.09, 46.06, 36.60, 13.68**;** MS (+ESI) m/z: 469.0894.

Synthesis of 3-(4-methoxybenzyl)-7-benzyl-1-ethyl-8-(3-isopropylphenyl)-1H-purine-2,6 (3H,7H)-dione (**5b1**)**:** To the mixture of compound **4b1** (1.66 g, 3.55 mmol), 3-isopropyl phenyl boronic acid (1.22 g, 7.45 mmol), anhydrous K_2CO_3 (1.03 g, 7.45 mmol) taken in 50 mL round bottom flask. Tertakis (triphenylphosphine) palladium (260 mg, 0.2 mmol) was added under argon atmosphere in the flask. The reaction was carried out in 10 mL DMF at 110°C for 48 h. After completion of the reaction, product mixture was allowed to cool at room temperature. Water (10 mL) was added to the product mixture and stirred for 10 minutes. Upon cooling, the reaction mixture darkened and black emulsion appeared on the upper layer of the solution. The reaction mixture was then diluted with ethyl acetate and transferred to a separating funnel. Two layers were formed; the organic layer was re-extracted with ethyl acetate. Organic extract was washed with 5% sodium carbonate solution and brine sequentially. After extraction, organic phase was transferred to a 250 mL Erlenmeyer flask equipped with a magnetic stir bar. Activated charcoal (0.50 g) and sodium sulfate (2g) were added to the flask. This mixture was stirred for 10 min. The solution was then filtered through 1 cm celite bed. The resulting pale yellow solution was concentrated under reduced pressure to yield the crude product in oil form. The product was purified by column chromatography (10%

ethyl acetate: 90% Hexane). The product **5b1** formed was light yellow and semisolid in nature with yield of 72.2 % (1.3 g). ^{1}H NMR (600 MHz, DMSO-d_6) δ: 7.455(t, *J*=8.58, 8.58 Hz, 1H), 7.409 (dd, *J*=5.98 Hz, 13.53, 2H), 7.374 (d, *J*=8.35 Hz, 2H), 7.345 (s, 1H), 7.289 (t, *J*=7.33, 7.33 Hz, 2H), 7.244 (d, *J*=7.26 Hz, 1H), 7.007 (d, *J*=7.30 Hz, 2H), 6.875 (d, *J*=8.13 Hz, 2H), 5.623 (s, 1H), 5.149 (s, 1H), 3.897 (dd, *J*=6.69, 13.63 Hz, 2H), 3.688(s, 1H), 2.834 (dt, *J*=6.72, 6.72, 13.55 Hz, 1H), 1.096 (t, *J*=6.55, 6.55 Hz, 3H); ^{13}C NMR (150 MHz, DMSO-d_6) δ: 159.35, 154.75, 152.54, 150.93, 149.61, 148.25, 137.77, 130.20, 129.66, 129.44, 127.35, 126.63, 114.49, 107.40, 60.43, 55.68, 49.21, 46.19, 36.45, 33.85, 24.20, 21.35, 14.73, 13.79.; MS (+ESI) m/z: 509.2611.

Synthesis of 7-benzyl-1-ethyl-8-(3-isopropylphenyl)-1H-purine-2,6(3H,7H)-dione (**6b1**)**:** A solution of Compound **5b1** (R_1=Et) (1.257 g, 2.47 mmol), concentrated sulfuric acid (10 drop), anisol (375 µL, 3.4 mmol) in TFA (5 mL) was taken in 25 mL flask equipped with magnetic bead. The flask was degassed and backfilled with argon alternatively for three times. The reaction mixture was refluxed for 22h. Oily residue was formed which was diluted with water and isopropyl ether. This was followed by neutralization with 20% NaOH till pH 5 was obtained. The resultant precipitate was filtered, washed with water and isopropyl ether, and dried. The product **6b1** was obtained in greenish powdered form with yield of 73 % (700 mg). ^{1}H NMR (600 MHz, DMSO-d_6): 12.036(s, 1H), 7.395(d, *J*=5.12 Hz, 1H), 7.36 (d, *J*=6.38, 6.38 Hz, 3H), 7.285 (t, *J*=7.30, 7.30 Hz, 2H), 7.232 (m, 1H), 6.989 (d, *J*=7.27 Hz, 2H), 5.604 (s, 1H), 3.845 (q, *J*=6.69, 6.69, 6.70 Hz, 2H), 2.832 (dt, *J*=6.76, 6.76 Hz, 13.58, 1H), 1.079 (d, *J*= 7.01 Hz, 6H); ^{13}C NMR (150 MHz, DMSO-d_6) δ: 154.95, 152.09, 150.62, 149.02, 147.29, 137.33, 128.92, 128.80, 128.64, 127.49, 126.45, 126.37, 125.93, 107.44, 48.64, 23.79, 23.59, 13.23; MS (+ESI) m/z: 389.199.

Synthesis of 7-benzyl-1-ethyl-3-isobutyl-8-(3-isopropylphenyl)-1H-purine-2,6(3H,7H)-dione **(7b1):** To a mixture of compound 6b1 (0.2 g, 0.515 mmol) and anhydrous K_2CO_3 (0.142 g, 1.028 mmol) in 2 mL anhydrous DMF, 59 µL isobutyl iodide (0.515 mmol) was added. The reaction was then stirred at 70°C for 12 h. After completion of the reaction, product mixture was allowed to cool at room temperature. The reaction mixture was then diluted with ethyl acetate and transferred to a separating funnel. Two layers were formed and the organic layer was re-extracted with ethyl acetate. The organic extract was washed with 5% sodium carbonate solution and brine sequentially. After extraction, organic phase was transferred to a 250 mL Erlenmeyer flask equipped with a magnetic stir bar. The resulting pale yellow solution was concentrated under reduced pressure to yield the crude product as oil. The product was then purified by column chromatography (10% ethyl acetate: 90% Hexane). Yellowish oil mixture was obtained. The product was purified by column chromatography. The purified compound 7b1 was obtained in yellowish oil form with yield of 84% (193 mg); ^{1}H NMR (600 MHz, DMSO-d_6) δ: 7.538(s, 1H), 7.43 (m, 2H), 7.39 (t, *J*=7.31 Hz, 1H), 7.32 (s, 1H), 7.29(t, *J*=7.40 Hz, 1H), 6.99 (d, *J*=7.31 Hz, 2H), 5.63 (s, 2H), 3.92 (q, *J*=7.10, 7.10, 6.99 Hz, 2H), 3.88 (d, *J*= 7.44 Hz, 2H), 2.99 (hept, 1H), 2.24 (ddq, 1H), 1.15 (d, 6H), 1.11(t, 3H), 1.08 (d, 6H); ^{13}C NMR (150 MHz, DMSO-d_6) δ: 154.70, 152.47, 151.13, 150.45, 149.63, 148.69, 137.83, 129.80, 129.61, 129.40, 128.37, 128.15, 128.15, 127.37, 127.01, 126.56, 107.76, 50.24, 49.40, 36.34, 34.00, 27.58, 24.52, 24.52, 24.19, 20.59, 13.76.; MS (+ESI) m/z: 445.2631.

Compound **7b2** was prepared by similar alkylation reaction as described above.

7-benzyl-3-butyl-1-ethyl-8-(3-isopropylphenyl)-1H-purine-2,6(3H,7H)-dione **(7b2):** Yield of 98 %, ^{1}H NMR (600 MHz, DMSO-d_6) δ: 7.355 (, d, *J*=7.18 Hz, 2H), 7.34 (m,

2H), 7.33 (d, *J*=7.82 Hz, 1H), 7.283 (m, J=7.67 Hz, 1H), 7.164 (s, *J*=1.79 Hz, 1H), 7.13 (s, *J*=7.67 Hz, 1H), 7.078 (d, *J*=8.05 Hz, 1H), 7.03 (t, *J*= 7.77 Hz, 2H), 5.41 (s, 2H), 3.90 (q, 2H) 3.82 (t, *J*= 7.14 Hz, 2H), 2.88 (hept, *J*=7.00, 6.99, 13.81 Hz, 1H), 2.75 (quint, 2H), 1.6 (sext, 2H), 1.13 (d, 6H), 1.10(t, *J*=7.05 Hz, 3H), 0.808 (t, *J*=7.36 Hz, 3H); ^{13}C NMR (150 MHz, DMSO-d_6) δ: 154.59, 152.06, 151.73, 150.97, 149.04, 148.04, 137.15, 128.99, 128.78, 127.51, 126.76, 126.39, 125.97, 107.39, 49.77, 48.77, 33.21, 27.71, 26.90, 23.90, 23.55, 19.93, 19.86, 19.23; MS (+ESI) m/z: 445.2622.

***Synthesis of 1-ethyl-3-isobutyl-8-(3-isopropylphenyl)-1H-purine-2,6(3H,7H)-dione* (8b1 or C5):** A mixture of compound **7b1** (315 mg, 0.778 mmol), 3-isopropyl phenyl boronic acid (268 mg, 1.63 mmol), anhydrous K_2CO_3 (225 mg, 1.63 mmol) was taken in 50 mL round bottom flask. Tertakis (triphenylphosphine) palladium (60 mg, 0.005 mmol) was added under argon atmosphere in the flask. The reaction was carried out in 6 mL DMF at 110°C for 48 h. After completion of the reaction, product mixture was allowed to cool at room temperature. Water (10 mL) was added to the product mixture and stirred for 10 minutes. Upon cooling, the reaction mixture darkened and black emulsion appeared on the upper layer of the solution. The reaction mixture was then diluted with ethyl acetate and transferred to a separating funnel. Two layers were formed, the organic layer was re-extracted with ethyl acetate. Organic layer was washed with 5% sodium carbonate solution and brine sequentially. After extraction organic phase was transferred to a 250 mL Erlenmeyer flask equipped with a magnetic stir bar. Activated charcoal (0.50 g) and sodium sulfate (2g) were added to the flask. This mixture was stirred for 10 min. The solution was then filtered through 1 cm celite bed. The resulting pale yellow solution was concentrated under reduced pressure to yield the crude product in oil form. The product was then purified by column chromatography (10% ethyl acetate: 90% Hexane). The product formed was semisolid and yellowish in color

(compound **8b1**) with a yield of 71%. ^{1}H NMR (600 MHz, DMSO-d_6) δ: 13.80 (s, 1H), 8.024 (s, 1H), 7.911 (d, *J*=7.62 Hz, 1H), 7.407 (t, *J*=7.68, 7.68 Hz, 1H Ar-H), 7.347 (d, J=7.67 Hz, 1H), 3.941 (q, *J*=6.95, 6.95, 6.97 Hz, 2H), 3.876 (d, *J*= 7.45 Hz, 2H), 2.94 (m, 1H), 2.244 (dp, *J*= 6.88, 6.88, 6.87, 6.87, 13.76 Hz, 1H), 1.237 (d, *J*=6.92 Hz, 6H), 1.125(t, *J*= 7.00, 7,00 Hz, 3H), 0.892 (d, *J*=6.71, 6H); ^{13}C NMR (150 MHz, DMSO-d_6)δ: 154.51, 151.34, 150.69, 149.81, 149.21, 129.60, 129.10, 128.21, 128.08, 124.87, 108.24, 50.49, 36.43, 34.11, 27.55, 24.42, 20.56, 13.85; MS (+ESI) m/z: 354.2182.

Compound **8b2** obtained from the deprotection of compound **7b2** using similar protocol as described above.

3-butyl-1-ethyl-8-(3-isopropylphenyl)-1H-purine-2,6(3H,7H)-dione **(8b2 or C6):** Yield, 77%; ^{1}H NMR (600 MHz, DMSO-d_6) δ: 8.017 (s, 1H), 7.906 (d, *J*=7.63 Hz, 1H), 7.385 (t, *J*=7.64, 7.64 Hz, 1H), 7.314 (d, *J*=7.55 Hz, 1H), 3.941 (t, *J*=7.12, 7.12 Hz, 2H), 3.929 (q, *J*= 6.89, 6.89, 6.92 Hz, 2H), 2.93 (dp, *J*=6.72, 6.72, 6.57, 6.57, 13.42 Hz, 1H), 1.686 (m, 2H), 1.314 (dq, *J*=7.41, 7.41, 7.46, 14.88 Hz, 2H), 1.236 (d, *J*=6.90, 6H), 1.119 (t, *J*= 6.96, 6.96 Hz, 3H), 0.913 (t, 3H); ^{13}C NMR (150 MHz, DMSO-d_6) δ: 154.76, 151.18, 151.13, 149.67, 149.07, 130.05, 129.48, 128.73, 124.73, 124.73, 109.10, 43.17, 36.33, 34.11, 30.28, 24.43, 20.02, 14.25, 13.92; MS (+ESI) m/z: 355.2142.

4.3. Results and Discussion

4.3.1. Selection of starting material

Availability, affordability and accessibility are the three main parameters considered in the drug development process to reduce the production cost. Therefore, the selection of the starting material was a very crucial step in the synthesis process. Xanthine derivatives are the modified forms of the original xanthine molecule. Abundance of xanthine, both biologically and synthetically makes it an excellent choice

as the reaction initiator for the organic synthesis of xanthine derivatives. In addition, using xanthine as a starting material for the synthesis of derivatives has other advantages, such as easy availability, cost effectiveness, time saving and scope of large scale synthesis. With this initiative only modifications at different positions of xanthine were required without disturbing the xanthine ring. The selective substitution at pre decided positions of xanthine using xanthine as a starting material for the synthesis of xanthine derivatives was the most challenging task because of the presence of three –NH groups at N_1, N_3 and N_7 positions of xanthine. Thus understanding the nature of these three –NH groups separately was needed for successful selective substitution reactions. **Figure 4.2** depicts the chemical structure of the starting material "xanthine".

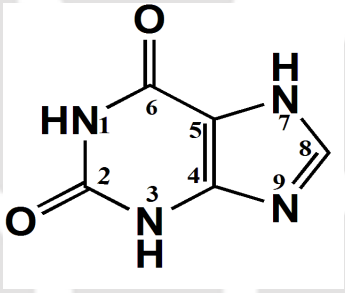

Figure 4.2 Molecular structure of starting material 'xanthine'

4.3.2. Development of new routes for synthesis of xanthine derivatives

In this study, two novel synthetic schemes (Scheme-I and Scheme-II) have been developed to synthesize 1, 3, 8-trisubstituted xanthine derivatives. Scheme-I is a six step synthesis procedure whereas, Scheme-II is of eight steps. Diverse set of compounds were developed using Scheme I and II. Both schemes begin with the use of common 'xanthine' molecule as a starting material. These schemes share two common initial steps and the final step is also common to both. In scheme-I, the three intermediate steps are exclusive while in scheme-II, five intermediate steps are exclusive.

Combined steps of scheme-I and scheme-II (suffix 'a' denotes scheme - I and 'b' denotes scheme – II)

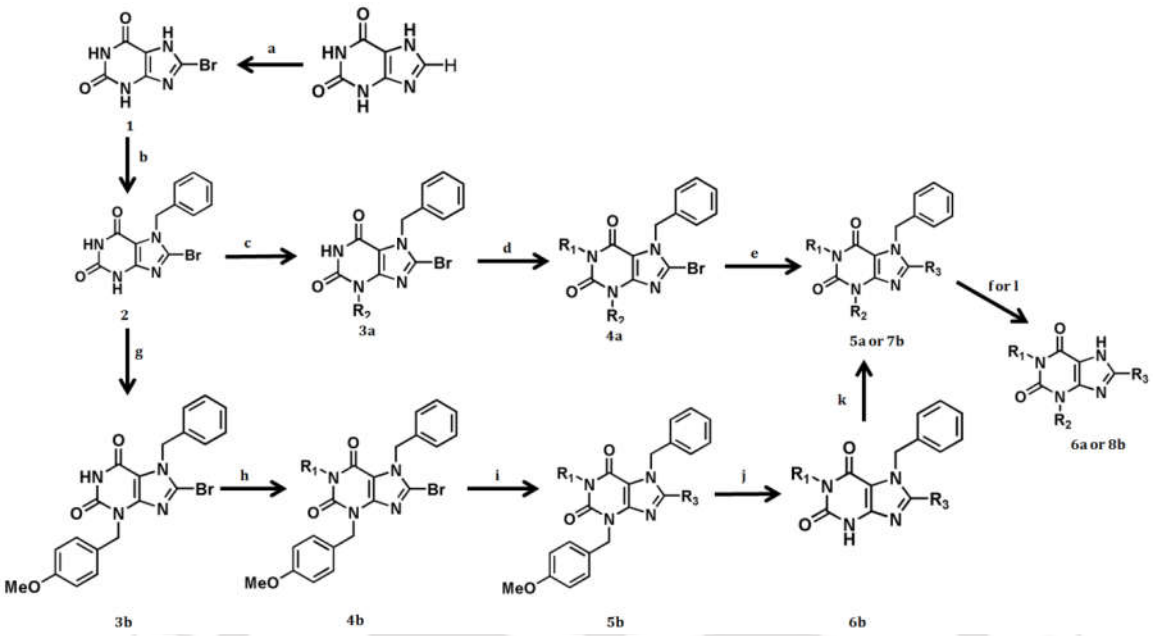

Reagents and Conditions: (a) Br_2, H_2O, 100°C, 3h; (b) benzyl chloride, Anhydrous K_2CO_3, Anhydrous DMF, 2.5 h, 70°C; (c) Alkyl iodide, Anhydrous K_2CO_3, Anhydrous DMF, 6h, 70°C; (d) Alkyl iodide, Anhydrous K_2CO_3, Anhydrous DMF, 12 h, 70°C; (e) Pd $(PPh_3)_4$, Anhydrous K_2CO_3, DMF, 48 h, 110°C, inert argon atmosphere; (g) 4-methoxy benzyl chloride, Anhydrous K_2CO_3, Anhydrous DMF, 2.5 h, 70°C; (h) Alkyl iodide, Anhydrous K_2CO_3, Anhydrous DMF, 12 h, 70°C; (i) Pd $(PPh_3)_4$, Anhydrous K_2CO_3, DMF, 48 h, 110°C, inert argon atmosphere; (j) TFA, conc. H_2SO_4, reflux, 22h (k) Alkyl iodide, Anhydrous K_2CO_3, Anhydrous DMF, 12 h (f or l) H_2, 10% Pd/H, Methanol, 48 h, rt.

The reaction starts in both the schemes with bromination reaction at C_8 position of xanthine. Bromination reaction at C_8 position in the first step and was essential because original xanthine has only one hydrogen atom at C_8 position with –CH group. The bromination reaction at C_8 position was required for C_8 arylation reaction to be carried out in the 5th step of both scheme-I and scheme-II. Selective bromination at C_8

position was not possible after protection with benzyl group because of the presence of methylene (-CH_2-) group. Therefore, bromination of xanthine was carried out first in both the schemes. In xanthine, presence of three –NH groups at N_1, N_3 and N_7 positions was the most challenging part in understanding the nature of the whole xanthine molecule. The three -NH sites of xanthine showed different reactivity because of their different atomic environment. In the development of schemes for synthesizing xanthine derivative, it was essential to go for selective reactions at different positions of xanthine.

In this study, substitution at N_1, N_3 and C_8 positions were selected for synthesis of xanthine derivatives. Substitution at these three positions (N_1, N_3 and C_8) of xanthine scaffold was to be selective. However, the presence of -NH groups at three different positions of xanthine and their different atomic environment was the major hinderance. Understanding the reactivity of three -NH positions of xanthine was imperative. In this study, by concentration optimization of reactant, it was found that -NH group at N_7 position was most reactive. This was because it faced less steric hinderance as compared to other –NH groups. Thus, to make the selective substitution reaction at N_3 and N_1 positions of xanthine, it was imperative to protect N_7 position first. This was because –NH group at N_7 position possessed highest reactivity among all -NH groups. For protecting –NH group at N_7 position, benzyl chloride was used in both scheme-I and scheme-II. With different concentration analysis of benzyl chloride to protect N_7 position it was found that –NH at N_7 position was protected first by benzyl group in all xanthine scaffold. When concentration of benzyl chloride was higher than the required concentration for selective protection of N_7 position, benzyl chloride acted at N_3 position because NH at N_3 position showed second higher reactivity among three –NH groups. Likewise, when all N_3 positions were occupied with the benzyl groups, then –NH at N_1 position was attacked by benzyl reactant. The –NH at N_1 position showed least reactivity

because -NH at N_1 position faced highest steric hindrance among the three –NH groups. This was because the reaction centre of -NH at N_1 position is surrounded by carbonyl groups at C_2 and C_6 positions. Due to these reasons, a sequential selectivity was generated at xanthine scaffold in order of N_7 substitution>N_3 substitution>N_1 substitution as shown in **figure 4.3**. Therefore, during synthesis, reactant gets attracted first to the N_7 position and uses all the available N_7 sites. Then it goes to the relatively lower reactive site i.e. N_3 site. After occupancy of the N_3 sites reactant attacked the N_1 site. The protection of N_7 position was carried out by S_N^2 mechanism where concentration of both the reactants have equal role in determining the product formation. The selective protection of –NH group at N_7 position was dependent on the concentration of both reactants (8-bromoxanthine and benzyl chloride). Multiple products were obtained when benzyl chloride was in higher concentration than the concentration actually needed for the occupancy of N_7 position only. When concentration was higher than the needed concentration for protection at N_7 position, the rest of the reactant (benzyl chloride) subsequently attacked the –NH group at N_3 position and occupied all N_3 position with formation of 3, 7- dibenzyl 8-bromo xanthine. After occupying all N_3 positions, rest of the reactant attacked the –NH group at N_1 position. The protection followed the order of 7-benzyl 8-bromoxanthine > 3,7–dibenzyl 8-bromoxanthine > 1,3,7- tribenzyl 8-bromoxanthine. Therefore, selective protection was completely dependent on the concentration of the benzyl reactant used. Hence, optimization of concentration of benzyl chloride for selective protection at N_7 position was carried out. The selective protection at N_7 position was achieved only when concentration of benzyl chloride was reduced to 0.5 equivalents of 8-bromoxanthine. Selective protection was necessary to achieve greater yield in shortest possible time bypassing the tedious workup and use of costly solvents for column chromatography. Thus, after protection at N_7 position of 8-bromo

xanthine, both Scheme-I and Scheme-II follow two different routes. In scheme-I, protection at N_7 position was followed by three independent steps while in scheme-II, it was followed by five independent steps, finally both schemes merge and shared the last common step. **Figure 4.3** represents the reaction affinity of different –NH positions of xanthine.

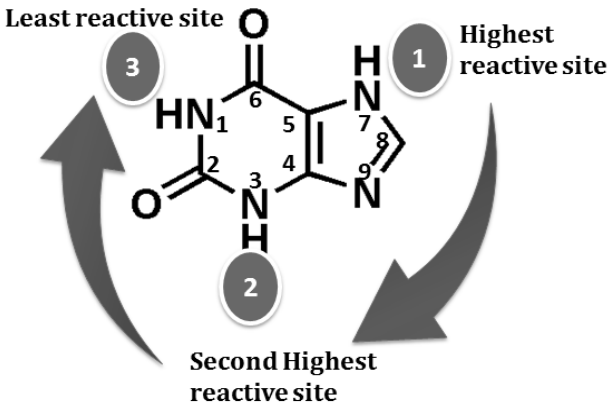

Figure 4.3 Reactivity pattern of –NH groups at N_1, N_3 and N_7 positions of xanthine

Scheme-I: Synthesis of compound 6a1-6a7

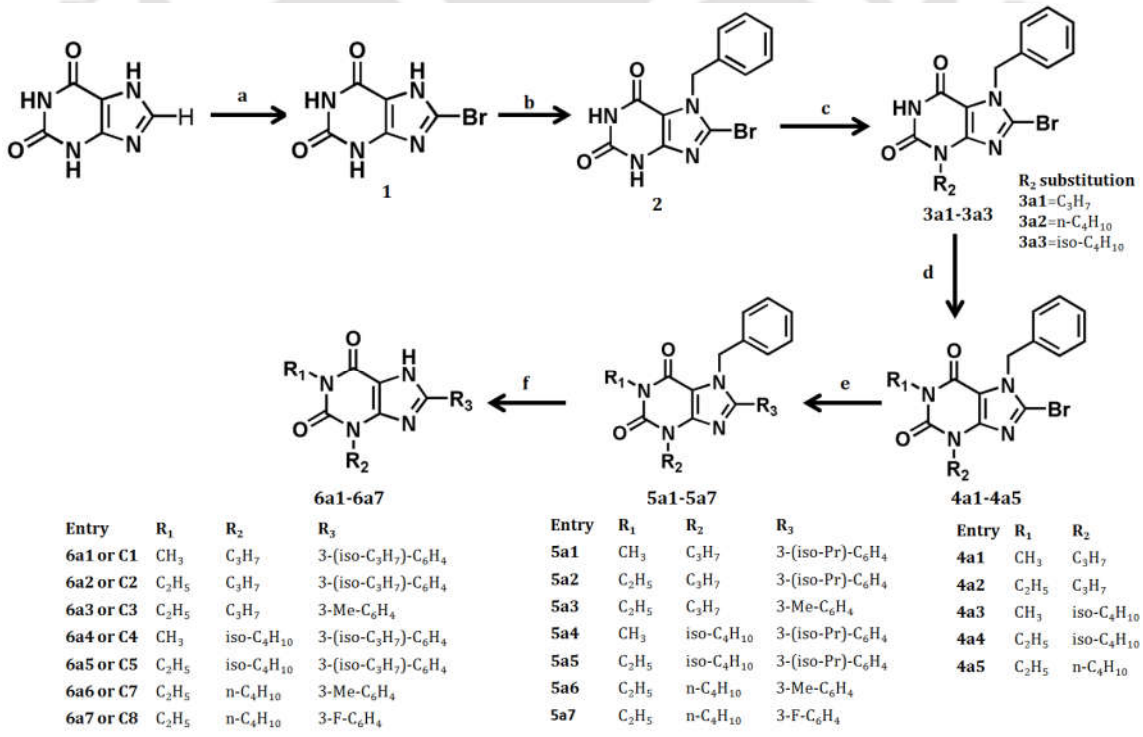

Entry	R_1	R_2	R_3
6a1 or C1	CH_3	C_3H_7	3-(iso-C_3H_7)-C_6H_4
6a2 or C2	C_2H_5	C_3H_7	3-(iso-C_3H_7)-C_6H_4
6a3 or C3	C_2H_5	C_3H_7	3-Me-C_6H_4
6a4 or C4	CH_3	iso-C_4H_{10}	3-(iso-C_3H_7)-C_6H_4
6a5 or C5	C_2H_5	iso-C_4H_{10}	3-(iso-C_3H_7)-C_6H_4
6a6 or C7	C_2H_5	n-C_4H_{10}	3-Me-C_6H_4
6a7 or C8	C_2H_5	n-C_4H_{10}	3-F-C_6H_4

Entry	R_1	R_2	R_3
5a1	CH_3	C_3H_7	3-(iso-Pr)-C_6H_4
5a2	C_2H_5	C_3H_7	3-(iso-Pr)-C_6H_4
5a3	C_2H_5	C_3H_7	3-Me-C_6H_4
5a4	CH_3	iso-C_4H_{10}	3-(iso-Pr)-C_6H_4
5a5	C_2H_5	iso-C_4H_{10}	3-(iso-Pr)-C_6H_4
5a6	C_2H_5	n-C_4H_{10}	3-Me-C_6H_4
5a7	C_2H_5	n-C_4H_{10}	3-F-C_6H_4

Entry	R_1	R_2
4a1	CH_3	C_3H_7
4a2	C_2H_5	C_3H_7
4a3	CH_3	iso-C_4H_{10}
4a4	C_2H_5	iso-C_4H_{10}
4a5	C_2H_5	n-C_4H_{10}

Reagents and Conditions: (a) Br_2, H_2O, 100°C, 3h, 71% (b) benzyl chloride, Anhydrous K_2CO_3, Anhydrous DMF, 2.5 h, 70°C, 67% (c) Alkyl iodide, Anhydrous

K_2CO_3, Anhydrous DMF, 6h, 70°C, 78-92 %; (d) Alkyl iodide, Anhydrous K_2CO_3, Anhydrous DMF, 12 h, 70°C, 90-95%; (e) Pd $(PPh_3)_4$, Anhydrous K_2CO_3, DMF, 48 h, 110°C, inert argon atmosphere, 63-99%; (f) H_2, 10% Pd/H, Methanol, 48 h, rt, 50-93%.

In scheme-I, the N_7 protection step was followed by substitution. First at N_3 position and then at N_1 position of xanthine by alkylation reaction. Alkyl groups such as methyl, ethyl, propyl, n-butyl and iso-butyl groups were selected for substitution reaction because of their positive biological implications such as inotropic effect, higher blood-brain barrier permeability level and plasma protein binding efficiency (Sanae et al., 1995). Alkylation reaction both at N_3 and N_1 positions followed the S_N^2 reaction mechanism. Therefore, in both schemes, alkylation reaction was dependent on the concentration of both reactants (xanthine intermediates and alkyl halides). Alkylation reaction was performed in anhydrous DMF in the presence of anhydrous K_2CO_3. In scheme-I, after selective protection at N_7 position with benzyl group, the first alkylation took place at N_3 position followed by alkylation reaction at N_1 position. Both were carried out with the optimized concentration of the respective alkyl halides. For N_3 substitution, propyl, butyl and isobutyl groups were used whereas, for N_1 substitution, methyl and ethyl groups were used. After sequential substitution at N_3 and N_1 positions, the intermediate product obtained were subjected to Suzuki coupling reaction for C_8 arylation to install phenyl ring with various functional groups and side chains at C_8 position. Suzuki coupling reaction was carried out with respective aryl-boronic acid in presence of palladium catalyst to give aryl substituted xanthine derivatives, **5a1-5a7**. For aryl substitution at C_8 position, meta-substituted phenyl ring was used. The substituent used at meta position was isopropyl, methyl and floro groups. After substitution at all selected positions (N_1, N_3 and C_8 positions) deprotection of N_7 position was carried out

by catalytic hydrogenation reaction. The final synthesized compounds obtained using scheme-I were **6a1-6a7**.

Scheme-II Synthesis of compound 8b1-8b2

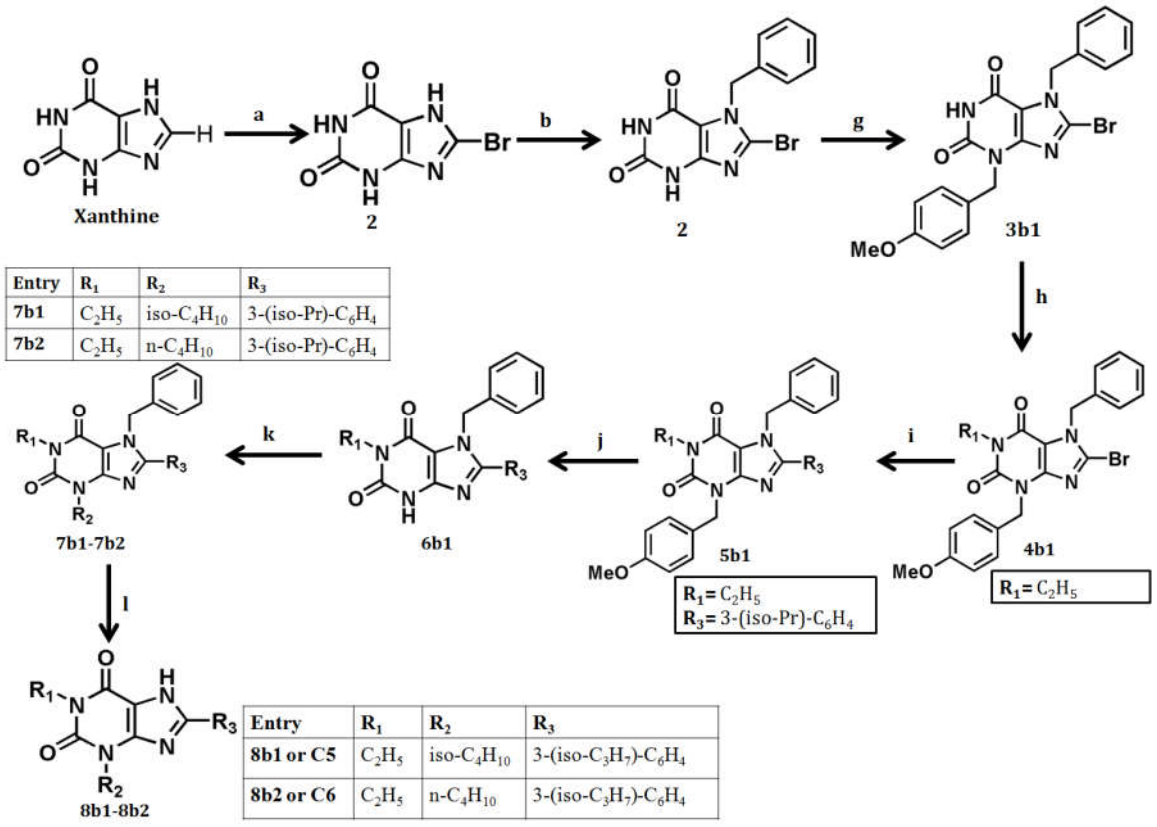

Entry	R_1	R_2	R_3
7b1	C_2H_5	iso-C_4H_{10}	3-(iso-Pr)-C_6H_4
7b2	C_2H_5	n-C_4H_{10}	3-(iso-Pr)-C_6H_4

Entry	R_1	R_2	R_3
8b1 or C5	C_2H_5	iso-C_4H_{10}	3-(iso-C_3H_7)-C_6H_4
8b2 or C6	C_2H_5	n-C_4H_{10}	3-(iso-C_3H_7)-C_6H_4

Reagents and Conditions: (a) Br_2, H_2O, 100°C, 3h, 71 %; (b) benzyl chloride, Anhydrous K_2CO_3, Anhydrous DMF, 2.5 h, 70°C, 67 %; (g) 4-methoxy benzyl chloride, Anhydrous K_2CO_3, Anhydrous DMF, 2.5 h, 70°C, 70%; (h) Alkyl iodide, Anhydrous K_2CO_3, Anhydrous DMF, 12 h, 70°C, 88 %; (i) Pd $(PPh_3)_4$, Anhydrous K_2CO_3, DMF, 48 h, 110°C, inert argon atmosphere; 72%; (j) TFA, conc H_2SO_4, reflux, 22h, 73%; (k) Alkyl iodide, Anhydrous K_2CO_3, Anhydrous DMF, 12 h, 84-95%; (l) H_2, 10% Pd/H, Methanol, 48 h, rt, 71-77% .

Scheme-II is an alternate scheme designed for the synthesis of analogous xanthine derivatives. In this scheme, N_7 protection with benzyl group was followed by

another protection with 4-methoxy benzyl chloride at N_3 position. The sequential double protection strategies at N_7 and N_3 position of 8-bromoxanthine was followed by alkylation reaction at N_1 position which was then followed by Suzuki coupling reaction for arylation reaction at C_8 position. The sequential alkylation at N_1 position and arylation at C_8 position were followed by deprotection of N_3 position by acid catalyzed method. The deprotection reaction was carried out selectively at N_3 position to make N_3 site available for various substituents to be used. After selective deprotection at N_3 position, alkylation reactions were carried out for N_3 substitutions. In scheme-II, after substitution at N_1, N_3 and C_8 positions of xanthine, another deprotection reaction was carried out to deprotect the N_7 position. This was similar to catalytic deprotection method which was employed in scheme-I. Thus, by using scheme-II, compound 8b1-8b2 were synthesized. Compound 8b1 (**C5**) was same as compound 6a5 (**C5**) obtained from scheme-I. Compound 8b2 (**C6**) was synthesized by exclusively using scheme-II.

Rational behind development of scheme-I and scheme-II

The foundation for the design and development of the above two schemes was their protection and deprotection strategies. In both scheme-I and scheme-II, the final step of the scheme was the deprotection of benzyl group at N_7 position. For this deprotection, different deprotection methods were attempted. Both acid deprotection method and catalytic hydrogenation method were used for deprotection at N_3 and N_7 position, but these methods worked differently at N_3 and N_7 position of xanthine derivatives. Acid deprotection method did not work for benzyl deprotection at N_7 position of xanthine derivatives. In both scheme-I and scheme-II, the catalytic hydrogenation was proved as the best method for selective deprotection at N_7 position of the xanthine derivatives when benzyl group was used as the protecting group. However, in scheme-II benzyl group was not appropriate protecting group for N_3 position. In scheme-II, two sequential protections

were required, first protection at N_7 position and second at N_3 position. In scheme-II, it was observed that when benzyl group was used as protecting group at both N_3 and N_7 positions, catalytic deprotection occurred only at N_7 position and did not affect the N_3 position. When 3,7-dibenzyl protected xanthine derivative was subjected to acidic deprotection, then it was found that acidic deprotection occurred selectively at N_3 position with very less product formation. From this study, it was analyzed that there was a strong possibility of selective deprotection at the N_3 position if a more appropriate protecting group was used. Hence, in scheme-II, p-methoxy benzyl chloride was used to protect N_3 position because of the presence of methoxy (an electron releasing) group that facilitated deprotection. The selective deprotection of p-methoxy benzyl group at N_3 position was carried out by acid deprotection method. The acid deprotection was selective for the N_3 position both in the case of benzyl and p-methoxy benzyl protecting groups. However, this method was more suitable for deprotection of p-methoxy benzyl group. The acid deprotection method was non-reactive to deprotection of benzyl protecting group at N_7 position. Therefore, this method was used for selective N_3 deprotection in scheme-II.

Catalytic deprotection of benzyl group at N_7 position of xanthine derivatives in scheme-I and scheme-II

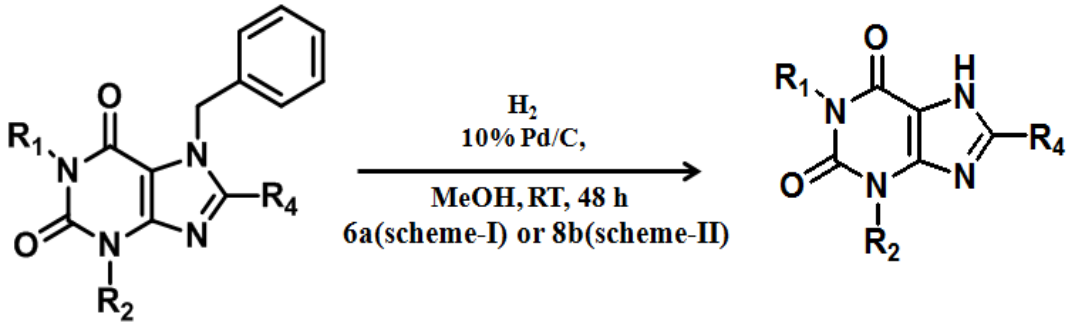

Selective deprotection of benzyl group at 7th position

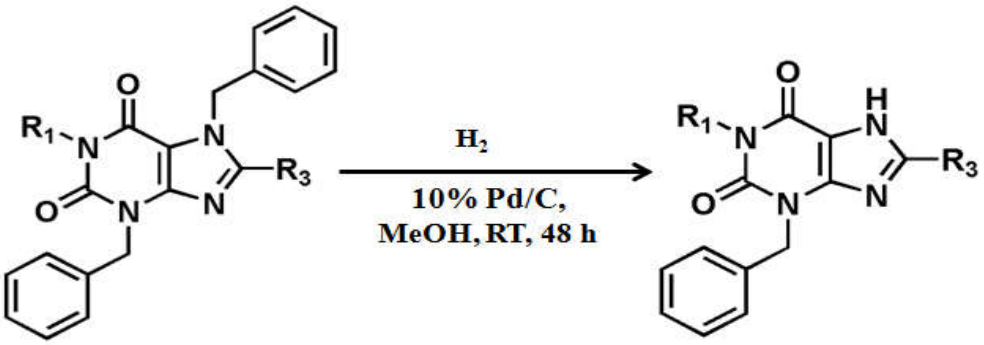

Scheme-II Step-6b: Acid deprotection of p-methoxy benzyl (PMB) group at N_3 position of xanthine derivative in scheme-II

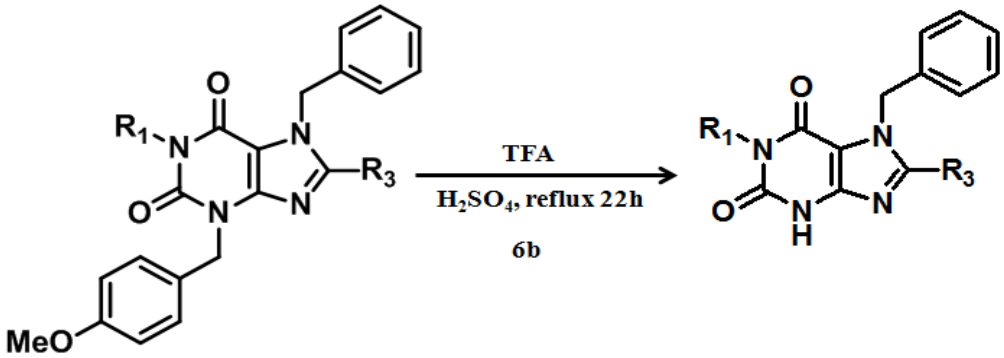

Thus, the whole synthesis work was divided into two schemes; scheme-I and scheme-II, which simplified the nature of xanthine derivatives by giving clear view on the reactivity and substitution pattern of different –NH groups of the xanthine scaffold. Scheme-I can be applied for those compounds which have common N_3 position with diverse N_1 and C_8 substitutions. Likewise scheme-II can be applied for synthesis of compounds having common N_1 and C_8 substituent but different N_3 substituent. It was apparent from the synthesis of two compounds (8b1 and 8b2) using one single synthesis pathway of scheme-II. These two compounds varied only at N_3 position. Compound 8b1 consists of iso-butyl group at N_3 position whereas, compound 8b2 consisted of n-butyl group. Thus, these two separate schemes are designed to construct diverse library of xanthine derivatives. Comparing with existing methods, xanthine initiated synthesis

mechanism has numerous advantages such as mild reaction conditions, cost-effectiveness and readily available reagents, use of non-hazardous chemicals, no need for chromatographic clean up in most of the steps, shorter reaction time, multiple compound generation using single scheme and better product yield. Due to these advantages, the above proposed schemes are better alternatives as compared to existing methods which has been used worldwide till date for the synthesis of xanthine derivatives.

4.4. Conclusion

The present study relates to the field of drug development and pharmaceutical chemistry, specifically to a class of substituted xanthine derivatives, preparation method and the use thereof, as therapeutic agents targeting phosphodiesterases 9A (PDE9A). Xanthines and its derivatives have been known for their non-specific PDE inhibition property. The modification at different positions of the xanthine molecule enhances the size and renders rigidity to the newly developed inhibitors which enhance the binding affinity of compounds towards PDE9A. By developing two novel schemes (scheme-I and scheme-II) for synthesis of xanthine derivatives, the current study has tried to fill the existing lacuna in the field of xanthine based drug development. These schemes have shown the standard pathway for synthesis of library of compounds and tried to simplify the understanding of the chemical nature of xanthine and its derivatives.

The present study focuses on the development of novel schemes for the synthesis of 1, 3, 8- tri substituted xanthine derivatives using xanthine as a starting material. But in proceeding with xanthine, the most challenging factor was presence of three –NH group at N_1, N_3 and N_3 positions of xanthine. The present study tried to understand the reactivity pattern of substitution at different –NH positions. By concentration optimization of reactant, it was identified that substitution followed in the order of N_7

substitution>N_3 substitution>N_1 substitution. This was because of reactivity of –NH groups of xanthine follows the order of N_7>N_3>N_1. Thus, due to higher affinity of N_7 position, protecting this position was imperative to precede further substitutions at N_1, N_3 and C_8 positions. The whole synthesis was based on protection and deprotection strategies. In both schemes, the protections were carried out in such a way that possible deprotection could be selectively taken up at N_7 and N_3 position. Acid deprotection method was the best method for selective deprotection of N_3, whereas, catalytic deprotection was the best method for selective deprotection of benzyl group at N_7 position. Alkylation was important step for substitution at N_1 and N_3 positions whereas, for selective arylation, Suzuki coupling method was applied. Thus, the two schemes (scheme-I and scheme-II) developed in the current study will have great significances in the long run for synthesizing a diverse library of xanthine based compounds.

CHAPTER 5

Biological Studies of Selected Compounds

Prologue

After an extensive work on the in silico studies and chemical synthesis, we landed with some selective inhibitors of PDE9A. Though these compounds were proved as potent inhibitors for PDE9A based on computational data, their biological studies were imperative for final validation of their potency as well as specificity towards PDE9A. In contrast to widely used radioactive method, new spectrophotometric MLG assay was used for structure activity relationship (SAR) analysis. The data obtained from spectrophotometric assay was used to calculate the biochemical half maximal inhibitory concentration (IC_{50}) and the inhibition constant (Ki) values. Based on the IC_{50} values of selected compounds, the pattern of potency was determined. The structural change at different positions of xanthine has significant impact in the inhibition affinity of compounds. Thermal shift assay were used to understand the stability of PDE9A with inhibitors bound form. The synthesized compounds showed better stability than the virtual screened compounds in PDE9A bound form. The comparative inhibition studies with other PDEs gave future perspectives for further drug development. The present work revealed the potential of xanthine scaffold in constructing potent compounds with requisite modification as per the active site requirement of particular member of PDE superfamily.

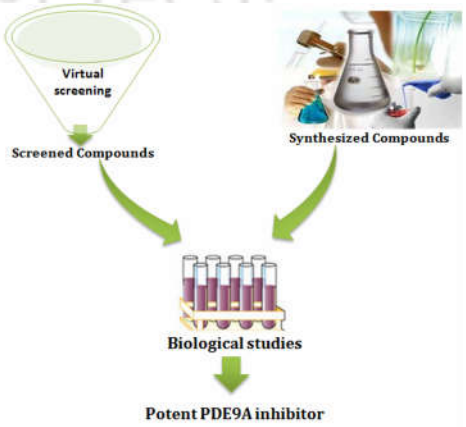

5.1. Introduction

In vitro studies are an essential part of research geared towards the discovery of drug candidates. Driven by predictive information obtained from *in silico* studies, *in vitro* techniques have been developed to study many other aspects of drug disposition such as structure activity relationship (SAR) analysis and temperature based stability analysis. Through both virtual screening of existing inhibitors and docking study of new inhibitors, the present study has tried to diversify the inhibitor based research in terms of introducing a new scaffold 'xanthine' for PDE9A inhibition. *In silico* study showed the potential of xanthine as a scaffold for future drug development process. However, the final validation was carried out by SAR analysis and thermal shift assay. Most of the earlier studies reported so far used radioactive approach which rests on the use of [^{3}H]-cAMP or [^{3}H]-cGMP as substrate. These methods were not favorable because of many reasons including the high cost of radioactive substrate, the harmful effect of the radiation and the radiation risk in operation (Feng et al., 2011; Zhu et al., 2009). Hence, there was a need to go for an alternative approach for inhibition studies. In 2009, Zhu *et al* gave spectrophotometric malachite green (MLG) assay for PDE4 inhibition studies. In the present study, this method was first time applied for activity assay and inhibition study of PDE5A and PDE9A. The MLG assay is coupled end point assay which depends on the catalytic action of two enzymes- PDE and calf intestinal alkaline phosphatase (CIAP).

A new series of compounds containing xanthine scaffold were discovered by the combinatorial studies such as virtual screening, molecular dynamic, structure-based design, molecular docking studies and drug-likeness property prediction. These procedures saved the load of chemical synthesis. Thus, one compound from virtual

screening and eight manual designed compounds of chemical synthesis were selected for structure activity relationship (SAR) analysis. Thermal shift assay was another important approach to determine the stability of compounds in PDE9A bound form. The thermal shift analysis ensured the stability of compounds during inhibition of targeted protein PDE9A. The *in vitro* analysis of selected compounds helped to understand the structural requirement of ligand targeting PDE9A for inhibition.

5.2. Materials and Methods

5.2.1. Cloning of selected PDEs (PDE9A, PDE5A and PDE4D)

Along with PDE9A two other PDEs- PDE5A and PDE4D were selected from PDE superfamily. These selections were based on their substrate specificity and their widely researched criteria. PDE4D was cAMP specific PDE whereas PDE5A was cGMP specific PDE. The Full length cDNA clone of PDE4D [IMAGE ID 4828512, Gene bank Accession no. AF012074], PDE5A [IMAGE ID 8991949, Gene bank Accession no. AM393036] and PDE9A [IMAGE ID 3874635, Gene bank Accession no. BC009047] were purchased from Source Bioscience Life sciences, UK. The coding domains of PDE4D (275-602), PDE5A (535-860) and PDE9A (181-506) were sub-cloned for inhibition studies and various other studies. **Figure 5.1** illustrates the cloning procedure used for sub-cloned the coding domain of selected PDEs in pET15b expression vector.

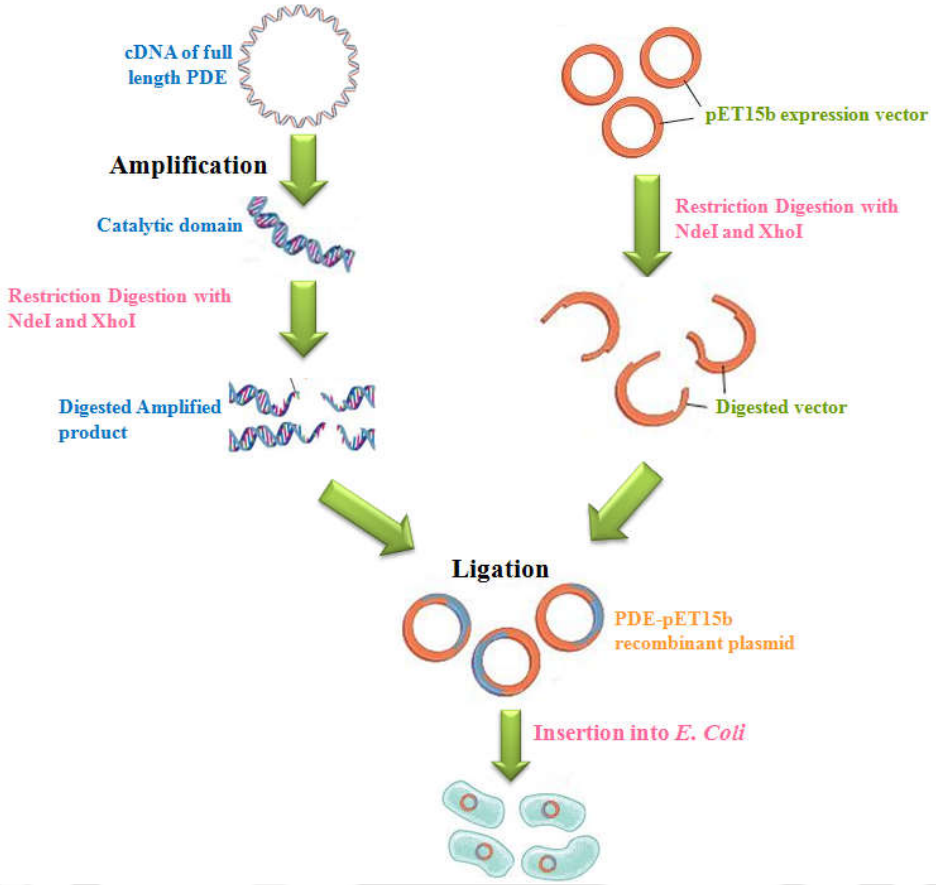

Figure 5.1 Schematic diagram of cloning procedure of coding domain of selected PDEs

Amplification of coding domain of selected PDEs

Amplification of coding domains from full length PDEs were carried out using gradient PCR. The amplification reactions were carried out with the help of a pair of synthesized oligonucleotide primers. The oligonucleotide primers were designed with the help of Sigma primer designing web tool and FastPCR software. The details of oligonucleotide primers for amplification of coding domain of PDE4D, PDE5A and PDE9A have been provided in the **Table 5.1.** For amplification of the coding domain from full length cDNA, the reaction components (given in **Table 5.2**) were mixed gently. Amplification was performed in a Gradient PCR (Takara Thermo cycler). Conditions used for gradient PCR amplification has been given in **Table 5.3**. PCR product were run

on 0.8 % agarose gel and visualized under UV light using ethidium bromide staining. The amplified fragments were purified with the help of gel elution technique.

Table 5.1 Oligonucleotide synthesized primers for the amplification of coding domains of PDE4D, PDE5A and PDE9A

Primers for PDE4D

Forward primer- ccgcgccatatgactgaacaagaagatgtcct

Reverse primer- ccatactcgagttagctctgagggattgtgct

Primers for PDE5A

Forward primer- cgcgcccatatggaagaaacaagagagcta

Reverse primer- ccatactcg agttactgctgttctgcaaggg

Primers for PDE9A

Forward primer- gacgcgatcata tgacttaccccaagtacctg

Reverse primer- cgggcctcgagttacttct tctgtaactctt

Table 5.2 Composition details of reactants for PCR amplification

Components	**Volume**	**Final Concentration**
cDNA	1 µL	10 ng
5X phusion High Fidelity Buffer	10 µL	1X
dNTPs	1 µL	200 µM
Forward Primer	2.5 µL	0.5 µM
Reverse Primer	2.5 µL	0.5 µM
DMSO	1.5 µL	3%
Phusion DNA polymerase	0.5 µL	1.0 units/50 µl PCR
Nuclease free Water	to 50 µL	

Table 5.3 Parameters for amplification of coding domains from full length cDNA clones

Gradient PCR programmes	Temperature	Time	Cycle
(1) Activation	98°C	30 seconds	1
(2) Denaturation	95°C	15 seconds	30
(3) Gradient temperature	55-65°C for PDE9A2 60-70°C for PDE5A1 62-72°C for PDE4D2	35 seconds	
(4) Extension	72°C	30 seconds	
(5) Final extension	72°C	8 minutes	1
(6) Preserve	4°C	indefinite	1

Restriction digestion and ligation reaction of coding domain of PDEs

The amplified coding domain of selected PDEs (PDE4D, PDE5A and PDE9A) and the expression vector (pET15b) were digested separately with the help of restriction enzymes NdeI and XhoI and then purified by gel elution technique. Ligation reaction of the digested coding domains with digested vector was carried out with the help of Quick T4 DNA ligation kit (m/s Merck Millipore) at 24°C for 1h. Thereafter, the resultant recombinant plasmid (PDE4D-pET15b, PDE5A-pET15b and PDE9A-pET15b) were transformed into *E. coli* DH5α for long term storage. The recombinant plasmids were isolated from their respective *E. coli* DH5α strain then clones were confirmed by restriction digestion and PCR. Final confirmation of the coding domains was carried out by sequencing of coding domain of recombinant plasmids from Europhin Genomics.

5.2.2. Expression and purification of selected PDEs (PDE9A, PDE5A and PDE4D)

The cloned catalytic domains of selected PDEs (PDE4D, PDE5A and PDE9A) were expressed in BL21 strain of *E. coli.* The recombinant clones were transformed into *E. coli* BL21. The BL21 strain carrying recombinant plasmid was grown in LB medium

at 37°C temperature and 180 rpm to absorption A_{600} = 0.7. After that culture was induced with optimized concentration of β-D-thiogalactopyranoside (IPTG) and further growth was allowed at 15°C for 16h. The culture was pelleted down at 4°C with 8000 rpm for 12 minutes. The pellet was dissolved in lysis buffer containing 20 mM Tris-HCl, 10 mM $MgCl_2$, and 5 mM β- mercaptoethanol at pH 7.5/7.8. The lysate was then sonicated for 25 cycles (7 second on and 20 second off). Sonicated samples were centrifuged at 4°C with 13000 rpm for 30 minutes. The supernatant was collected for Ni-NTA affinity purification. The purified PDE4D, PDE5A and PDE9A proteins were confirmed by SDS-PAGE. The concentration of purified protein was determined by extinction coefficient determination method using ExPASy-ProtParam tool and protein estimation tool [http://christoph-leidig.de/tprot.html]. The details of buffer composition have been provided into **Table 5.4.**

Table 5.4 Optimized conditions for expression of PDEs

Condition	**Buffer for protein purification**
Lysis buffer	20 mM Tris-HCl, 10 mM $MgCl_2$, 5mM β-mercaptoethanol (pH 7.5 for PDE5A and PDE4D, pH 7.8 for PDE9A)
Extraction buffer	20 mM Tris-HCl, 10 mM $MgCl_2$, (pH 7.5 for PDE5A and PDE4D, pH 7.8 for PDE9A)
Washing buffer	20 mM Tris-HCl, 10 mM $MgCl_2$, 20 mM imidazole (pH 7.5 for PDE5A and PDE4D, pH 7.8 for PDE9A)
Elution buffer	20 mM Tris-HCl, 10 mM $MgCl_2$, 250 mM imidazole (pH 7.5 for PDE5A and PDE4D, pH 7.8 for PDE9A)

5.2.3. Spectrophotometric activity assay of expressed PDEs

The activity of expressed PDE proteins was analyzed by malachite green (MLG) assay- a spectrometric assay (Feng et al., 2011; Zhu et al., 2009). This assay is basically dependent on the coupled action of two enzymes- phosphodiesterase (PDEs) and calf intestinal alkaline phosphatase (CIAP). Activity assay of PDE9A and PDE5A was

performed in the presence of their common substrate cGMP, whereas activity assay of PDE4D was carried out with its substrate cAMP. MLG assay comprised several steps such as preparation of phosphate standard, optimization of concentration of CIAP by separate assay, etc.

Requirements for spectrophotometric MLG assay:

(a) Molybdate solution- solution of 50 mM Ammonium molybdate and 3.4 M sulphuric acid in milliQ water

(b) MLG reagent – Solution of 1 mM malachite green, 0.16 % Poly vinyl alcohol, 6.0 mM sulphuric acid in milliQ water

(c) 1 mM Phosphate buffer- 1mM of potassium di-hydrogen phosphate (KH_2PO_4) + 1mM of di-potassium hydrogen phosphate (K_2HPO_4) in milliQ water

(d) A reaction buffer used for assay contained 20 mM Tris-HCl at pH 7.5, 10 mM $MgCl_2$, 0.10 mM EDTA at pH 7.5 in milliQ water.

Preparation of phosphate standard

Spectrophotometric phosphodiesterase activity assay was the combined action of two enzymes- one was the expressed PDE and other was commercially available CIAP. At the end phosphate released due to combined catalytic action of two proteins. The released phosphate was quantified by using phosphate standard graph. Phosphate standard graph was prepared in the reaction buffer containing 10 mM $MgCl_2$, 0.10 mM EDTA, 6.3% $HClO_4$ and 2.8% glycerol. Phosphate solution used for the standard was prepared by addition of potassium di-hydrogen phosphate (KH_2PO_4) and di-potassium hydrogen phosphate (K_2HPO_4). 0.7 mL of phosphate solution of different concentrations (1-60 µM) were taken in a series of eppendorf tubes. 70 µL of molybdate solution was

added in the respective tubes. Each reaction tubes were allowed to incubate for 2 min then 130 µL of MLG reagent was added. Subsequently, all reaction tubes were incubated at 30°C in water bath for 30 minutes. Final absorbance was taken at 630 nm in single beam spectrophotometer (Toshvin Analytical). All concentrations were taken in duplicate.

Concentration optimization of CIAP to act as second enzyme in couple end point assay

In MLG spectrophotometric assay role of CIAP was to release phosphate (PO_4^{3-}) from the intermediate product (AMP or GMP) which was obtained by the catalytic action of PDE on the substrate (cAMP or cGMP). For this, the optimized amount of CIAP was required. The amount of CIAP needed for assay and inhibition studies was estimated by separate MLG assay. For CIAP catalytic reaction, the reaction mixture at 30°C in 1.35 mL contains different concentrations of properly-diluted CIAP (1-100 U/L) in the buffer (20 mM Tris-HCl, 10 mM $MgCl_2$ and 0.10 mM EDTA at pH 7.5) containing 28% glycerol. Reaction was started by adding 60 µM GMP or 40 µM AMP. After the indicated reaction duration, CIAP action was terminated by the addition of 157µL $HClO_4$ solution (60%). The reaction samples were then centrifuged at 5000g for 10 min to remove denatured proteins. After that, 0.70 mL of the acidified supernatant from different reaction tubes was withdrawn to the fresh eppendorf tubes. Then 70 µL molybdate solution was added to each tube and then solution was incubated for 2 minutes. It was followed by addition of 130 µL MLG reagents in each tube. Reaction was then allowed to incubate at 30°C for 30 minutes. The amount of phosphate released from GMP or AMP by the catalytic action of CIAP was estimated at the absorbance of 630nm wavelength. This experiment gave the estimation of concentration of CIAP needed further for both PDE activity assays and inhibition studies.

Activity assay of selected PDEs (PDE9A, PDE5A and PDE4D)

For PDE activity assay, the reaction mixture of 1.35 mL at 30°C contained 1.26 mL reaction buffer and optimized concentration of CIAP (70 U/L for GMP or 80 U/L for AMP) was taken in a series of eppendorf tubes. Various concentrations (1-50 µg/mL) of PDE (PDE9A or PDE5A or PDE4D) were added into each tube. In reaction mixture the final concentration of glycerol was of 2.8%. The enzymatic reaction was started at 30°C with the addition of 50 µL of cGMP or cAMP in each reaction tube. The reaction was carried out at 30°C for 30 minutes in water bath. The reaction was terminated by the addition of 157 µL $HClO_4$ (40%) after an indicated reaction duration. After centrifugation at 5000 g for 10 min to remove denaturated proteins, 0.70 mL of the acidified supernatant was withdrawn in fresh tube to quantify the released phosphate. After that 70 µL molybdate solution was added to the acidified supernatant first and then 130 µL MLG reagents was added after a lag time of 2 min. The reaction mixtures were incubated at 30°C for 30 min. Absorbance was measured at 630 nm in a microcell of 1.00 cm light path.

Kinetics studies of selected PDEs (PDE9A, PDE4D and PDE5A)

PDEs are crucial enzymes in the of mammalian cell signaling pathway. They fall under the hydrolase group in enzyme classification with E.C. number 3.1.4. (3.1.4.35 for PDE9A, 3.1.4.17 for PDE5A and 3.1.4.53 for PDE4D). Michaelis-Menten model is best kinetic studies model to understand the kinetic behavior of enzyme. This kinetic studies model is typically referred as Michaelis-Menten equation.

$$V = \frac{[S]\,V_{max}}{[S] + K_m}$$

Where,

v = rate of reaction

V_{max} = maximal reaction rate

S= substrate concentration

K_m = Michaelis-Menten constant

In this study, K_m and V_{max} of selected PDEs (PDE9A, PDE5A and PDE4D) were calculated by non-linear regression analysis. The K_m is substrate concentration at which enzyme achieves rate of reaction half of the maximum velocity (V_{max}).

5.2.4. Spectrophotometric inhibition studies of selected PDEs

Inhibition study of PDE9A was imperative to understand the binding efficiency of compounds derived from chemical synthesis and virtual screening. For PDE inhibition studies similar spectrophotometric malachite green assay was used. Inhibition study was a key analysis to determine the structure-activity relationship of newly synthesized compounds. For PDE inhibition study, the reaction mixture at 30°C in 1.35 mL contained 0.90 mL reaction buffer plus an indicated PDE inhibitor, 0.15 mL of CIAP solution, 0.20 mL solution of a PDE, 0.10 mL aqueous cGMP or cAMP for the final concentration at 16 µM (as optimized). In reaction mixture the final concentration of glycerol was 2.8%. Enzymatic reactions were initiated at 30°C with the addition of cGMP or cAMP and were terminated with the addition of 0.25 mL $HClO_4$ (40%) after an indicated reaction duration. After centrifugation at 5000 g for 10 min to remove denaturated proteins, 0.70 mL of the acidified supernatant was withdrawn to fresh eppendorf tubes to quantify the inorganic phosphate released from the combined action of PDE and CIAP. Thereafter, 70 µL molybdate solution was added to the acidified supernatant at first and then 130 µL MLG reagent was added after a time lag of 2 min.

The incubation time for the dye binding was kept 30 min at 30°C before the absorbance was measured at 630 nm. More than 10 different concentrations (1-200 µM) of selected inhibitors were used. Three independent reactions were carried out to validate the result. MLG inhibition assay was carried out with both virtual screened and chemically synthesized compounds. Four top hit (ZINC62579975, ZINC12231988, ZINC12231966 and ZINC12232141) obtained from virtual screening were purchased from Enamine Ltd (US). cGMP were purchased from Sigma Aldrich. **Figure 5.2** illustrates the protocol used for spectrophotometric MLG inhibition assay.

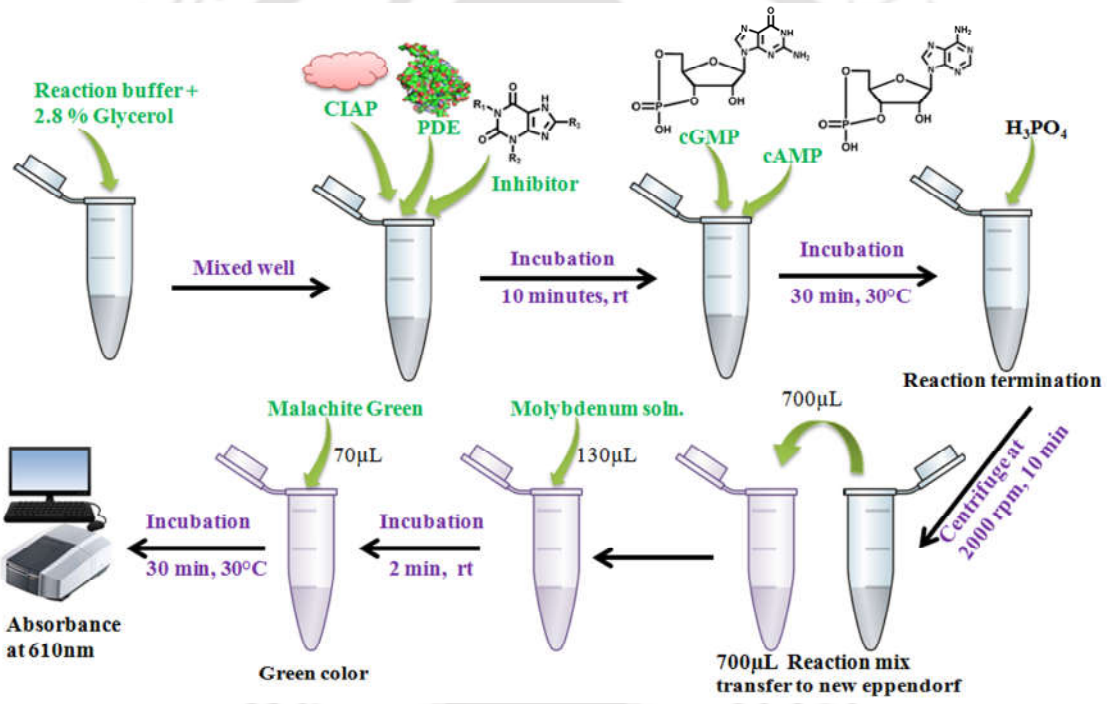

Figure 5.2 General procedure for spectrophotometric inhibition assay of PDEs

Structure activity relationship (SAR) analysis for selected inhibitors (synthesized and virtual screened compounds)

IC_{50} is the concentration of inhibitor where the enzymatic reaction and product release was reduced to half. Dose-response plot was used to determine the role of inhibitor on reducing the catalytic activity of PDEs. These experiments were carried out

with MLG spectrophotometric inhibition assay at the constant concentration of enzyme and substrate with varying (1-200 µM) inhibitor concentration. This was crucial analysis to determine the structure activity relationship of selected compounds. The IC_{50} values obtained from SAR analysis were crucial to determine the changes which were responsible for improving the potency of synthesized compounds towards PDE9A inhibition. The IC_{50} graph was plotted to determine the percentages inhibition of PDE9A activities against logarithmic concentrations of a candidate inhibitor. The linear part of such plots was used for regression analysis which gave IC_{50} of the candidate inhibitor. For measurement of IC_{50} value at least ten different concentrations of each inhibitor were used. Each experiment was repeated at least three times. Results were represented as mean ± standard deviation. Kinetic studies using cGMP as substrate at various concentrations gave K_m values; this enabled the estimation of K_i of all synthesized compounds from experimental IC_{50} values using web-tool (Cer et al., 2009).

K_i determination assay of most promising synthesized compound

The compound which showed best potency among eight synthesized compounds targeting PDE9A was chosen for K_i determination assay**.** Three independent reactions were carried out with different concentration of inhibitors (0 µM, 25 µM and 50 µM). The substrate (cGMP) concentrations were varied from 0-30 µM whereas the protein (PDE9A) concentration was kept constant at 16 µg/mL. The reaction was carried out at 30°C. The assay procedure for K_i determination was similar to inhibition studies. Ki was calculated using non-linear regression analysis.

5.2.5. Real time differential scanning fluorimetry thermal shift assay

Differential scanning fluorimetry (DSF) thermal shift assay was performed to determine the stability of ligand bound protein. The reaction buffer used for this assay

was 20 mM Tris-HCl at pH 7.5, 10 mM $MgCl_2$, 0.10 mM EDTA, 10% Glycerol. The reaction was carried out in presence of 200X SYPRO Orange (Invitrogen). The excitation and emission spectra of the dye was performed at 492nm and 610nm respectively. The concentration of protein and inhibitor used for this assay were 20 µM and 200 µM (1:10) respectively. DSF was performed in Real Time PCR instruments (Agilent Mx3005P QPCR System). The protocol followed for DSF assay was taken from published article by Niesen et al in 2007. For this assay, the reaction buffer was taken in a series of PCR tubes. Reactions were carried out in triplicates. For this study Lysozyme was used as standard whereas 'buffer with dye' was used as control. In this study, a simple fitting procedure was used for quick calculation of melting temperature (T_m). The midpoint temperatures (T_m) of the transitions were calculated for melting curves from the midpoint of transition. The midpoint of transition was the temperature at which 50% of the proteins were denatured, and was a measure of the protein's inherent thermal stability (Niesen et al., 2007). DSF thermal shift assay was performed to determine the stability of inhibitor bound protein by the comparative study of change in melting temperature or ΔT_m of inhibitor bound PDE9A with the substrate bound protein complex.

5.2.6. Comparative biological studies of synthesized compound and selected ZINC compound

Present study was based on mainly two kinds of compounds- one compound obtained from virtual screening and eight novel compounds derived from manual design, molecular docking and chemical synthesis. The compounds obtained from these two paths were further compared by using all assay data. This comparison was imperative to understand the nature of compounds and modification sites in relation to protein inhibition.

5.3. Results and Discussion

5.3.1. Cloning of selected Phosphodiesterases

In PDE superfamily the catalytic domain perform catalytic function independently. Hence, most of the studies used catalytic domain for biological studies (Huai et al., 2004; Liu et al., 2008). The amplification of coding domain of selected PDEs (PDE9A, PDE5A and PDE4D) was carried out successfully from their full length cDNA clones. The best amplification of PDE9A, PDE5A and PDE4D were carried out at 61.8°C, 63.2°C and 67.6°C respectively. The size of products obtained after amplification were of 978 base pairs (PDE9A), 978 base pairs (PDE5A) and 984 base pairs (PDE4D) as shown in **figure 5.3.** The amplified coding domains of all selected PDEs were cloned successfully in the pET15b expression vector. The clones were confirmed by both restriction digestion and PCR of recombinant clones. The clones were finally confirmed by sequencing from Europhin Genomics. The sequencing data has been provided in Appendix-III.

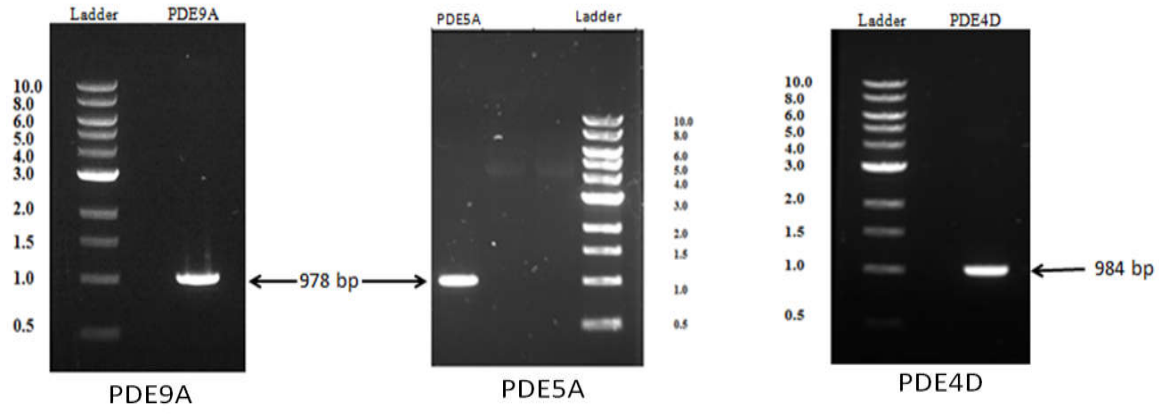

Figure 5.3 Amplified catalytic domains of PDE9A, PDE5A and PDE4D

5.3.2. Protein expression and Purification

Expression of selected PDEs (PDE9A, PDE5A and PDE4D)

Protein expression was achieved in following four steps. Step-I: The culture was inoculated and allowed for growth at 37°C and after 2-3 hrs of growth IPTG was added for inducing the expression of His-tagged PDE proteins. Step-II: After induction the cells were allowed to grow for 20 hours at 15°C with 120 rpm agitation. Step-III: The cells were pelleted down and lysed and supernatant and pellet both were collected separately. Step-IV: Protein expression was confirmed by SDS-PAGE.

Purification of selected PDEs (PDE9A, PDE5A and PDE4D)

Ni-NTA affinity chromatography method was best method for the purification of PDE proteins. The best suited expression and binding buffer were 20 mM Tris-HCl at pH 7.8 (pH 7.5 for PDE5A and PDE4D), 10 mM $MgCl_2$ and 5 mM β-mercaptoethanol. The lysate were allowed to bind for 3 hours at 4°C. The washing buffer used for purification consisted of 20 mM Tris-HCl at pH 7.8 (pH 7.5 for PDE5A and PDE4D), 10 mM $MgCl_2$ and 20 mM imidazole. Using imidazole more than 20 mM had negative impact on the yield of purified protein. As very low concentration of imidazole was used in washing step, thus the washing time was increased with increasing the volume of washing buffer (100 mL) to elute all impurities. Simultaneously the content of impurity was checked with Bradford solution. The purified protein was eluted with good yield with same buffer containing 250 mM imidazole. 250 mM imidazole was good enough to release all the purified protein from Ni-NTA column. The purified protein was confirmed by 12 % SDS-PAGE. Concentration yield obtained after Ni-NTA were for 1 mg/mL (PDE9A), 2 mg/mL (PDE5A) and 2 mg/mL (PDE4D). Selected PDEs (PDE9A, PDE5A and PDE4D)

were successfully purified to single band as shown in **figure 5.4**. Coomassie Brilliant Blue staining revealed a single protein band with a molecular weight of about 40.06 kDa (PDE9A), 40.06 kDa (PDE5A) and 40.7 kDa (PDE4D). The concentration of purified proteins was determined by extinction coefficient.

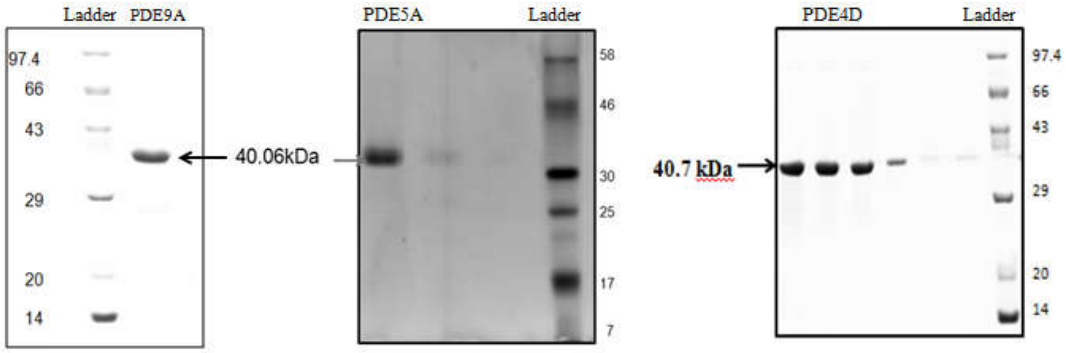

Figure 5.4 SDS PAGE of purified PDE proteins (a) PDE9A (b) PDE5A and (c) PDE4D

5.3.3. Spectrophotometric Malachite green activity assay of selected PDEs

In the present study, the activity of purified PDEs was determined by using MLG assay, a spectrophotometric assay (Zhu et al., 2009). MLG assay is a fast, reproducible, and non-radioactive method for measuring inorganic free phosphate released from the catalytic action of reaction enzymes in aqueous solutions. This simple assay method is based on the complex formed between malachite green molybdate and free orthophosphate under acidic conditions. This method was based on the estimation of inorganic phosphate released from cGMP or cAMP by the combined catalytic action of PDE and CIAP. **Figure 5.5** depicts the mechanism of the spectrophotometric MLG assay.

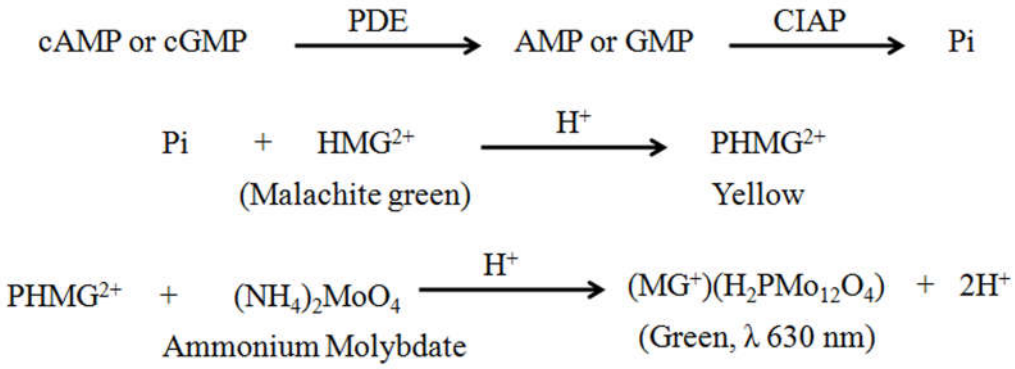

Figure 5.5 Mechanism of action of couple end point MLG assay which depends on the combined action of PDE and CIAP

Phosphate standard for MLG assay

Inorganic phosphate released from intermediate substrate (AMP or GMP) by the catalytic action of CIAP in the MLG assay was quantified by using the phosphate standard. Phosphate standard was created by carrying out the similar assay. For this, phosphate buffer of different concentration (0.5 µM- 60 µM) were used to quantify the content of phosphate through absorbance at 630 nm. Linear range for MLG assay was obtained between 1 µM - 20 µM of phosphate from phosphate buffer. **Figure 5.6** depicts the phosphate standard graph for further spectrometric activity assay and inhibition studies

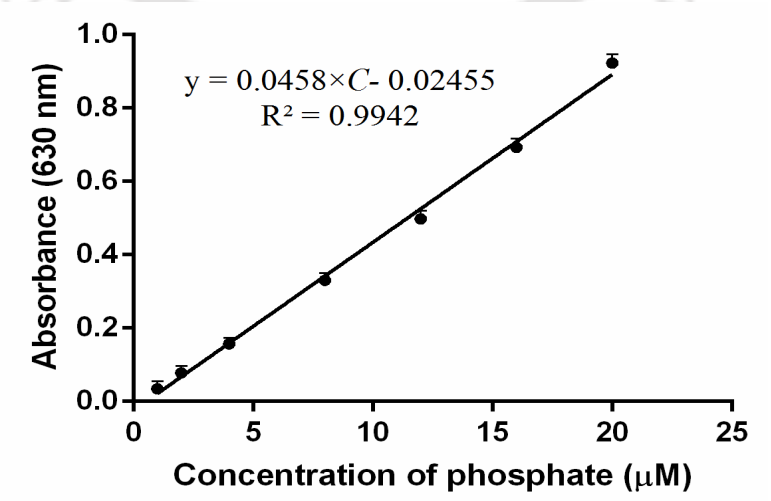

Figure 5.6 Standard graph of inorganic Phosphate for malachite green assay

Optimization of CIAP concentration for hydrolysis of AMP or GMP

CIAP acted as second enzyme to release inorganic phosphate (P_i) from intermediate products (AMP or GMP). In malachite green spectrophotometric assay, cyclic AMP or cyclic GMP acts as a substrate. The catalytic action of PDE breaks the 3'5'-cycle of the substrate and linearised the cyclic phosphate and the product obtained from this catalytic action was AMP or GMP. AMP or GMP acted as substrate for CIAP. CIAP then released inorganic phosphate from 5' end of the intermediate products (AMP or GMP). The released inorganic phosphates were further quantified by MLG assay. For this purpose quantification of commercial CIAP was needed for coupled end point assay. Quantification of CIAP was carried out by similar malachite green assay. By quantification of CIAP it was found that 80 U/L was the maximum required concentration for breaking AMP and/or GMP both, hence, this concentration was used in further PDE MLG assay. In principle, the CIAP concentration should be taken the upper limit of saturation to ensure the full potential of CIAP to breakdown most of GMP or AMP release by the catalytic action of PDEs.

Enzyme Kinetics studies of selected PDEs (PDE9A, PDE5A and PDE4D)

Malachite green phosphodiesterase assay is absorbance based spectrophotometric assay. It is high throughput method for measuring cyclic nucleotide phosphodiesterase activity. To measure PDE9A activity, coupled end-point assay was used that depends on the combined action of both PDE and CIAP to produce inorganic phosphate which was finally quantified by the MLG assay. Both PDE and CIAP require magnesium ion for their activity (Zhu et al., 2009). Hence $MgCl_2$ was used in the reaction buffer.

In PDE9A, initial rate of reaction was carried out at 60 µM cGMP and 80 U/L of CIAP to estimate the required quantity of protein in further reactions. The concentration of PDE9A was varied from 1-30 µg/mL. At the concentration of 18 µg/mL, PDE9A protein got saturated and precipitation started. Phosphate release from 60 µM of cGMP at 18µg/mL of PDE9A was 9 µM. Therefore, for kinetic studies, this concentration (18 µg/mL) of PDE9A was taken. The concentration of substrate was varied from 1-30 µM. Maximum consumption of cGMP occurred at 12 µM after that saturation started. Inorganic phosphate released from 12 µM of cGMP was 5.467 µM. Hence, 12 µM cGMP was used for further inhibition studies of PDE9A with selected compounds.

Similarly, kinetic studies of PDE4D and PDE5A were carried out with MLG assay. In the presence of initial substrate concentration of 60 µM, the proteins started to saturate at 14 µg/mL and 16 µg/mL of PDE4D and PDE5A respectively. Beyond these concentrations precipitation started to appear. cAMP and cGMP were used as substrate for PDE4D and PDE5A respectively. Hence 14 µg/mL and 16 µg/mL concentrations of PDE4D and PDE5A were taken for kinetic studies and further inhibition studies. In PDE4D kinetic studies, substrate (cAMP) concentrations were varied from 1-40 µM. At 20 µM, maximum phosphate released with concentration of 12.56 µM. Thus 20 µM concentration of cAMP was used for further inhibition studies. For PDE5A kinetic studies, substrate (cGMP) concentrations were varied from 1-30 µM at constant PDE5A concentration (16 µg/mL). At 14 µM of cGMP, saturation started. From 16 µM, precipitation was visualized. Hence 14 µM of cGMP was taken for further inhibition studies.

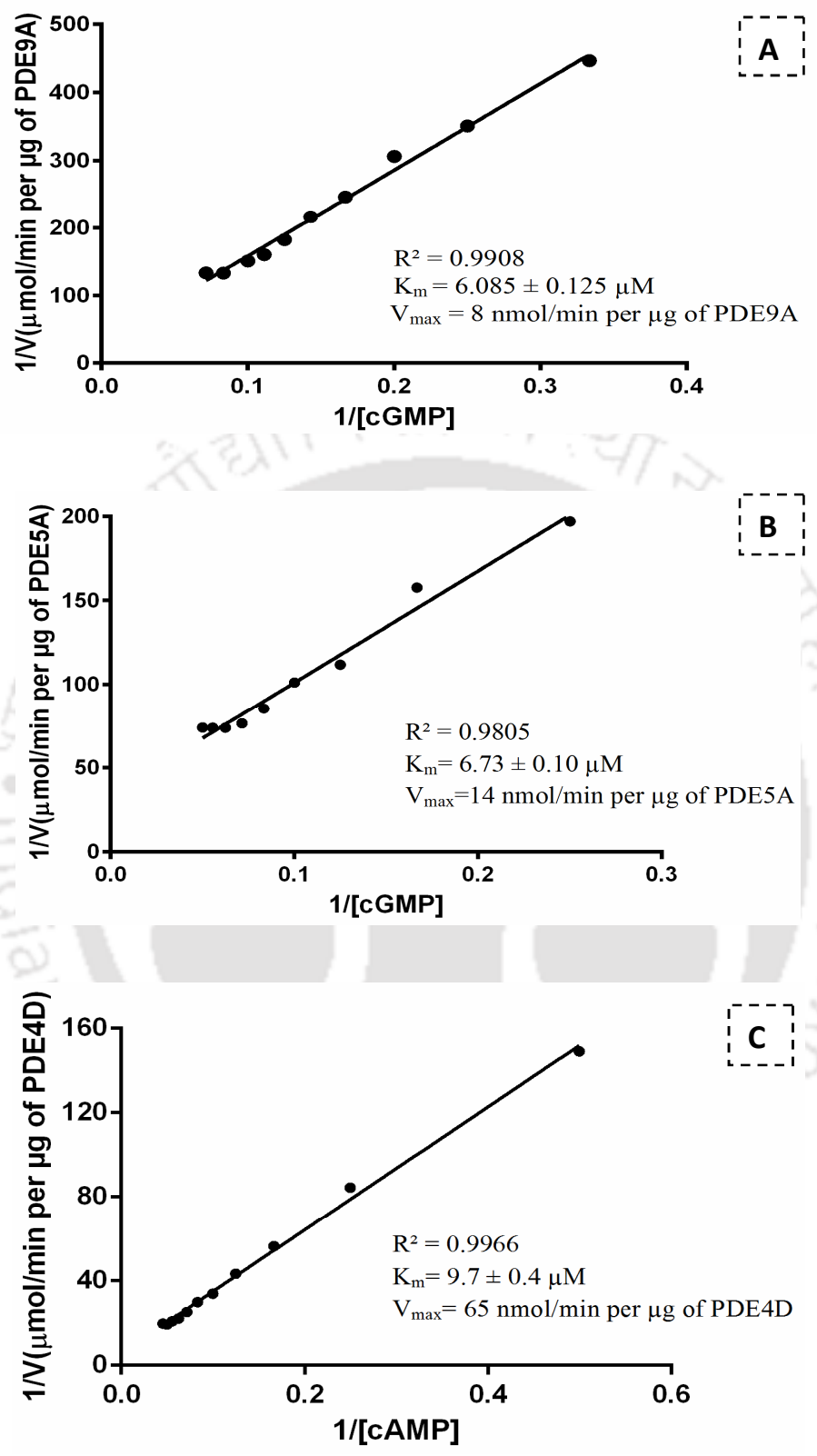

Figure 5.7 Lineweaver-Burk plots of (A) PDE9A, (B) PDE5A and (C) PDE4D

K_m, and V_{max} were calculated using the non-linear regression analysis of Michaelis Menten equation. From the experimental data, K_m and V_{max} were calculated

for PDE9A (6.085±0.12 µM cGMP and 8 nmol/min per µg of PDE9A), PDE5A (9.7±0.4 µM cGMP and V_{max}= 65 nmol/min per µg of PDE5A) and PDE4D (K_m= 6.73±0.1 µM cAMP and V_{max} =14 nmol/min per µg of PDE4D).

5.3.4. Structure activity relationship (SAR) analysis of selected compounds from virtual screening and manual designing

The SAR analysis is a tool to understand the relationship between molecular changes in compounds with their biological effects. The IC_{50} is a quantitative tool for SAR analysis which represents the effectiveness of substance (inhibitor) in protein active site. SAR analysis helped to understand the biological behaviour of selected compounds obtained from both virtual screening and manual designing approaches in physical environment. For this study, BAY73-6691 (a known PDE9A inhibitor) was used as reference compound to examine the sensitivity of spectrophotometric assay and affinity of selected compounds towards PDE9A. IC_{50} value for BAY73-6691 in PDE9A was 5.5±2.2 µM. In previous studies IC_{50} values of BAY73-6691 was reported as 45 nM which may be attributed to the sensitivity of the radioactive assay method [Lin et al., 2015]. Thus, spectrophotometric method was less sensitive as compared to radioactive method. However, non-hazardous, cost-effective and reproducible nature of spectrophotometric assay was the major factor for choosing it for SAR analysis in the present study. IBMX is a known synthetic xanthine derivative which does not inhibit PDE9A; hence it was used as a negative control (Huai et al., 2004). The inactivity of IBMX as an inhibitor of PDE9A was validated in the present study too. IC_{50} value calculated from the experimental data gave insight to understand the potency of selected compounds.

(a) SAR analysis of virtual screened compounds

Through the combinatorial virtual screening approach, ZINC62579975 obtained as potent compound for PDE9A. Further validation was carried out by inhibition studies. In the inhibition studies, purified PDE9A was used with different concentrations (1-100 μM) of ZINC compound. The inhibition studies were performed in presence of 12 μM of cGMP because at this concentration of substrate (cGMP) PDE9A enzyme gets completely saturated in the activity assay. IC_{50} value (46.96 μM) calculated from the experimental data showed good potency of ZINC62579975 towards PDE9A proteins. Inhibition studies were also carried out with PDE5A and PDE4D. IC_{50} of ZINC62579975 with PDE5A and PDE4D were 61.023 μM and 70.04 μM respectively. **Figure 5.8** represents the IC_{50} value of ZINC62579975 with the selected purified PDEs (PDE9A, PDE5A and PDE4D). Based on the inhibition data ZINC62579975 showed comparatively higher potency towards PDE9A over other selected PDEs (PDE5A and PDE4D). To confirm the binding efficiency of ZINC62579975 towards PDE9A among four top hits (obtained after virtual screening studies) inhibition studies were carried out. But the other three compounds (ZINC12231988, ZINC12231966 and ZINC12232141) were not showing good inhibition with PDE9A. Hence, they were not taken up further. The presence of unsubstituted N_1 position of ZINC62579975 was the most probable reason for showing inhibition properties among four hits because in other three ZINC compounds N_1 position was occupied by substituent. The presence of substituent at N_1 position hindered the hydrogen bond formation with active site residues. While in ZINC62579975, -NH at N_1 position interacted with active site residues by forming Hydrogen bond. The inhibition properties of xanthine derivative, ZINC62579975 also showed modification at N_3, C_8 and N_7 could have positive impact on increasing inhibition affinity towards PDE9A. Thus the inhibition potential of the screened

compound (ZINC62579975) makes it suitable candidate for future drug development. K_i is the inhibition constant of inhibitor, it was calculated by using the experimental data of IC_{50} and K_m of the respective proteins. **Table 5.5** represents the experimental IC_{50} data of ZINC62579975 with purified PDEs and the predicted K_i values derived from experimental IC_{50} values and K_m of the respective PDEs.

Table 5.5 Determination of IC_{50} and predicted K_i values of the screened compound with PDE9A, PDE5A and PDE4D

Purified PDEs	IC_{50} (in µM)	Predicted K_i (in µM)
PDE9A	46.96 ± 1.78	15.8
PDE5A	61.023 ± 1.71	24.9
PDE4D	70.04 ± 1.98	20.74

The predicted K_i was calculated by using web tool [https://botdb-abcc.ncifcrf.gov/]. The equation used for calculating *Ki* was $IC_{50} = K_i(1 + [S]/K_m$, where [S] = 12 µM and K_m = 6.085 µM for PDE9A, [S] = 14 µM and K_m = 9.7±0.4 µM cGMP for PDE5A, [S] = 16 µM and K_m = 6.73±0.1 µM cAMP for PDE4D were used.

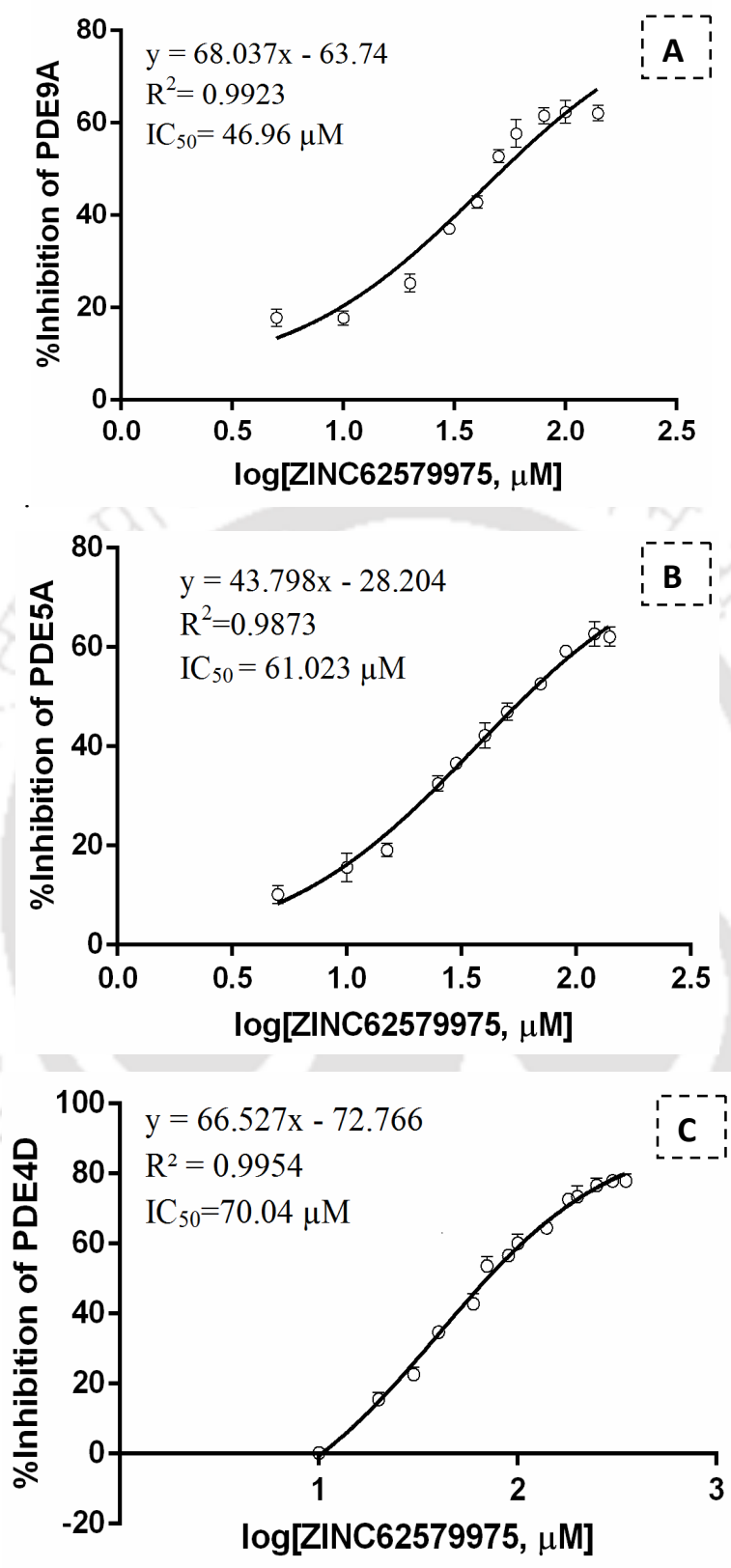

Figure 5.8 IC_{50} graph of ZINC62579975 with (A) PDE9A (B) PDE5A and PDE4D

(b) SAR analysis of manually designed chemically synthesized compound (C1-C8)

With the development of two novel schemes (Scheme-I and Scheme-II), a series of xanthine based derivatives was synthesized. To carry out their SAR analysis, all synthesized compounds were used as inhibitor for PDE9A. *In vitro* inhibition assay determined inhibitor potency and selectivity towards PDE9A. In the present study, IBMX was used as reference compound to analyze the improvement in inhibitory affinity of the synthesized compounds (C1-C8) targeting PDE9A. **Table 5.6** represents the experimental IC_{50} values of all synthesized compounds. This table also shows the predicted K_i values derived from experimental IC_{50} values and K_m of the PDE9A using formula $IC_{50} = K_i (1 + [S]/K_m$. Among all synthesized compounds, compound **C6** showed best inhibition result targeting PDE9A in a dose dependent manner (IC_{50}= 38.27 µM). The compound **C5** showed similar potency (IC_{50}= 38.55 µM) towards PDE9A. The presence of isomeric fragment at N_3 position of these compounds might be a reason for such similarity. In this study it was found that increasing chain length has immense impact in increasing the inhibition affinity of synthesized compounds. This was evident by the IC_{50} value obtained with alkyl chain length at both N_1 and N_3 positions. At C_8 position, increase in alkyl chain length at meta position of phenyl ring also showed increase in inhibition affinity towards PDE9A. Increasing alkyl chain length at N_1 position showed relatively better inhibition affinity than increasing alkyl chain length at N_3 position. It was evident from the PDE9A inhibition result of compound **C1** and compound **C2** because the two compounds vary at N_1 position**.** In Compound **C1**, substitution of methyl group at N_1 position showed nearly two fold less inhibition affinity (IC_{50}= 91.83 µM) than ethyl group substituted compound **C2** (IC_{50}= 50.46 µM) at N_1 position. The inhibition results of compound **C4** (IC_{50}=76.188) and compound **C5** (**IC_{50}**=38.55 µM) showed similar finding. Compounds having modifications with

isomeric fragments showed very little difference in the inhibitory affinity for PDE9A. For instance, in compound **C5,** substitution at N_3 position with isobutyl chain (branching) showed relatively less inhibition than compound **C6** with n-butyl substitution at N_3 position.

Substitution at C_8 position with aryl fragment created significant change in inhibitory effect of compounds. The non-inhibitory affinity of IBMX towards PDE9A was evident from the previous studies. The addition of aryl fragment (phenyl ring with aliphatic side chain/functional group at meta position) at C_8 position of xanthine ring had significant role in increasing the inhibitory affinity of the compounds. For instance, in compound **C4** (3-isobutyl 1-methyl 8-(3- isopropyl) phenyl xanthine), the presence of isopropyl phenyl ring at C_8 position led to bring inhibitory efficiency in compound **C4** (IC_{50}= 76.19 µM). It can be compared with IBMX as in the absence of C_8 substitution IBMX does not possess inhibitory affinity towards PDE9A. **Figure 5.9** illustrates the improvement in inhibition affinity with substitution at C_8 position of xanthine derivatives.

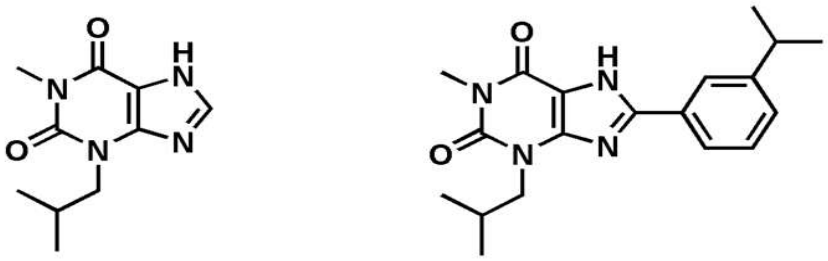

Figure 5.9 Comparative study of compound having C_8 substitution with non substituted IBMX

Furthermore, replacing functional group (such as floro group) at meta-position of phenyl ring increased the potency of compound towards PDE9A. However, increase in alkyl chain length had more impact in enhancing the inhibitory affinity of compound

than using phenyl ring with functional group at C_8 position of xanthine derivatives. Thus phenyl substituent has significant role in generating the inhibition potential in compounds.

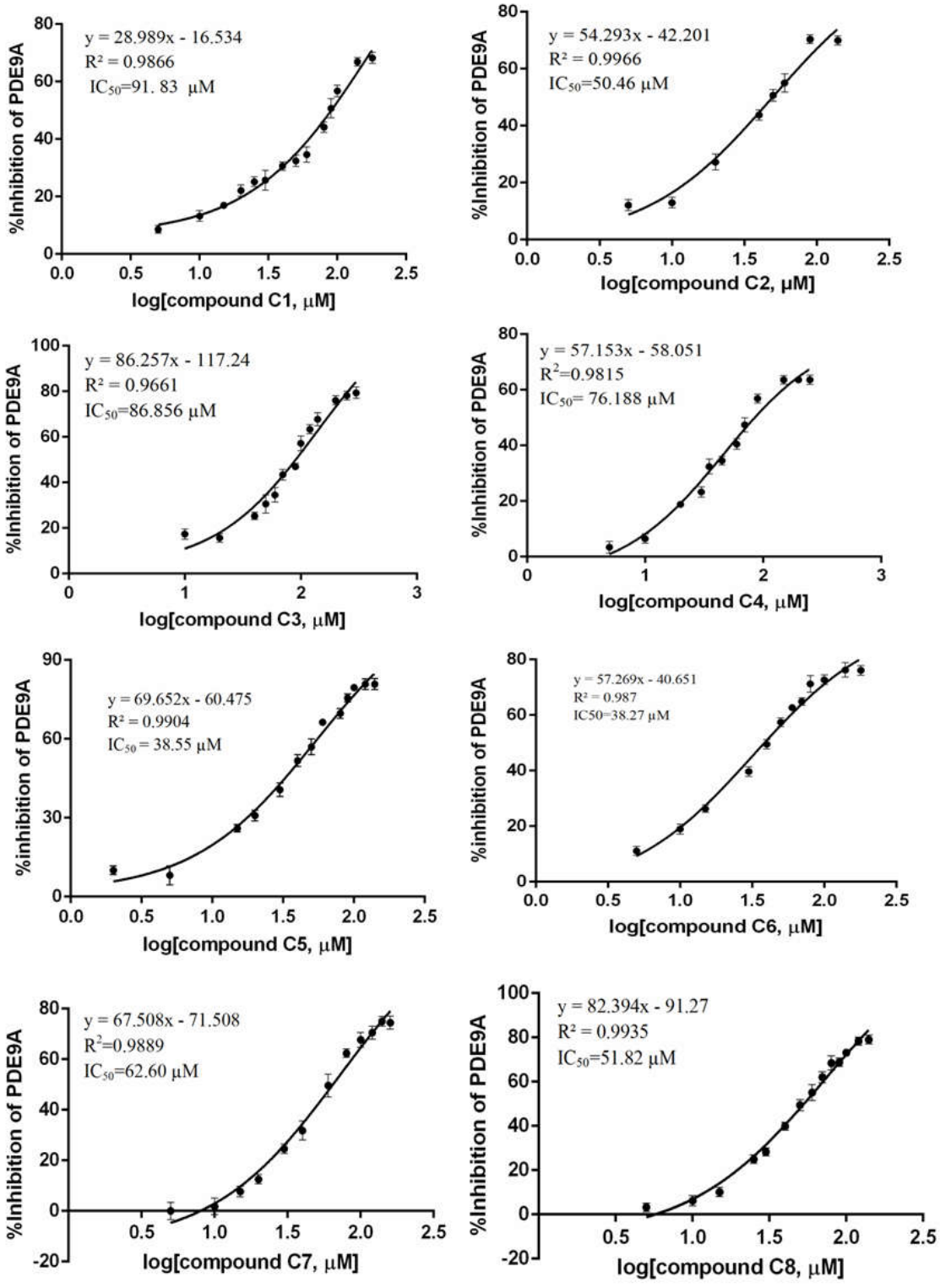

Figure 5.10 IC_{50} graph of chemically synthesized compounds (C1-C8) with PDE9A

Table 5.6 Chemical structure of inhibitors (C1-C8) and their SAR analysis (IC_{50}) with PDE9A (amino acid 181-506)

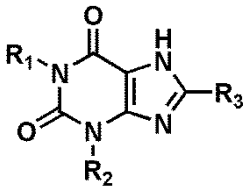

Entry	Substituted positions at the xanthine scaffold			IC_{50} of PDE9A (in µM)	Predicted K_i (in µM) #
	R_1	R_2	R_3		
C1	$-CH_3$	$-C_3H_7$	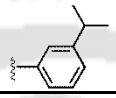	**91.83 ± 1.98**	**30.84**
C2	$-C_2H_5$	$-C_3H_7$	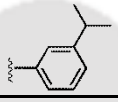	**50.46 ± 2.21**	**16.92**
C3	$-C_2H_5$	$-C_3H_7$	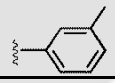	**86.86 ± 2.43**	**29.16**
C4	$-CH_3$	$-CH_2CH(CH_3)_2$	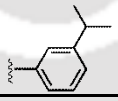	**76.19 ± 1.60**	**25.57**
C5	$-C_2H_5$	$-CH_2CH(CH_3)_2$	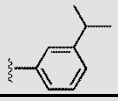	**38.55 ± 1.90**	**12.91**
C6	$-C_2H_5$	$-C_4H_{10}$	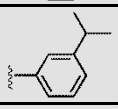	**38.28 ± 1.63**	**12.82**
C7	$-C_2H_5$	$-C_4H_{10}$	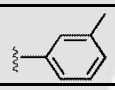	**62.60 ± 2.6**	**21**
C8	$-C_2H_5$	$-C_4H_{10}$	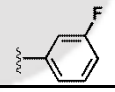	**51.82 ± 2.25**	**17.37**

The predicted K_i was calculated by using web tool [https://botdb-abcc.ncifcrf.gov/]. The equation used for calculating *Ki* was $IC_{50} = K_i(1 + [S]/K_m)$, where [S] = 12 µM and K_m = 6.085 µM were used.

(c) Comparative studies of compound C6 with PDE4D and PDE5A

Compound **C6** was selected for comparative studies with other purified PDEs because of its highest inhibition affinity for PDE9A. The comparative study was only to check the specificity of compounds towards the target. The comparative study indicated that compound **C6** showed higher potency towards PDE5A (with IC_{50} of

9.98±1.23 μM) among selected purified PDEs. This might be because of the fact that PDE5A is also cGMP specific protein as PDE9A. Despite this, Compound **C6** can be considered as potent inhibitor for PDE9A while treating neurodegenerative diseases as PDE5A has negligible presence in brain. Compound **C6** showed comparatively less potency (IC_{50}= 44.33±1.4μM) towards PDE4D among selected PDEs. This study paved the way to understand structural implication of xanthine derivatives in inhibition of PDE9A and other PDEs as well. Schemes developed in this study can have significance in the development of more potent inhibitor based on xanthine scaffold. This may be extended to other disease targets as well. **Figure 5.11** shows the IC_{50} graph of compound **C6** with PDE5A and PDE4D.

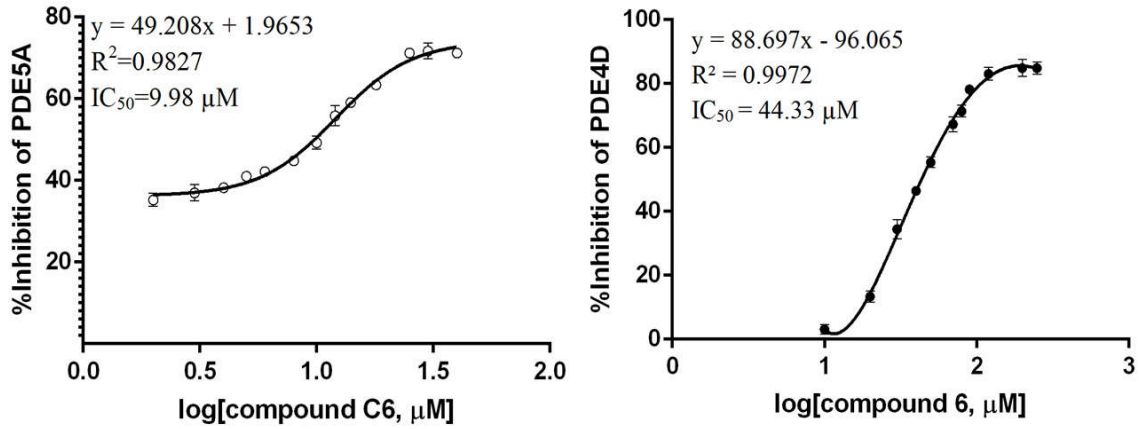

Figure 5.11 IC_{50} graph of compound **C6** with (a) PDE5A and (b) PDE4D

(d) K_i determination of most promising Compound C6 with PDE9A to understand the inhibitory nature of synthesized inhibitors

K_i is an intrinsic inhibitor constant which shows the affinity of an inhibitor to binds with an enzyme. The K_i value is a reproducible and reliable value which shows how promising is the inhibitor. It also gives an indication for need of future *in vivo* studies. Preliminary IC_{50} determination gave a direction to choose inhibitor

concentrations for a K_i determination. IC_{50} of compound **C6** was 38.28±1.63 µM. Therefore, the concentration of inhibitor for K_i determination was used in range of 0-50 µM. The K_i LB plot generated from the experimental data was determined the "competitive" nature of xanthine based inhibitors. For compound $\mathbf{C_6}$ experimentally determined K_i was 10.3±2.4 µM. Based on this result it can be said that the $\mathbf{C_6}$ showed competitive inhibition towards PDE9A as it possessed same V_{max} with different K_m in presence of inhibitors. The predicted K_i for compound **C6** was 12.82 µM as shown in **Table 5.6**. Therefore the difference of K_i between predicted and experimental data of K_i was of 2.52 µM. This suggested that the K_i which was calculated from the IC_{50} value were not much differed from experimental K_i. **Figure 5.12** represents the K_i graph of PDE9A in presence of compound **C6**.

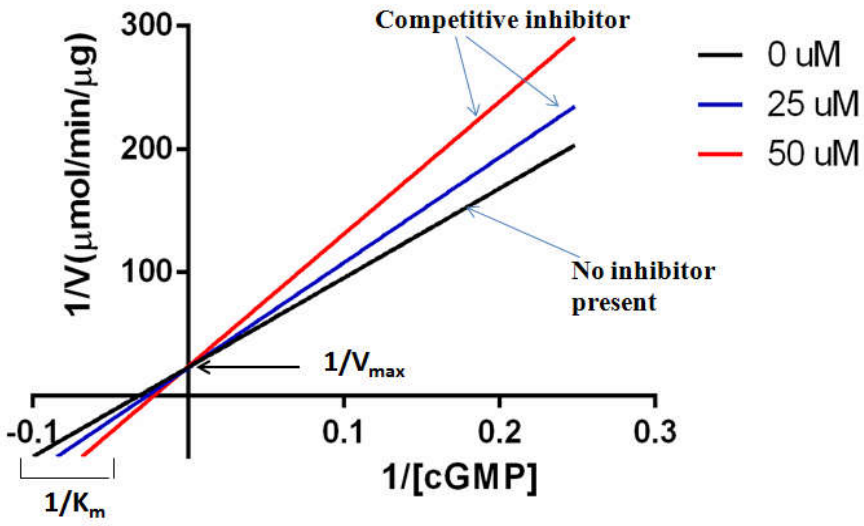

Figure 5.12 Line Weaver Burk plot of PDE9A in presence of Compound **C6**

5.3.5. Real time Differential scanning fluorimetry thermal shift assay

Differential scanning fluorimetry (DSF) is a rapid and inexpensive screening method to identify stability of purified proteins in presence of ligands. In drug development process, thermal stability of protein is important to examine the binding

interaction of ligand in protein (Niesen et al, 2007). **Figure 5.13** depicts the stages of protein behaviour during thermal shift assay.

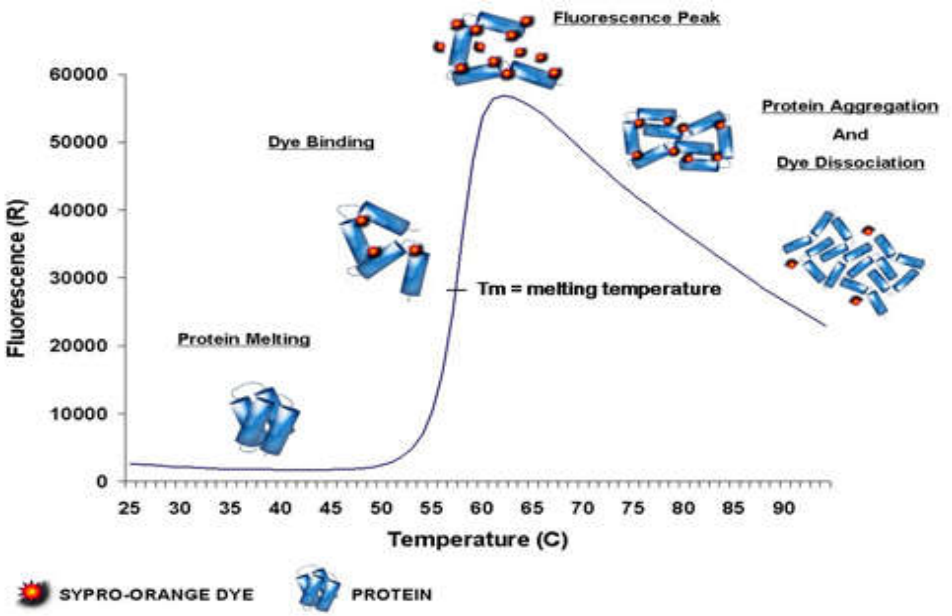

Figure 5.13 Typical thermograph showing protein behaviour during Thermal Shift Assay

In most of the cases, protein stability decreases with increasing temperature. With increasing temperature, change in free energy (ΔG°) decreases. ΔG° becomes zero when equilibrium achieves where the concentration of both folded and unfolded proteins become equal. Here, temperature is considered as melting temperature (T_m). In this study, the stability of the PDE9A in complex with synthesized compounds was determined by Differential scanning fluorimetry (DSF). T_m of substrate (cGMP) bound PDE9A was used as a reference point to analyze the stability of protein in inhibitor bound state. The calculated T_m of cGMP-PDE9A complex was 53.35°C. The magnitude of T_m shift was more or less similar for all the synthesized compounds. However, these values do not always reflect the relative binding affinities (Niesen et al., 2007). The magnitude of T_m depends on the contribution of enthalpy and entropy of the compounds (Niesen et al., 2007). Among all synthesized compounds, compound **C5**-PDE9A

complex showed highest T_m of 54.35°C. From this analysis it was concluded that the synthesized compounds were bound and stabilized the protein in similar manner as was analyzed in the case of substrate (cGMP) bound protein. **Figure 5.14** illustrates the thermograph of all synthesized compounds in PDE9A bound form. **Table 5.7** represents the calculated melting temperature of substrate bound PDE9A and inhibitor bound PDE9A.

Table 5.7 Melting temperature of substrate bound PDE9A and inhibitor (**C1-C8**) bound PDE9A

Compounds	**cGMP**	**C1**	**C2**	**C3**	**C4**	**C5**	**C6**	**C7**	**C8**
ΔT_m (°C)	53.35	53.75	53.75	52.7	53.35	54.35	53.35	52.75	52.7

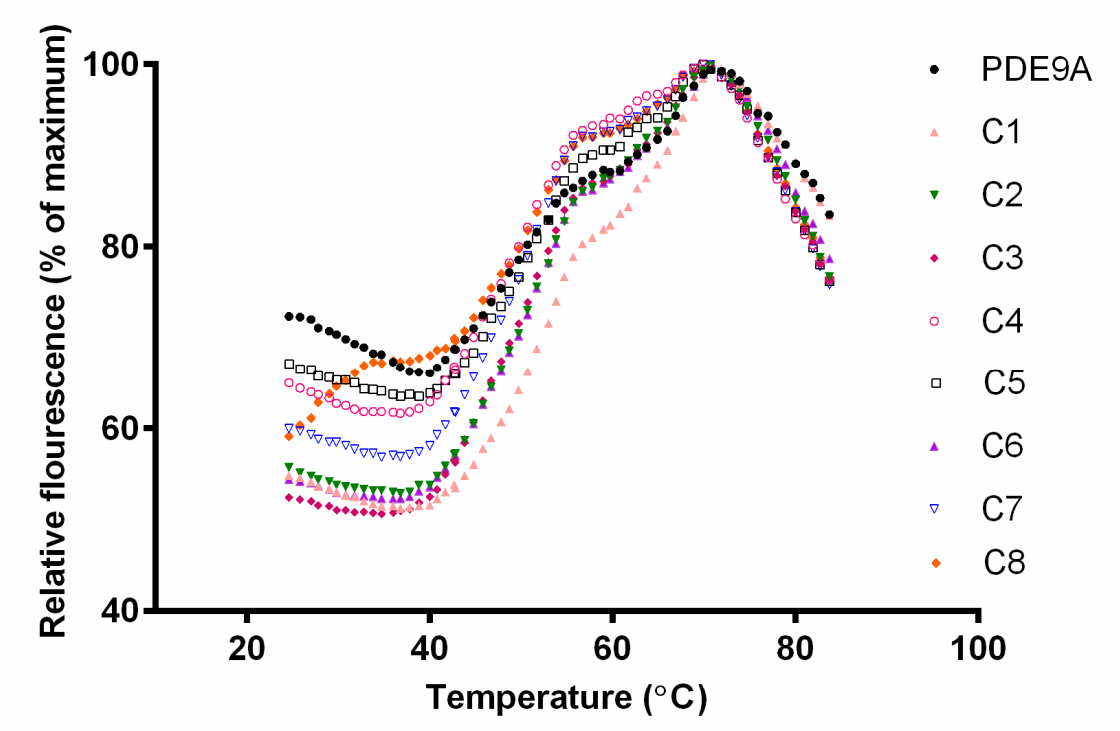

Figure 5.14 Thermograph of PDE9A protein bound with chemically synthesized inhibitors

5.3.6 Comparative study of chemically synthesized compounds (C1-C8) and virtual screened compound ZINC62579975 with PDE9A

Comparison based on the SAR analysis

The comparative SAR analysis of both synthesized and virtual screened compounds gave understanding over the modification required for generating potency in compound towards PDE9A. Based on the *in silico* interaction analysis it was found that unsubstituted –NH at N_1 position and carbonyl group at C_8 position together in ZINC62579975 were responsible for creating strong Hydrogen bond interaction with GLN453. Similarly the presence of unsubstituted –NH group at N_7 position and carbonyl group at C_8 position together in the manually designed compounds were responsible for such interaction with GLN453. Interaction with GLN453 was important for generating potency towards PDE9A. This finding was validated by inhibition studies. Among four top hits of virtual screening, only ZINC62579975 showed potency towards PDE9A in inhibition studies because of the presence of unsubstituted N_1 position whereas other three hits devoid of unsubstituted N_1 position. The presence of alkyl group at N_3 position has important role in creating binding strength of xanthine derivatives. It was evident from the IC_{50} data of both synthesized compounds and ZINC62579975 provided in **Table 5.5** and **Table 5.6.** Compound **C5** and **C6** showed highest potency because of the presence of butyl group which was the largest fragment used for N_3 substitution. In ZINC62579975 also N_3 position consisted butyl group. C_8 position was occupied in both types of compounds. However, the presence of phenyl substituent at C_8 position in synthesized compound showed better interaction than alkylated aryl substituent in ZINC62579975. In synthesized compound, phenyl substituent placed towards hydrophobic reason. In ZINC62579975 the aryl part of C_8 substituent move towards the

HIS rich site of the active site pocket of PDE9A which might be the reason for its good interaction with protein. The presence of phenyl substituent in synthesized compounds has greater implication in generating the potency towards PDE9A because of hydrophobic-hydrophobic interaction developed between protein and ligand that was lacking in ZINC62579975. This was apparent from the comparative interaction pattern analysis of compound $\mathbf{C_6}$ and ZINC62579975 in PDE9A active site as shown in **figure 5.15.** Thus by *in silico* SAR analysis, manually designed compounds (**C5** and **C6**) showed better potency than ZINC62579975. Subsequently, this finding was validated by *in vitro* inhibition studies. Compound **C6** (38.27 µM) showed better potency than ZINC62579975 (46.96 µM).

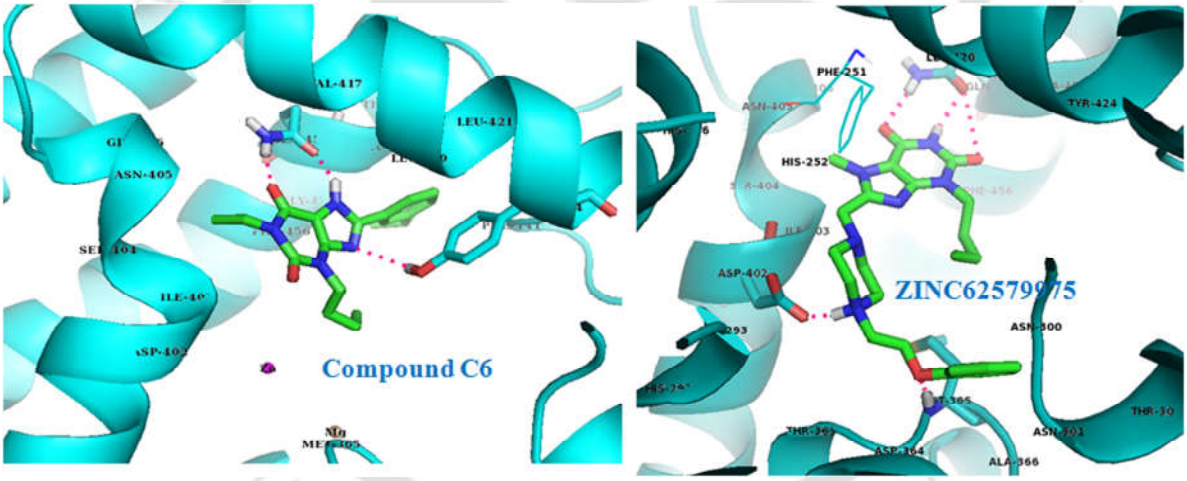

Figure 5.15 Comparative *in silico* SAR analysis of compound C6 and ZINC62579975

Comparison based on the thermal shift study

The assay for analyzing the stability of PDE9A in the presence of compound **C6** and ZINC62579975 were performed by similar thermal shift assay. Surprisingly, ZINC62579975 showed comparatively lower T_m than the synthesized compounds. T_m of ZINC62579975 was 47.75°C which was 5.6°C lower than T_m of Compound **C6**

(53.35°C), the compound showed best potency towards PDE9A among all synthesized compounds. This result showed that as compared to synthesized compounds, ZINC62579975 was lower in capacity to thermally stabilize the PDE9A protein during binding. Hence from this comparative study we can conclude that PDE9A bound with synthesized compounds showed better stability than with ZINC compound. The higher T_m shift of synthesized compounds was due to more entropically driven binding. The entropically driven binding is mainly hydrophobic binding. This is because of the presence of phenyl substituent with alkyl groups at C_8 position. The phenyl substituent with alkyl fragment established hydrophobic-hydrophobic interaction between ligand and protein and stabilized the interaction. The stability of protein in inhibitor bound form was important to ensure the stability of interaction between protein and ligand. **Figure 5.16** represents the comparative thermograph of compound **C6** and ZINC62579975.

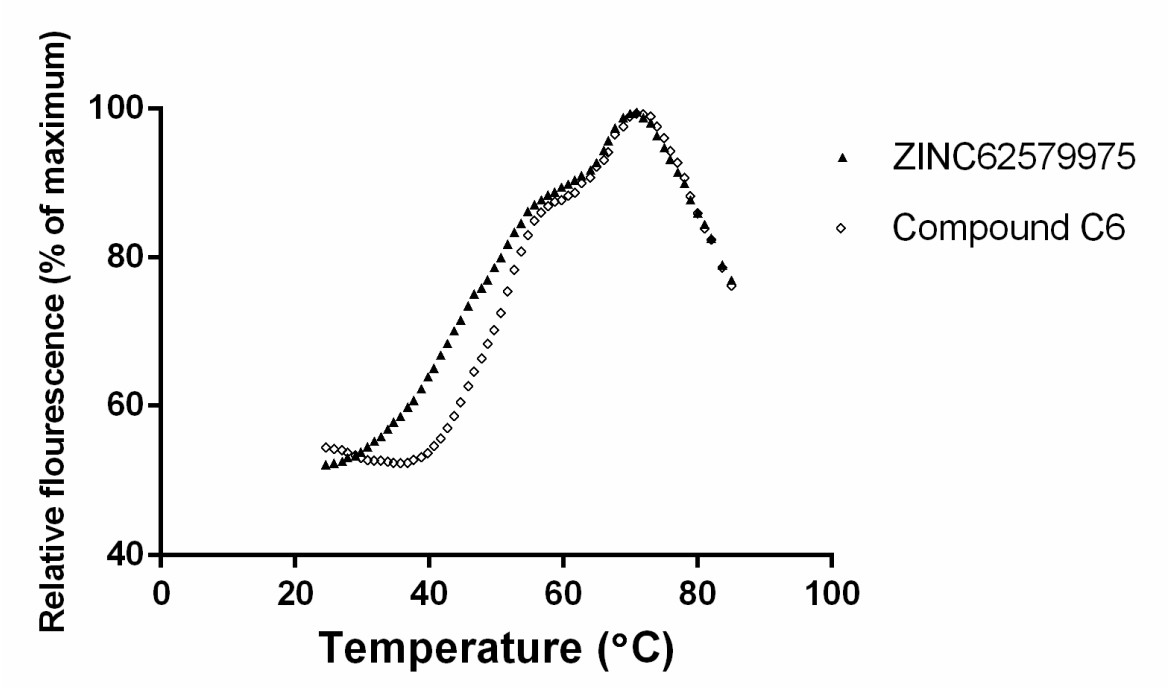

Figure 5.16 Thermograph of PDE9A in complex with compound **C6** and ZINC62579975

5.4 Conclusion

Through the *in silico* studies and chemical synthesis total nine compounds were identified as potent and selective for PDE9A. Among these nine compounds one compound (ZINC62579975) was obtained from the virtual screening of the ZINC database. Other eight compounds (**C1-C8**) were designed using structure based drug designing accompanied by parallel molecular docking studies followed by their subsequent chemical synthesis. SAR analysis of these compounds revealed the inhibitory affinity towards PDE9A. The virtual screened compound ZINC62579975 showed comparatively higher potency towards PDE9A with IC_{50} value of 46.96 µM among selected PDEs. The inhibitory activity for PDE5A and PDE4D are 61.023 µM and 70.04 µM respectively. Thus ZINC62579975 can be considered as a potential drug candidate for further modification based on the active site requirement of PDE9A to make it more specific for PDE9A. Among eight newly designed chemically synthesized compounds, compound **C6** showed highest inhibitory activity towards PDE9A with IC_{50} value of 38.27 µM. The inhibition potential of compound **C5** was similar to compound **C6** because of the presence of isomeric fragment at N_3 position. The structural modification has significant impact on the inhibition affinity of synthesized compounds. With increasing chain length at both N_1 and N_3 positions, the inhibition affinity of synthesized compounds increased. Increasing chain length at N_1 position was more effective in increasing the potency of compounds towards PDE9A. Substitution at C_8 position with phenyl substituent (having modification at meta-position with aliphatic chains) showed significant impact in generating inhibition potential in the synthesized compounds. It was evident from the comparative study of IBMX and 8-substituted IBMX that is compound **C4**. IBMX does not inhibit PDE9A whereas compound **C4** (IC_{50}=76.19 ± 1.60) inhibit PDE9A because of the presence of alkylated phenyl substituent. The presence of alkyl

group at phenyl substituent was imperative to built hydrophobic-hydrophobic interaction between protein and ligand. In docking study it was found that aryl substituent at C_8 position placed towards the hydrophobic region of the PDE9A active site and established strong hydrophobic interaction with protein. This finding was confirmed by SAR analysis. With increasing the alkyl group at meta-position increased the binding strength of compounds and made the compound more potent towards PDE9A. Thus conclusively all the synthesized compounds showed inhibitory capacity towards PDE9A. Thermal shift assay showed the stability of protein-ligand complex. All synthesized compounds showed better stability in PDE9A than ZINC62579975. The comparative studies of compound **C6** with other PDEs such as PDE5A and PDE4D revealed some interesting facts about this series of compound. Compound **C6** showed better affinity towards PDE5A with IC_{50} value of 9.98 μM. Based on the comparative biological studies it can be said that synthesized compounds showed good potency towards two cGMP specific PDEs- PDE9A and PDE5A. This would not create much hurdle while treating neurodegenerative diseases because PDE5A has negligible presence in the brain. However, the present study is preliminary phase of xanthine based drug discovery targeting PDE9A. By using the experimental analysis of the present study compounds with better specificity can be achieved in future drug development process. Most interesting fact is that this study has opened scope for introducing new scaffold not only for PDE9A but for other PDEs too. The increasing chain length at N_1 and N_3 positions, aryl substitution at C_8 position and choosing N_1, N_3, C_8 sites together for modification at xanthine scaffold have been the essence of the present study. If the above divulged factors are taken into consideration for further substitution with different fragments at xanthine scaffold as per the requirement of the active site composition and size of the targeted protein, a better drug candidate can be reached for.

Conclusion and Future Perspectives

Thesis Conclusion

Introducing new scaffolds in PDE9A drug development process was imperative to bring out structural diversification. Using xanthine as scaffold was one step towards the realization of structural diversification. The present thesis used two approaches- one was virtual screening of existing xanthine derivatives for PDE9A and another was manual designing of xanthine derivatives for PDE9A. After introduction and literature review, chapter-2 concentrated on the screening of existing inhibitors from ZINC database targeting PDE9A using "xanthine ring" as a scaffold. Out of 2055 available xanthine derivatives in database only one ZINC compound (ZINC62579975) was proved as potent specific inhibitor for PDE9A. Due to low success rate of existing xanthine derivatives towards PDE9A, it became necessity to look for manual design approach for generating suitable inhibitors as per the requirement of PDE9A active site pocket. The subsequent chapter-3 dealt with manual designing and simultaneous docking study of xanthine based compounds as per the requirement of active site pocket of PDE9A. From this study, N_1, N_3 and C_8 positions of xanthine together were considered as the best sites for substitution. The compounds with substitution N_1, N_3 and C_8 positions were categorized into two sets- set-1 and set-2. Both sets were similar in substitution at N_1 position with alkyl groups and at C_8 position with phenyl substituent. These groups varied at N_3 substitution. In set-1, N_3 position was substituted by alkyl groups whereas, in set-2, aromatic fragment was used. With comparative studies between two sets, it was found that some compounds from both sets selectively targeted PDE9A. However, the set-1 compounds showed higher pharmaceutical activity because of the presence of alkyl group at N_3 position. Hence, eight most potent set-1 compounds were selected for further chemical synthesis. Chapter 4

focused on the chemical synthesis of selected compounds. Two novel schemes (scheme-I and scheme-II) were developed using 'xanthine' as starting material. With development of new routes we got clear understanding over the chemical nature of xanthine and its three –NH sites which have been matter of concern for researchers. Due to lack of structural understanding, the use of xanthine has been negligible in obtaining derivative compounds. The present study found the reactivity pattern of three –NH sites which follows $N_7>N_3>N_1$ substitution. This finding was contrary to the earlier reports but similar to the sequence of transmethylation occurring in the living system. By understanding the nature of xanthine structure, the derivatisation of xanthine becomes easier than before. Development of whole synthesis strategies was based on the protection and deprotection steps. Finally, the present study ended with the biological studies of compounds obtained from virtual screening and chemical synthesis. Chapter-5 focused on biological study part. Spectrophotometric inhibition method was applied to check the inhibitory nature of selected xanthine derivatives. The selected ZINC compound showed better potency for PDE9A (IC_{50}=46.96 ± 1.78) than PDE4D (IC_{50}=61.023 ± 1.71) and PDE5A (IC_{50}=70.04 ± 1.98). Based on the structure activity analysis of eight compounds, compound **C6** (IC_{50}= 38.28 ± 1.63) showed highest affinity for PDE9A. The increasing chain length at N_1, N_3 and C_8 positions showed significant impact in increasing the inhibition affinity of compounds towards PDE9A specificity. Substitution with isomeric fragments showed negligible difference in binding affinity towards the target. The substitution at C_8 position has considerable impact in generating the inhibition potential in the newly developed compounds by establishing the strong hydrophobic-hydrophobic interaction with PDE9A. This was apparent from the fact that in absence of C_8 substitution IBMX showed non-inhibitory potential towards PDE9A.

Thermal stability of PDE9A in inhibitor bound form was confirmed by thermal shift assay. This study suggested the stable nature of chemically synthesized compounds over virtual screened compound towards PDE9A. By carrying out extensive combinatorial studies, the present thesis was an attempt to explore the wide potential of 'xanthine' both as 'scaffold' and 'reaction initiator' to bring out structural diversification in derivatisation of xanthine based drug development.

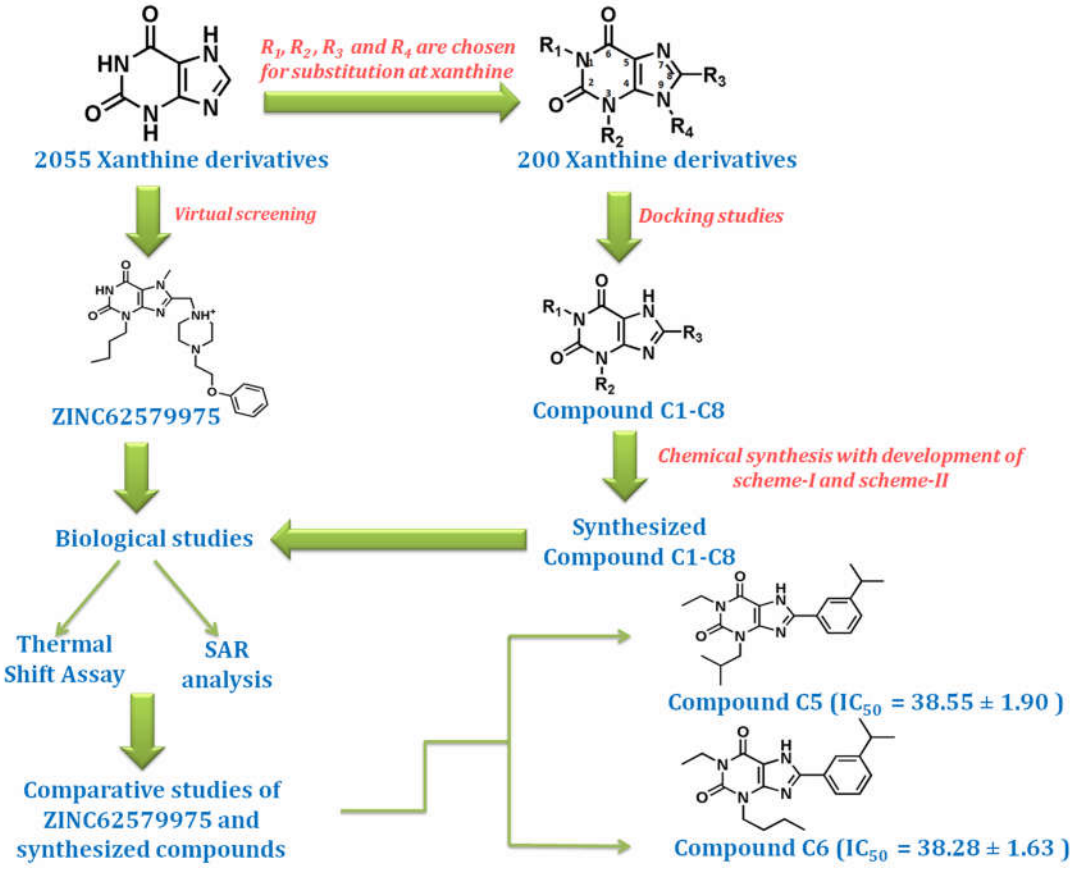

Figure S1 Thesis conclusion

Future Perspectives for xanthine based research

With the availability of three –NH groups at N_1, N_3 and N_7 positions and one –CH group at C_8 position, xanthine provides maximum possibility for derivatisation. Despite enormous ground available for substitution/modification the use full potential of xanthine has been limited in drug development process. Till date no research has been carried out using xanthine as starting material for xanthine derivatives. This is mainly because of the 'lacking' in understanding over the molecular/structural nature of xanthine. According to reports available till date on xanthine, N_3 position has been considered as most reactive position in xanthine because of the highest acidity of –NH group at N_3 position and substitution follows the order of $N_3>N_7>N_1$ positions (Gulevskaya et al., 1991). This analysis was contradictory to the transmethylation process of xanthine in living organism. The transmethylation of xanthine occurs in sequence of $N_7>N_3>N_1$. This thesis has tried to fill this lacuna with understanding the true nature of reactivity pattern of xanthine. This study suggest the reactivity pattern of xanthine in chemical synthesis unquestionably follows the natural transmethylation sequences i.e. $N_7>N_3>N_1$ positions. The reactivity differences in –NH groups are due to their different atomic environment. With development of two new synthesis routes, xanthine can become an ideal choice for reaction initiator for future xanthine based drug developments because of its easy availability cost effective, time saving and high yield producing nature. It would be a better alternative of any existing synthesis method. The clear understanding over reactivity pattern would be useful to generate library of xanthine based compounds. The present thesis has given two novel schemes for synthesis of xanthine derivatives. Beside this more schemes can be developed by targeting particular sites of xanthine for substitution. Newly developed

compounds can be subjected to x-ray diffraction analysis and pharmaceutical analysis for understanding the physical, molecular behaviour and biological of these molecules. The ligand-protein complex can be subjected to crystallization for understanding the positioning and interaction pattern of compounds inside the active site pocket of protein. Using xanthine as scaffold, functioning of other proteins can also be targeted. The present study has tried to solve the constraint existed in xanthine based drug development process by developing novel schemes which can bring out structural diversification in xanthine based research. This study has given new platform for xanthine based research by utilizing the full potential of 'xanthine' both as scaffold and as reaction initiator in drug development.

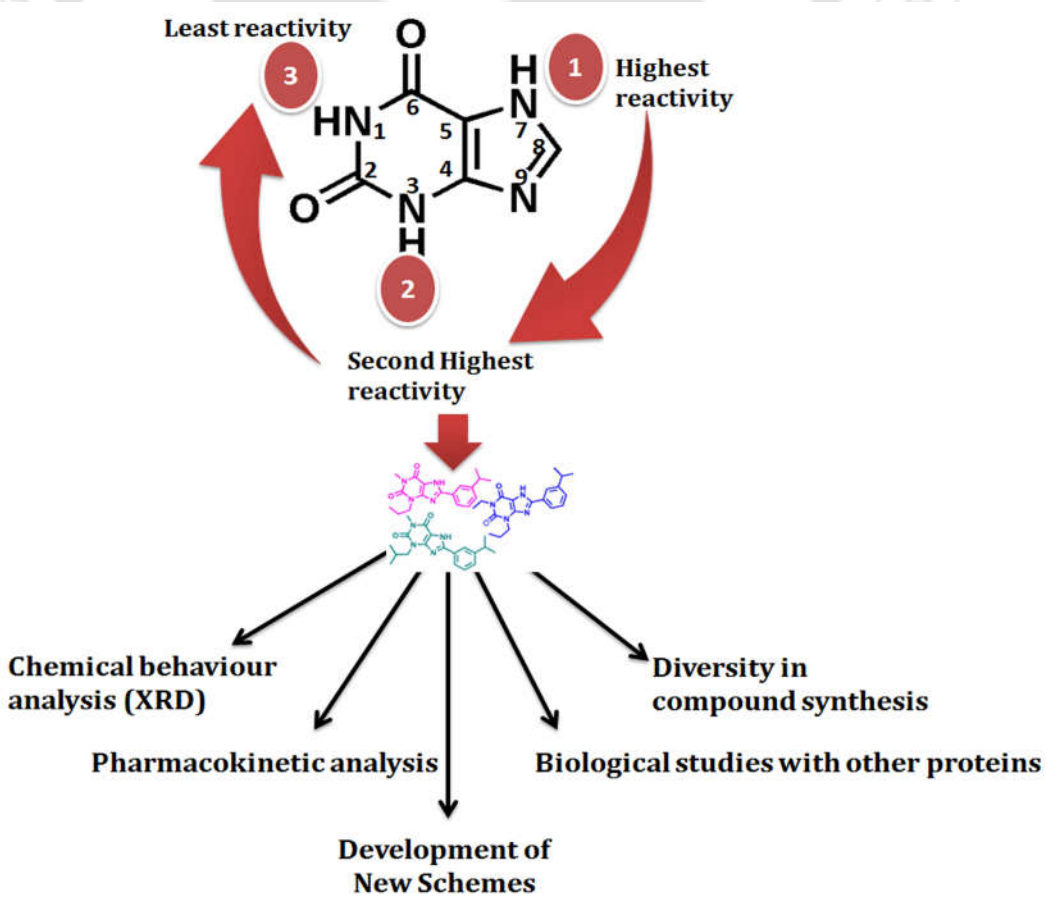

Figure S2 Future outlook in xanthine based research

BIBLIOGRAPHY

Abdel-Magid, A.F., 2013. PDE10 Inhibitors as Potential Treatment for Schizophrenia. *ACS Med. Chem. Lett.* 4, 161–2.

Abdulrahman, L.K., Al-Mousilly, M.M., Al-Halaibeh, T.S., Al-Azzawii, K.M., 2012. International research journal of pharmacy synthesis of new 1, 3, 7, 8-tetrasubstituted xanthenes analogue. *Int. Res. J. Pharm.* 3, 83–5.

Agulló, L., Garcia-Dorado, D., Escalona, N., Ruiz-Meana, M., Inserte, J., Soler-Soler, J., 2003. Effect of ischemia on soluble and particulate guanylyl cyclase-mediated cGMP synthesis in cardiomyocytes. *Am. J. Physiol. - Hear. Circ. Physiol*. 284, H2170-6.

Agulló, L., Garcia-Dorado, D., Escalona, N., Ruiz-Meana, M., Mirabet, M., Inserte, J., Soler-Soler, J., 2005. Membrane association of nitric oxide-sensitive guanylyl cyclase in cardiomyocytes. *Cardiovasc. Res*. 68, 65-74.

Ahmad, M., Abdel-Wahab, Y.H.A., Tate, R., Flatt, P.R., Pyne, N.J., Furman, B.L., 2000. Effect of type-selective inhibitors on cyclic nucleotide phosphodiesterase activity and insulin secretion in the clonal insulin secreting cell line BRIN-BD11. *Br. J. Pharmacol.* 129, 1228–34.

Aleksandrova Katherine, Igor Belenichev, Alexander Shkoda, Sergey Levich, Darja Yurchenko, Nina Buchtiyarova, 2014. Research of antioxidant properties of theophyllinyl-7-acetic acid derivatives. *Med. Sci.* 3, 187–94.

Allwood, M.B., Cannan, B., van Aalten, D.M.F., Eggleston, I.M., 2007. Efficient synthesis of 1,3,7-substituted xanthines by a safety-catch protection strategy. *Tetrahedron* 63, 12294–302.

Amirkia, V., Heinrich, M., 2014. Alkaloids as drug leads – A predictive structural and biodiversity-based analysis. Phytochem. Lett. 10, xlviii–liii.

Andreeva, S.G., Dikkes, P., Epstein, P.M., Rosenberg, P.A., 2001. Expression of cGMP-Specific Phosphodiesterase 9A mRNA in the Rat Brain. *J. Neurosci.* 21, 9068-76.

Antoni, F.A., 2000. Molecular Diversity of Cyclic AMP Signalling. *Front. Neuroendocrinol.* 21, 103–32.

Azam, F., Ibn-Rajab, I.A., Alruiad, A.A., Azam, F., 2009. Adenosine A 2A receptor antagonists as novel anti-Parkinsonian agents: a review of structure-activity relationships. *Pharmazie* 64, 771–95.

Bandyopadhyay, P., Agrawal, S.K., Sathe, M., Sharma, P., Kaushik, M.P., 2012. A facile and rapid one-step synthesis of 8-substituted xanthine derivatives via tandem ring closure at room temperature. *Tetrahedron* 68, 3822–27.

Bansal, R., Kumar, G., Gandhi, D., Yadav, R., Young, L.C., Harvey, A.L., 2010. Synthesis of 8-(cyclopentyloxy)phenyl substituted xanthine derivatives as adenosine A2A ligands. *Arzneimittelforschung*. 60, 131–6.

Baraldi, P.G., Fruttarolo, F., Tabrizi, M.A., Romagnoli, R., Preti, D., 2007. Novel 8-heterocyclyl xanthine derivatives in drug development - an update. *Expert Opin Drug Discov* 2, 1161–83.

Barcz, E., Sommer, E., Janik, P., Marianowski, L., Skopinska-Rózewska, E., 2000. Adenosine receptor antagonism causes inhibition of angiogenic activity of human ovarian cancer cells. *Oncol. Rep.* 7, 1285–91.

Bell, A., DeNinno, M., Palmer, M., Visser, M., 2004. PDE9 inhibitors for treating type 2 diabetes,metabolic syndrome, and cardiovascular disease. US 20040220186 A1.

Bender, A.T., 2006. Cyclic Nucleotide Phosphodiesterases: Molecular Regulation to Clinical Use. *Pharmacol. Rev.* 58, 488–520.

Black, Shawn, C., Gibbs, Earl, M., Mcneish, John, D., 2005. Phosphodiesterase 9 inhibition as treatment for obesity-related conditions, US Patent, WO2005041972 A1.

Boess, F.G., Hendrix, M., van der Staay, F.-J., Erb, C., Schreiber, R., van Staveren, W., de Vente, J., Prickaerts, J., Blokland, A., Koenig, G., 2004. Inhibition of phosphodiesterase 2 increases neuronal cGMP, synaptic plasticity and memory performance. *Neuropharmacol.* 47, 1081–1092.

Bondan, E.F., De Fátima, M., Martins, M., Bernardi, M.M., 2015. Propentofylline reverses delayed remyelination in streptozotocin- induced diabetic rats. *Arch. Endocrinol. Metab.* 59, 47-53.

Boswell-Smith, V., Cazzola, M., Page, C.P., 2006. Are phosphodiesterase 4 inhibitors just more theophylline? *J. Allergy Clin. Immunol.* 117, 1237–43.

Braumann, T., Erneux, C., Petridis, G., Stohrer, W.-D., Jastorff, B., 1986. Hydrolysis of cyclic nucleotides by a purified cGMP-stimulated phosphodiesterase: structural requirements for hydrolysis. Biochim. Biophys. Acta - Protein Struct. Mol. Enzymol. 871, 199–206.

Burbiel, J.C., Hockemeyer, J., Müller, C.E., 2006. Microwave-assisted ring closure reactions : Synthesis of 8-substituted xanthine derivatives and related pyrimido- and diazepinopurinediones. *Beilstein J. Org. Chem.* 63, 1–6.

Burley, D.S., Ferdinandy, P., Baxter, G.F., 2007. Cyclic GMP and protein kinase-G in myocardial ischaemia-reperfusion: opportunities and obstacles for survival signaling. *Br. J. Pharmacol.* 152, 855–69.

Bussi, G., Gervasio, F.L., Alessandro Laio, Parrinello, M., 2006. Free-Energy Landscape for β Hairpin Folding from Combined Parallel Tempering and Metadynamics. *J. Am. Chem. Soc*. 128, 13435–41.

Cahill, K.B., Quade, J.H., Carleton, K.L., Cote, R.H., 2012. Identification of amino acid residues responsible for the selectivity of tadalafil binding to two closely related phosphodiesterases, PDE5 and PDE6. *J. Biol. Chem.* 287, 41406–16.

Castaño, T., Wang, H., Campillo, N.E., Ballester, S., González-García, C., Hernández, J., Pérez, C., Cuenca, J., Pérez-Castillo, A., Martínez, A., Huertas, O., Gelpí, J.L., Luque, F.J., Ke, H., Gil, C., 2009. Synthesis, Structural Analysis, and Biological Evaluation of Thioxoquinazoline Derivatives as Phosphodiesterase 7 Inhibitors. *ChemMedChem* 4, 866–76.

Cer, R.Z., Mudunuri, U., Stephens, R., Lebeda, F.J., 2009. IC_{50}-to-Ki: A web-based tool for converting IC_{50} to Ki values for inhibitors of enzyme activity and ligand binding. *Nucleic Acids Res.* 37, 441–5.

Chappe, V., Mettey, Y., Vierfond, J.M., Hanrahan, J.W., Gola, M., Verrier, B., Becq, F., 1998. Structural basis for specificity and potency of xanthine derivatives as activators of the CFTR chloride channel. *Br. J. Pharmacol.* 123, 683–93.

Chen, Y., Wang, B., Guo, Y., Zhou, Y., Pan, L., Xiong, L., Yu, S., Li, Z., Youwei, C., Baolei, W., Yanjun, G., Yunyun, Z., Li, P., Lixia, X., Shujing, Y., Zhengming, L., 2014. Synthesis and biological activities of novel methyl xanthine derivatives. *Chem. Res. Chinese Univ.* 30, 98–102.

Chung, H.H., Dai, Z.-K., Wu, B.N., Yeh, J.L., Chai, C.Y., Chu, K.S., Liu, C.P., Chen, I.J., 2010. The xanthine derivative KMUP-1 inhibits models of pulmonary artery hypertension via increased NO and cGMP-dependent inhibition of RhoA/Rho kinase. *Br. J. Pharmacol.* 160, 971–86.

Claffey, M.M., Helal, C.J., Verhoest, P.R., Kang, Z., Fors, K.S., Jung, S., Zhong, J., Bundesmann, M.W., Hou, X., Lui, S., Kleiman, R.J., Vanase-Frawley, M., Schmidt, A.W., Menniti, F., Schmidt, C.J., Hoffman, W.E., Hajos, M., McDowell, L., O'Connor, R.E., MacDougall-Murphy, M., Fonseca, K.R., Becker, S.L., Nelson, F.R., Liras, S., 2012. Application of Structure-Based Drug Design and Parallel Chemistry to Identify Selective, Brain Penetrant, In Vivo Active Phosphodiesterase 9A Inhibitors. *J. Med. Chem.* 55, 9055–68.

Conti, M., Beavo, J., 2007. Biochemistry and Physiology of Cyclic Nucleotide Phosphodiesterases: Essential Components in Cyclic Nucleotide Signaling. *Annu. Rev. Biochem.* 76, 481–511.

Cosio, B.G., Tsaprouni, L., Ito, K., Jazrawi, E., Adcock, I.M., Barnes, P.J., 2004. Theophylline Restores Histone Deacetylase Activity and Steroid Responses in COPD Macrophages. J. Exp. Med. 200, 689-95.

Currie, M.G., Fok, K.F., Kato, J., Moore, R.J., Hamra, F.K., Duffin, K.L., Smith, C.E., 1992. Guanylin: an endogenous activator of intestinal guanylate cyclase. *Proc. Natl. Acad. Sci*. 89, 947–51.

Cushley, M.J., Holgate, S.T., 1985. Bronchodilator actions of xanthine derivatives administered by inhalation in asthma. *Thorax* 40, 176–9.

Cushnie, T.P.T., Cushnie, B., Lamb, A.J., 2014. Alkaloids: an overview of their antibacterial, antibiotic-enhancing and antivirulence activities. *Int. J. Antimicrob. Agents* 44, 377–86.

da Silva, F.H., Pereira, M.N., Franco-Penteado, C.F., De Nucci, G., Antunes, E., Claudino, M.A., 2013. Phosphodiesterase-9 (PDE9) inhibition with BAY 73-6691 increases corpus cavernosum relaxations mediated by nitric oxide–cyclic GMP pathway in mice. *Int. J. Impot.* Res. 25, 69–73.

Dai, Z.-K., Liu, Y.-W., Hsu, J.-H., Yeh, J.-L., Chen, I.-J., Wu, J.-R., Wu, B.-N., 2015. The Xanthine Derivative KMUP-1 Attenuates Serotonin-Induced Vasoconstriction and K^+-Channel Inhibitory Activity via the PKC Pathway in Pulmonary Arteries. *Int. J. Biol. Sci.* 11, 633–42.

Daly, J.W., Hide, I., Bridson, P.K., 1990. Imidazodiazepinediones: a new class of adenosine receptor antagonists. *J. Med. Chem.* 33, 2818–21.

Daly, J.W., Hong, O., Padgett, W.L., Shamim, M.T., Jacobson, K.A., Ukena, D., 1988. Non-xanthine heterocycles: Activity as antagonists of A1 and A2-adenosine receptors.

Biochem. Pharmacol. 37, 655–64.

Das, A., Xi, L., Kukreja, R.C., 2005. Phosphodiesterase-5 inhibitor sildenafil preconditions adult cardiac myocytes against necrosis and apoptosis. Essential role of nitric oxide signaling. *J. Biol. Chem.* 280, 12944–55.

de Vente, J., 2004. cGMP: a second messenger for acetylcholine in the brain? *Neurochem. Int.* 45, 799–812.

Deguchi, A., Thompson, W.J., Weinstein, I.B., 2004. Activation of protein kinase G is sufficient to induce apoptosis and inhibit cell migration in colon cancer cells. *Cancer Res.* 64, 3966–73.

DeNinno, M.P., Andrews, M., Bell, A.S., Chen, Y., Eller-Zarbo, C., Eshelby, N., Etienne, J.B., Moore, D.E., Palmer, M.J., Visser, M.S., Yu, L.J., Zavadoski, W.J., Michael Gibbs, E., 2009. The discovery of potent, selective, and orally bioavailable PDE9 inhibitors as potential hypoglycemic agents, *Bioorg. Med. Chem. Lett*. 19, 2537-41.

Dini, F.L., Cogo, R., 2000. Doxofylline: A New Generation Xanthine Bronchodilator Devoid of Major Cardiovascular Adverse Effects. *Curr. Med. Res. Opin.* 16, 258–68.

Dunkern, T.R., Hatzelmann, A., 2007. Characterization of inhibitors of phosphodiesterase 1C on a human cellular system. *FEBS* J. 274, 4812–24.

Erceg, S., Monfort, P., Hernandez-Viadel, M., Llansola, M., Montoliu, C., Felipo, V., 2005. Restoration of learning ability in hyperammonemic rats by increasing extracellular cGMP in brain. *Brain Res.* 1036, 115–21.

Erickson, R.H., Hiner, R.N., Feeney, S.W., Blake, P.R., Rzeszotarski, W.J., Hicks, R.P., Costello, D.G., Abreu, M.E., Neurosci, S.H.A.R., 1991. 1,3,8-Trisubstituted Xanthines. Effects of Substitution Pattern upon Adenosne A1/A2 Affinity. *J. Med. Chem.* 34, 1431–5.

Essmann, U., Perera, L., Berkowitz, M.L., Darden, T., Lee, H., Pedersen, L.G., 1995. A smooth particle mesh Ewald method. *J. Chem. Phys.* 103, 8577–93.

Evgenov, O. V., Busch, C.J., Evgenov, N. V., Liu, R., Petersen, B., Falkowski, G.E., Pethő, B., Vas, Á., Bloch, K.D., Zapol, W.M., Ichinose, F., 2006. Inhibition of phosphodiesterase 1 augments the pulmonary vasodilator response to inhaled nitric oxide in awake lambs with acute pulmonary hypertension. *Am. J. Physiol. Lung Cell. Mol. Physiol.* 290, L723-9.

Feng, J., Chen, Y., Pu, J., Yang, X., Zhang, C., Zhu, S., Zhao, Y., Yuan, Y., Yuan, H., Liao, F., 2011. An improved malachite green assay of phosphate: Mechanism and application. *Anal. Biochem.* 409, 144–9.

Fisher, D.A., Smith, J.F., Pillar, J.S., St Denis, S.H., Cheng, J.B., 1998. Isolation and characterization of PDE9A, a novel human cGMP-specific phosphodiesterase. *J. Biol. Chem.* 273, 15559–64.

Foukas, L.C., Daniele, N., Ktori, C., Anderson, K.E., Jensen, J., Shepherd, P.R., 2002. Direct effects of caffeine and theophylline on p110δ and other phosphoinositide 3-kinases: Differential effects on lipid kinase and protein kinase activities. *J. Biol. Chem.* 277, 37124–30.

Franchetti, P., Messini, L., Cappellacci, L., Grifantini, M., Lucacchini, A., Martini, C., Senatore, G., 1994. 8-Azaxanthine Derivatives as Antagonists of Adenosine Receptors. *J. Med. Chem.* 37, 2970–5.

Francis, S.H., 2010. The Role of cGMP-Dependent Protein Kinase in Controlling Cardiomyocyte cGMP. *Circ. Res.* 107, 1164–6.

Francis, S.H., Blount, M.A., Corbin, J.D., 2011. Mammalian Cyclic Nucleotide Phosphodiesterases: Molecular Mechanisms and Physiological Functions. *Physiol. Rev.* 91, 651-90.

Franco, R., Oñatibia-Astibia, A., Martínez-Pinilla, E., 2013. Health Benefits of Methylxanthines in Cacao and Chocolate. *Nutrients* 5, 4159–4173.

Friebe, A., Koesling, D., 2003. Regulation of Nitric Oxide-Sensitive Guanylyl Cyclase. *Circ. Res.* 93.

Fryburg, D., Gibbs, E., 2004. Treatment of insulin resistance syndrome and type 2 diabetes with PDE9 inhibitors, US Patent, WO 2003037432 A1.

Ganoth, A., Friedman, R., Nachliel, E., Gutman, M., 2006. A Molecular Dynamics Study and Free Energy Analysis of Complexes between the Mlc1p Protein and Two IQ Motif Peptides. *Biophys. J.* 91, 2436–50.

Geisbuhler, T.P., Schwager, T.L., Ervin, H.D., 2002. 3-Isobutyl-1-methylxanthine (IBMX) sensitizes cardiac myocytes to anoxia. *Biochem. Pharmacol.* 63, 2055–62.

Glennon, R.A., Gaines, J.J., Rogers, M.E., 1981. Benz-fused mesoionic xanthine analogs as inhibitors of cyclic-AMP phosphodiesterase. *J. Med. Chem.* 24, 766–9.

Gómez-Pinedo, U., Rodrigo, R., Cauli, O., Cabrera-Pastor, A., Herraiz, S., Garcia-Verdugo, J.-M., Pellicer, B., Pellicer, A., Felipo, V., Gómez-Pinedo, U., Rodrigo, R., Cauli, O., Herraiz, S., Garcia-Verdugo, J., Pellicer, B., Pellicer, A., Felipo, V., Cauli, O., Herraiz, S., Pellicer, B., Pellicer, A., Felipo, V., 2011. cGMP modulates stem cells differentiation to neurons in brain in vivo pathological implications. *BMC Pharmacol.* 11, O29.

Gonçalves, R.L., Lugnier, C., Keravis, T., Lopes, M.J., Fantini, F.A., Schmitt, M., Cortes, S.F., Lemos, V.S., 2009. The flavonoid dioclein is a selective inhibitor of cyclic nucleotide phosphodiesterase type 1 (PDE1) and a cGMP-dependent protein kinase (PKG) vasorelaxant in human vascular tissue. *Eur. J. Pharmacol.* 620, 78–83.

Graham, T.E., Rush, J.W.E., Soeren, M.H. van, 1994. Caffeine and Exercise: Metabolism and Performance. *Can. J. Appl. Physiol.* 19, 111–38.

Grome, J.J., Hofmann, W., Gojowczyk, G., Stefanovich, V., 1996. Effects of a xanthine derivative, propentofylline, on local cerebral blood flow and glucose utilization in the rat. *Brain Res*. 740, 41–6.

Guipponi, M., Scott, H.S., Kudoh, J., Kawasaki, K., Shibuya, K., Shintani, A., Asakawa, S., Chen, H., Lalioti, M.D., Rossier, C., Minoshima, S., Shimizu, N., Antonarakis, S.E., 1998. Identification and characterization of a novel cyclic nucleotide phosphodiesterase gene (PDE9A) that maps to 21q22.3: alternative splicing of mRNA transcripts, genomic structure and sequence. *Hum. Genet.* 103, 386–92.

Gulevskaya, A. V., Pozharskii, A.F., 1991. Synthesis of N-substituted xanthines (review). *Chem. Heterocycl. Comp.* 27, 1–23.

Gupta, A., Yadav, V., Yadav, J.S., Rawat, S., 2011. An Analytical Approach of Doxofylline: A Review. *Asian J. Pharm. Anal.* 1, 67–70.

Gwak, Y.S., Crown, E.D., Unabia, G.C., Hulsebosch, C.E., 2008. Propentofylline attenuates allodynia, glial activation and modulates GABAergic tone after spinal cord injury in the rat. *Pain* 138, 410–22.

Haghgoo, S., Hasegawa, T., Nadai, M., Wang, L., Ishigaki, T., Miyamoto, K.-I., Nabeshima, T., 1995. Brain Distribution Characteristics of Xanthine Derivatives and Relation to their Locomotor Activity in Mice. *J. Pharm. Pharmacol.* 47, 412–9.

Hamra, F.K., Forte, L.R., Eber, S.L., Pidhorodeckyj, N. V, Krause, W.J., Freeman, R.H., Chin, D.T., Tompkins, J.A., Fok, K.F., Smith, C.E., 1993. Uroguanylin: structure and activity of a second endogenous peptide that stimulates intestinal guanylate cyclase. *Proc. Natl. Acad. Sci.* 90, 10464–8.

Hasegawa, T., Nadai, M., Apichartpichean, R., Muraoka, I., Nabeshima, T., Takagi, K., 1991. Pharmacokinetic Characteristics of N7-Substituted Theophylline Derivatives and Their Interaction with Quinolone in Rats. *J. Pharm. Sci.* 80, 962–965.

Hatzelmann, A., Tenor, H., Schudt, C., 1995. Differential effects of non-selective and selective phosphodiesterase inhibitors on human eosinophil functions. *Br. J. Pharmacol.* 114, 821–31.

Hayallah, A.M., Sandoval-Ramírez, J., Reith, U., Schobert, U., Preiss, B., Schumacher, B., John W. Daly, Müller, C.E., 2002. 1,8-Disubstituted Xanthine Derivatives: Synthesis of Potent A2B-Selective Adenosine Receptor Antagonists. *J. Med. Chem.* 45, 1500–10.

Heizmann, G., Eberle, A.N., 1997. Xanthines as a scaffold for molecular diversity. *Mol. Divers.* 2, 171–4.

Hess, B., Bekker, H., Berendsen, H.J.C., Fraaije, J.G.E.M., 1997. LINCS: A linear constraint solver for molecular simulations. *J. Comput. Chem.* 18, 1463–72.

Hofmann, F., Ammendola, A., Schlossmann, J., 2000. Rising behind NO: cGMP-dependent protein kinases. *J. Cell Sci.* 113, 1671–6.

Hofmann, F., Bernhard, D., Lukowski, R., Weinmeister, P., 2009. cGMP regulated protein kinases (cGK). *Handb. Exp. Pharmacol.* 137–62.

Hofmann, F., Feil, R., Kleppisch, T., Schlossmann, J., 2006. Function of cGMP-dependent protein kinases as revealed by gene deletion. *Physiol. Rev.* 86, 1–23.

Hong, T.Y., Guh, J.Y., Wu, B.N., Chai, C.Y., Huang, H.T., Chen, I.J., 2014. Kmup-1 Protects Kidney from Streptozotocin-Induced Pro-Inflammation in Early Diabetic Nephropathy by Restoring Enos/Pparγ and Inhibiting MMP-9. *Eur. J. Inflamm.* 12, 89–100.

Hosseinzadeh, H., Fazly Bazzaz, B.S., Moaddab Sadati, M., 2006. In vitro Evaluation of Methylxanthines and Some Antibiotics: Interaction against Staphylococcus aureus and Pseudomonas aeruginosa. *Iran. Biomed. J.* 10, 163–167.

Hou, J., Xu, J., Liu, M., Zhao, R., Luo, H.-B., Ke, H., 2011. Structural Asymmetry of Phosphodiesterase-9, Potential Protonation of a Glutamic Acid, and Role of the

Invariant Glutamine. *PLoS One* 6, e18092.

Hu, F., Ren, J., Zhang, J., Zhong, W., Luo, M., 2012. Natriuretic peptides block synaptic transmission by activating phosphodiesterase 2A and reducing presynaptic PKA activity. *Proc. Natl. Acad. Sci.* 109, 17681–6.

Huai, Q., Wang, H., Zhang, W., Colman, R.W., Robinson, H., Ke, H., 2004. Crystal structure of phosphodiesterase 9 shows orientation variation of inhibitor 3-isobutyl-1-methylxanthine binding. *Proc. Natl. Acad. Sci.* 101, 9624–9.

Hutson, P.H., Finger, E.N., Magliaro, B.C., Smith, S.M., Converso, A., Sanderson, P.E., Mullins, D., Hyde, L.A., Eschle, B.K., Turnbull, Z., Sloan, H., Guzzi, M., Zhang, X., Wang, A., Rindgen, D., Mazzola, R., Vivian, J.A., Eddins, D., Uslaner, J.M., Bednar, R., Gambone, C., Le-Mair, W., Marino, M.J., Sachs, N., Xu, G., Parmentier-Batteur, S., 2011. The selective phosphodiesterase 9 (PDE9) inhibitor PF-04447943 (6-[(3S,4S)-4-methyl-1-(pyrimidin-2-ylmethyl)pyrrolidin-3-yl] -1-(tetrahydro-2H-pyran-4-yl)-1,5-dihydro-4H-pyrazolo[3,4-d]pyrimidin-4-one) enhances synaptic plasticity and cognitive function. *Neuropharmacol.* 61, 665–76.

Ito, K., Caramori, G., Lim, S., Oates, T., Chung, K.F., Barnes, P.J., Adcock, I.M., 2002. Expression and Activity of Histone Deacetylases in Human Asthmatic Airways. *Am. J. Respir. Crit. Care Med.* 166, 392–6.

Ivanov, E.I., Polishchuk, A.A., Kalayanov, G.D., 1992. Synthesis of crown-containing xanthine derivatives. Chem. *Heterocycl. Compd.* 28, 1266–9.

Jacobson, K.A., Gao, Z.-G., 2006. Adenosine receptors as therapeutic targets. *Nat. Rev. Drug Discov.* 5, 247–64.

Jeon, Y.H., Heo, Y.-S., Kim, C.M., Hyun, Y.-L., Lee, T.G., Ro, S., Cho, J.M., 2005. Phosphodiesterase: overview of protein structures, potential therapeutic applications and recent progress in drug development. *Cell. Mol. Life Sci.* 62, 1198–220.

Jiang, X., Li, J., Paskind, M., Epstein, P.M., 1996. Inhibition of calmodulin-dependent phosphodiesterase induces apoptosis in human leukemic cells. *Proc. Natl. Acad. Sci.* 93, 11236–41.

Joghataie, M.T., Roghani, M., Negahdar, F., Hashemi, L., 2004. Protective effect of caffeine against neurodegeneration in a model of Parkinson's disease in rat: behavioral and histochemical evidence. *Parkinsonism Relat. Disord.* 10, 465–8.

Kadi, A.A., El-Tahir, K.E.H., Jahng, Y., Rahman, A.F.M.M., 2015. Synthesis, biological evaluation and Structure Activity Relationships (SARs) study of 8-(substituted) aryloxycaffeine. *Arab. J. Chem.*

Kakuyama (nee Iwazaki), A., Sadzuka, Y., 2001. Effect of Methylxanthine Derivatives on Doxorubicin Transport and Antitumor Activity. *Curr. Drug Metab.* 2, 379–95.

Kass, D.A., Champion, H.C., Beavo, J.A., 2007. Phosphodiesterase Type 5 Expanding Roles in Cardiovascular Regulation. *Circ. Res.* 101, 1084-95.

Ke, H., Wang, H., 2007. Crystal Structures of Phosphodiesterases and Implications on Substrate Specificity and Inhibitor Selectivity. *Curr. Top. Med. Chem.* 7, 391–403.

Ke, H., Wang, H., Ye, M., 2011. Structural insight into the substrate specificity of phosphodiesterases. *Handb. Exp. Pharmacol.* 121–34.

Kieback, A.G., Baumann, G., 2006. Saterinone, a Phosphodiesterase (PDE) III Inhibitor and α1-Adrenergic Antagonist. *Cardiovasc. Drug Rev.* 17, 374–83.

Kim, D., Jun, H., Lee, H., Hong, S.S., Hong, S., 2010. Development of new fluorescent xanthines as kinase inhibitors. *Org. Lett.* 12, 1212–15.

Kim, E., Park, J.M., 2003. Identification of Novel Target Proteins of Cyclic GMP Signaling Pathways Using Chemical Proteomics. *J. Biochem. Mol. Biol.* 36, 299–304.

Kleiman, R.J., Chapin, D.S., Christoffersen, C., Freeman, J., Fonseca, K.R., Geoghegan, K.F., Grimwood, S., Guanowsky, V., Hajós, M., Harms, J.F., Helal, C.J., Hoffmann, W.E., Kocan, G.P., Majchrzak, M.J., McGinnis, D., McLean, S., Menniti, F.S., Nelson, F., Roof, R., Schmidt, A.W., Seymour, P.A., Stephenson, D.T., Tingley, F.D., Vanase-Frawley, M., Verhoest, P.R., Schmidt, C.J., 2012. Phosphodiesterase 9A Regulates Central cGMP and Modulates Responses to Cholinergic and Monoaminergic Perturbation In Vivo. *J. Pharmacol. Exp. Ther.* 341, 396-409.

Kleppisch, T., 2009. Phosphodiesterases in the Central Nervous System, in: cGMP: Generators, Effectors and Therapeutic Implications. *Springer Berlin Heidelberg, Berlin, Heidelberg,* pp. 71–92.

Kroker, K.S., Rast, G., Giovannini, R., Marti, A., Dorner-Ciossek, C., Rosenbrock, H., 2012. Inhibition of acetylcholinesterase and phosphodiesterase-9A has differential effects on hippocampal early and late LTP. *Neuropharmacology* 62, 1964–74.

Kuhn, M., 2003. Structure, regulation, and function of mammalian membrane guanylyl cyclase receptors, with a focus on guanylyl cyclase-A. *Circ. Res.* 93, 700–9.

Kumar, M., Dagar, A., Gupta, V.K., Sharma, A., 2014. In silico docking studies of bioactive natural plant products as putative DHFR antagonists. *Med. Chem. Res.* 23, 810–17.

Laddha, S.S., Wadodkar, S.G., Meghal, S.K., 2009. CAMP-dependent phosphodiesterase inhibition and SAR studies on novel 6,8-disubstituted 2-phenyl-3-(substituted benzothiazole-2-yl)-4[3H]- quinazolinone. *Med. Chem. Res.* 18, 268–76.

Lazzaroni, M., Grossi, E., Porro, G.B., 2007. The effect of intravenous doxofylline or aminophylline on gastric secretion in duodenal ulcer patients. *Aliment. Pharmacol. Ther.* 4, 643–9.

Lee, D., Lee, S., Liu, K.H., Bae, J.S., Baek, D.J., Lee, T., 2016. Solid-Phase Synthesis of 1,3,7,8-Tetrasubstituted Xanthine Derivatives on Traceless Solid Support. *ACS Comb. Sci.* 18, 70–4.

Lee, I., Kamba, A., Low, D., Mizoguchi, E., 2014. Novel methylxanthine derivative-mediated anti-inflammatory effects in inflammatory bowel disease. *World J. Gastroenterol*. 20, 1127–38.

Li, Z., Lu, X., Feng, L.-J., Gu, Y., Li, X., Wu, Y., Luo, H.-B., 2015. Molecular dynamics-based discovery of novel phosphodiesterase-9A inhibitors with non-pyrazolopyrimidinone scaffolds. *Mol. BioSyst.* 11, 115–25.

Lin, R.J., Wu, B.N., Shen, K.P., Huang, C.H., Liu, Z.I., Lin, C.Y., Cheng, C.J., Chen, I.J., 2002. Xanthine-analog, KMUP-2, enhances cyclic GMP and K^+ channel activities in rabbit aorta and corpus cavernosum with associated penile erection. *Drug Dev. Res.* 55, 162–72.

Liou, S.F., Hsu, J.H., Lin, I.L., Ho, M.L., Hsu, P.-C., Chen, L.W., Chen, I.J., Yeh, 2013. KMUP-1 Suppresses RANKL-Induced Osteoclastogenesis and Prevents Ovariectomy-Induced Bone Loss: Roles of MAPKs, Akt, NF-κB and Calcium/Calcineurin/NFATc1 Pathways. *PLoS One* 8, e69468.

Liu, C.P., Yeh, J.L., Wu, B.N., Chai, C.Y., Chen, I.J., Lai, W.T., 2011. KMUP-3 attenuates ventricular remodelling after myocardial infarction through eNOS enhancement and restoration of MMP-9/TIMP-1 balance. *Br. J. Pharmacol.* 162, 126–35.

Liu, S., Mansour, M.N., Dillman, K.S., Perez, J.R., Danley, D.E., Aeed, P.A., Simons, S.P., Lemotte, P.K., Menniti, F.S., 2008. Structural basis for the catalytic mechanism of human phosphodiesterase 9. *Proc. Natl. Acad. Sci.* 105, 13309–14.

Lucas, K.A., Pitari, G.M., Kazerounian, S., Ruiz-Stewart, I., Park, J., Schulz, S., Chepenik, K.P., Waldman, S.A., 2000. Guanylyl cyclases and signaling by cyclic GMP. *Pharmacol. Rev.* 52, 375–414.

Lugnier, C., 2006. Cyclic nucleotide phosphodiesterase (PDE) superfamily: A new target for the development of specific therapeutic agents. *Pharmacol. Ther.* 109, 366–98.

Mackenzie, S.J., Houslay, M.D., 2000. Action of rolipram on specific PDE4 cAMP phosphodiesterase isoforms and on the phosphorylation of cAMP-response-element-binding protein (CREB) and p38 mitogen-activated protein (MAP) kinase in U937 monocytic cells. *Biochem. J.* 347, 571–8.

Makhlouf, A., Kshirsagar, A., Niederberger, C., 2006. Phosphodiesterase 11: a brief review of structure, expression and function. *Int. J. Impot. Res.* 18, 501–9.

Malde, A.K., Zuo, L., Breeze, M., Stroet, M., Poger, D., Nair, P.C., Oostenbrink, C., Mark, A.E., 2011. An Automated Force Field Topology Builder (ATB) and Repository: Version 1.0. *J. Chem. Theory Comput.* 7, 4026–37.

Matissek, R., 1997. Evaluation of xanthine derivatives in chocolate - nutritional and chemical aspects. *Zeitschrift fur Leb. und forsch. A.* 205, 175–184.

Maurice, D.H., Ke, H., Ahmad, F., Wang, Y., Chung, J., Manganiello, V.C., 2014. Advances in targeting cyclic nucleotide phosphodiesterases. *Nat. Rev. Drug Discov.* 13, 290–314.

Medina, A.E., 2011. Therapeutic utility of phosphodiesterase type I inhibitors in neurological conditions. *Front. Neurosci.* 5, 21.

Mehats, C., Andersen, C.B., Filopanti, M., Jin, S.-L.C., Conti, M., 2002. Cyclic nucleotide phosphodiesterases and their role in endocrine cell signaling. *Trends Endocrinol. Metab.* 13, 29–35.

Meng, F., Hou, J., Shao, Y.X., Wu, P.Y., Huang, M., Zhu, X., Cai, Y., Li, Z., Xu, J., Liu, P., Luo, H.-B., Wan, Y., Ke, H., 2012. Structure-Based Discovery of Highly Selective Phosphodiesterase-9A Inhibitors and Implications for Inhibitor Design. *J. Med. Chem.* 55, 8549–58.

Meskini, N., Némoz, G., Okyayuz-Baklouti, I., Lagarde, M., Prigent, A.-F., 1994. Phosphodiesterase inhibitory profile of some related xanthine derivatives pharmacologically active on the peripheral microcirculation. *Biochem. Pharmacol.* 47,

781–788.

Michie, A.M., Lobban, M., Müller, T., Harnett, M.M., Houslay, M.D., 1996. Rapid regulation of PDE-2 and PDE-4 cyclic AMP phosphodiesterase activity following ligation of the T cell antigen receptor on thymocytes: Analysis using the selective inhibitors erythro-9-(2-hydroxy-3-nonyl)-adenine (EHNA) and rolipram. *Cell. Signal.* 8, 97–110.

Mielke, R., Kittner, B., Ghaemi, M., Kessler, J., Szelies, B., Herholz, K., Heiss, W.D., 1996. Propentofylline improves regional cerebral glucose metabolism and neuropsychologic performance in vascular dementia. *J. Neurol. Sci.* 141, 59–64.

Miguel, L.I., Almeida, C.B., Traina, F., Canalli, A.A., Dominical, V.M., Saad, S.T.O., Costa, F.F., Conran, N., 2011. Inhibition of phosphodiesterase 9A reduces cytokine-stimulated in vitro adhesion of neutrophils from sickle cell anemia individuals. *Inflamm. Res.* 60, 633–42.

Miyamoto, K., Kurita, M., Ohmae, S., Sakai, R., Sanae, F., Takagi, K., 1994. Selective tracheal relaxation and phosphodiesterase-IV inhibition by xanthine derivatives. *Eur. J. Pharmacol.* 267, 317–22.

Miyamoto, K., Yamamoto, Y., Kurita, M., Sakai, R., Konno, K., Sanae, F., Ohshima, T., Takagi, K., Hasegawa, T., 1993. Bronchodilator activity of xanthine derivatives substituted with functional groups at the 1- or 7-position. *J. Med. Chem.* 36, 1380–6.

Müller, C.E., Deters, D., Dominik, A., Pawlowski, M., 1998. Synthesis of paraxanthine and isoparaxanthine analogs (1,7- and 1,9- substituted xanthine derivatives). Synthesis. 1428–36.

Mullershausen, F., Russwurm, M., Koesling, D., Friebe, A., 2004. In vivo reconstitution of the negative feedback in nitric oxide/cGMP signaling: role of phosphodiesterase type 5 phosphorylation. *Mol. Biol. Cell.* 15, 4023–30.

Nehlig, A., Daval, J.L., Debry, G., 1992. Caffeine and the central nervous system: mechanisms of action, biochemical, metabolic and psychostimulant effects. Brain Res. *Brain Res. Rev.* 17, 139–70.

Nicholas, T., Park, Y., Choo, H.W., Plotka, A., Martin, W., Martin, D., Schwam, E., 2011. Pharmacokinetic and safety interactions between a novel PDE9 inhibitor, PF-04447943, and donepezil in healthy volunteers. *Alzheim. Dement.* 7, S786.

Niesen, F.H., Berglund, H., Vedadi, M., 2007. The use of differential scanning fluorimetry to detect ligand interactions that promote protein stability. *Nat. Protoc.* 2, 2212–21.

Ogawa, K., Takagi, K., Satake, T., 1989. Mechanism of xanthine-induced relaxation of guinea-pig isolated trachealis muscle 542–46.

Omori, K., Kotera, J., 2007. Overview of PDEs and their regulation. *Circ. Res.* 100, 309–27.

Oostenbrink, C., Villa, A., Mark, A.E., Van Gunsteren, W.F., 2004. A biomolecular force field based on the free enthalpy of hydration and solvation: The GROMOS force-field parameter sets 53A5 and 53A6. *J. Comput. Chem.* 25, 1656–1676.

Osswald, H., Schnermann, J., 2011. Methylxanthines and the Kidney. *Springer Berlin Heidelberg*. 391–412.

Parrinello, M., 1981. Polymorphic transitions in single crystals: A new molecular dynamics method. *J. Appl. Phys.* 52, 7182.

Paterniti, I., Mazzon, E., Gil, C., Impellizzeri, D., Palomo, V., Redondo, M., Perez, D.I., Esposito, E., Martinez, A., Cuzzocrea, S., 2011. PDE 7 Inhibitors: New Potential Drugs for the Therapy of Spinal Cord Injury. *PLoS One* 6, e15937.

Pennella, S., Vittoria Mattioli, A., 2015. Caffeine, Energy Drinks and Atrial Fibrillation: A Mini-Review. *BAOJ Nutr.* 1, 1-4.

Perviz, S., Khan, H., Pervaiz, A., 2016. Plant alkaloids as an emerging therapeutic alternative for the treatment of depression. *Front. Pharmacol*. 7, 1–7.

Pronk, S., Páll, S., Schulz, R., Larsson, P., Bjelkmar, P., Apostolov, R., Shirts, M.R., Smith, J.C., Kasson, P.M., Van Der Spoel, D., Hess, B., Lindahl, E., 2013. GROMACS 4.5: A high-throughput and highly parallel open source molecular simulation toolkit. *Bioinformatics* 29, 845–54.

Rabe, K.F., 2011. Update on roflumilast, a phosphodiesterase 4 inhibitor for the treatment of chronic obstructive pulmonary disease. *Br. J. Pharmacol.* 163, 53–67.

Rabe, K.F., Magnussen, H., Dent, G., 1995. Theophylline and selective PDE inhibitors as bronchodilators and smooth muscle relaxants. *Eur. Respir. J.* 8, 637–42.

Rao, Y.J., Xi, L., 2009. Pivotal effects of phosphodiesterase inhibitors on myocyte contractility and viability in normal and ischemic hearts. *Acta Pharmacol. Sin.* 30, 1–24.

Rentero, C., Monfort, A., Puigdomènech, P., 2003. Identification and distribution of different mRNA variants produced by differential splicing in the human phosphodiesterase 9A gene. Biochem. *Biophys. Res. Commun.* 301, 686–92.

Rentero, C., Puigdomènech, P., 2006. Specific use of start codons and cellular localization of splice variants of human phosphodiesterase 9A gene. *BMC Mol. Biol.* 7, 39.

Rieg, T., Steigele, H., Schnermann, J., Richter, K., Osswald, H., Vallon, V., 2005. Requirement of Intact Adenosine A1 Receptors for the Diuretic and Natriuretic Action of the Methylxanthines Theophylline and Caffeine. *J. Pharmacol. Exp. Ther.* 313, 403-9.

Roy, U., Pal, M., Datta, S., Harlalka, S., 2015. Has Oxidative Stress any Role on Mechanisms of Aminophylline – Induced Seizures? An Animal Study. *Kathmandu Univ. Med. J.* 12, 269.

Russell, T.R., Terauki, W.L., Appleman, M.M., 1973. Separate Phosphodiesterases for the

Hydrolysis of Cyclic Adenosine 3', 5'-Monophosphate and Cyclic Guanosine 3', 5'-Monophosphate in Rat Liver. *J. Biol. Chem.* 248, 1334–40.

Rutherford, J.D., Vatner, S.F., Braunwald, E., 1981. Effects and mechanism of action of aminophylline on cardiac function and regional blood flow distribution in conscious dogs. *Circulation* 63, 378-87.

Ruttikorn, A., Takagi, K., Nadai, M., Kuzuya, T., Ogawa, K., Miyamoto, K., Hasegawa, T., 1988. Studies on Alkyl-Xanthine Derivatives II. Pharmacokinetic and Pharmacodynamic Studies of a New Bronchodilator, 1-Methyl-3-Propylxanthine (MPX). *Jpn. J. Pharmacol.* 48, 341–47.

Sachdeva, S., Gupta, M., 2013. Adenosine and its receptors as therapeutic targets: An overview. *Saudi Pharm. J.* 21, 245–53.

Sadzuka, Y., Iwazaki, A., Miyagishima, A., Nozawa, Y., Hirota, S., 1995. Effects of methylxanthine derivatives on adriamycin concentration and antitumor activity. *Jpn. J. Cancer Res.* 86, 594–9.

Sakai, R., Konno, K., Yamamoto, Y., Sanae, F., Takagi, K., Hasegawa, T., Iwasaki, N., Kakiuchi, M., Kato, H., Miyamoto, K., 1992. Effects of alkyl substitutions of xanthine skeleton on bronchodilation. *J. Med. Chem.* 35, 4039–44.

Sanae, F., Ohmae, S., Kurita, M., Sawanishi, H., Takagi, K., Miyamotol, K. I., 1995. Structure-Activity Relationships of Alkylxanthines: Alkyl Chain Elongation at the NI-or N7-Position Decreases Cardiotonic Activity in the Isolated Guinea Pig Heart. *Jpn. J. Pharmacol.* 69, 75–82.

Saravani, R., Karami-Tehrani, F., Hashemi, M., Aghaei, M., Edalat, R., 2012. Inhibition of phosphodiestrase 9 induces cGMP accumulation and apoptosis in human breast cancer cell lines, MCF-7 and MDA-MB-468. *Cell Prolif.* 45, 199–206.

Schett, G., Sloan, V.S., Stevens, R.M., Schafer, P., 2010. Apremilast: a novel PDE4 inhibitor in the treatment of autoimmune and inflammatory diseases. *Ther. Adv. Musculoskelet. Dis.* 2, 271–8.

Schneller, S.W., Ibay, A.C., Christ, W.J., Bruns, R.F., 1989. Linear and proximal benzo-separated alkylated xanthines as adenosine-receptor antagonists. *J. Med. Chem.* 32, 2247–54.

Scholz, N., Goy, M., Truman, J., Graubard, K., 1996. Nitric oxide and peptide neurohormones activate cGMP synthesis in the crab stomatogastric nervous system. *J. Neurosci.* 16, 1614-22.

Schwabe, U., Ukena, D., Lohse, M.J., 1985. Xanthine derivatives as antagonists at A1 and A2 adenosine receptors. *Naunyn. Schmiedebergs. Arch. Pharmacol.* 330, 212–21.

Schwam, E., Evans, R., Nicholas, T., Chew, R., Davidson, W., Ambrose, D., Altstiel, L., 2011. PF-04447943: A phase II controlled clinical trial of a selective PDE9A inhbitor in Alzheimer's disease. *Alzheimer's Dement.* 7, S695.

Sebastido, A.M., Ribeiro, J.A., 1989. Substituted xanthines: relative potency as adenosine receptor antagonists at the frog neuromuscular junction. *Br. J. Pharmacol* 9633, 211–19.

Semmler, J., Gebert, U., Eisenhut, T., Moeller, J., Schonharting, M.M., 1993. Xanthine derivatives: comparison between suppression of tumour necrosis factor-a production and inhibition of cAMP phosphodiesterase activity. *Immunology* 78, 520–25.

Shao, Y., Huang, M., Cui, W., Feng, L.-J., Wu, Y., Cai, Y., Li, Z., Zhu, X., Liu, P., Wan, Y., Ke, H., Luo, H.B., 2014. Discovery of a Phosphodiesterase 9A Inhibitor as a Potential Hypoglycemic Agent. *J. Med. Chem.* 57, 10304–13.

Shimizu-Albergine, M., Patrucco, E., Tsai, L., Campbell, J.S., Beavo, J.A., 2008. Role of phosphodiesterase 8A (PDE8A) in lipid metabolism in the liver. *FASEB J.* 22, 909.4.

Singh, N., Patra, S., 2014. Phosphodiesterase 9: Insights from protein structure and role in therapeutics. *Life Sci.* 106, 1–11.

Skinhøj, E., Paulson, O.B., 1970. The mechanism of action of aminophylline upon cerebral vascular disorders. *Acta Neurol. Scand.* 46, 129–40.

Slattery, M.L., West, D.W., 1993. Smoking, alcohol, coffee, tea, caffeine, and theobromine: risk of prostate cancer in Utah (United States). *Canc. Caus. Contr.* 4, 559–63.

Sledz, W., Los, E., Paczek, A., Rischka, J., Motyka, A., Zoledowska, S., Jacek Piosik, Lojkowska, E., 2015. Antibacterial activity of caffeine against plant pathogenic bacteria. *Acta Biochim. Pol.* 62, 605–12.

Soderling, S.H., Bayuga, S.J., Beavo, J.A., 1998. Identification and characterization of a novel family of cyclic nucleotide phosphodiesterases. *J. Biol. Chem.* 273, 15553–8.

Stefanovich, V., 1985. Effect of propentofylline on cerebral metabolism of rats. *Drug Dev. Res.* 6, 327–38.

Steinleitner, A., Lambert, H., Kazensky, C., Danks, P., Roy, S., 1990. Pentoxifylline, a methylxanthine derivative, prevents postsurgical adhesion reformation in rabbits. *Obstet. Gynecol.* 75, 926–8.

Su, J., Scholz, P.M., Weiss, H.R., 2005. Differential effects of cGMP produced by soluble and particulate guanylyl cyclase on mouse ventricular myocytes. *Exp. Biol. Med. (Maywood)*. 230, 242–50.

Sugimura, K., Mizutani, A., 1979. The inhibitory effect of xanthine derivatives on alkaline phosphatase in the rat brain. *Histochem.* 61, 131–7.

Surapisitchat, J., Jeon, K.-I., Yan, C., Beavo, J.A., 2007. Differential Regulation of Endothelial Cell Permeability by cGMP via Phosphodiesterases 2 and 3. *Circ. Res.* 101, 811-8.

Suravajhala, R., Poddar, R., Nallapeta, S., Ullah, S., 2014. Xanthine Derivatives: A Molecular Modeling Perspective, in: Agricultural Bioinformatics. *Springer India, New Delhi,* 283–91.

Takagi, K., Hasegawa, T., Kuzuya, T., Ogawa, K., Watanabe, T., Satake, T., Miyamoto, K., Wakusawa, S., Koshiura, R., 1988. Structure-activity relationship in N3-alkyl-xanthine derivatives. *Jpn. J. Pharmacol*. 46, 373–8.

Tanaka, H., Ogawa, K., Takagi, K., Satake, T., Hidaka, H., 1991. Inhibition of cyclic gmp phosphodiesterase by xanthine derivatives relaxes guinea-pig trachealis smooth muscle. *Clin. Exp. Pharmacol. Physiol.* 18, 163–68.

Tarhan, O.R., Barut, I., Sutcu, R., Akdeniz, Y., Akturk, O., 2006. Pentoxifylline, a Methyl Xanthine Derivative, Reduces Peritoneal Adhesions and Increases Peritoneal Fibrinolysis in Rats. *Tohoku J. Exp. Med.* 209, 249–55.

Tedford, R.J., Hemnes, A.R., Russell, S.D., Wittstein, I.S., Mahmud, M., Zaiman, A.L., Mathai, S.C., Thiemann, D.R., Hassoun, P.M., Girgis, R.E., Orens, J.B., Shah, A.S., Yuh, D., Conte, J. V, Champion, H.C., 2008. PDE5A inhibitor treatment of persistent pulmonary hypertension after mechanical circulatory support. *Circ. Heart Fail.* 1, 213–9.

Trong, H. Le, Beier, N., Sonnenburg, W.K., Stroop, S.D., Walsh, K.A., Beavo, J.A., Charbonneau, H., 1990. Amino acid sequence of the cyclic GMP stimulated cyclic nucleotide phosphodiesterase from bovine heart. *Biochem.* 29, 10280–8.

Usachev, Y., Verkhratsky, A., 1995. IBMX induces calcium release from intracellular stores in rat sensory neurones. Cell Calcium 17, 197–206.

Usmani, O.S., Belvisi, M.G., Patel, H.J., Crispino, N., Birrell, M.A., Korbonits, M., Korbonits, D., Barnes, P.J., 2005. Theobromine inhibits sensory nerve activation and cough. *FASEB J.* 19, 231–3.

Vaandrager, A.B., de Jonge, H.R., 1996. Signalling by cGMP-dependent protein kinases. *Mol. Cell. Biochem.* 157, 23–30.

van der Staay, F.J., Rutten, K., Bärfacker, L., DeVry, J., Erb, C., Heckroth, H., Karthaus, D., Tersteegen, A., van Kampen, M., Blokland, A., Prickaerts, J., Reymann, K.G., Schröder, U.H., Hendrix, M., 2008. The novel selective PDE9 inhibitor BAY 73-6691 improves learning and memory in rodents. *Neuropharmacol.* 55, 908–18.

van Galen, P.J.M., Stiles, G.L., Michaels, G., Jacobson, K.A., 1992. Adenosine A1 and A2 receptors: Structure–function relationships. *Med. Res. Rev.* 12, 423–71.

van Mastbergen, J., Jolas, T., Allegra, L., Page, C.P., 2012. The mechanism of action of doxofylline is unrelated to HDAC inhibition, PDE inhibition or adenosine receptor antagonism. *Pulm. Pharmacol. Ther.* 25, 55–61.

Vang, A.G., Ben-Sasson, S.Z., Dong, H., Kream, B., DeNinno, M.P., Claffey, M.M., Housley, W., Clark, R.B., Epstein, P.M., Brocke, S., 2010. PDE8 Regulates Rapid Teff Cell Adhesion and Proliferation Independent of ICER. *PLoS One* 5, e12011.

Vardigan, J.D., Converso, A., Hutson, P.H., Uslaner, J.M., 2011. The Selective Phosphodiesterase 9 (PDE9) Inhibitor PF-04447943 Attenuates a Scopolamine-Induced Deficit in a Novel Rodent Attention Task. J. Neurogenet. 25, 120–6.

Verhoest, P.R., Fonseca, K.R., Hou, X., Proulx-LaFrance, C., Corman, M., Helal, C.J., Claffey, M.M., Tuttle, J.B., Coffman, K.J., Liu, S., Nelson, F., Kleiman, R.J., Menniti, F.S., Schmidt, C.J., Vanase-Frawley, M., Liras, S., 2012. Design and Discovery of 6-[(3S,4S)-4-Methyl-1-(pyrimidin-2-ylmethyl)pyrrolidin-3-yl]-1-(tetrahydro-2H-pyran-4-yl)-1,5-dihydro-4H-pyrazolo[3,4-d]pyrimidin-4-one (PF-04447943), a Selective Brain Penetrant PDE9A Inhibitor for the Treatment of Cognitive Disor. *J. Med. Chem.* 55, 9045–54.

Verhoest, P.R., Proulx-Lafrance, C., Corman, M., Chenard, L., Helal, C.J., Hou, X., Kleiman, R., Liu, S., Marr, E., Menniti, F.S., Schmidt, C.J., Vanase-Frawley, M.,

Schmidt, A.W., Williams, R.D., Nelson, F.R., Fonseca, K.R., Liras, S., 2009. Identification of a Brain Penetrant PDE9A Inhibitor Utilizing Prospective Design and Chemical Enablement as a Rapid Lead Optimization Strategy. *J. Med. Chem* 52,7946–9.

Vignoli, J.A., Bassoli, D.G., Benassi, M.T., 2011. Antioxidant activity, polyphenols, caffeine and melanoidins in soluble coffee: The influence of processing conditions and raw material. *Food Chem.* 124, 863–868.

Vukadinovica, V., Stefanovich, V., Rakica, L., 1986. Effect of propentofylline on the GABA system of a rat brain. *Drug Dev. Res.* 7, 87–94.

Wall, M.E., Francis, S.H., Corbin, J.D., Grimes, K., Richie-Jannetta, R., Kotera, J., Macdonald, B.A., Gibson, R.R., Trewhella, J., 2003. Mechanisms associated with cGMP binding and activation of cGMP-dependent protein kinase. *Proc. Natl. Acad. Sci.* 100, 2380–5.

Wallace, A.C., Laskowski, R.A., Thornton, J.M., 1995. LIGPLOT: a program to generate schematic diagrams of protein-ligand interactions. Protein Eng. 8, 127–34.

Wang, H., Liu, Y., Huai, Q., Cai, J., Zoraghi, R., Francis, S.H., Corbin, J.D., Robinson, H., Xin, Z., Lin, G., Ke, H., 2006. Multiple conformations of phosphodiesterase-5: implications for enzyme function and drug development. *J. Biol. Chem.* 281, 21469–79.

Wang, H., Luo, X., Ye, M., Hou, J., Robinson, H., Ke, H., 2010. Insight into Binding of Phosphodiesterase-9A Selective Inhibitors by Crystal Structures and Mutagenesis. *J. Med. Chem.* 53, 1726–31.

Wang, P., Wu, P., Egan, R.W., Billah, M.M., 2003. Identification and characterization of a new human type 9 cGMP-specific phosphodiesterase splice variant (PDE9A5): Differential tissue distribution and subcellular localization of PDE9A variants. *Gene* 314, 15–27.

Ward, A., Clissold, S.P., 1987. Pentoxifylline. A review of its pharmacodynamic and pharmacokinetic properties, and its therapeutic efficacy. *Drugs* 34, 50–97.

Westermann, D., Becher, P.M., Lindner, D., Savvatis, K., Xia, Y., Fröhlich, M., Hoffmann, S., Schultheiss, H.P., Tschöpe, C., 2012. Selective PDE5A inhibition with sildenafil rescues left ventricular dysfunction, inflammatory immune response and cardiac remodeling in angiotensin II-induced heart failure in vivo. *Basic Res. Cardiol.* 107, 308.

Weyler, S., Fülle, F., Diekmann, M., Schumacher, B., Hinz, S., Klotz, K.-N., Müller, C.E., 2006. Improving Potency, Selectivity, and Water Solubility of Adenosine A1 Receptor Antagonists: Xanthines Modified at Position 3 and Related Pyrimido[1,2,3-cd]purinediones. *ChemMedChem* 1, 891–902.

Witzenrath, M., Gutbier, B., Schmeck, B., Tenor, H., Seybold, J., Kuelzer, R., Grentzmann, G., Hatzelmann, A., van Laak, V., Tschernig, T., Mitchell, T.J., Schudt, C., Rosseau, S., Suttorp, N., Schütte, H., 2009. Phosphodiesterase 2 inhibition diminished acute lung injury in murine pneumococcal pneumonia. *Crit. Care Med.* 37, 584–90.

Wong, E.H.A., Ooi, S.O., 1985. Methylxanthine and non-xanthine phosphodiesterase inhibitors: Their effects on adenosine uptake and the low Km cyclic AMP phosphodiesterase in intact rat adipocyte. *Biochem. Pharmacol.* 34, 2891–6.

Wu, B.N., Chen, I.C., Lin, R.J., Chiu, C.C., An, L.M., Chen, I.J., 2005. Aortic Smooth Muscle Relaxants KMUP-3 and KMUP-4, Two Nitrophenylpiperazine Derivatives of Xanthine, Display cGMP-Enhancing Activity. *J. Cardiovasc. Pharmacol.* 46, 600–8.

Wu, B.N., Lin, R.J., Lin, C.Y., Shen, K.P., Chiang, L.C., Chen, I.J., 2001. A xanthine-based KMUP-1 with cyclic GMP enhancing and K^+ channels opening activities in rat aortic smooth muscle. *Br. J. Pharmacol.* 134, 265–74.

Wunder, F., Gnoth, M.J., Geerts, A., Barufe, D., 2009. A Novel PDE2A Reporter Cell Line: Characterization of the Cellular Activity of PDE Inhibitors. *Mol. Pharm.* 6, 326–36.

Wunder, F., Tersteegen, A., Rebmann, A., Erb, C., Fahrig, T., Hendrix, M., 2005. Characterization of the first potent and selective PDE9 inhibitor using a cGMP reporter cell line. *Mol. Pharmacol.* 68, 1775–81.

Yashin, A., Yashin, Y., Wang, J.Y., Nemzer, B., 2013. Antioxidant and Antiradical Activity of Coffee. *Antioxidants* 2, 230–45.

Yeh, J.-L., Liu, C.-P., Hsu, J.-H., Tseng, C.-J., Wu, P.-J., Wang, Y.-Y., Wu, J.-R., Chen, I.-J., 2012. KMUP-1 inhibits hypertension-induced left ventricular hypertrophy through regulation of nitric oxide synthases, ERK1/2, and calcineurin. *Kaohsiung J. Med. Sci.* 28, 567–76.

Yougbare, I., Morin, C., Senouvo, F.Y., Sirois, C., Albadine, R., Lugnier, C., Rousseau, E., 2011. NCS 613, a potent and specific PDE4 inhibitor, displays anti-inflammatory effects on human lung tissues. *Am. J. Physiol. Lung Cell. Mol. Physiol*. 301.

Zainab, S., Djafarian, K., 2016. Coffee Consumption and Coronary Heart Diseases: A Mini-Review. *J. Clin. Nutr. Diet.* 2, 1–7.

Zhang, K.Y.., Card, G.L., Suzuki, Y., Artis, D.R., Fong, D., Gillette, S., Hsieh, D., Neiman, J., West, B.L., Zhang, C., Milburn, M. V, Kim, S.-H., Schlessinger, J., Bollag, G., 2004. A Glutamine Switch Mechanism for Nucleotide Selectivity by Phosphodiesterases. *Mol. Cell* 15, 279–86.

Zhu, S., Gan, Z., Li, Z., Liu, Y., Yang, X., Deng, P., Xie, Y., Yu, M., Liao, H., Zhao, Y., Zhao, L., Liao, F., 2009. The measurement of cyclic nucleotide phosphodiesterase 4 activities via the quantification of inorganic phosphate with malachite green. *Anal. Chim. Acta* 636, 105–10.

Zoraghi, R., Francis, S.H., Corbin, J.D., 2007. Critical amino acids in phosphodiesterase-5 catalytic site that provide for high-affinity interaction with cyclic guanosine monophosphate and inhibitors. *Biochemistry* 46, 13554–63.

Zuidema, J., Merkus, F.W.H.M., 1981. Pharmacokinetics and pharmacodynamics of diprophylline. Pharm. *Weekbl. Sci. Ed.* 3, 1320–5.

PUBLICATIONS

Journal Papers

1. Nivedita Singh, Sanjukta Patra. Phosphodiesterase 9: insights from protein structure and role in therapeutics. *Life Science* 2014, 106, 1-11.

2. Nivedita Singh, Parameswaran Saravanan, M. S. Thakur, Sanjukta Patra. Development of Xanthine based inhibitors targeting Phosphodiesterase 9A. *Letters in Drug Design & Discovery* (**Accepted**).

3. Nivedita Singh, Swagata Patra, Sanjukta Patra. Identification of potent xanthine based inhibitor by Virtual screening studies and biological studies for phosphodiesterase 9A (**Communicated**).

4. Nivedita Singh, Akhtar Hussain Malik, Parameswar Krishnan Iyer, Sanjukta Patra. Novel synthetic routes for generation of xanthine derivatives: potential inhibitors for phosphodiesterase 9A (**Communicated**).

5. Nivedita Singh, M. S. Thakur, Sanjukta Patra. Xanthine scaffold: Scope and potential in drug development (**Communicated**)

Patent applied

Nivedita Singh, Akhtar Hussain Malik, P. K. Iyer, Sanjukta Patra. Xanthine as a scaffold for synthesis of novel compounds. [Temporary Patent Number- 201631028745]

Conferences

1. Nivedita Singh, Sanjukta Patra. BioSangam 2013 - International Conference on Health, Environment & Industrial Biotechnology, MNNIT Allahabad (**Poster Presentation**).

2. Nivedita Singh, Swagata Patra, Sanjukta Patra. Virtual screening of existing xanthine derivatives from ZINC database with phosphodiesterase 9A. 5th Annual International Conference on Advances in Biotechnology-2015- IIT Kanpur (**Poster Presentation**).

Appendix-I

^{1}H and ^{13}C NMR Spectra Data

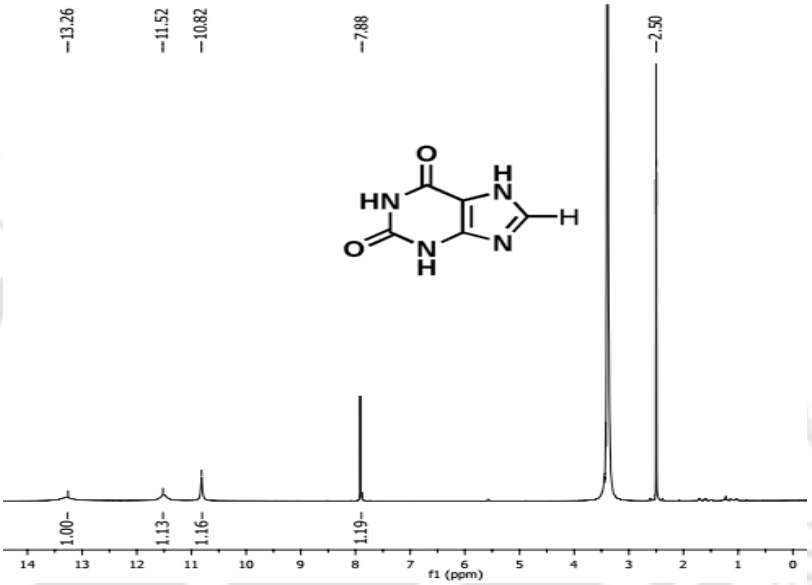

Figure A1.1 ^{1}H NMR spectra of Xanthine

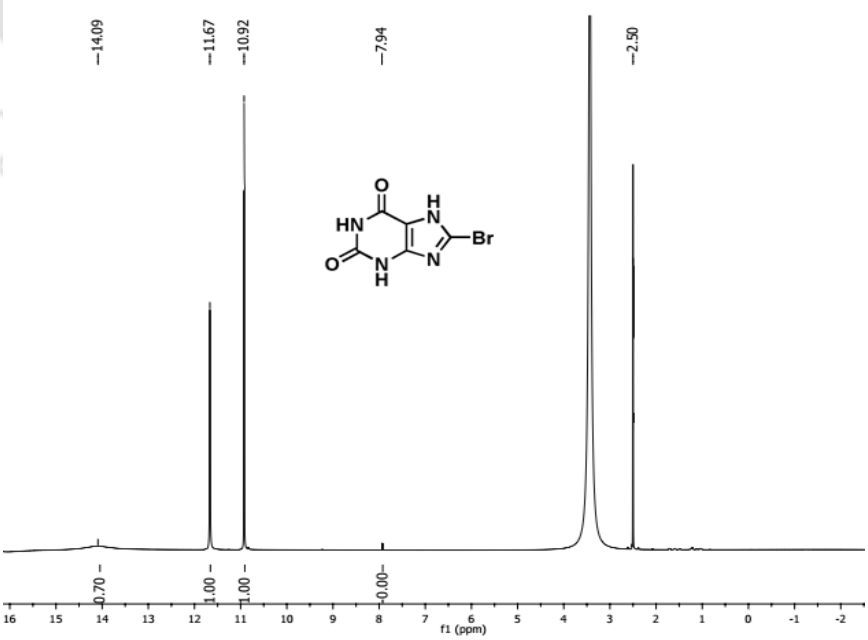

Figure A1.2 ^{1}H NMR (DMSO-d6, 600 MHz) spectra of Compound 1

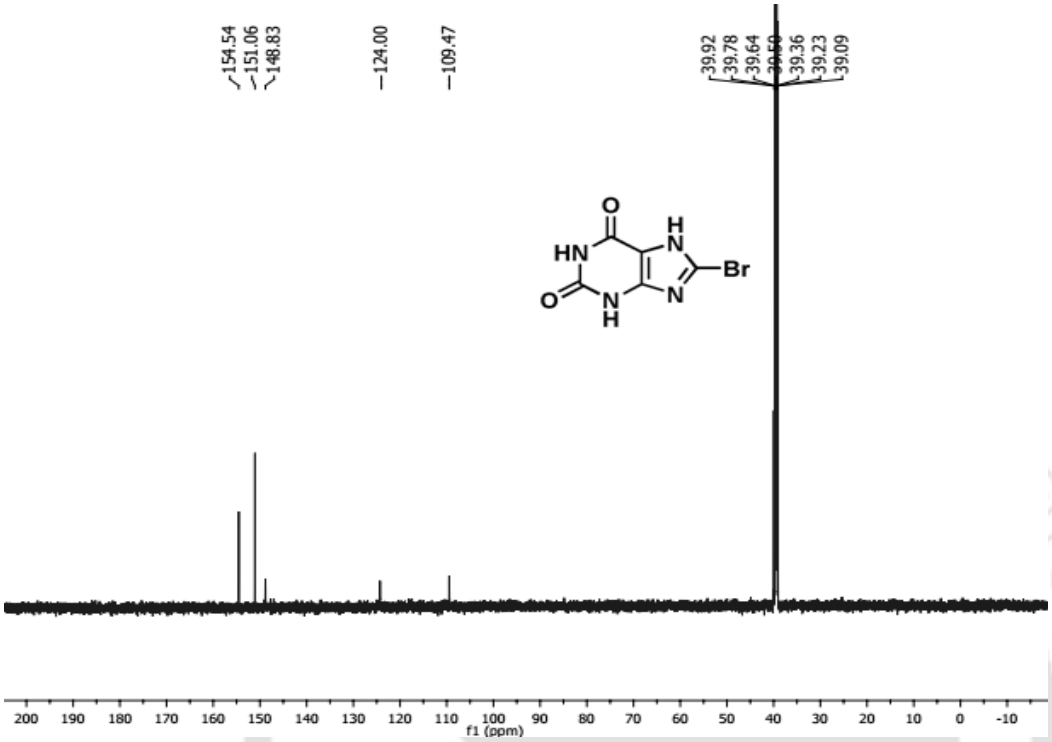

Figure A1.3 ^{13}C NMR (DMSO-d6, 150 MHz) spectra of Compound 1

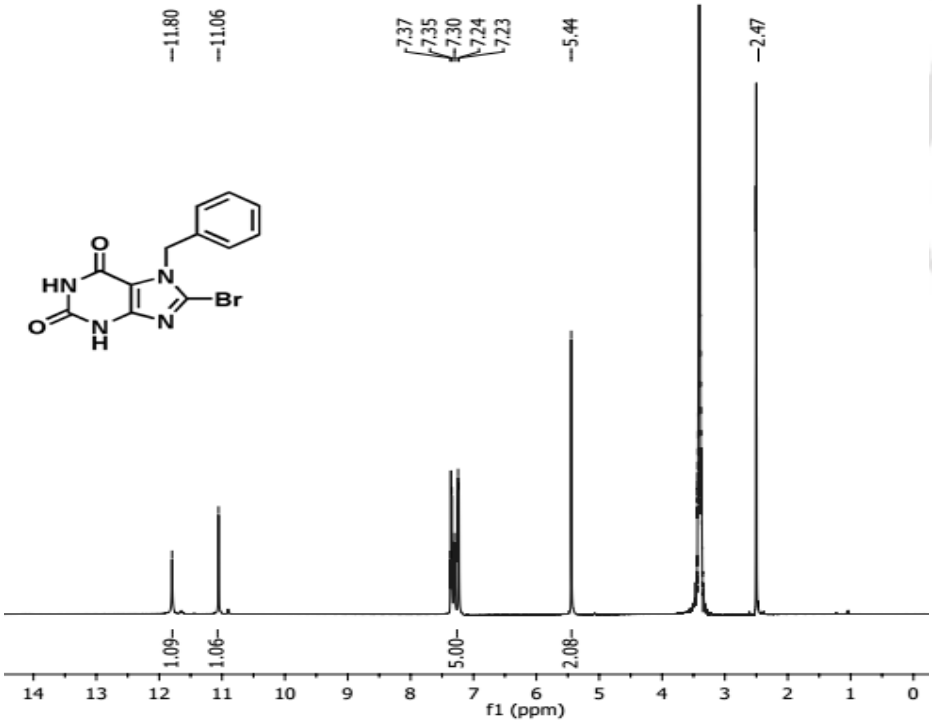

Figure A1.4 ^{1}H NMR (in DMSO-d6, 600 MHz) spectra of compound 2

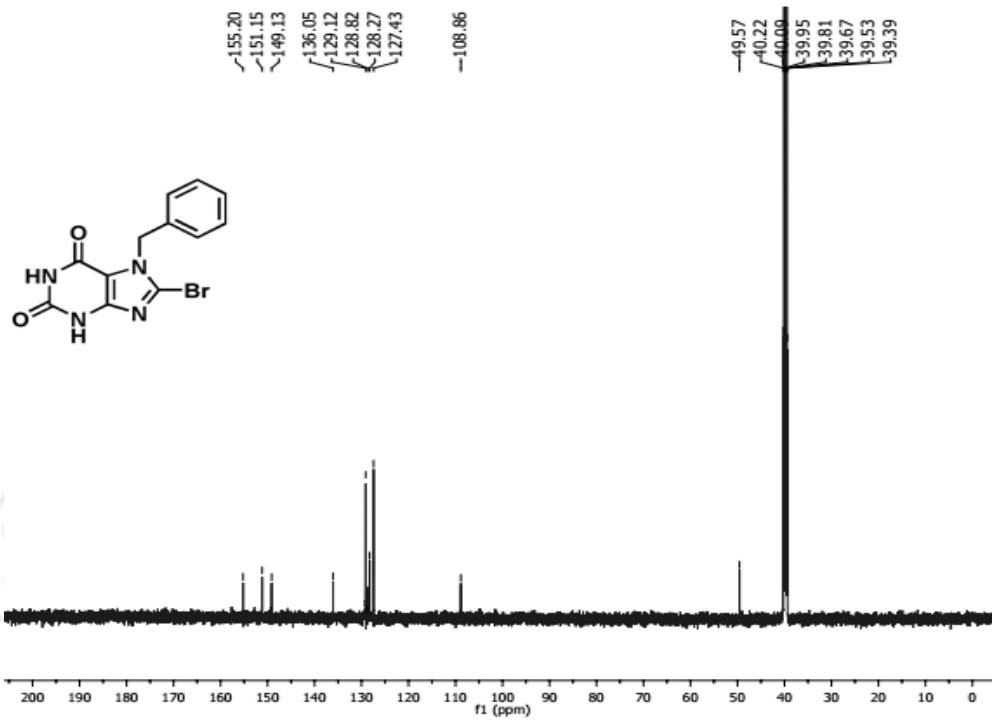

Figure A1.5 ^{13}C NMR (in DMSO-d6, 150 MHz) spectra of compound 2

Scheme-I Step-3a: Alkylation reaction at N_3 position of xanthine derivatives

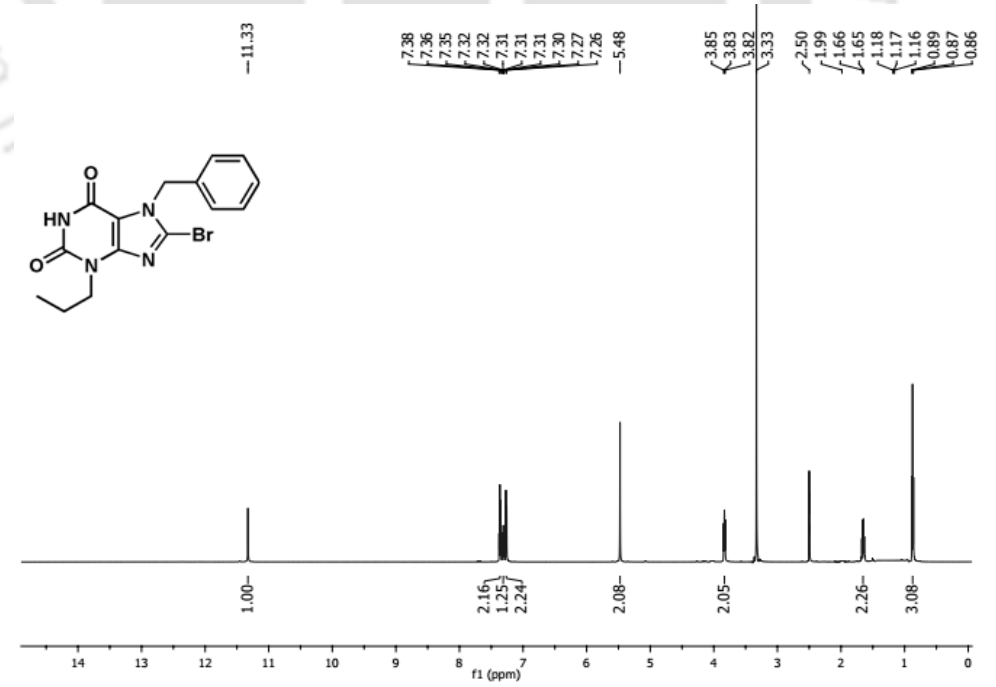

Figure A1.6 ^{1}H NMR spectra of compound 3a1

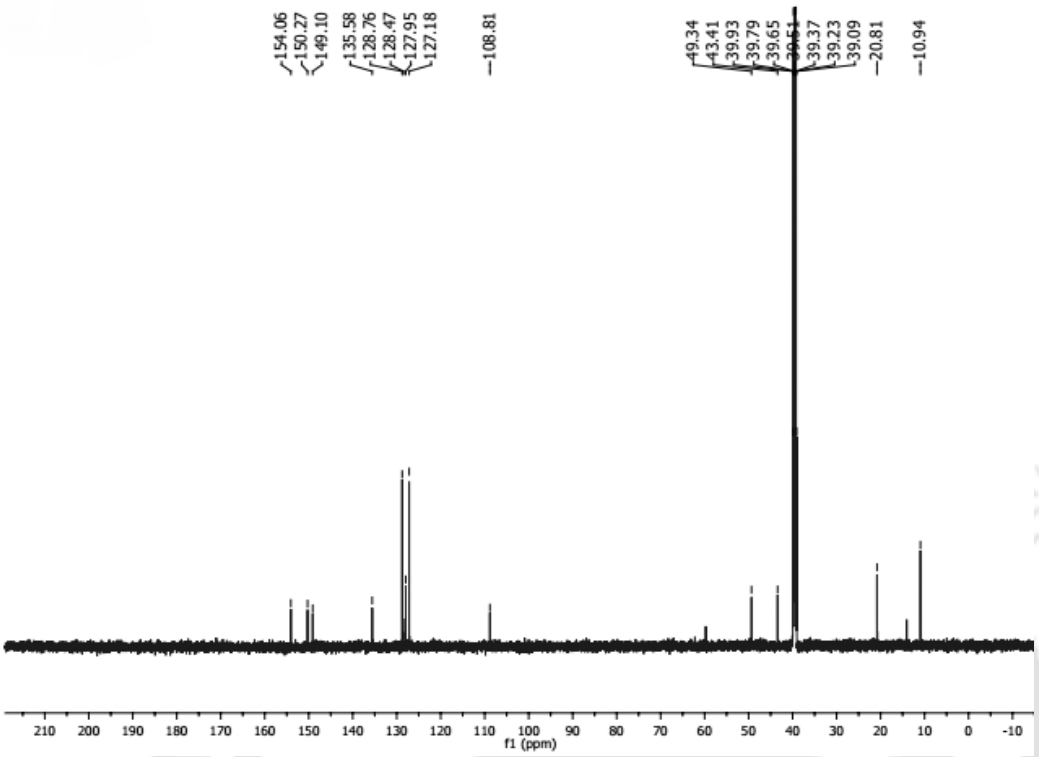

Figure A1.7 ^{13}C NMR (DMSO-d6, 150 MHz) spectra of compound 3a1

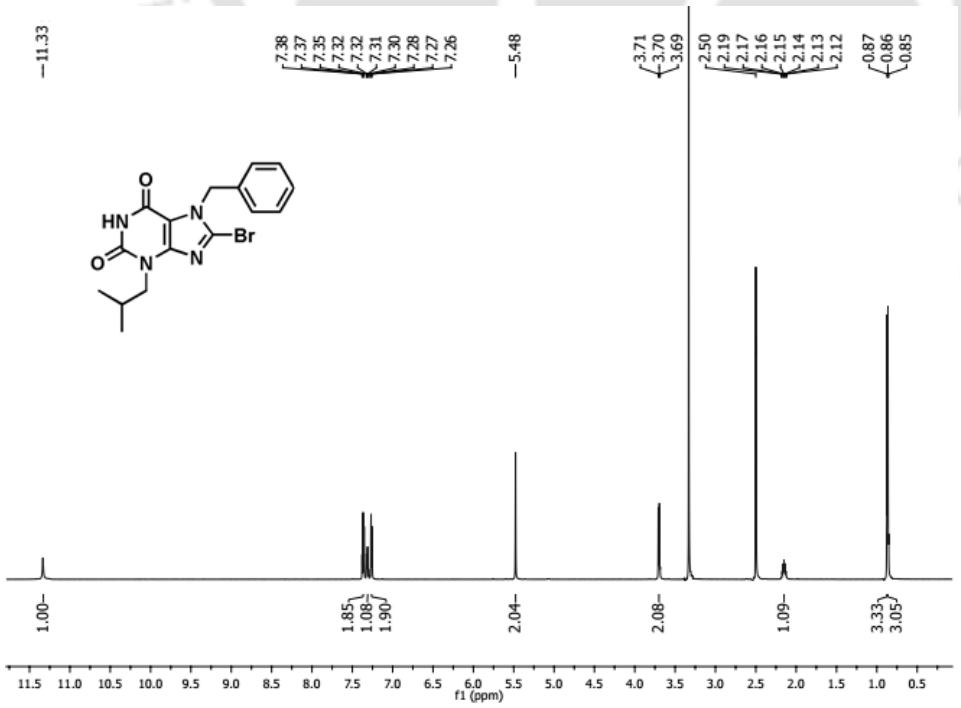

Figure A1.8 ^{1}H NMR (DMSO-d6) spectra of compound 3a2

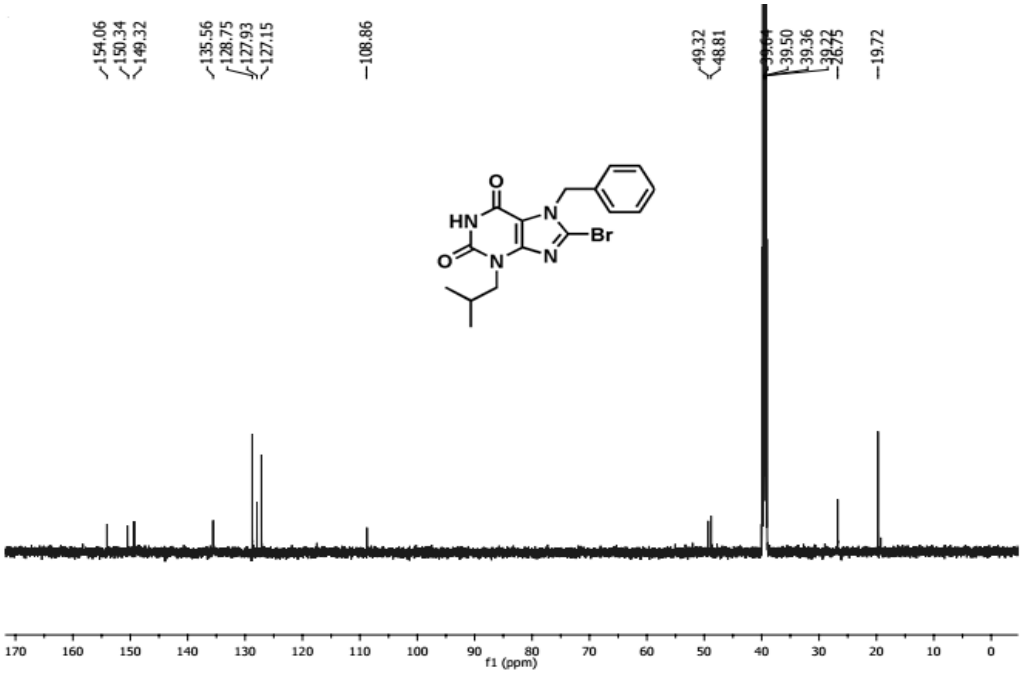

Figure-S1.9 ^{13}C NMR (DMSO-d6, 150 MHz) spectra of compound 3a2

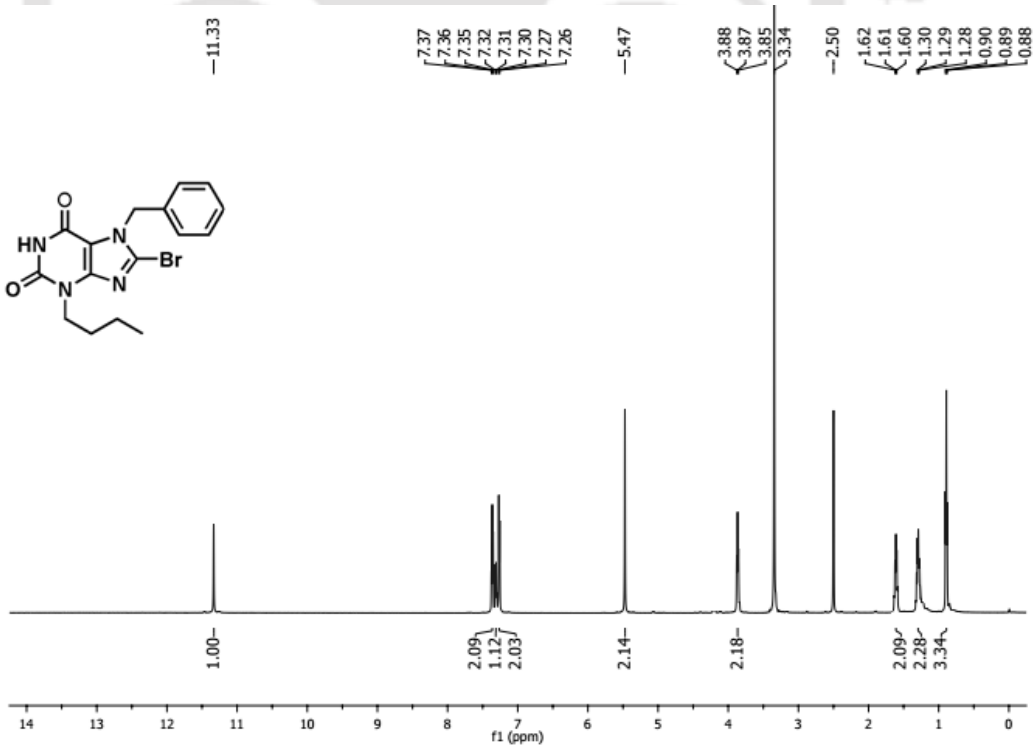

Figure A1.10 ^{1}H NMR (DMSO-d6) spectra of compound 3a3

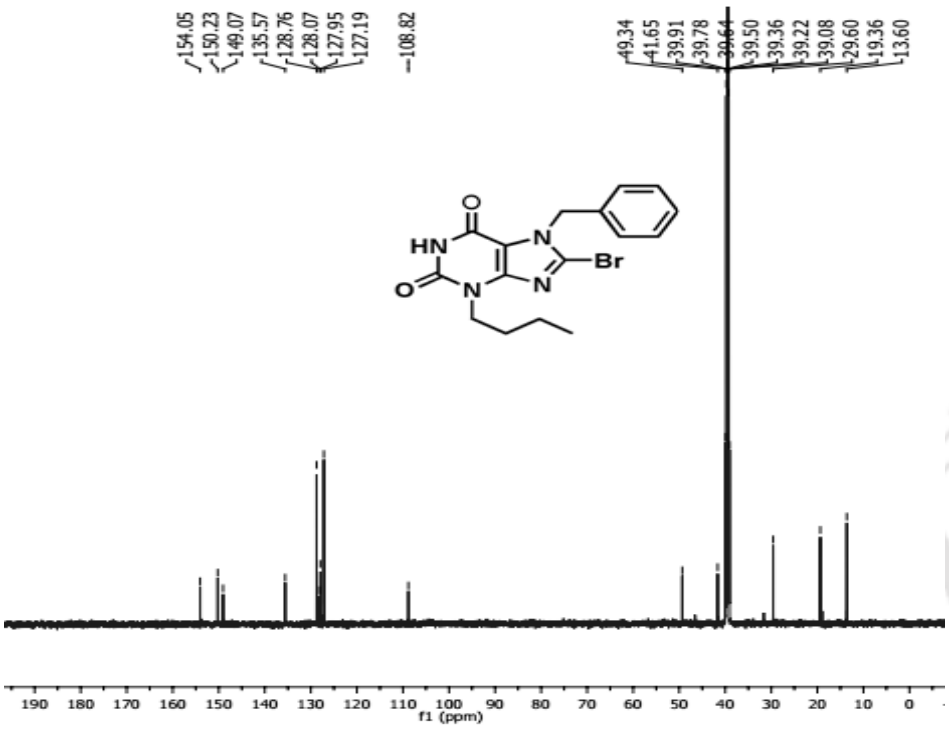

Figure A1.11 ^{13}C NMR (DMSO-d6, 150 MHz) spectra of compound 3a3

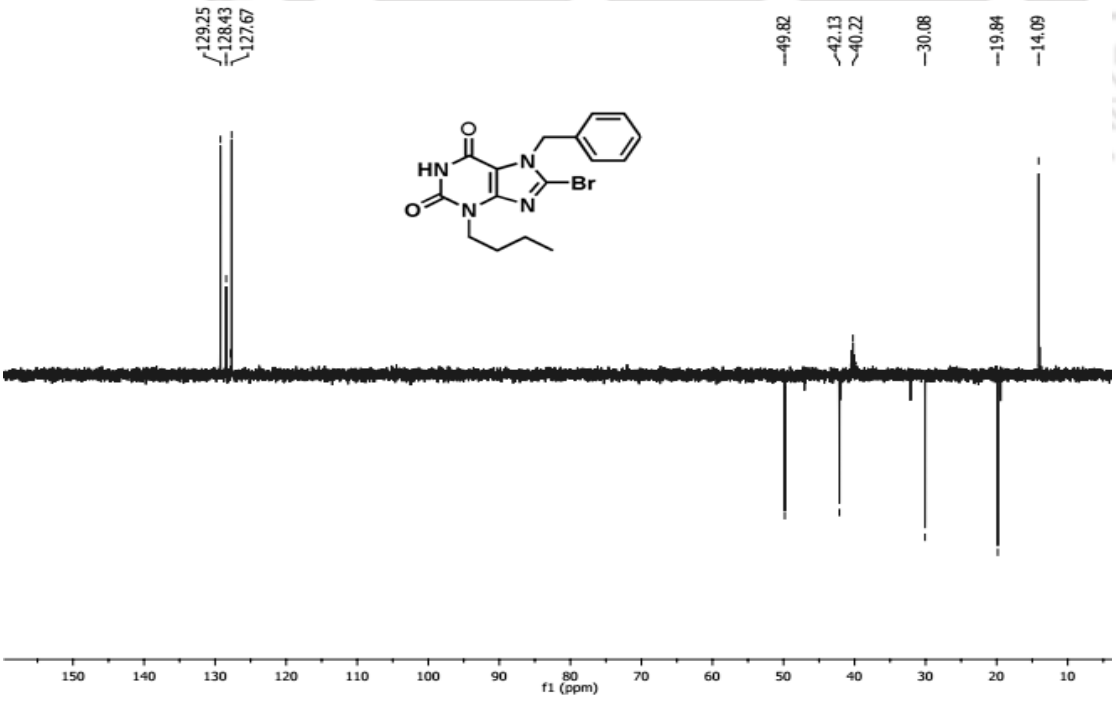

Figure A1.12: ^{135}DEPT NMR (DMSO-d6) spectra of compound 3a3

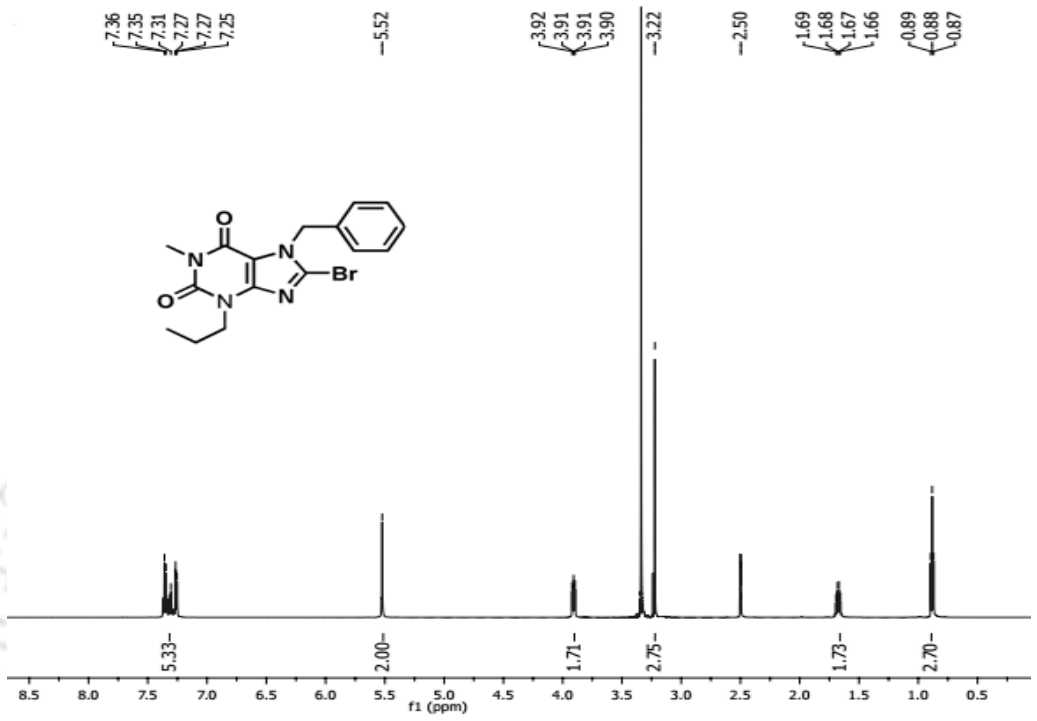

Figure A1.13 ^{1}H NMR (DMSO-d6, 600 MHz) spectra compound 4a1

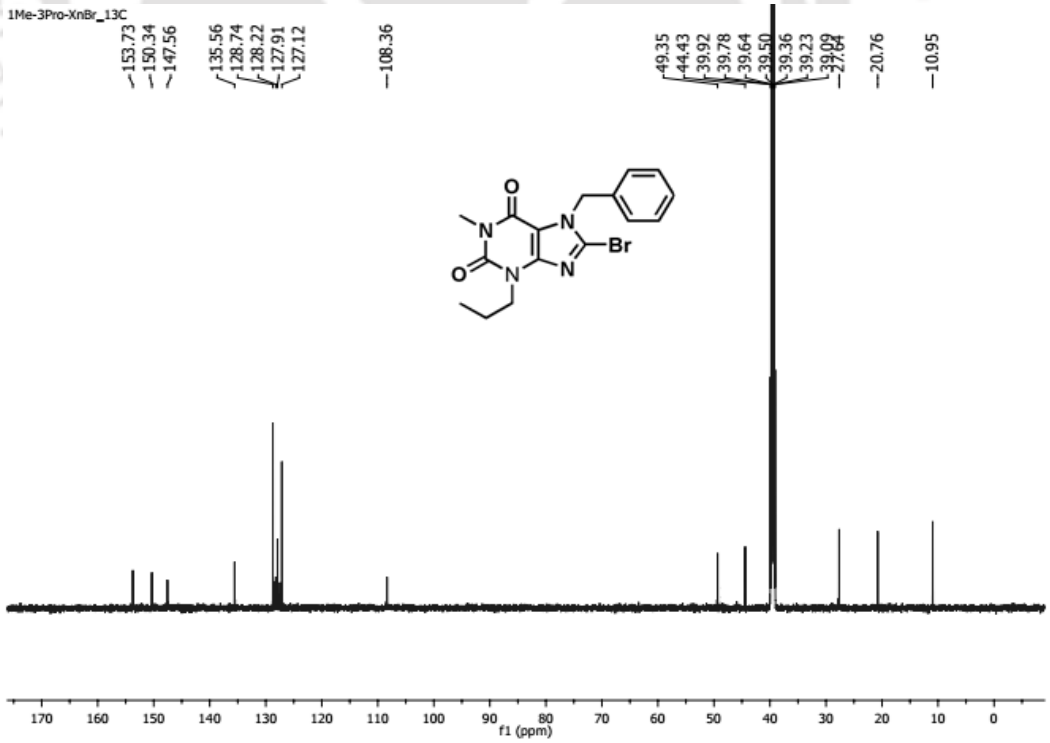

Figure A1.14 ^{13}C NMR (DMSO-d6, 150 MHz) spectra of compound 4a1

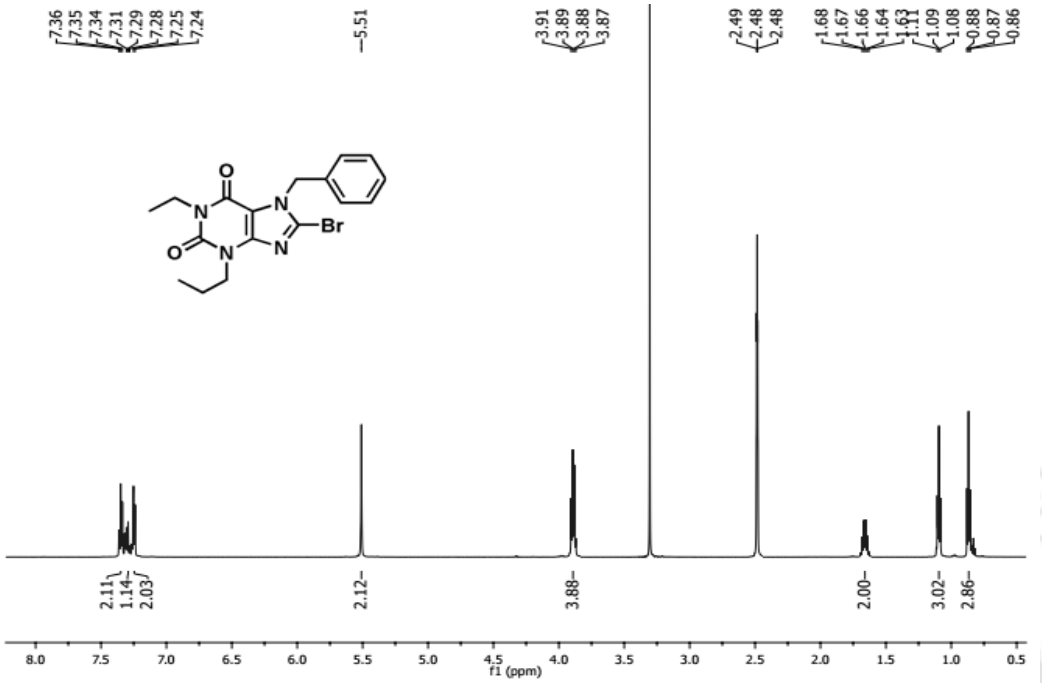

Figure A1.15 ^{1}H NMR (DMSO-d6, 600 MHz) spectra of compound 4a2

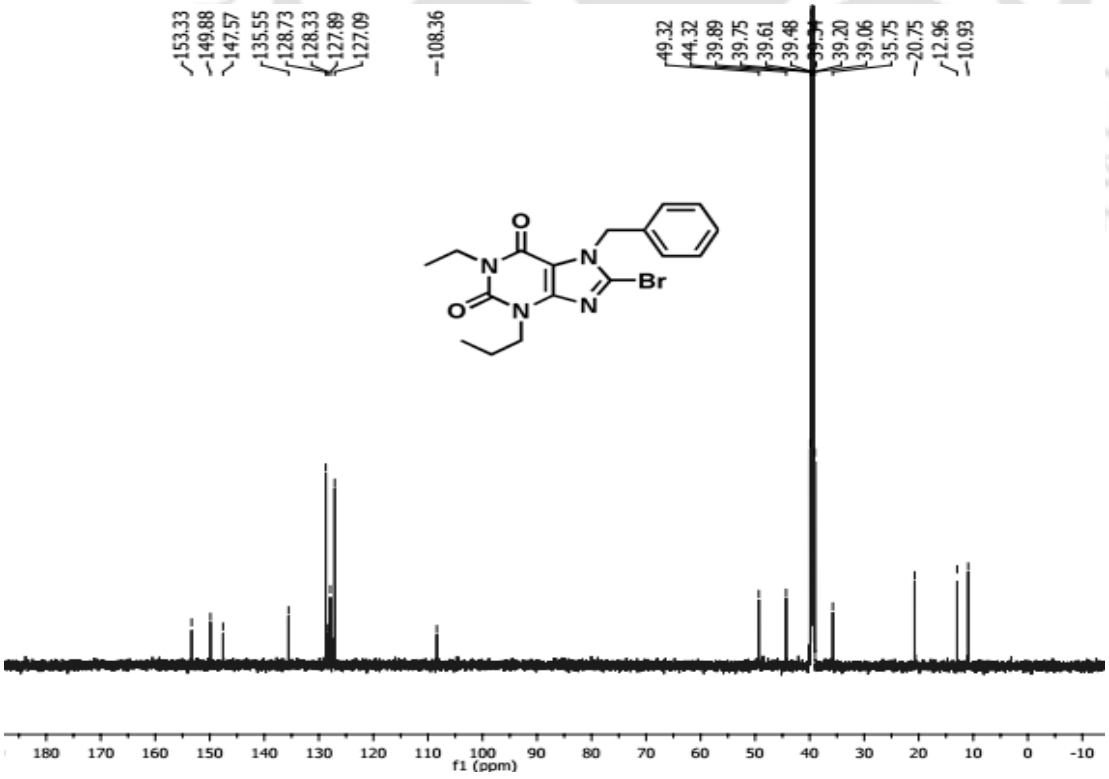

Figure A1.16 ^{13}C NMR (DMSO-d6, 150 MHz) spectra of compound 4a2

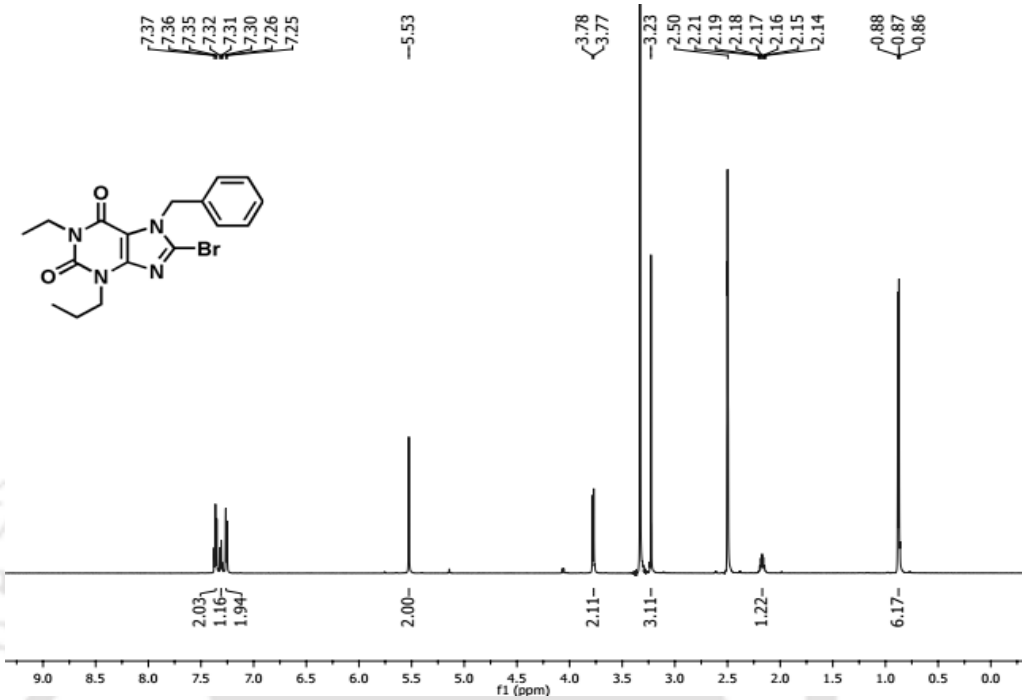

Figure A1.17 ^{1}H NMR (DMSO-d6) spectra of compound 4a3

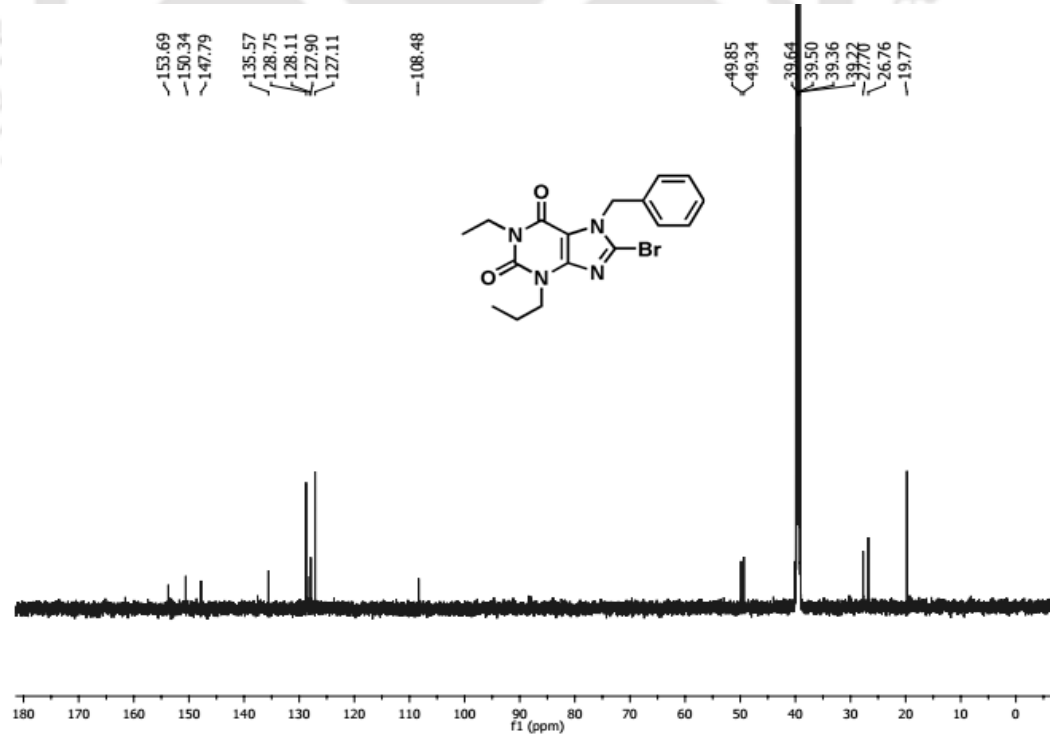

Figure A1.18 ^{13}C NMR (DMSO-d6, 150 MHz) spectra of compound 4a3

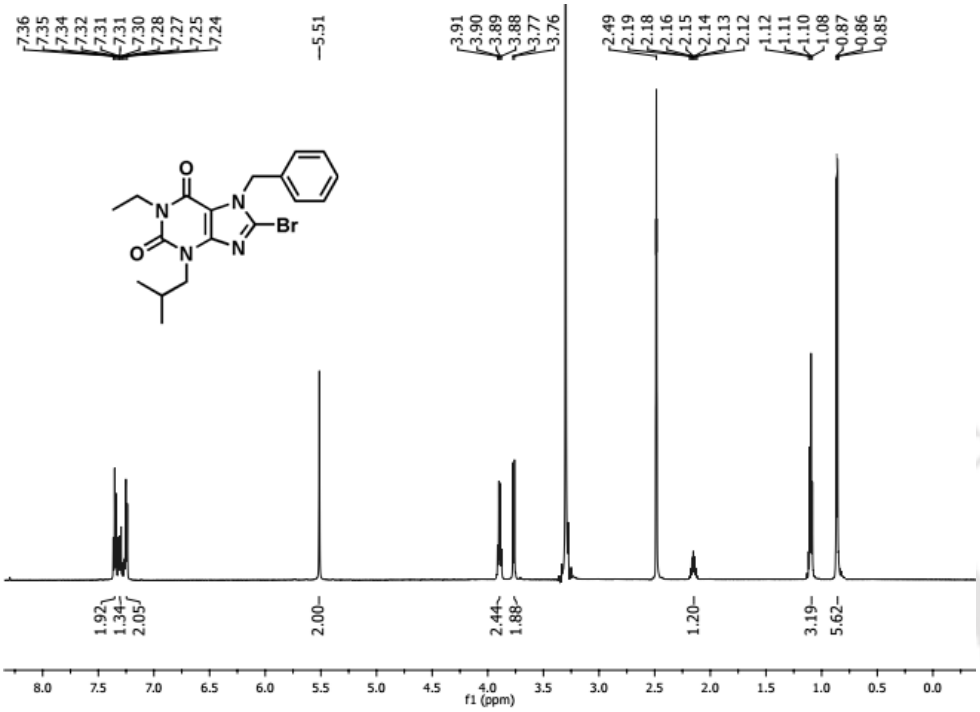

Figure A1.19 ^{1}H NMR (DMSO-d6, 600 MHz) spectra of compound 4a4

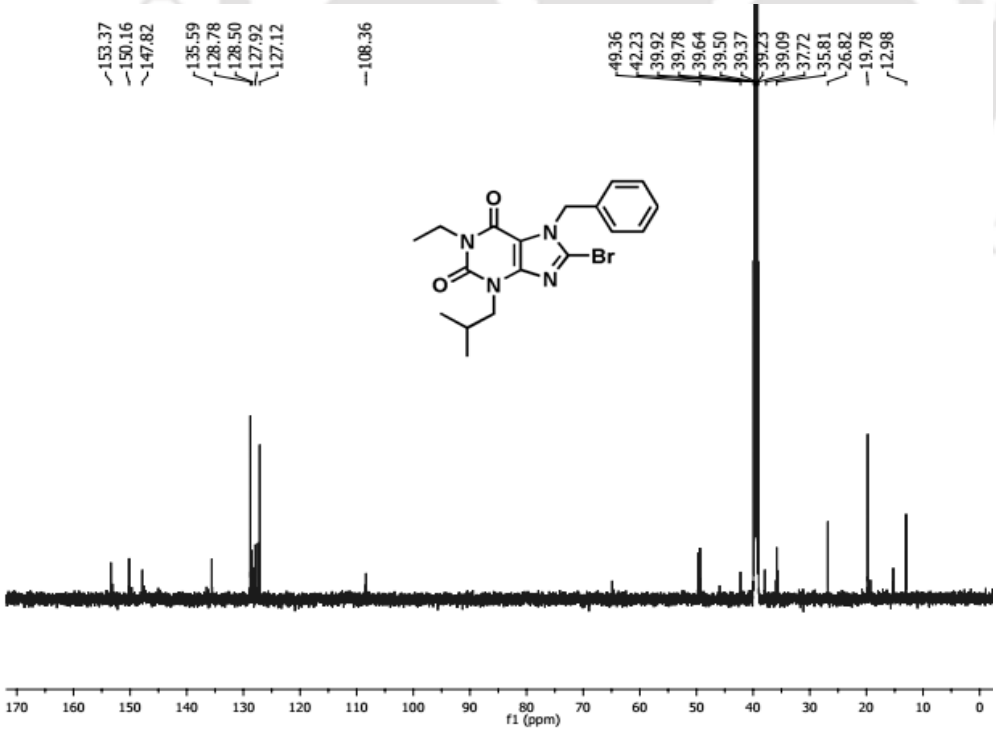

Figure A1.20 ^{13}C NMR (DMSO-d6, 150 MHz) spectra of compound 4a4

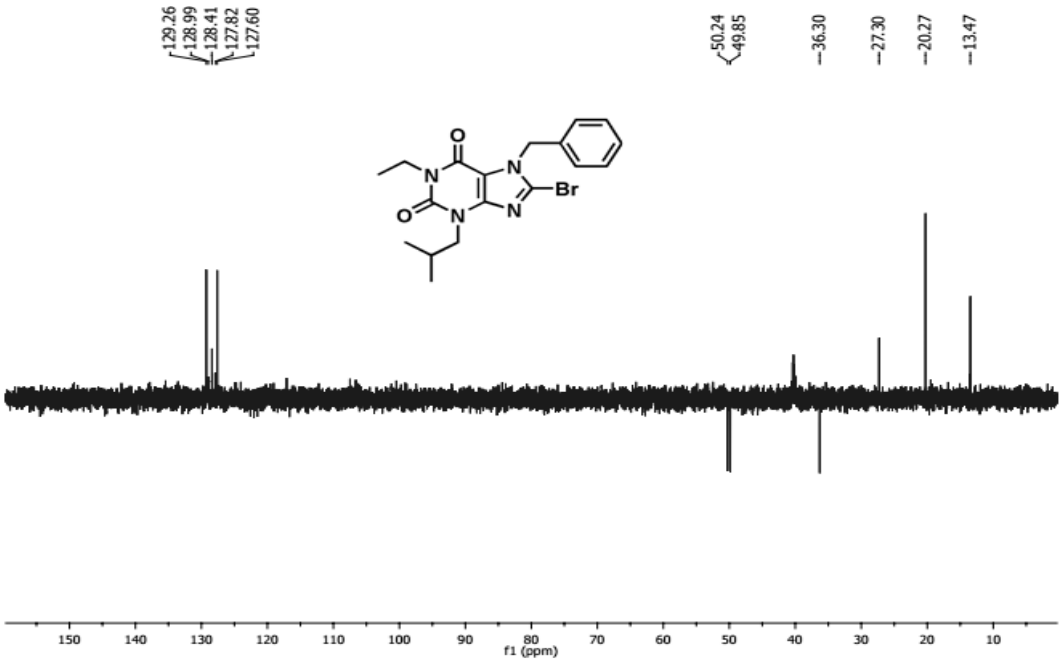

Figure A1.21 [135]DEPT NMR (DMSO-d6, 150 MHz) spectra of compound4a4

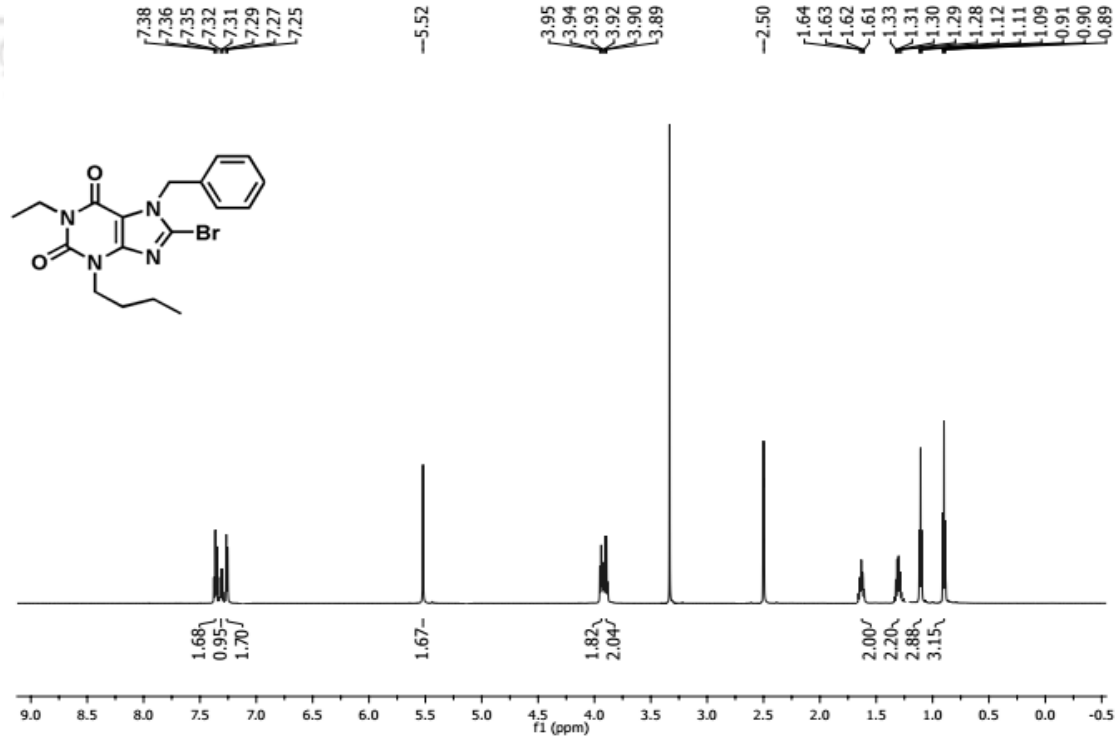

Figure A1.22 [1]H NMR (DMSO-d6, 600 MHz) spectra of compound 4a5

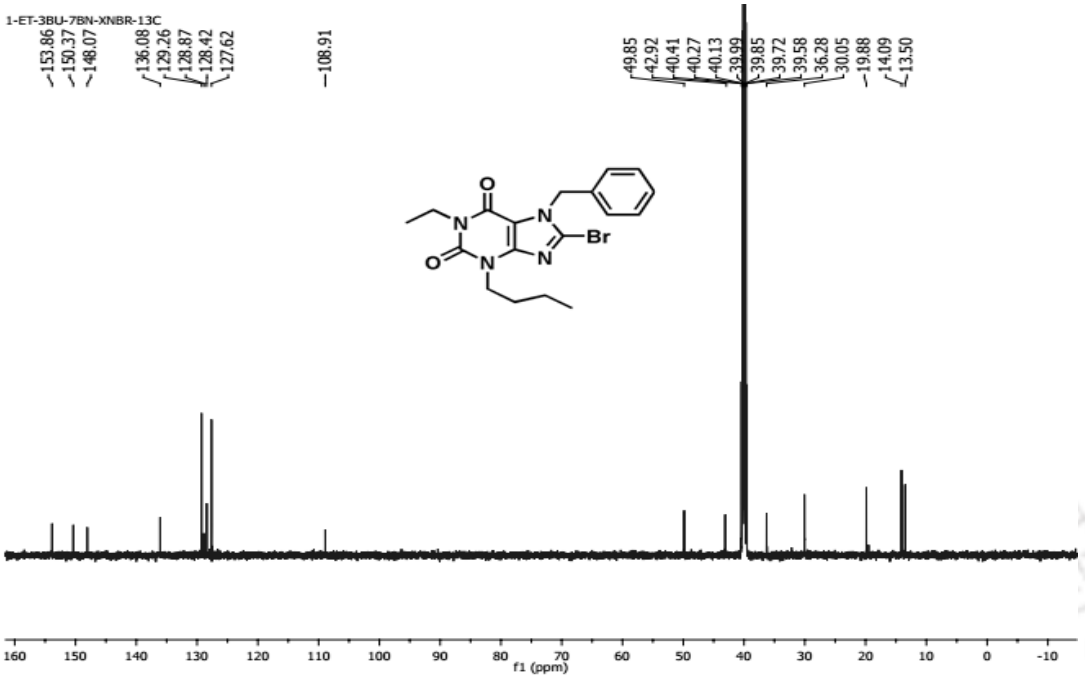

Figure A1.23 ^{13}C NMR (DMSO-d6, 150 MHz) spectra of compound 4a5

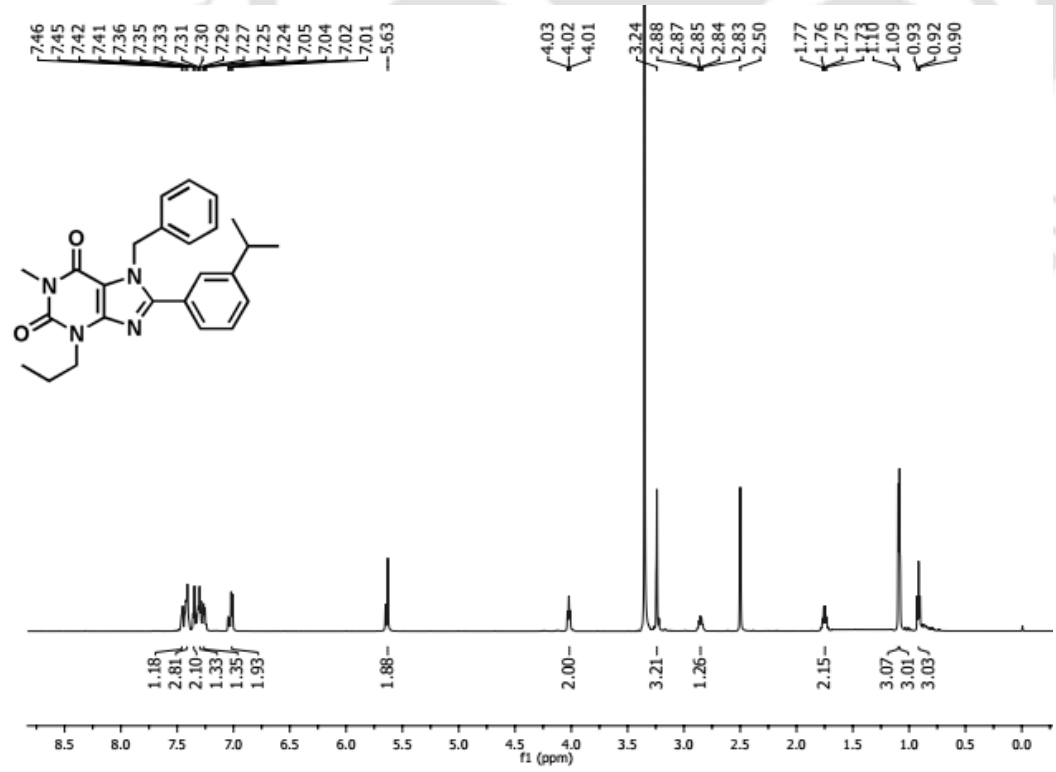

Figure A1.24 ^{1}H NMR (DMSO-d6) spectra of compound 5a1

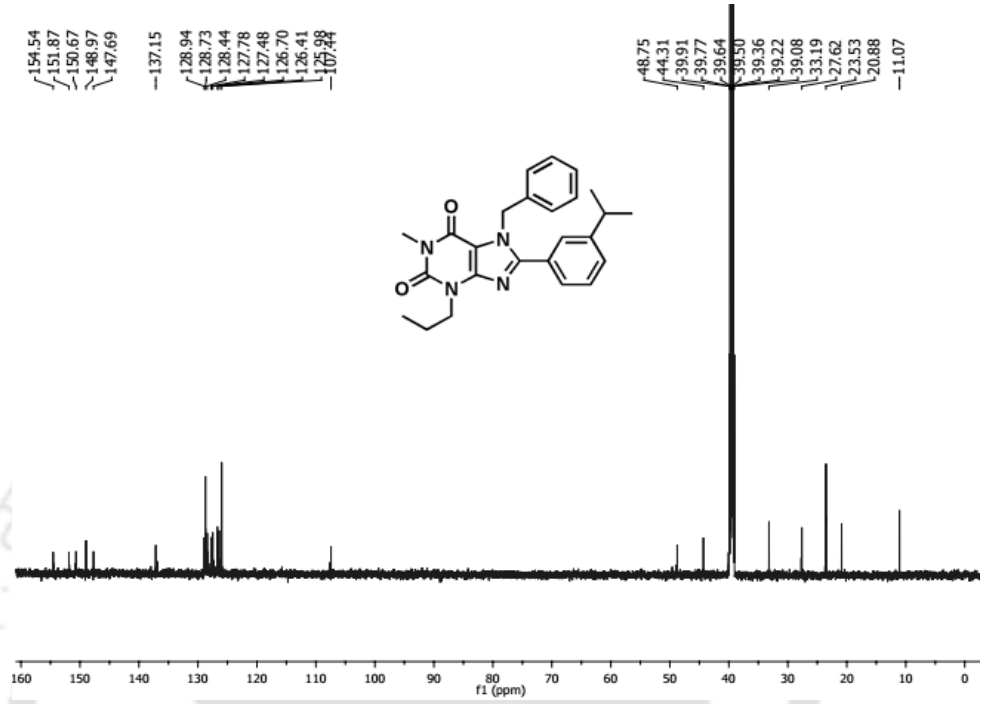

Figure A1.25 ^{13}C NMR (DMSO-d6, 150 MHz) spectra of 5a1

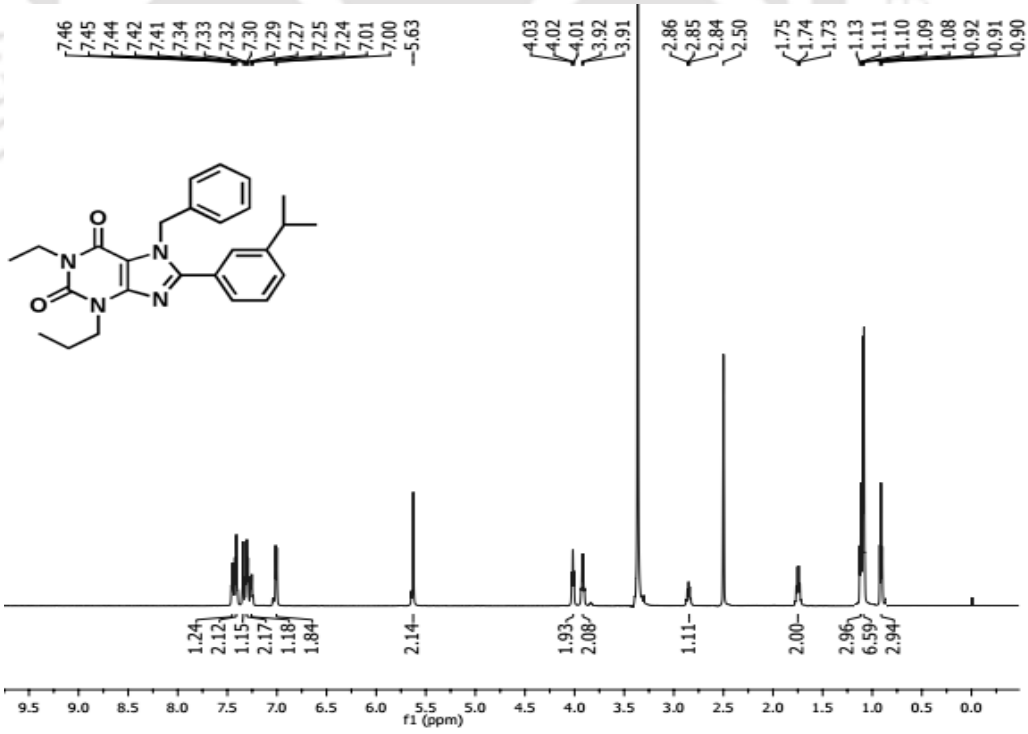

Figure A1.26 ^{1}H NMR (DMSO-d6) of compound 5a2

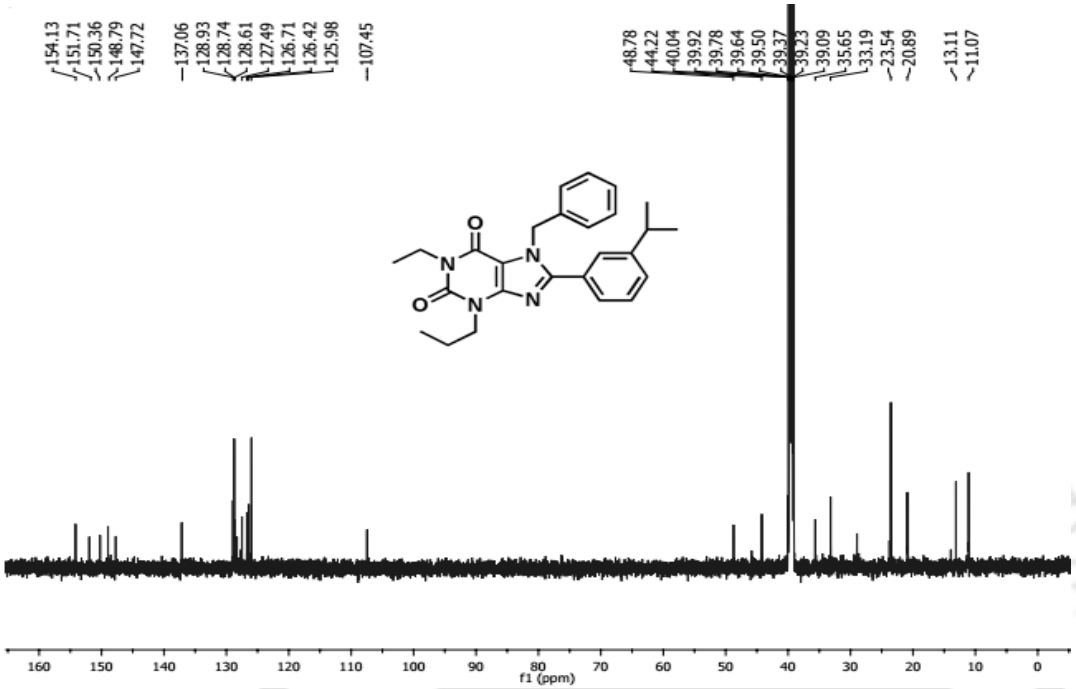

Figure A1.27 ^{13}C NMR (DMSO-d6, 150 MHz) of compound 5a2

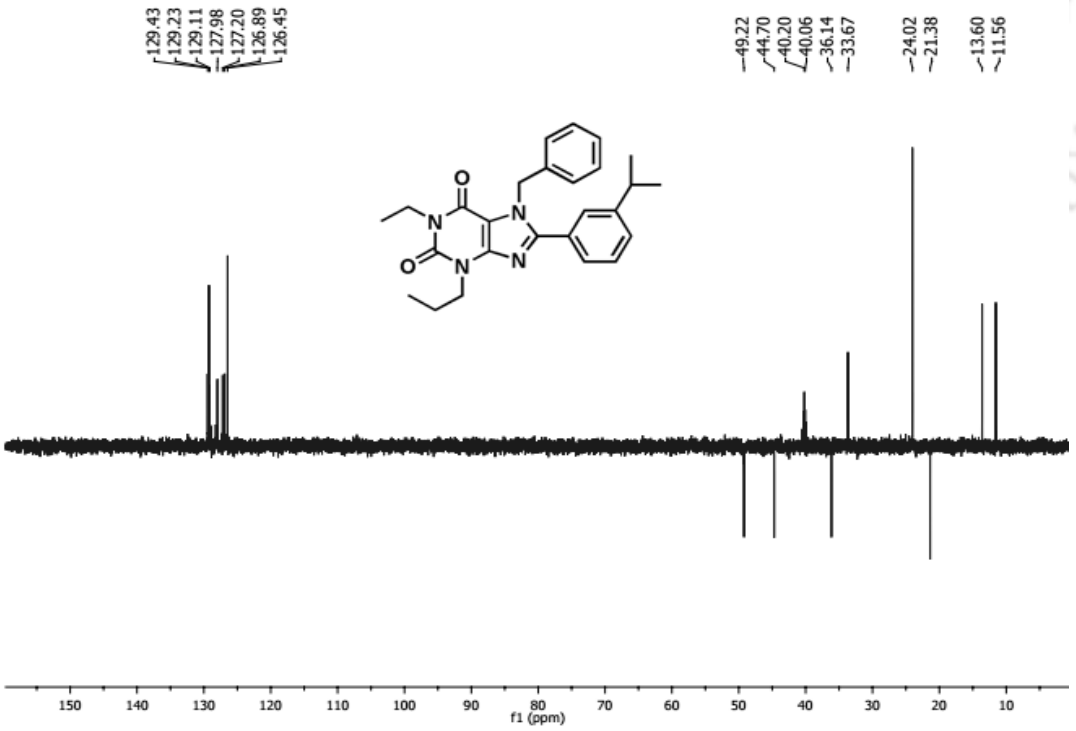

Figure A1.28 600 MHz ^{135}DEPT NMR (DMSO-d6) of compound 5a2

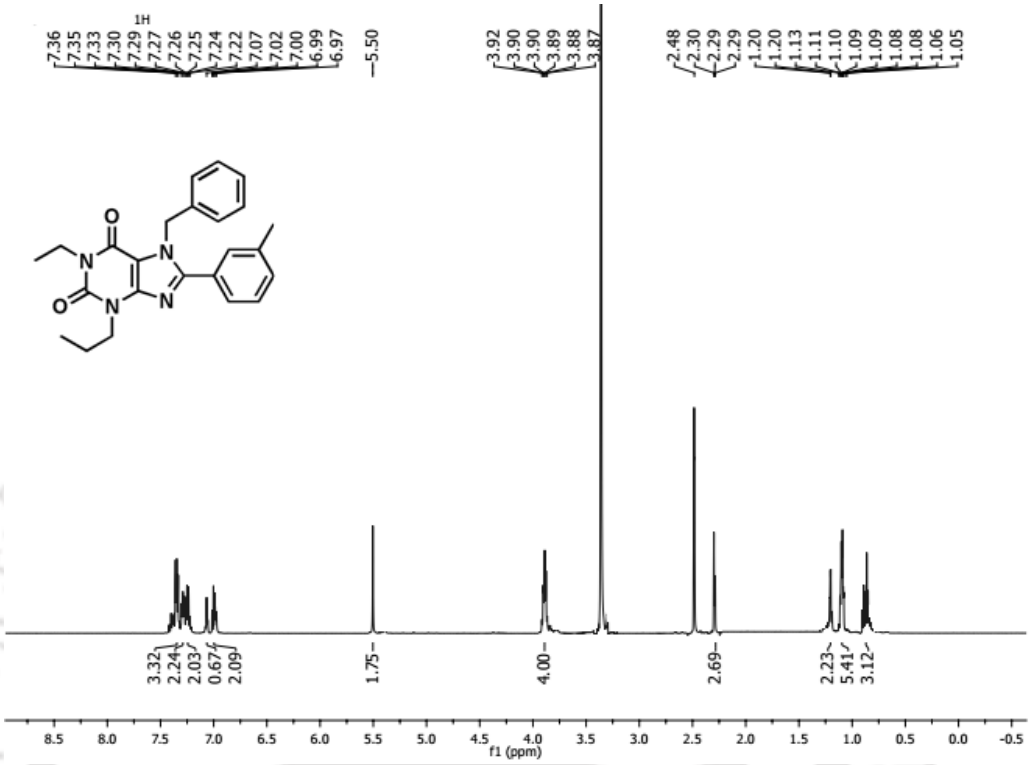

Figure A1.29 600 MHz ^{1}H NMR (in DMSO-d6) spectra of compound 5a3

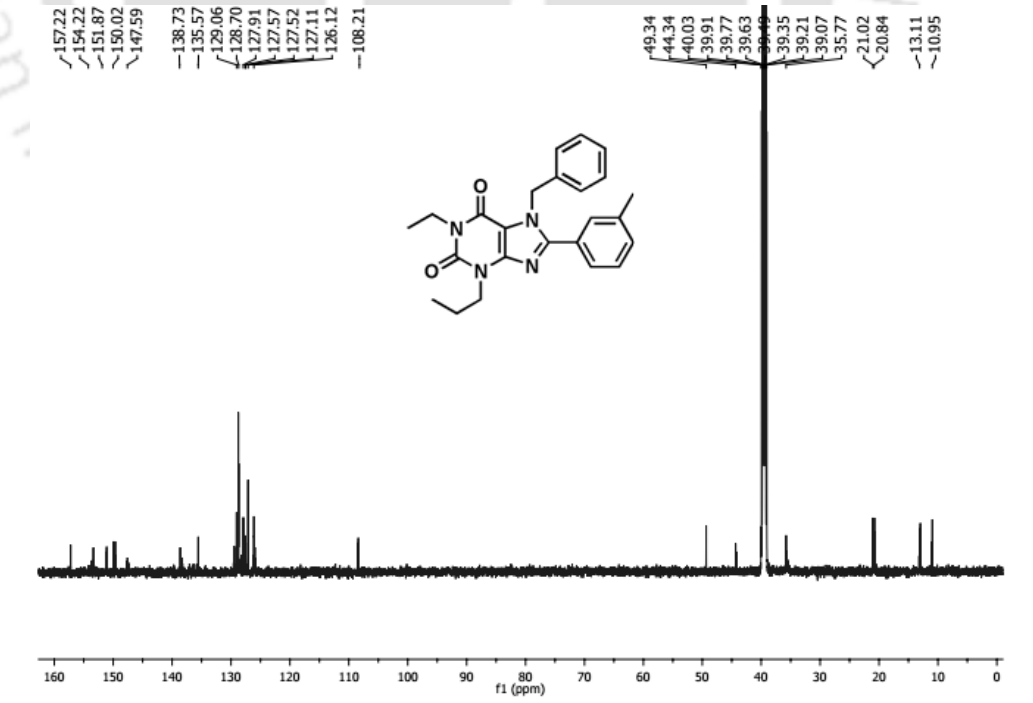

Figure A1.30 ^{13}C NMR (in DMSO-d6, 150 MHz) spectra of compound 5a3

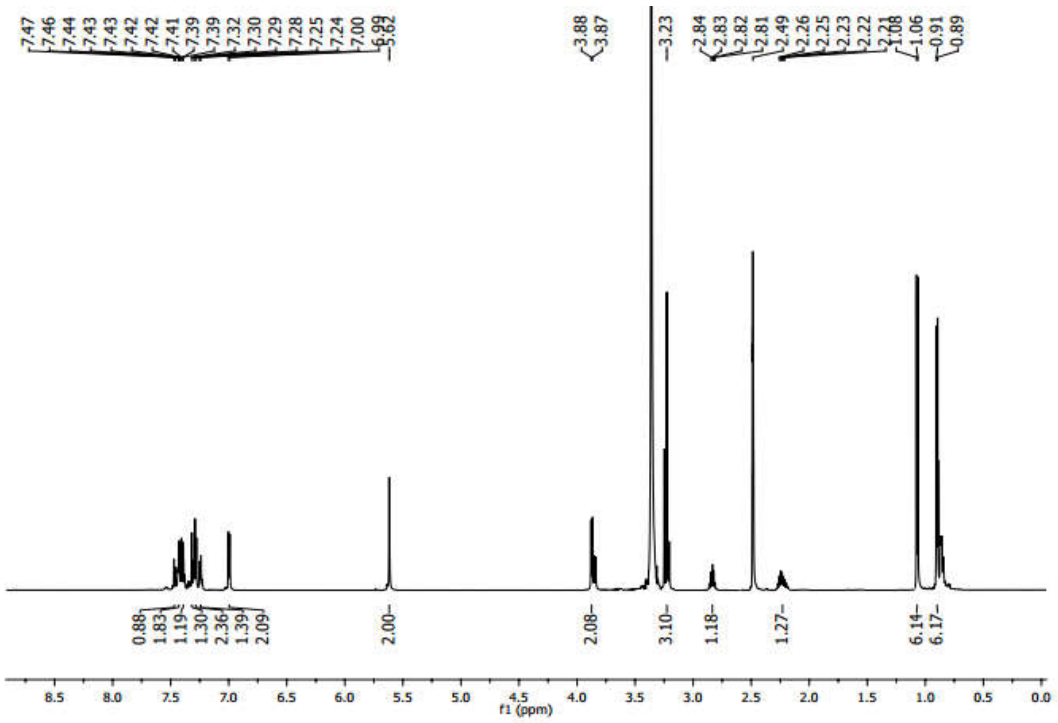

Figure A1.31 ^{1}H NMR (DMSO-d6, 600 MHz) spectra of Compound 5a4

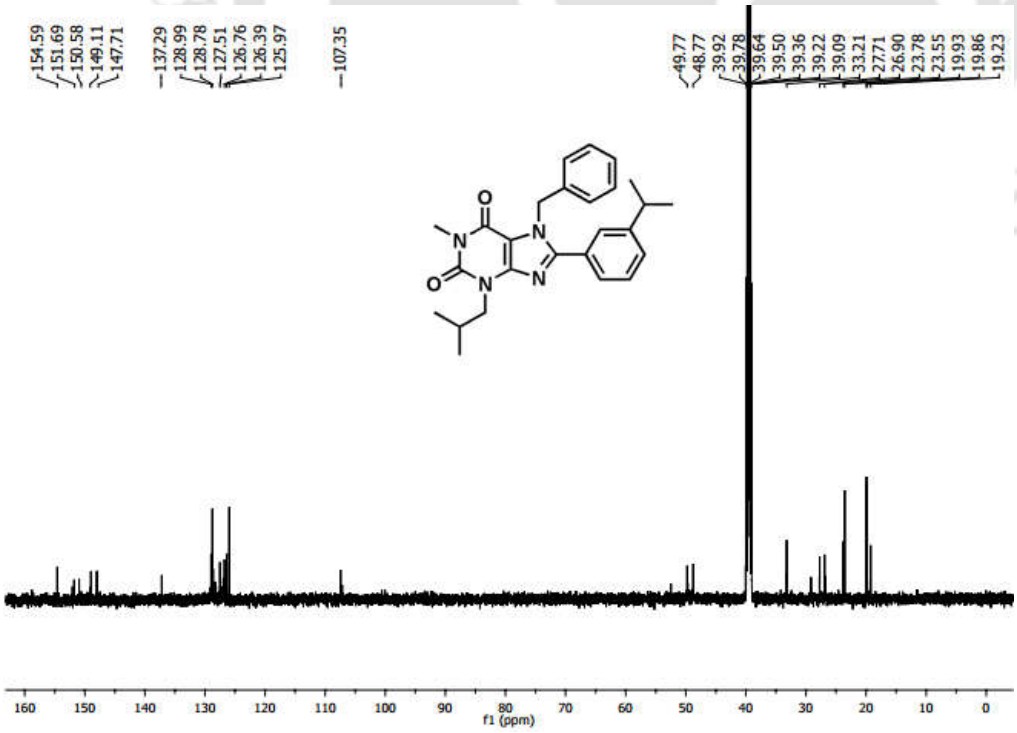

Figure A1.32 ^{13}C NMR (DMSO-d6, 150 MHz) spectra of compound 5a4

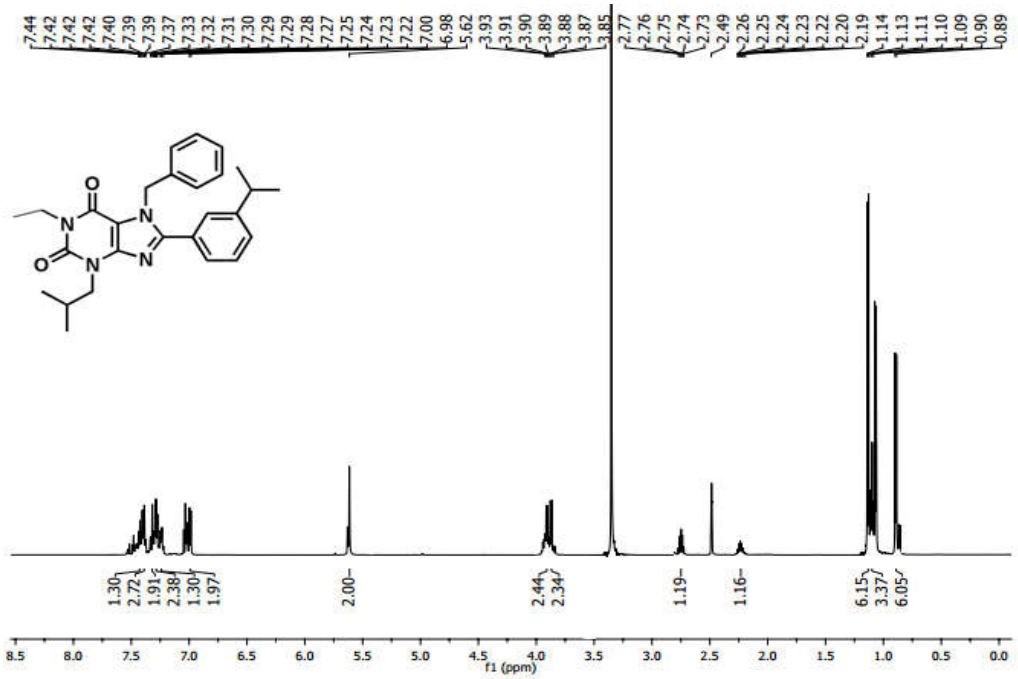

Figure A1.33 ^{1}H NMR (DMSO-d6, 600 MHz) spectra of compound 5a5

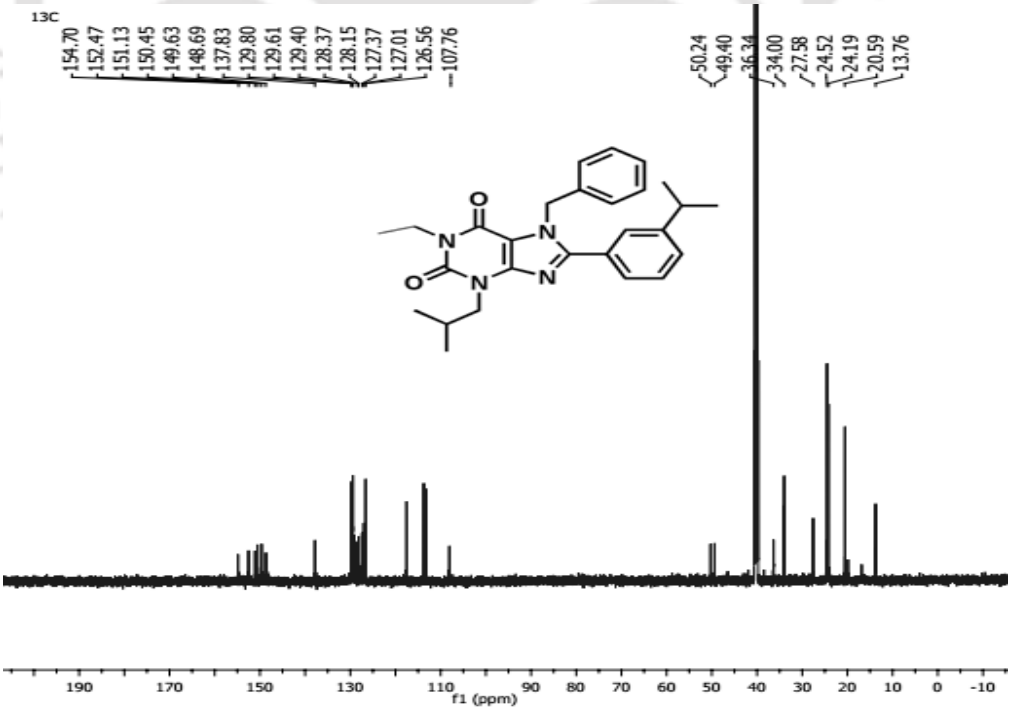

Figure A1.34 ^{13}C NMR (DMSO-d6, 150 MHz) of compound 5a5

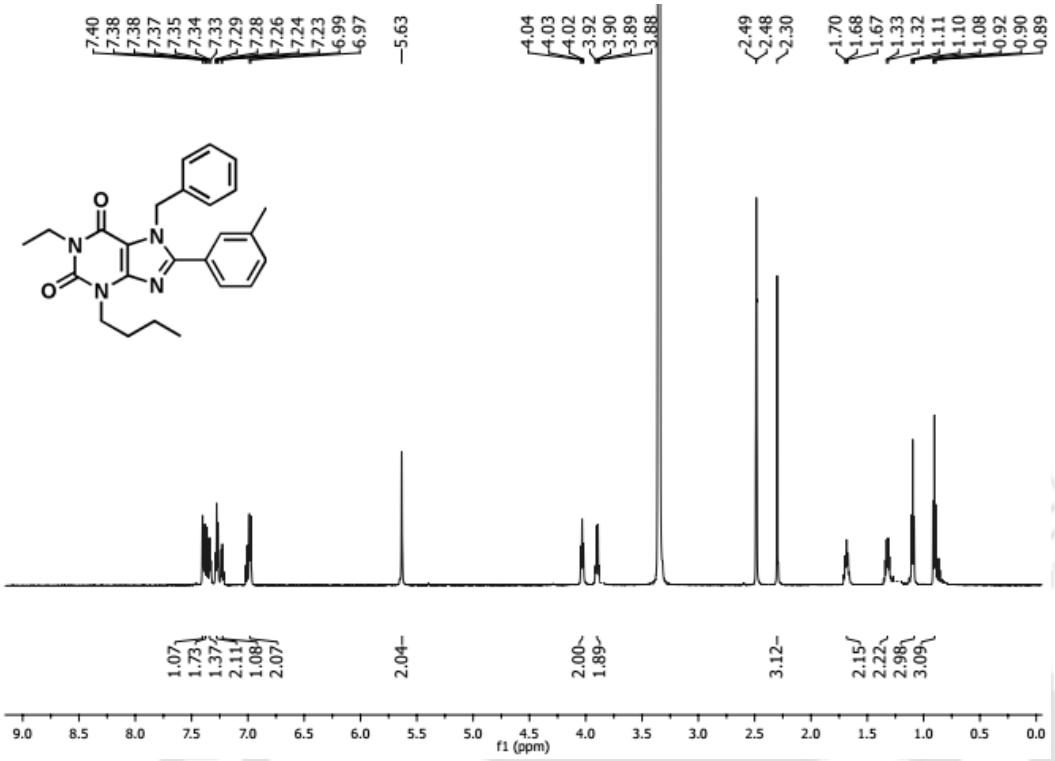

Figure A1.35 ^{1}H NMR (DMSO-d6; 600 MHz) spectra of compound 5a6

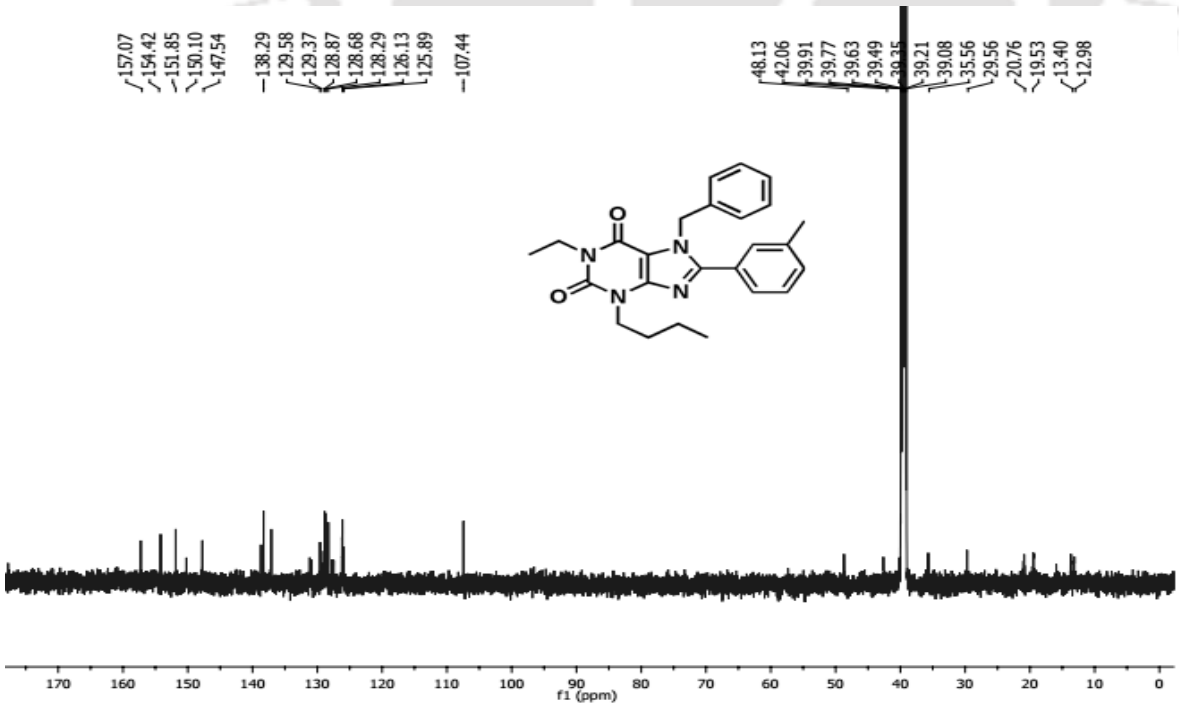

Figure A1.36 ^{13}C NMR (DMSO-d6; 150 MHz) spectra of compound 5a6

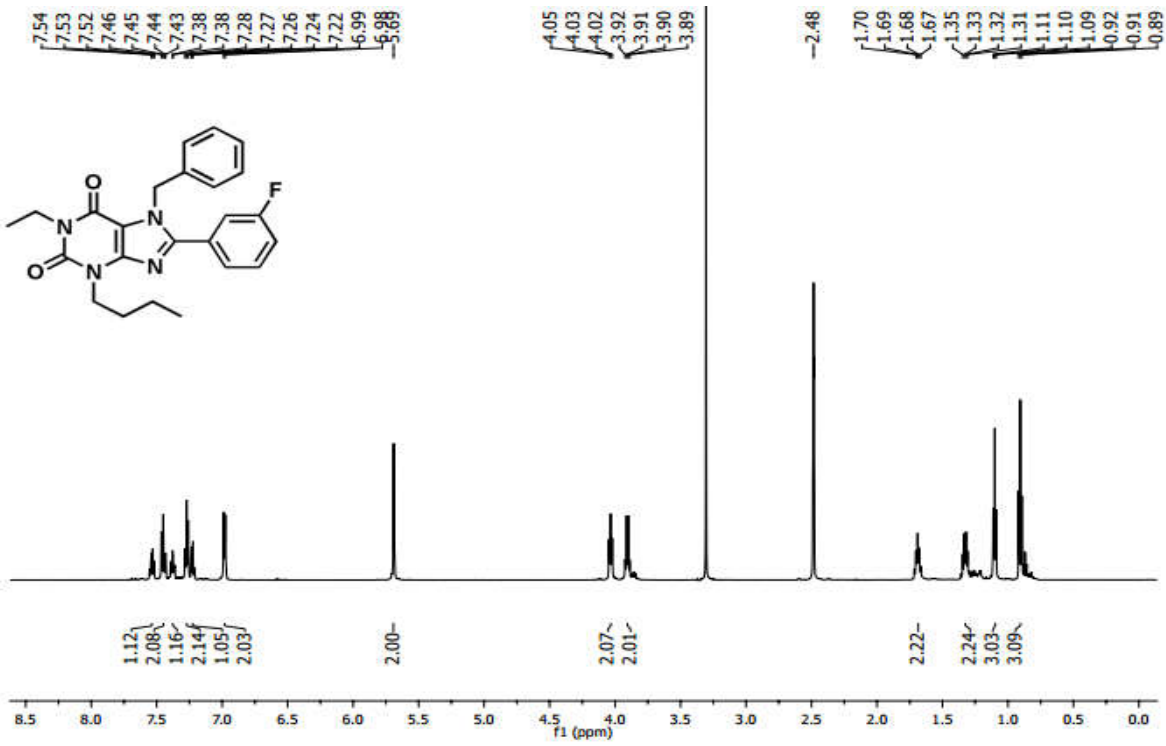

Figure A1.37 ^{1}H NMR (DMSO-d6; 600 MHz) spectra of compound 5a7

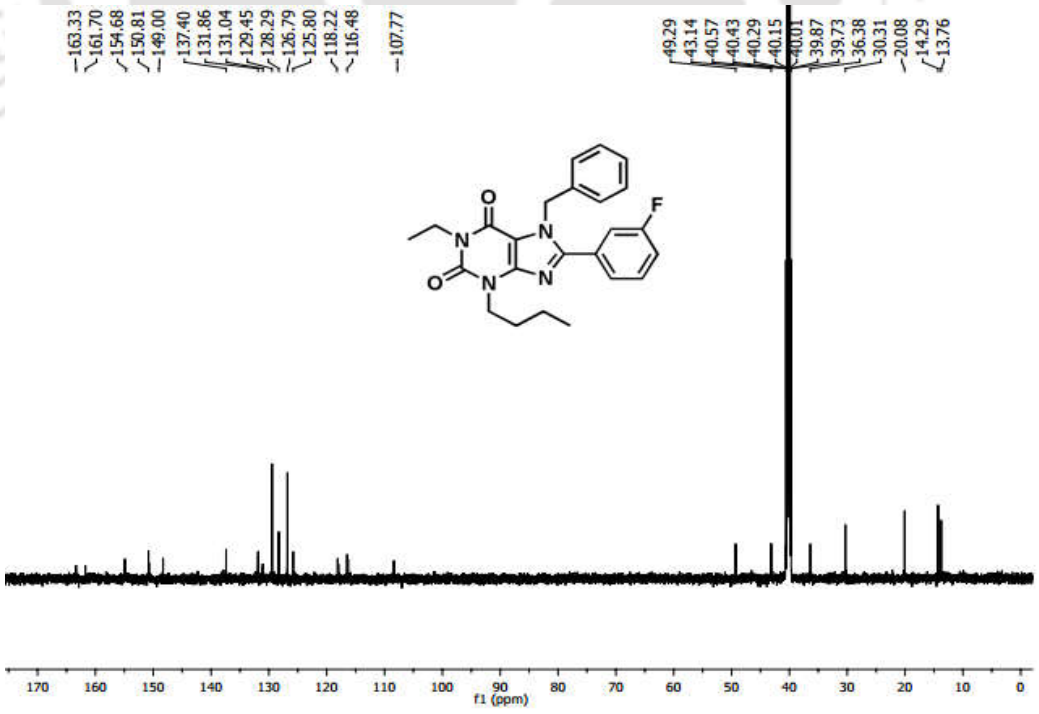

Figure A1.38 ^{13}C NMR (DMSO-d6; 150 MHz) spectra of 5a7

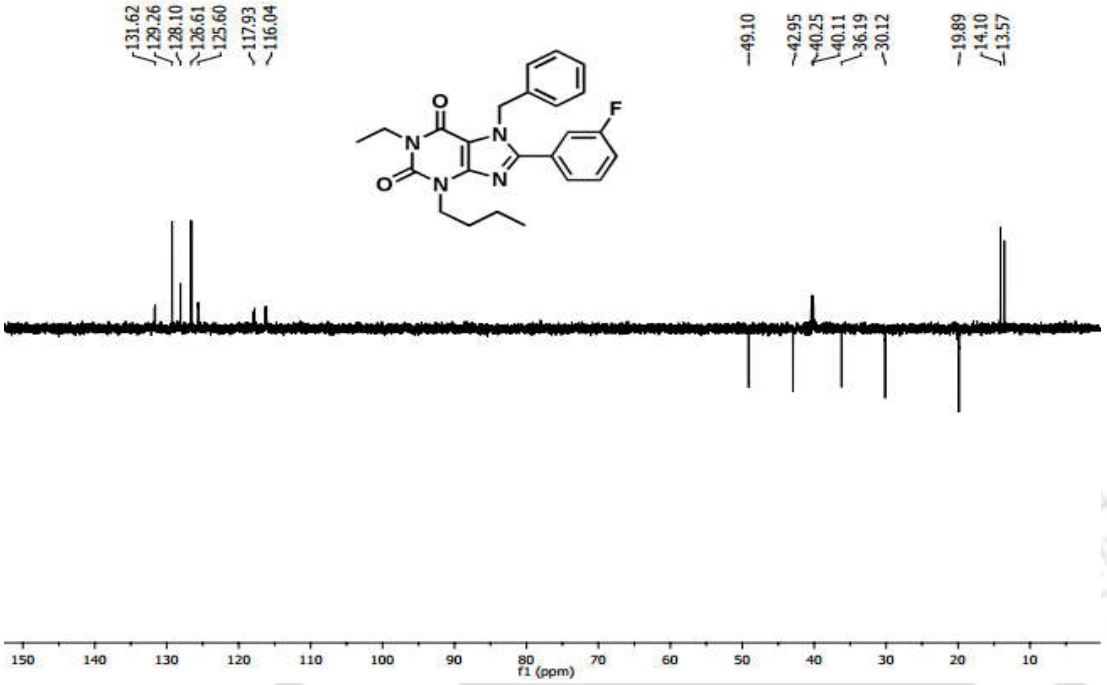

Figure A1.39 [135]DEPT NMR (DMSO-d6; 150 MHz) spectra of compound 5a7

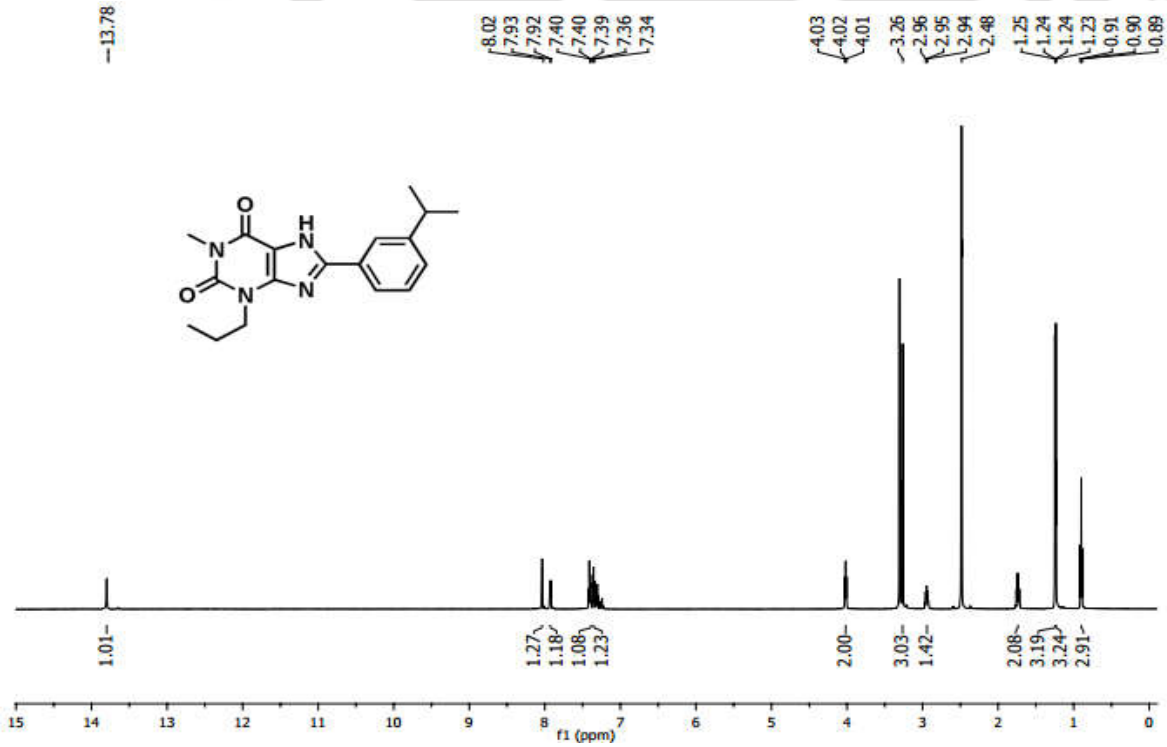

Figure A1.40 [1]H NMR (DMSO-d6; 600 MHz) spectra of Compound 6a1 or C1

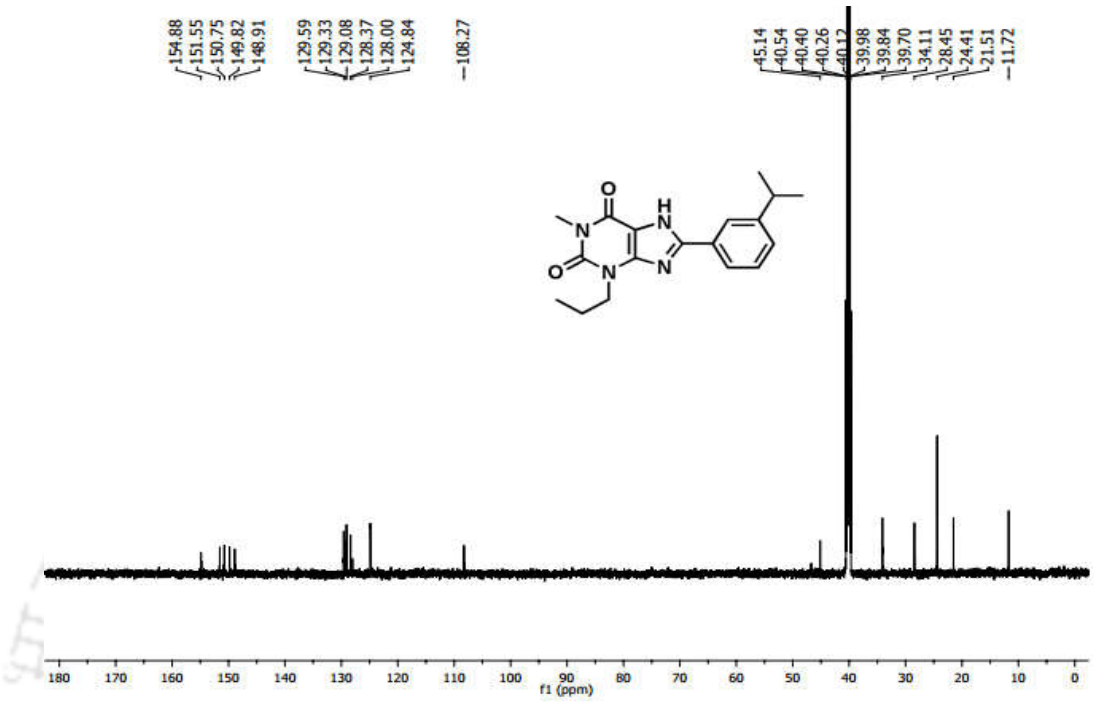

Figure A1.41 ^{13}C NMR (DMSO-d6; 150 MHz) spectra of Compound 6a1 or C1

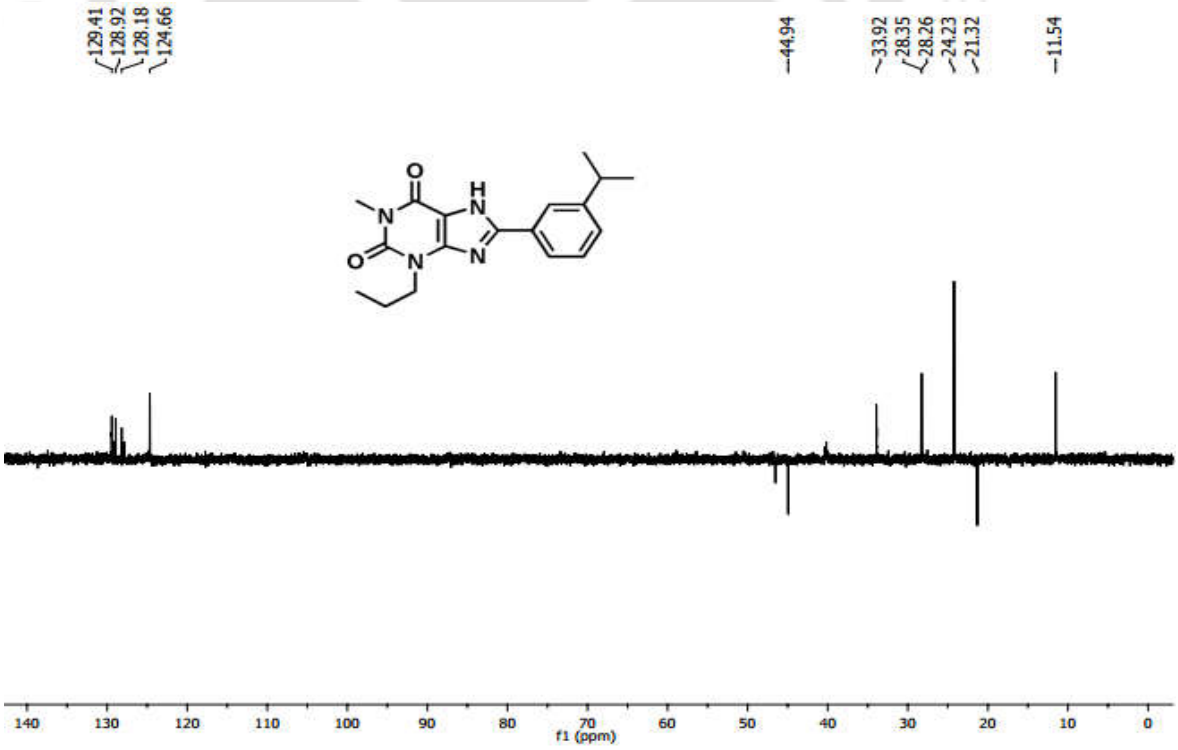

Figure A1.42 ^{135}DEPT NMR (DMSO-d6; 150 MHz) spectra of Compound 6a1 or C1

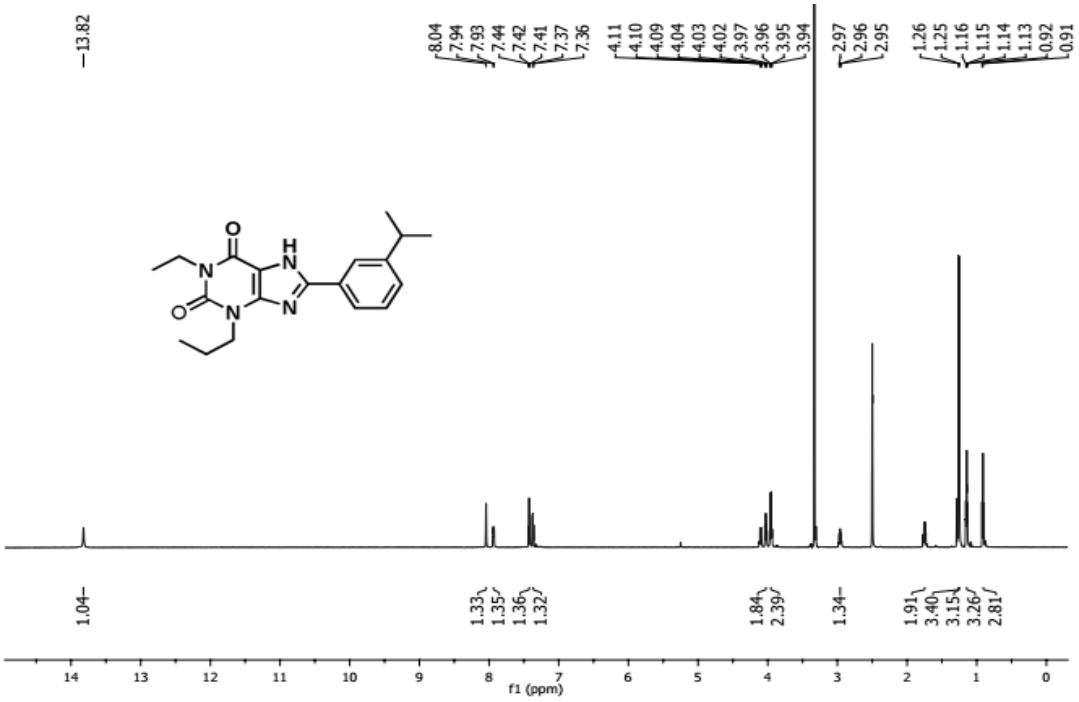

Figure A1.43 ^{1}H NMR (DMSO-d6; 600 MHz) spectra of compound 6a2 or C2

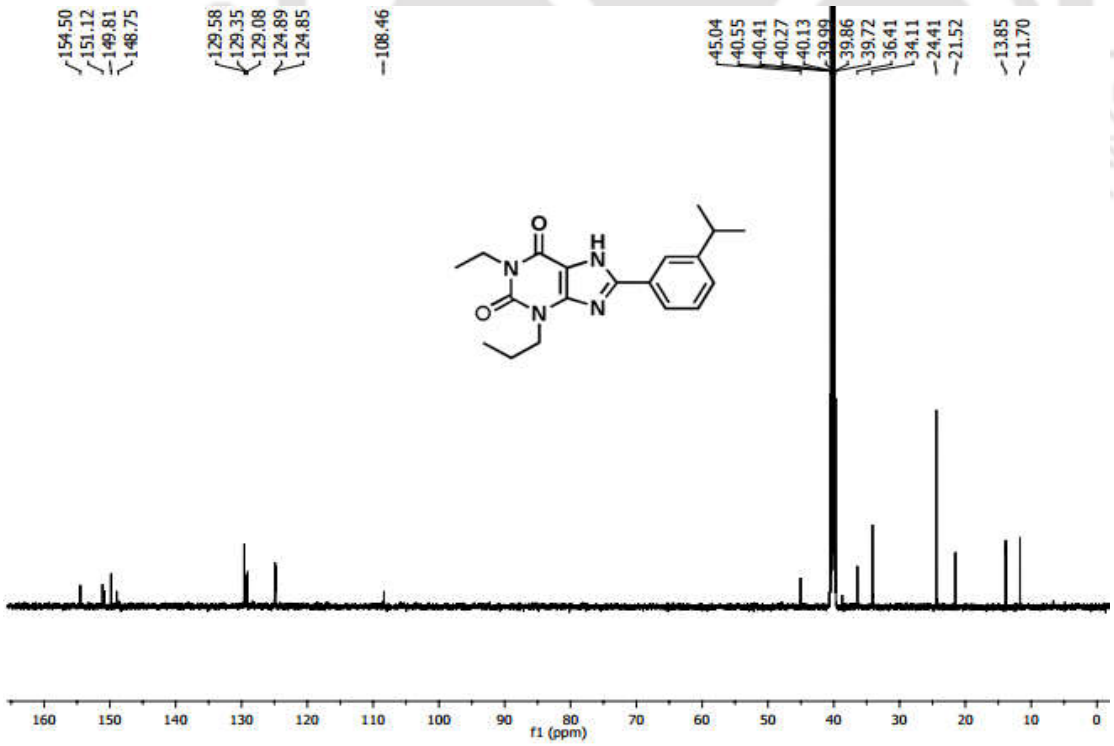

Figure A1.44 ^{13}C NMR (DMSO-d6; 150 MHz) spectra of compound 6a2 or C2

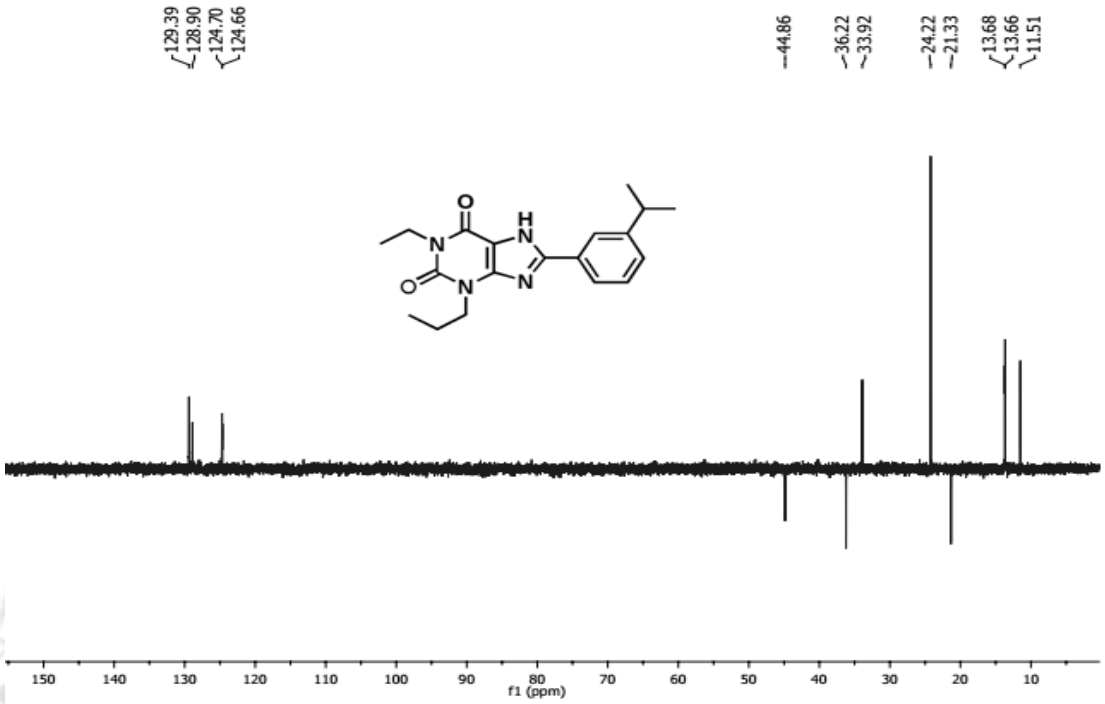

Figure A1.45 [135]DEPT NMR (DMSO-d6; 150 MHz) spectra of compound 6a2 or C2

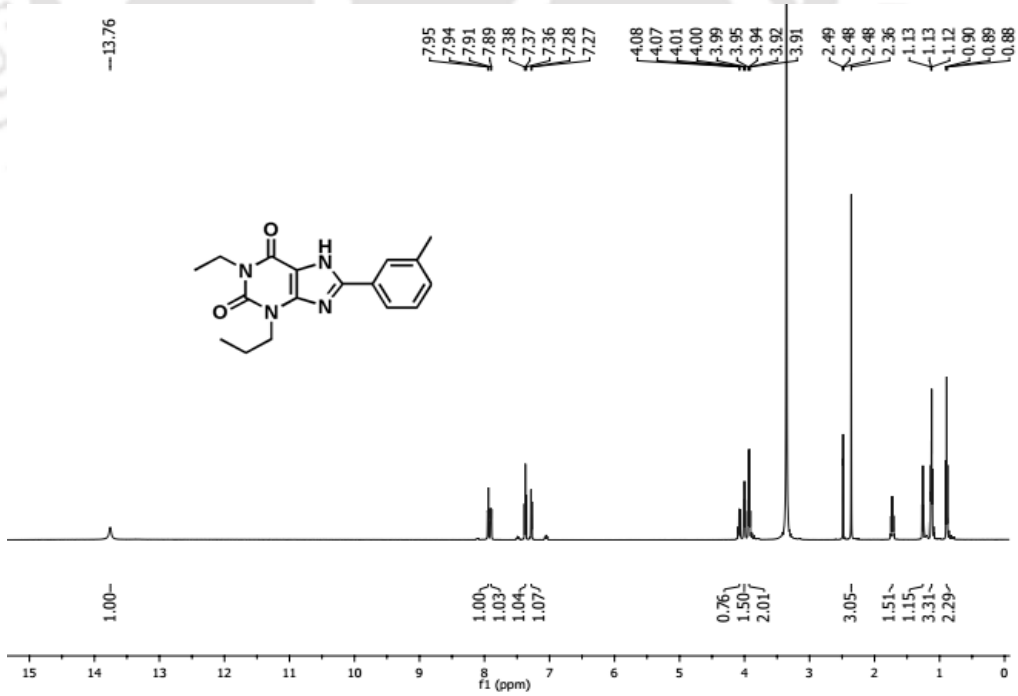

Figure A1.46 [1]H NMR (DMSO-d6; 600 MHz) spectra of Compound 6a3 or C3

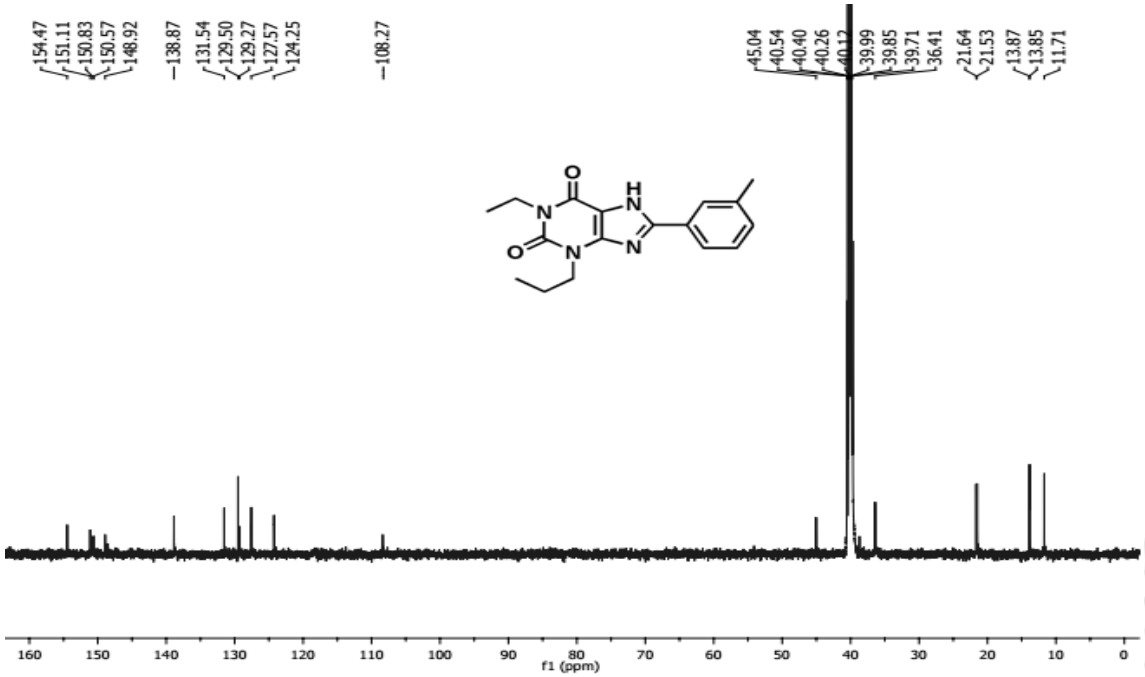

Figure A1.47 ^{13}C NMR (DMSO-d6; 150 MHz) spectra of Compound 6a3 or C3

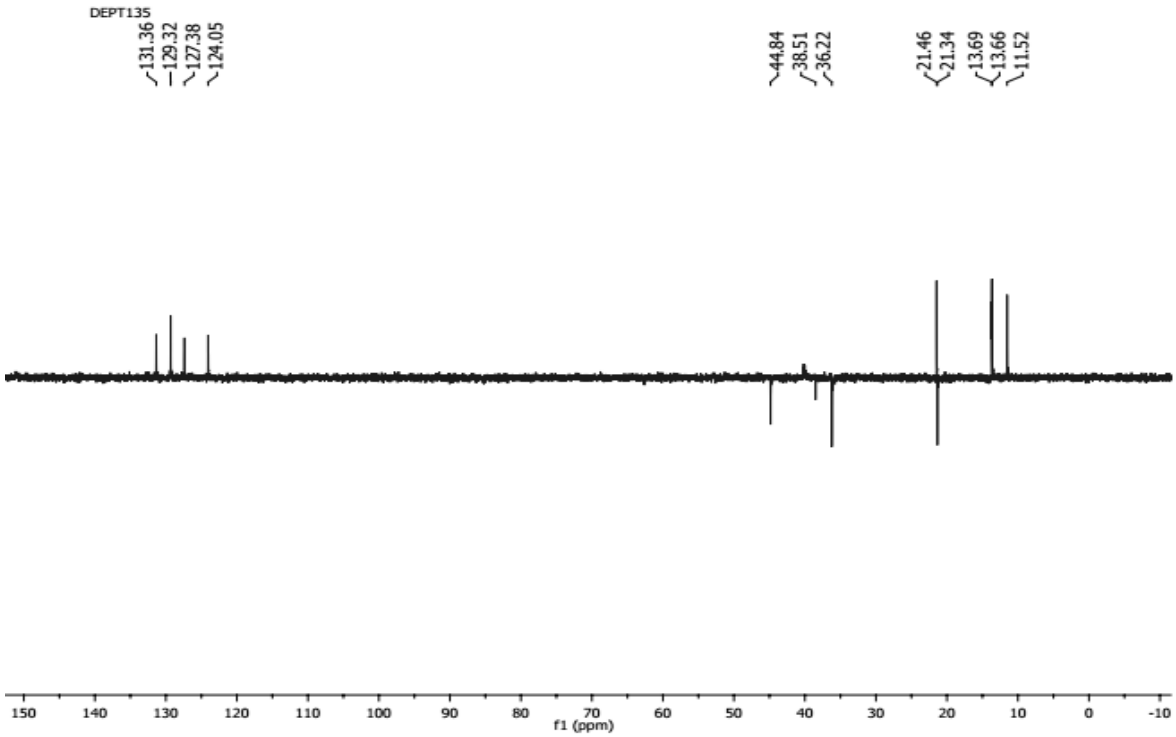

Figure A1.48 ^{135}DEPT NMR (DMSO-d6; 150 MHz) spectra of Compound 6a3 or C3

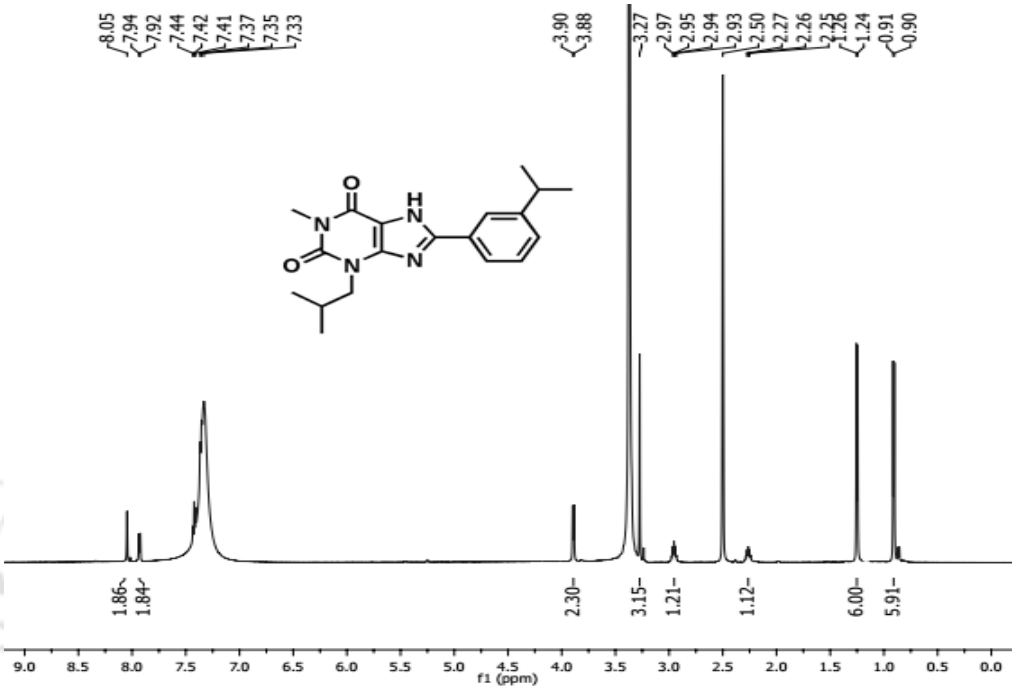

Figure A1.49 ^{1}H NMR (DMSO-d6; 600 MHz) spectra of Compound 6a4 or C4

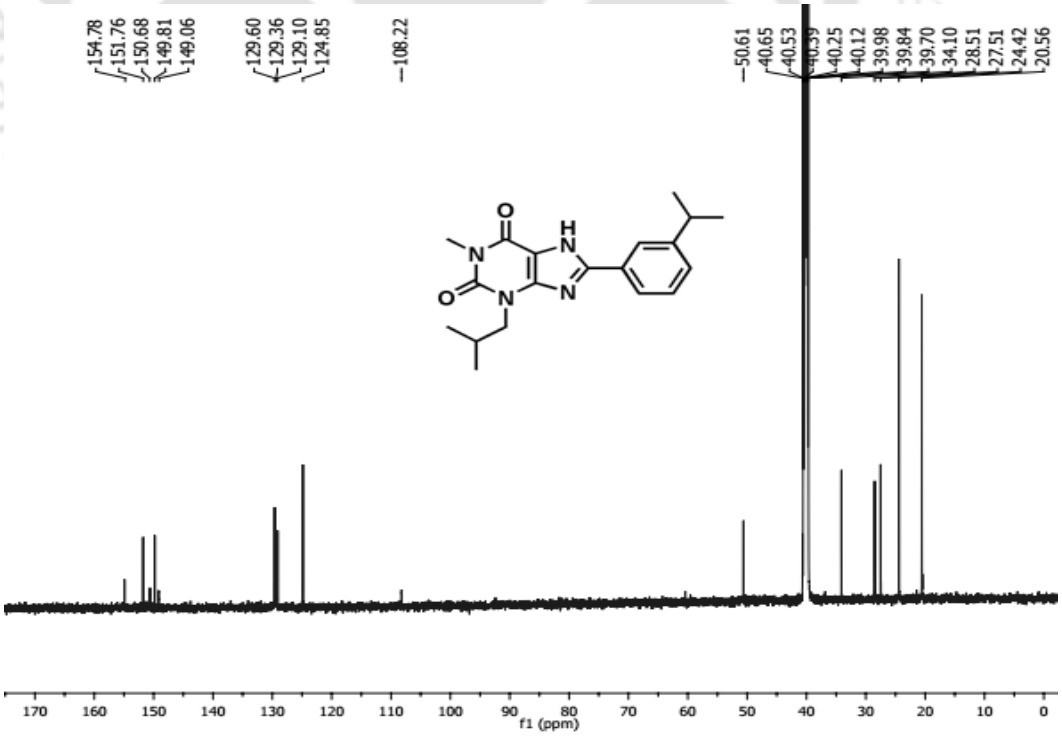

Figure A1.50 ^{13}C NMR (DMSO-d6; 150 MHz) spectra of Compound 6a4 or C4

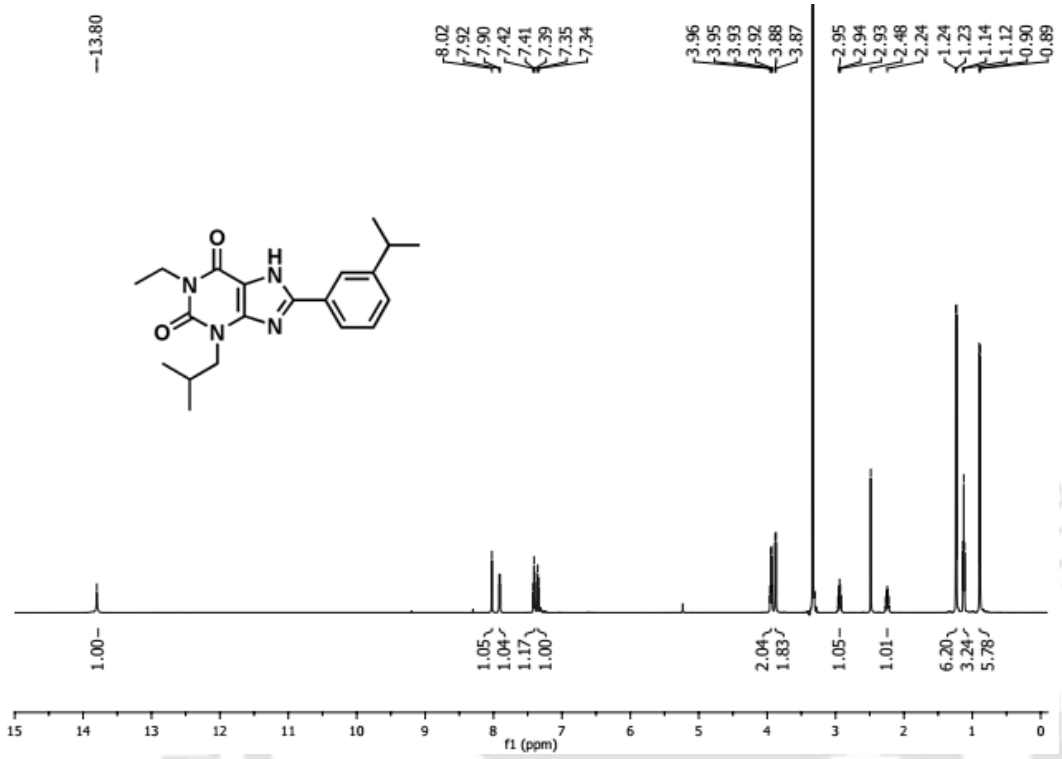

Figure A1.51 ^{1}H NMR (DMSO-d6; 600 MHz) spectra of compound 6a5 or C5

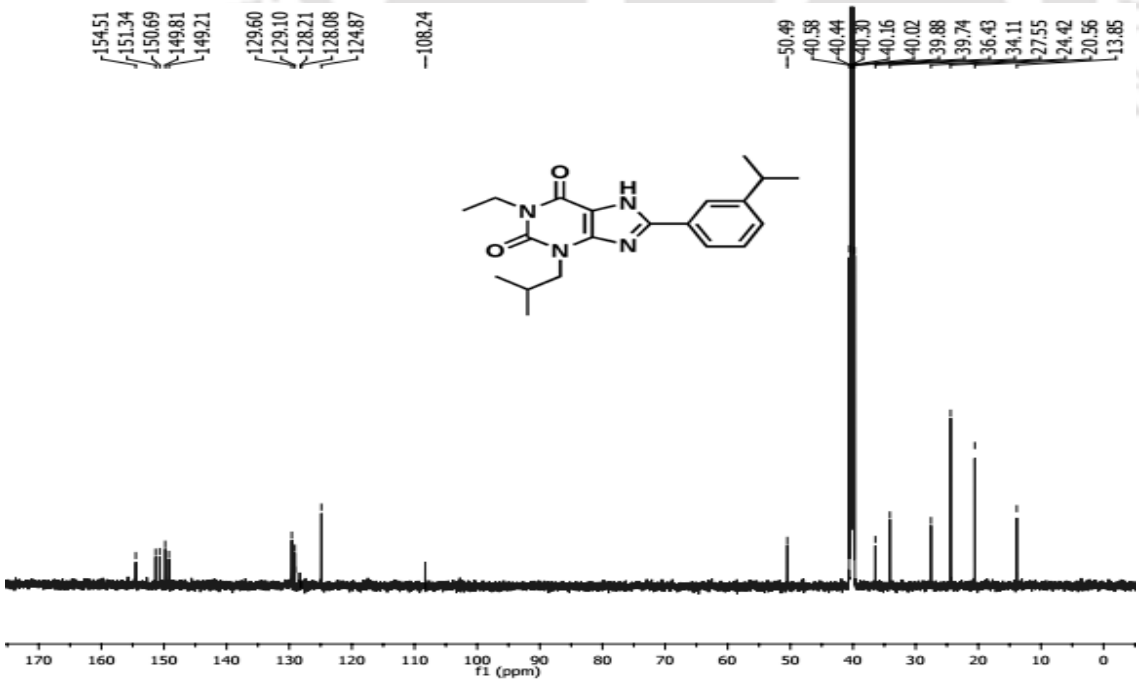

Figure A1.52 ^{13}C NMR (DMSO-d6; 150 MHz) spectra of compound 6a5 or C5

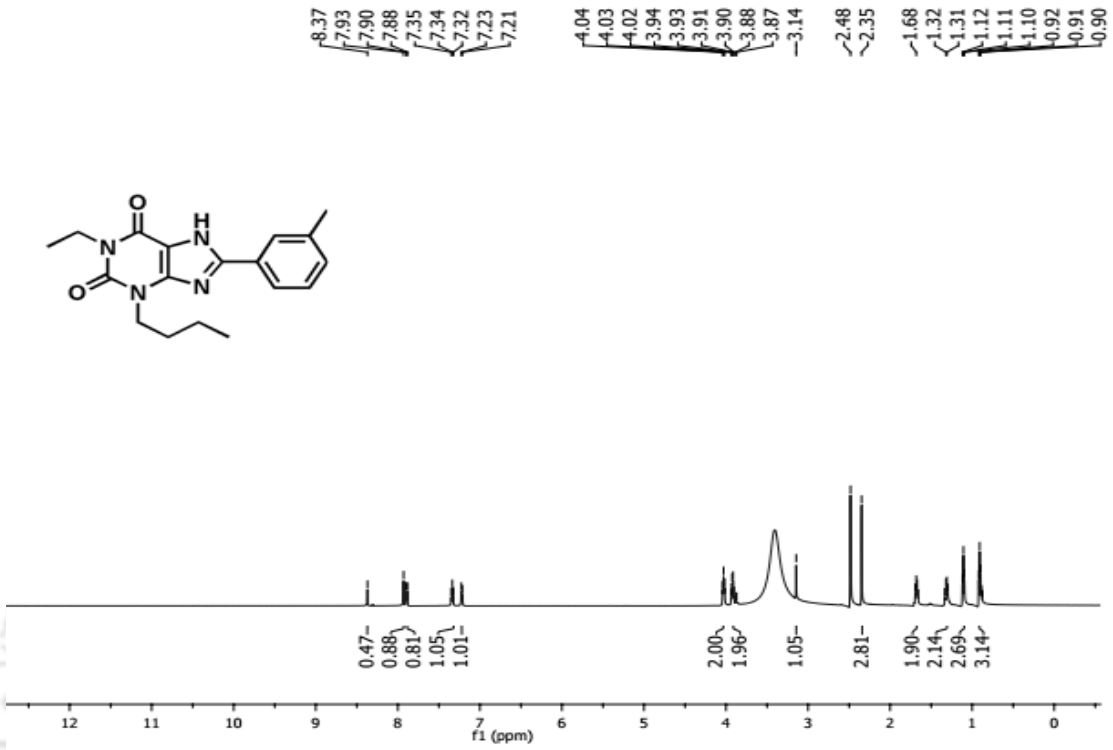

Figure A1.53 ^{1}H NMR (DMSO-d6; 600 MHz) spectra of compound 6a6 or C7

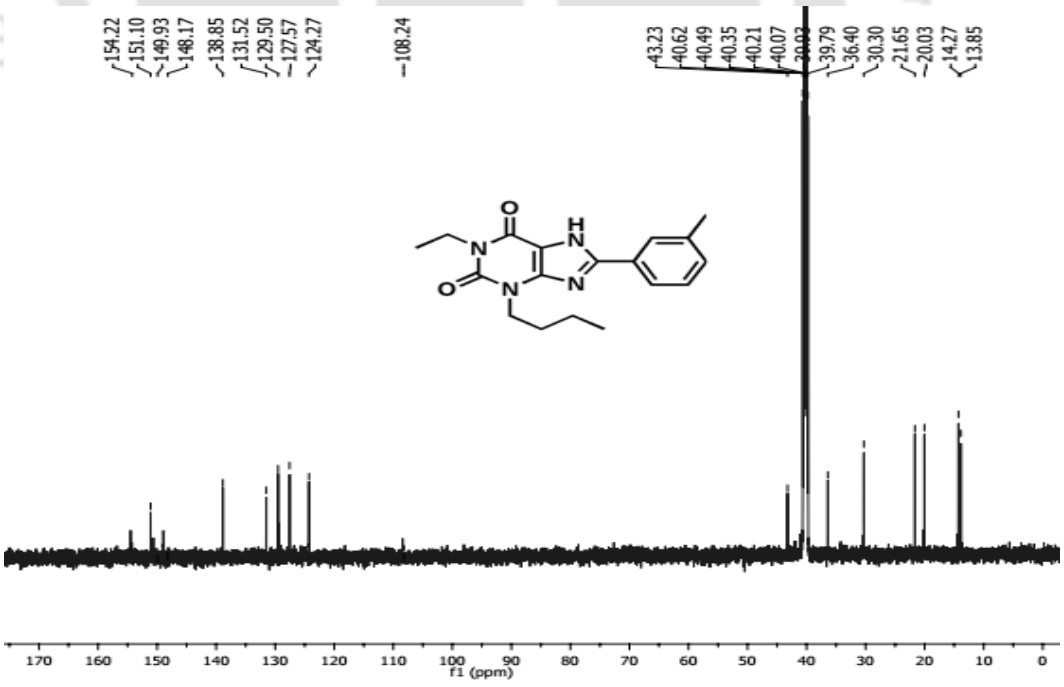

Figure A1.54 ^{13}C NMR (DMSO-d6; 150 MHz) spectra of compound 6a6 or C7

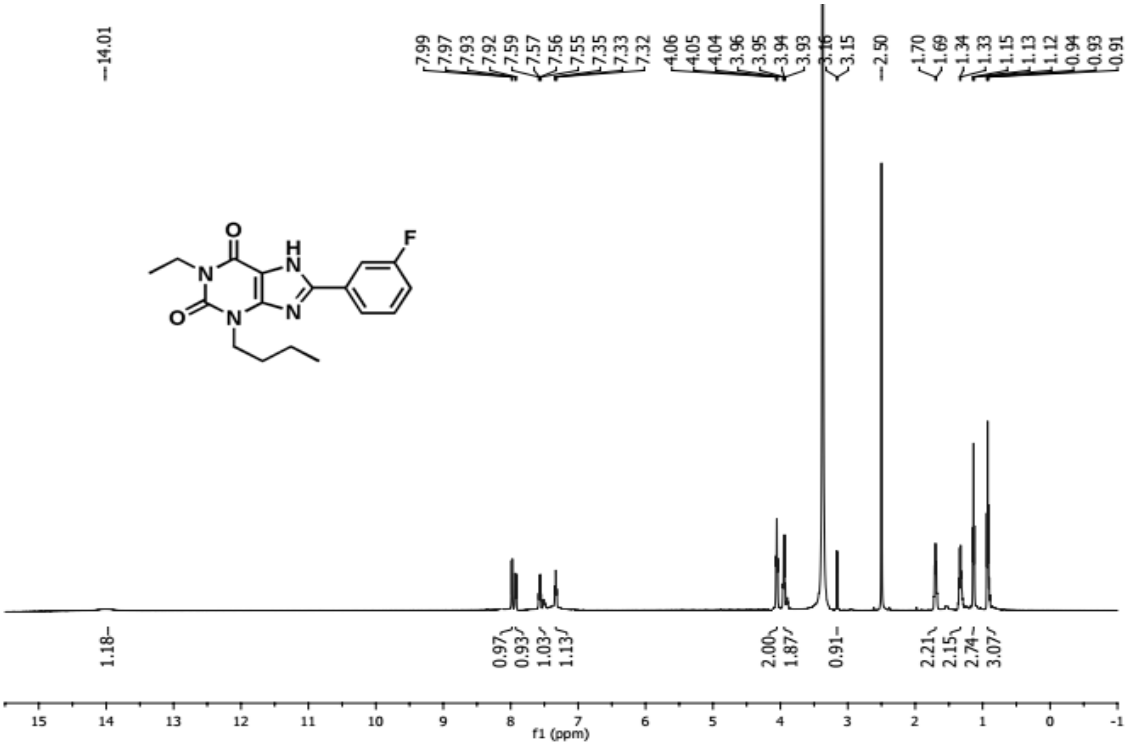

Figure A1.55 [1]H NMR (DMSO-d6; 600 MHz) spectra of compound 6a7 or C8

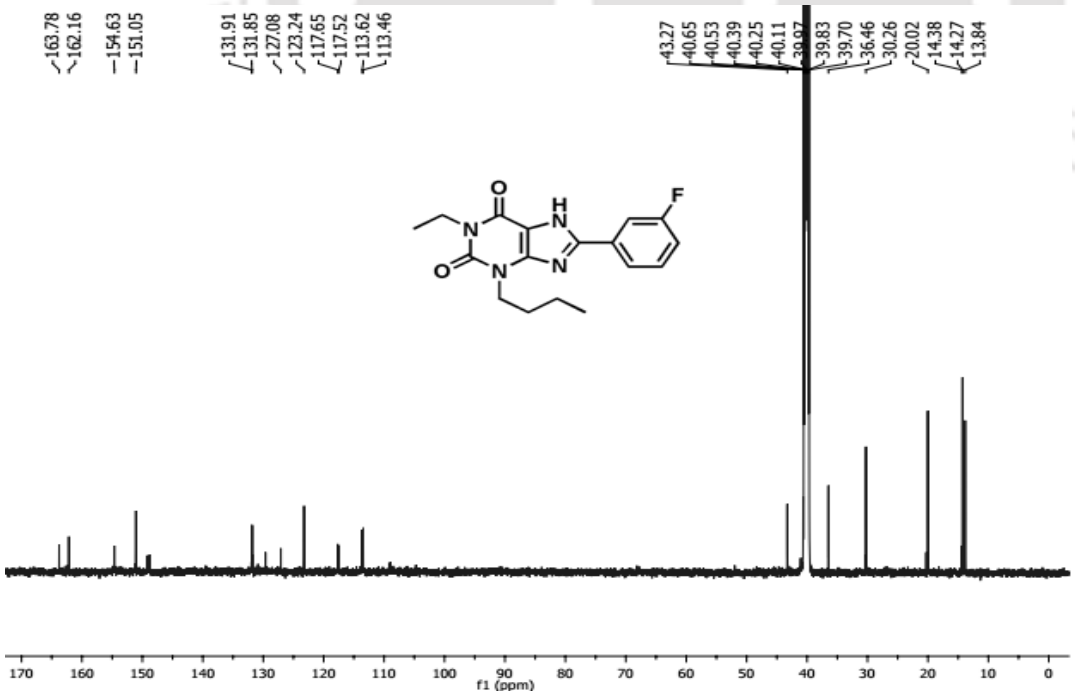

Figure A1.56 [13]C NMR (DMSO-d6; 150 MHz) spectra of compound 6a7 or C8

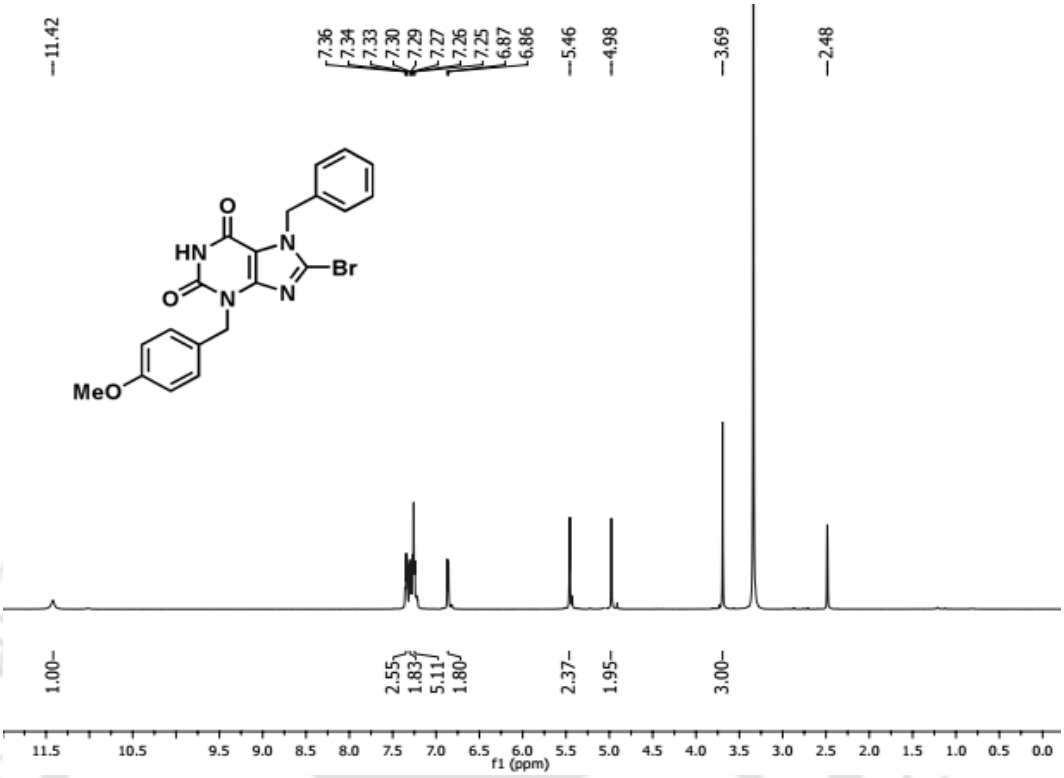

Figure A1.57 ^{1}H NMR (DMSO-d6; 600 MHz) spectra compound 3b1

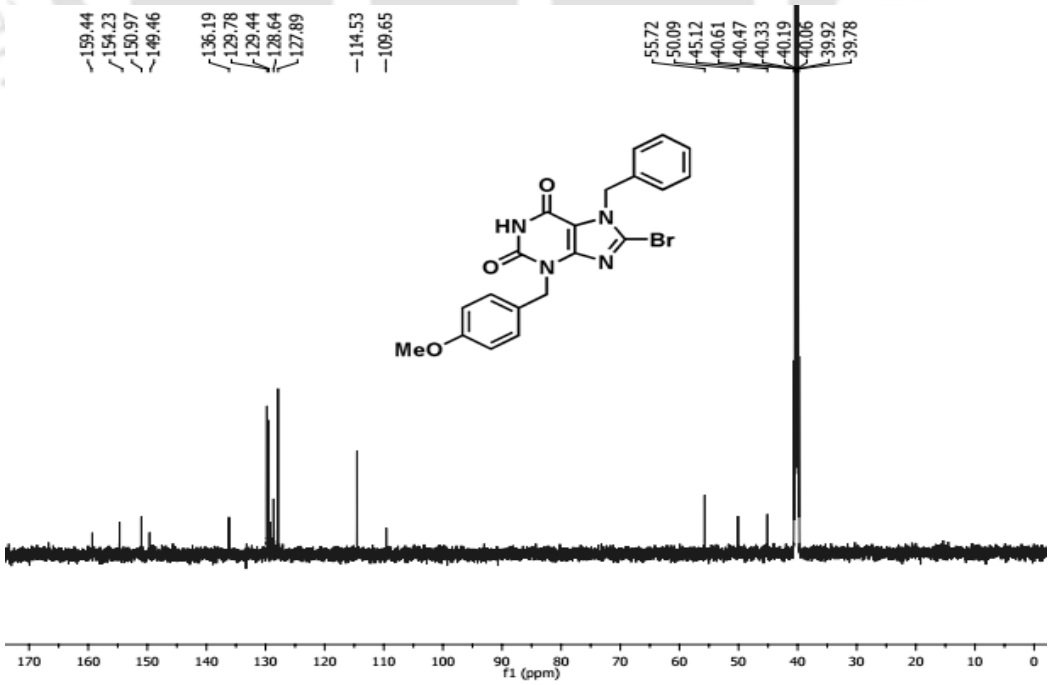

Figure A1.58 ^{13}C NMR (DMSO-d6; 150 MHz) spectra of compound 3b1

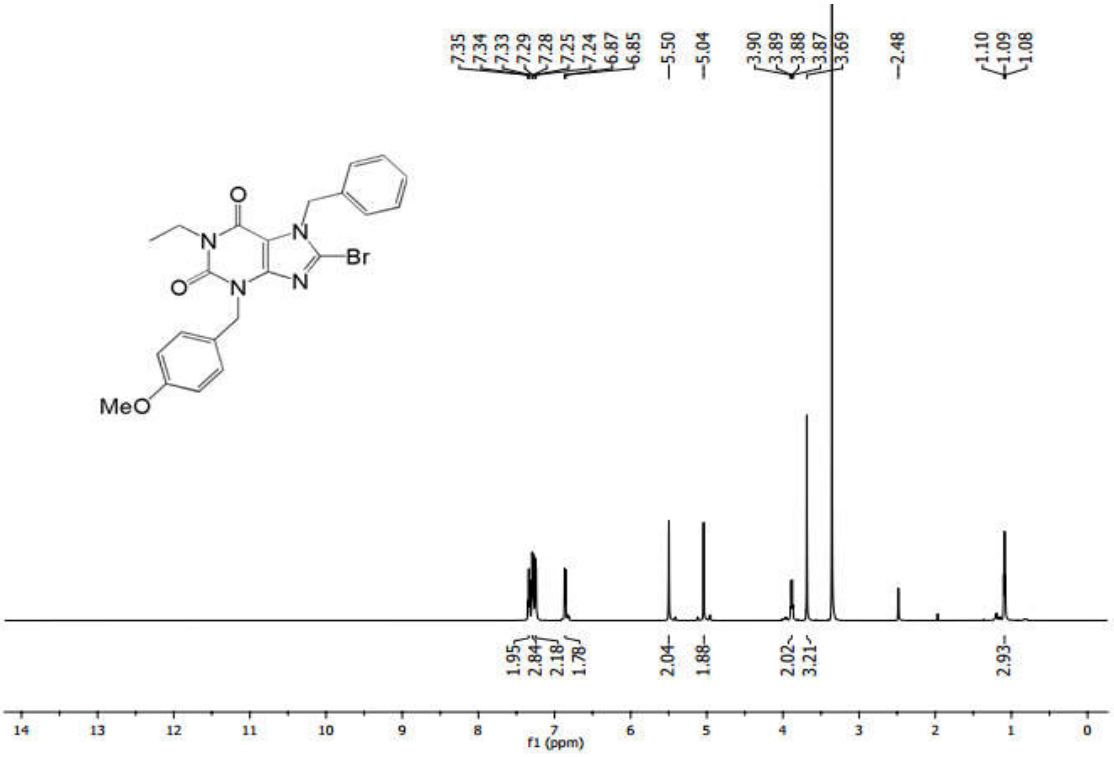

Figure A1.59 ^{1}H NMR (DMSO-d6; 600 MHz) spectra of Compound 4b1

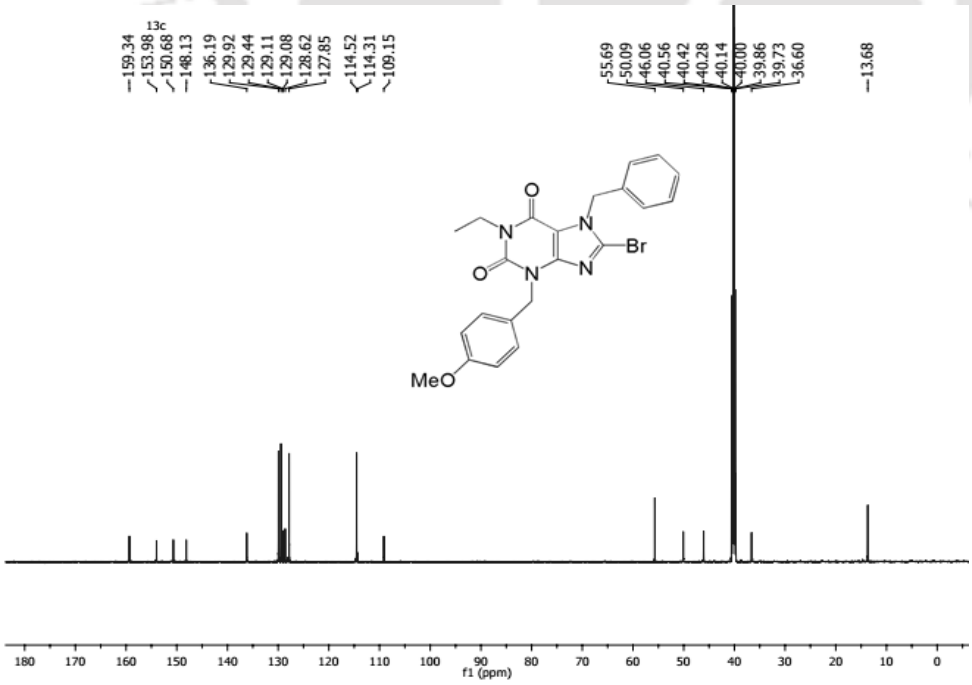

Figure A1.60 ^{13}C NMR (DMSO-d6; 150 MHz) spectra of compound 4b1

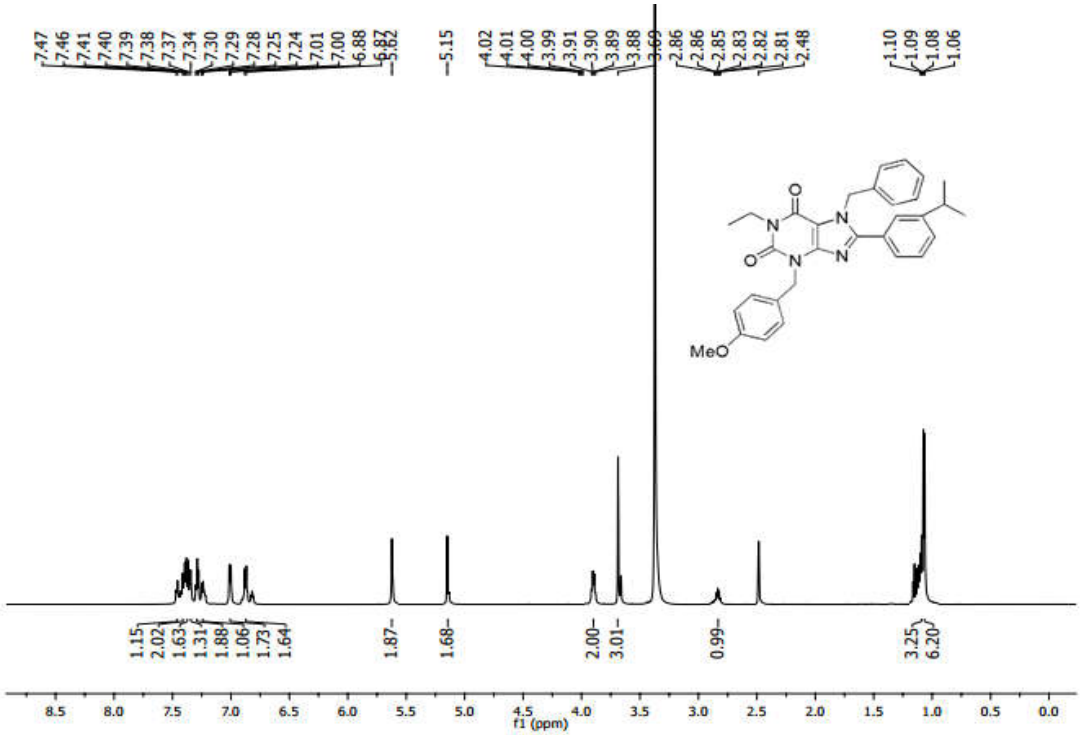

Figure A1.61 ^{1}H NMR (DMSO-d6, 600 MHz) spectra of compound 5b1

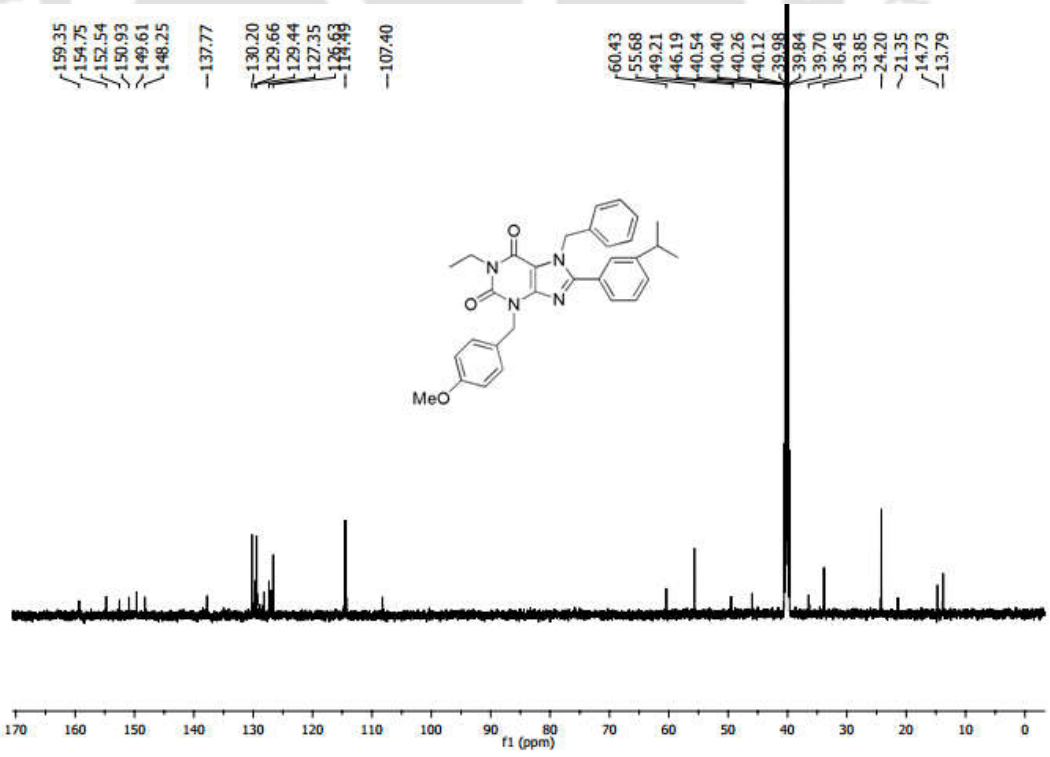

Figure A1.62 ^{13}C NMR (DMSO-d6, 150 MHz) spectra of compound 5b1

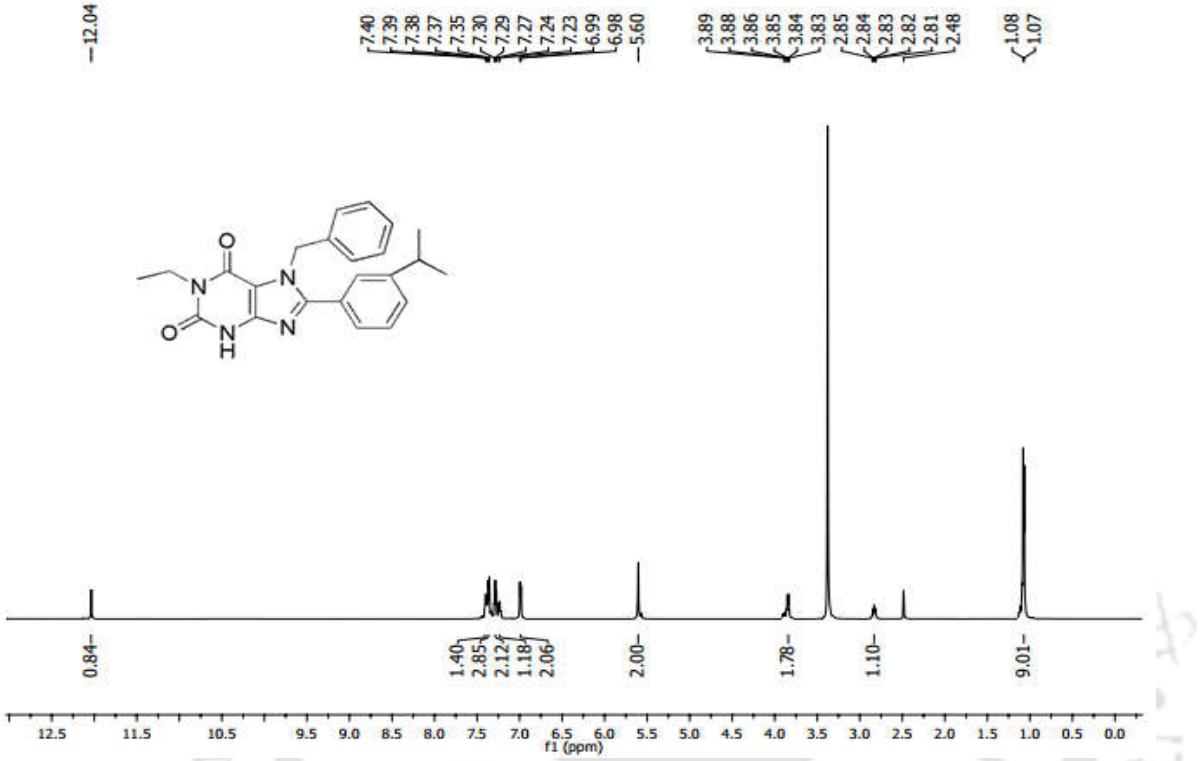

Figure A1.63 ^{1}H NMR (DMSO-d6, 600 MHz) spectra of compound 6b1

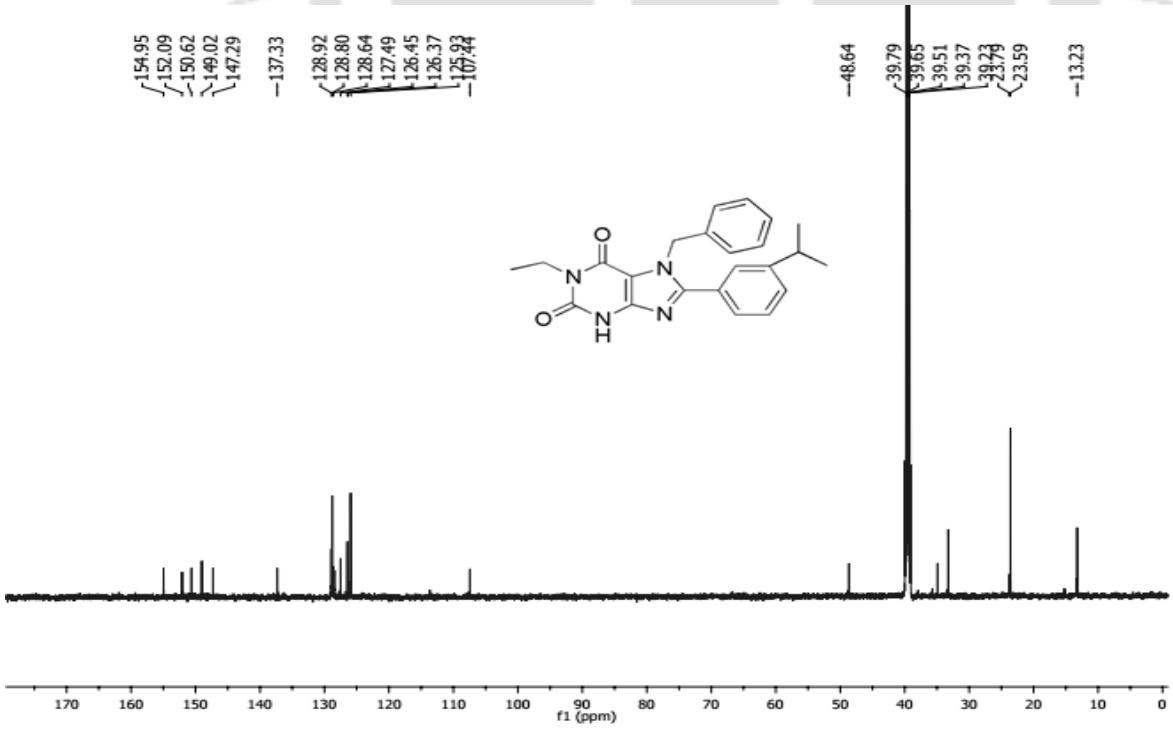

Figure A1.64 ^{13}C NMR (DMSO-d6, 150 MHz) spectra of compound 6b1

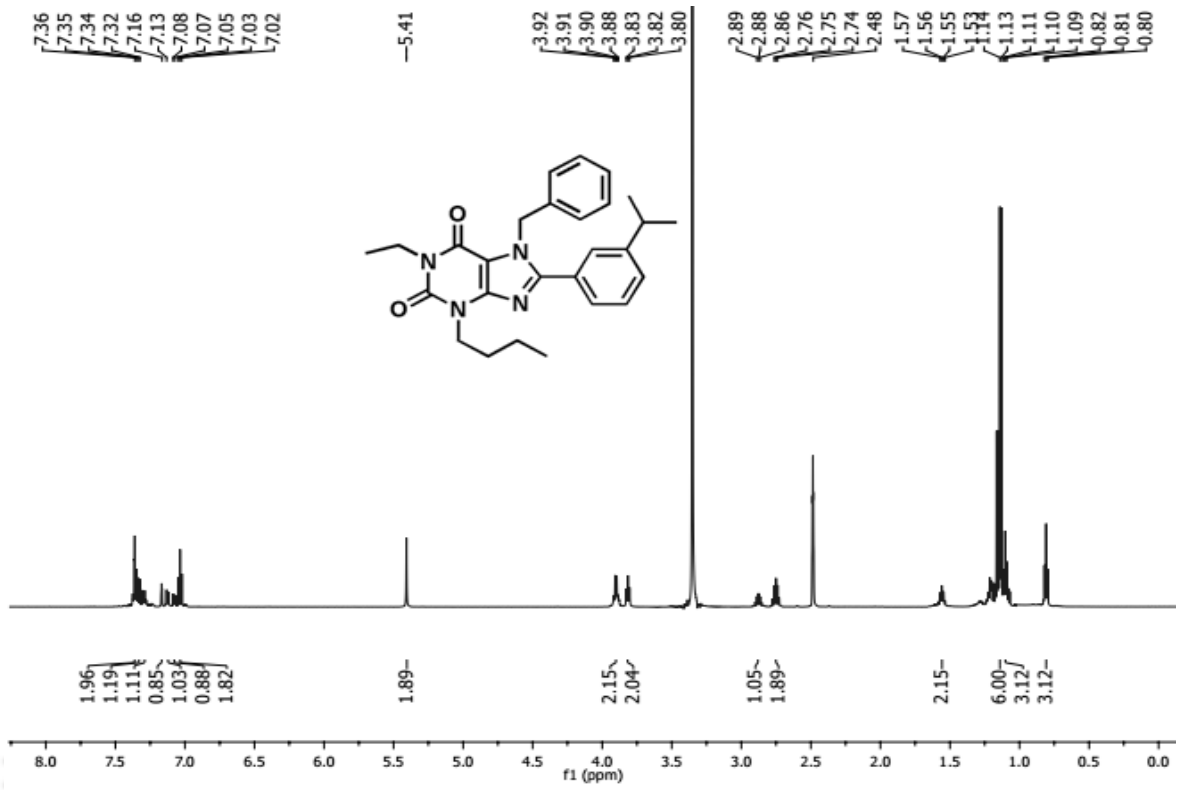

Figure A1.65 ^{1}H NMR (DMSO-d6, 600 MHz) spectra of compound 7b2

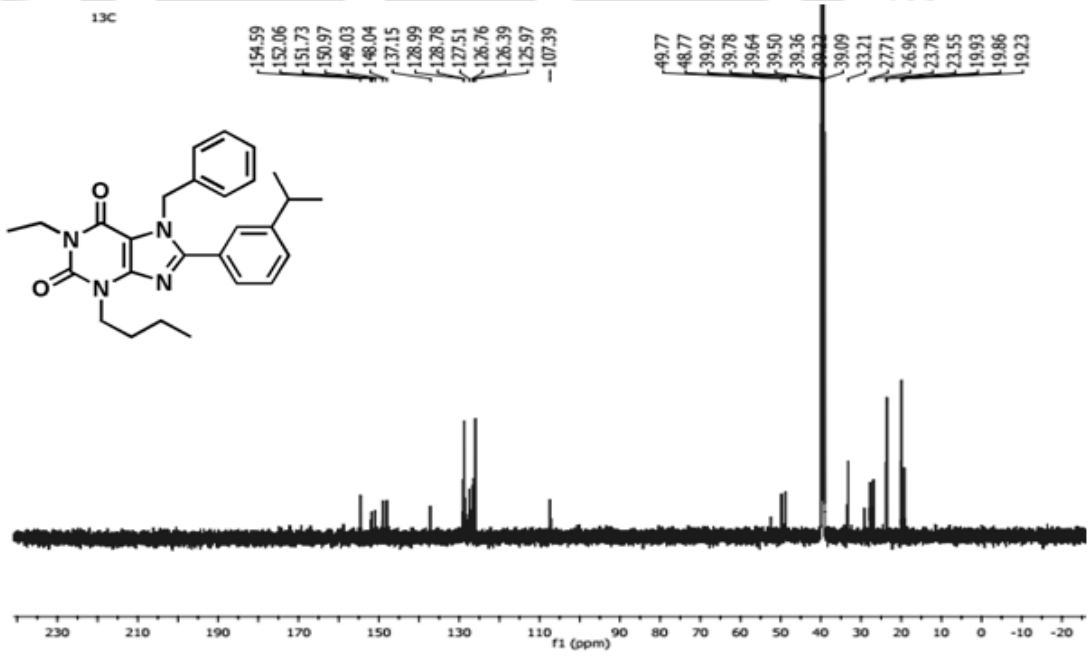

Figure A1.66 ^{13}C NMR (DMSO-d6, 150 MHz) spectra of compound 7b2

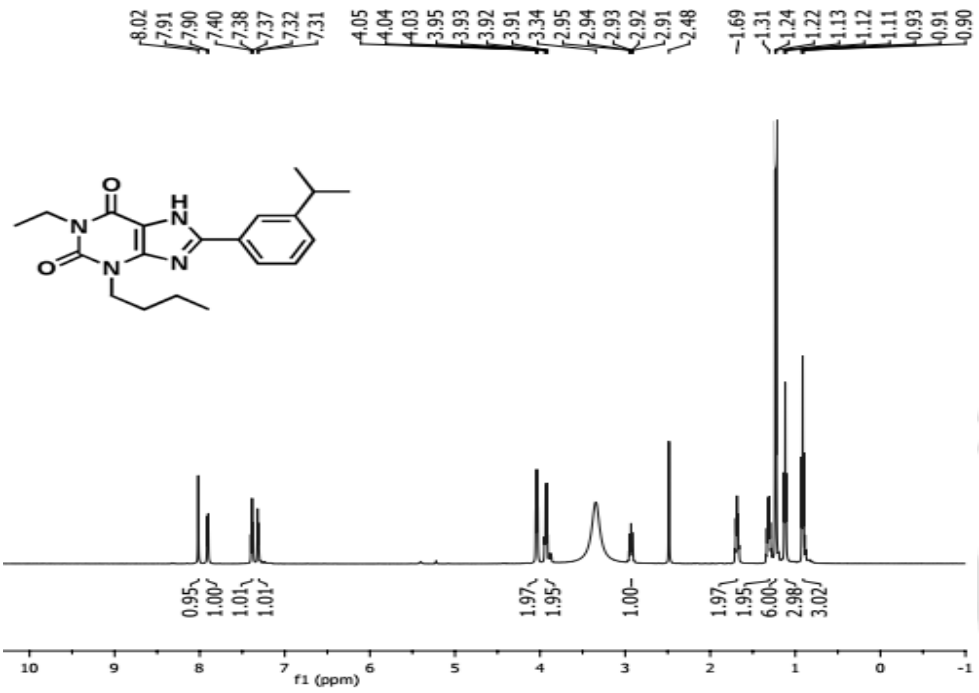

Figure A1.67 ^{1}H NMR (DMSO-d6; 600 MHz) spectra of compound 8b1 or C6

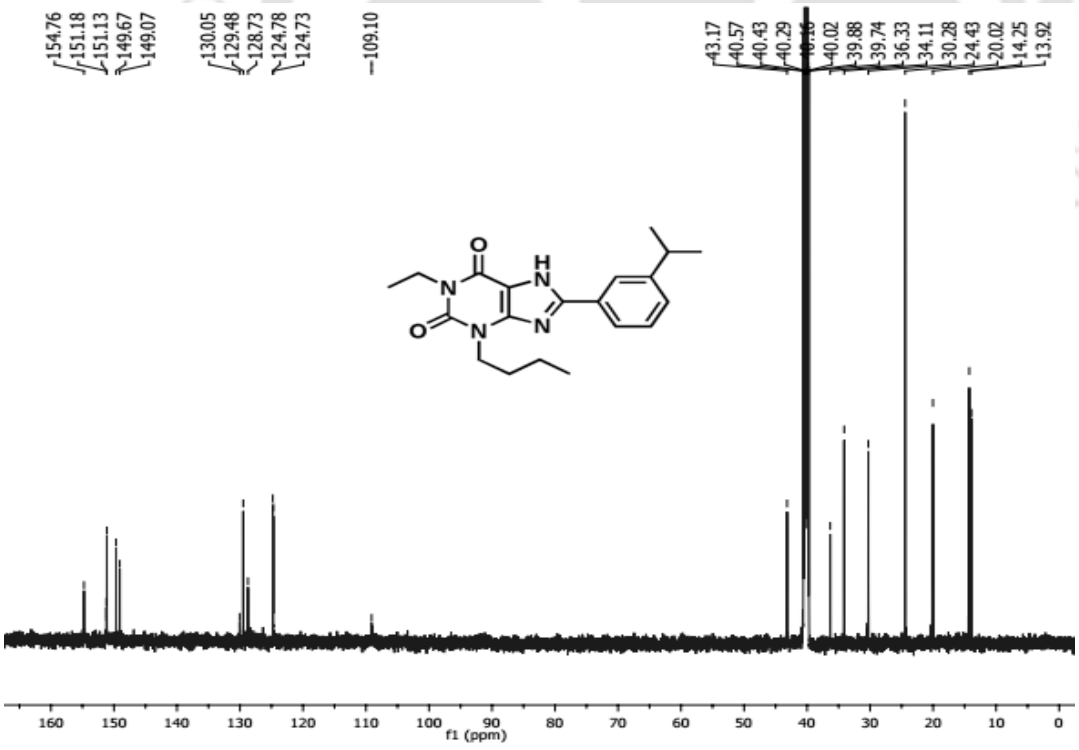

Figure A1.68 ^{13}C NMR (DMSO-d6; 150 MHz) spectra of compound 8b1 or C6

Appendix-II

Mass spectra of synthesized compounds

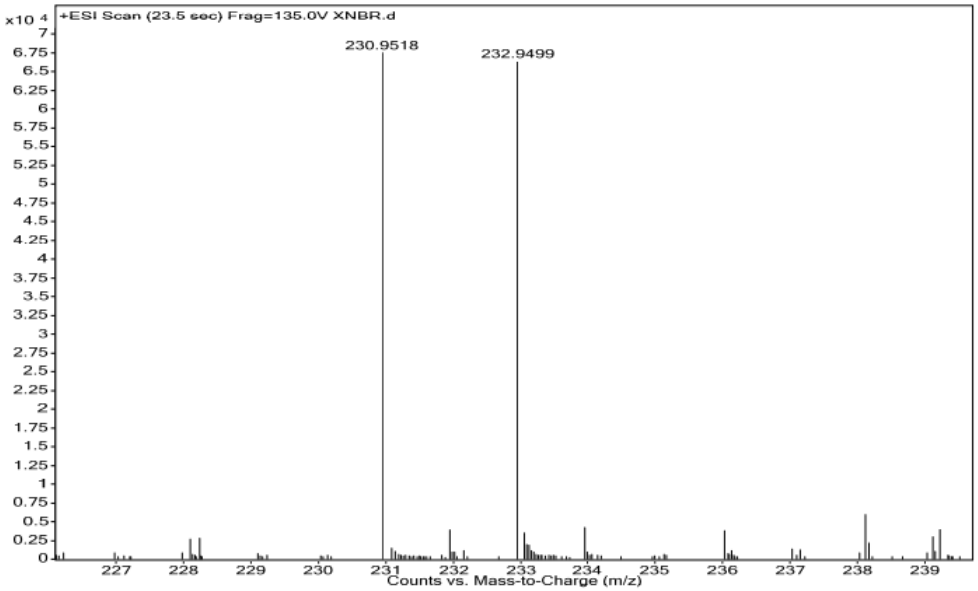

Figure A2.1 Mass spectra of compound **1**

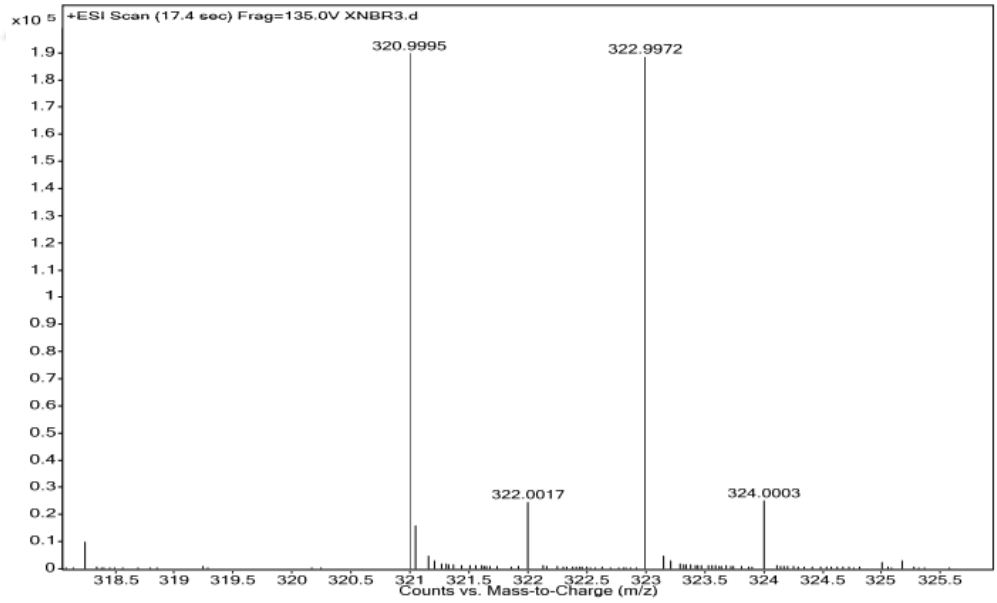

Figure A2.2 Mass spectra of compound **2**

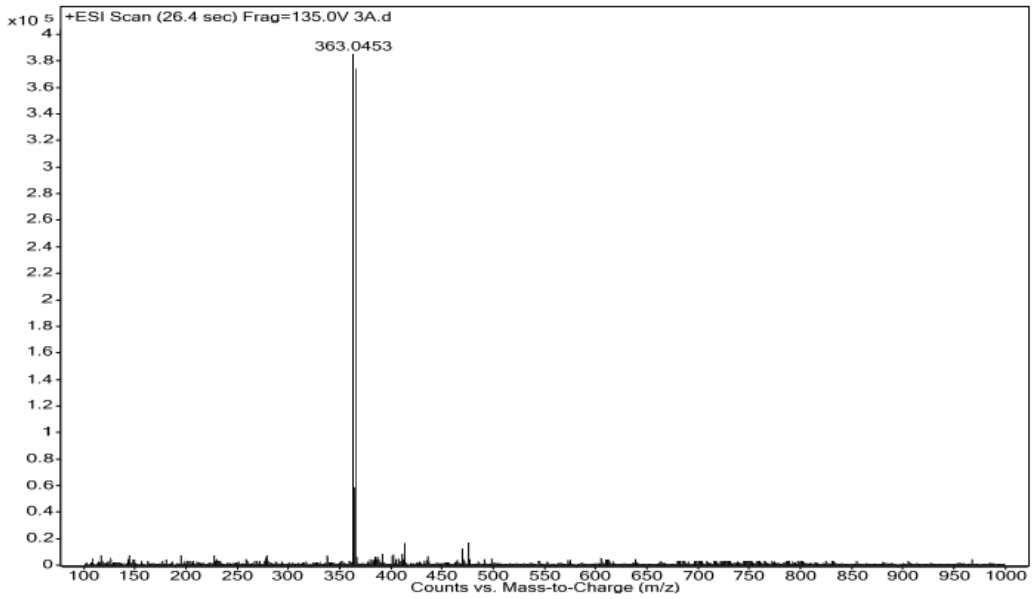

Figure A2.3 Mass spectra of compound **3a1**

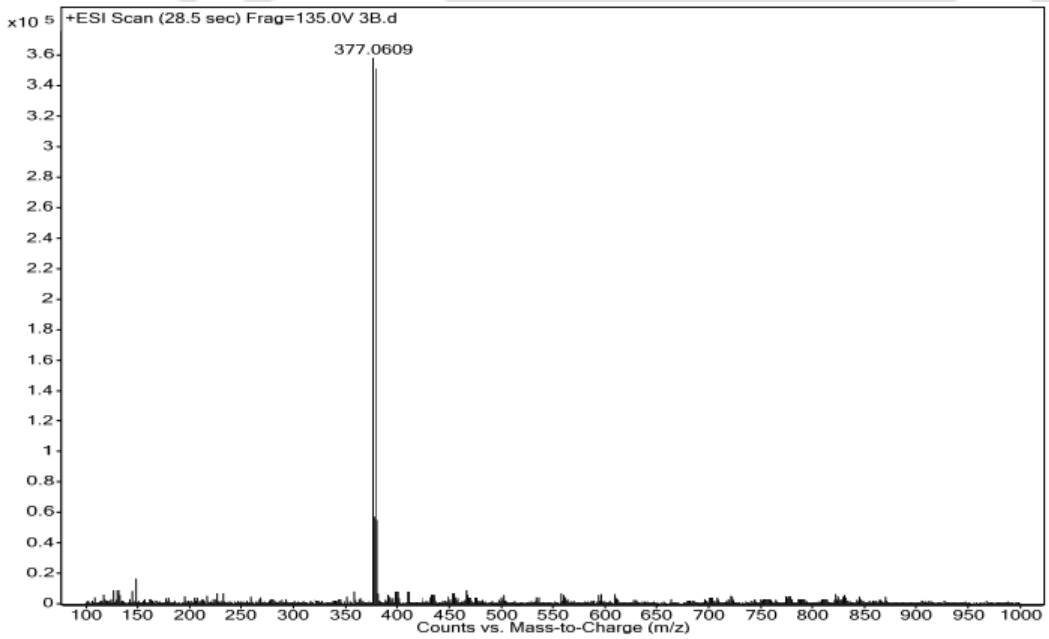

Figure A2.4 Mass spectra of compound **3a2**

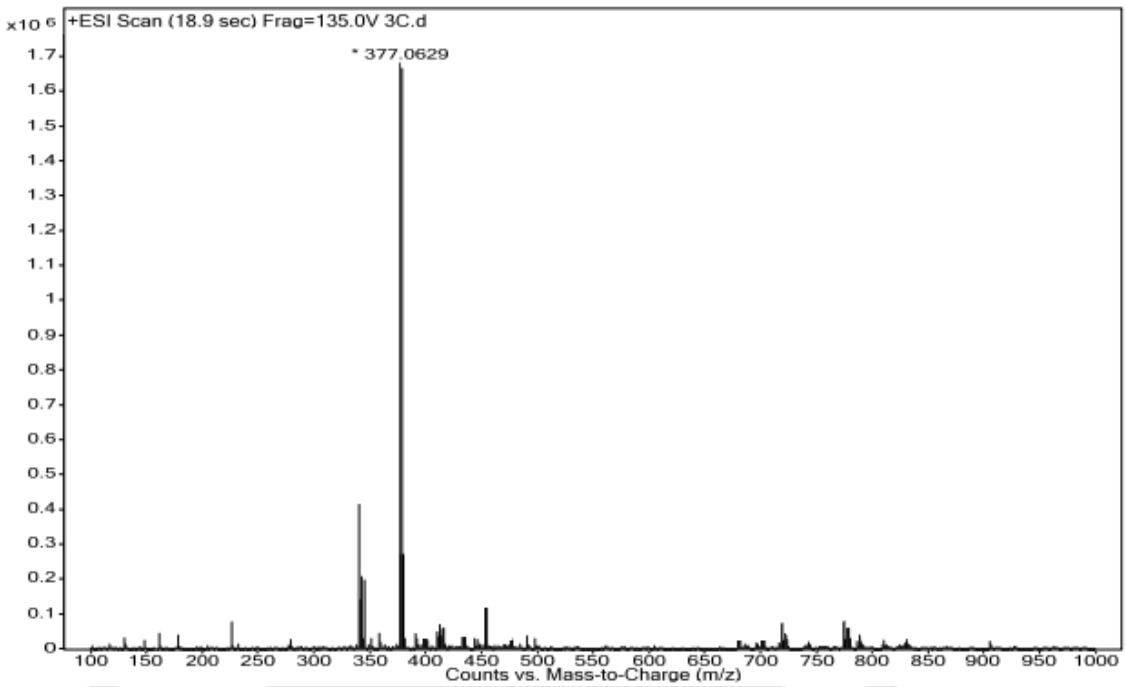

Figure A2.5 Mass spectra of compound **3a3**

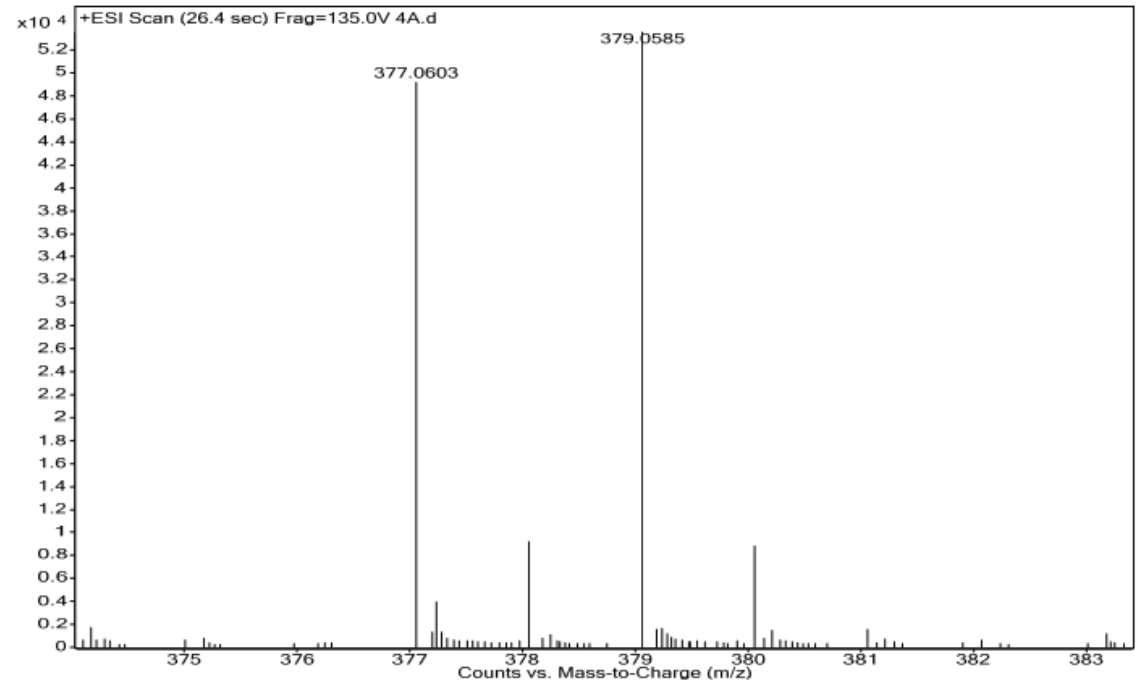

Figure A2.6 Mass spectra of compound **4a1**

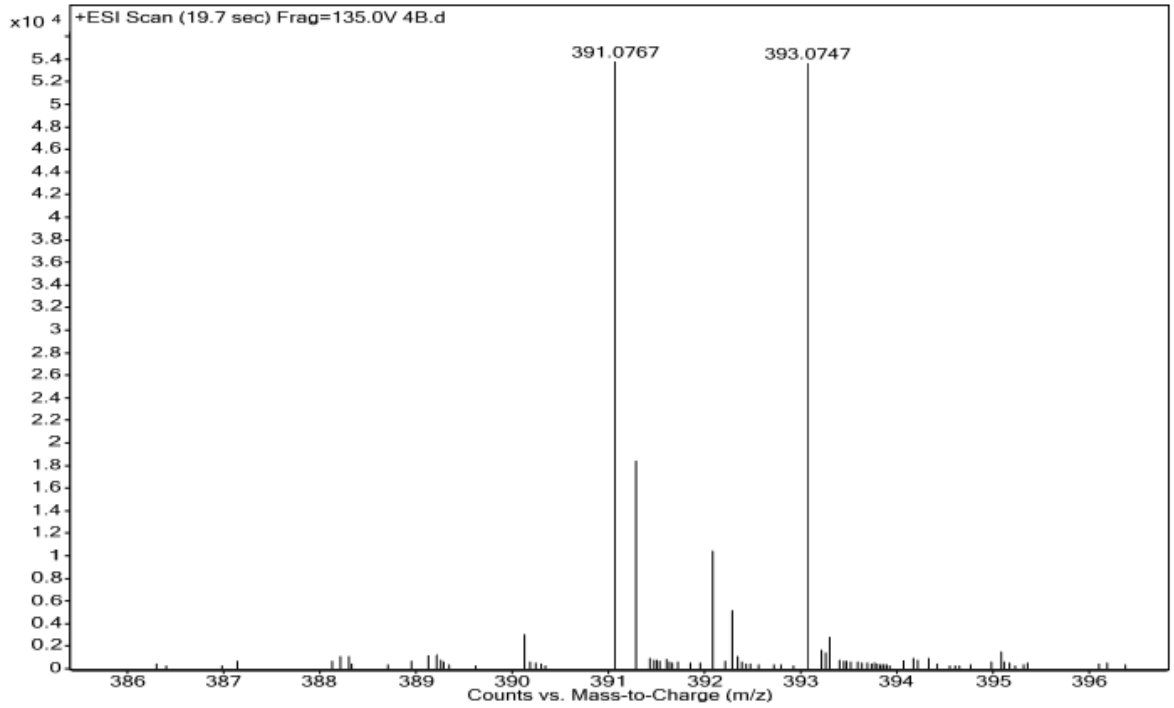

Figure A2.7 Mass spectra of compound **4a2**

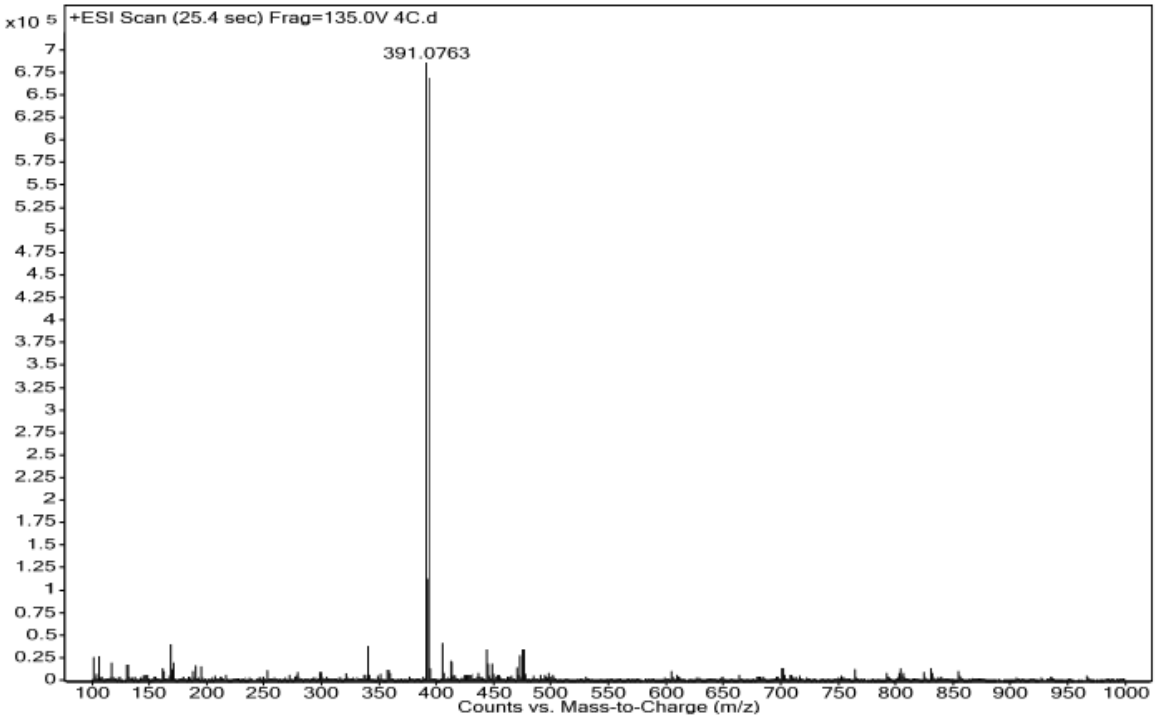

Figure A2.8 Mass spectra of compound **4a3**

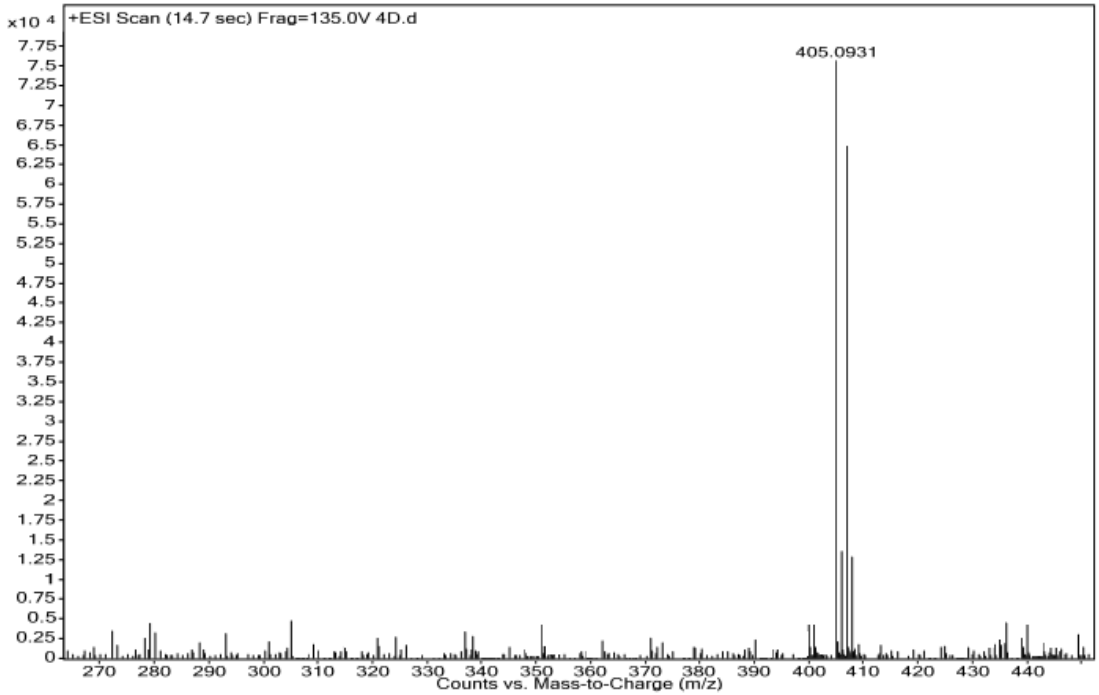

Figure A2.9 Mass spectra of compound **4a4**

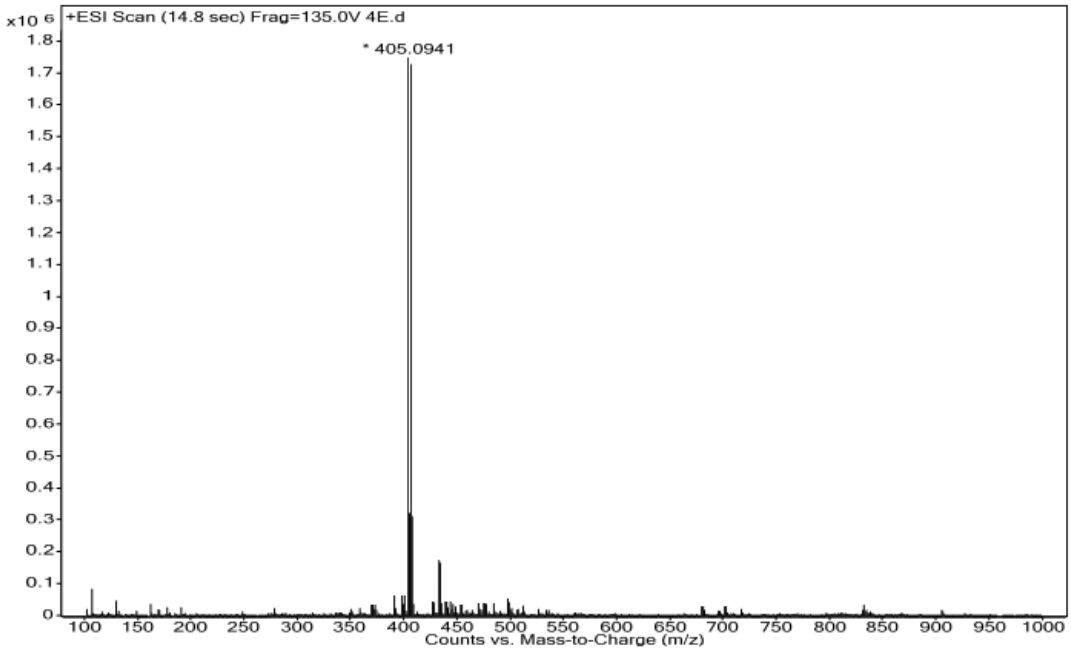

Figure A2.10 Mass spectra of compound **4a5**

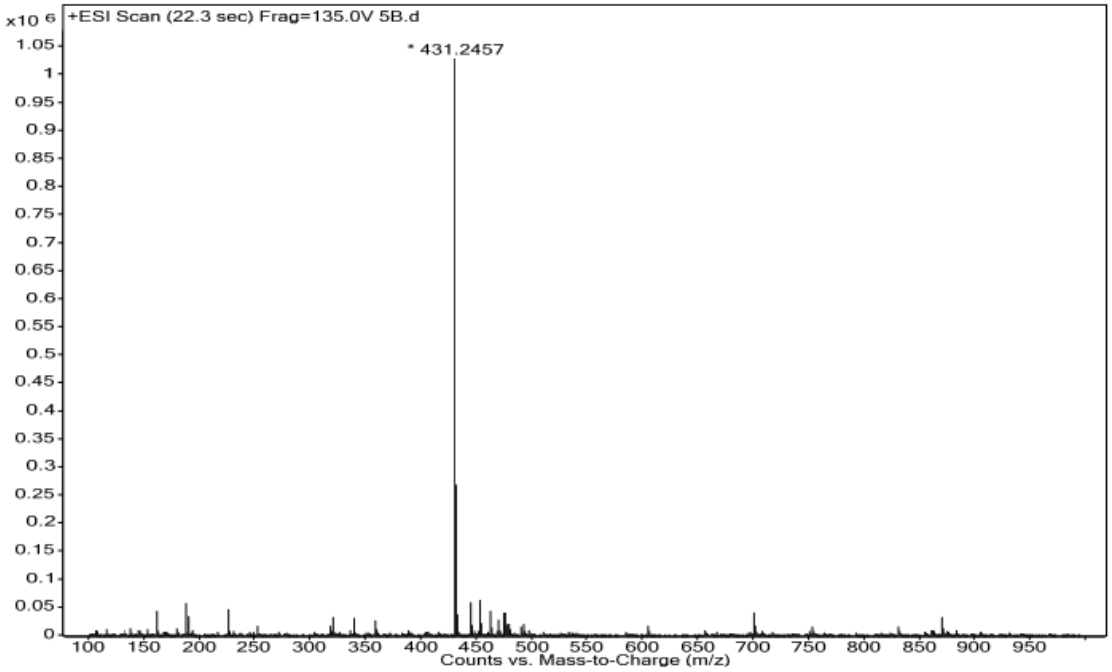

Figure A2.11 Mass spectra of compound **5a2**

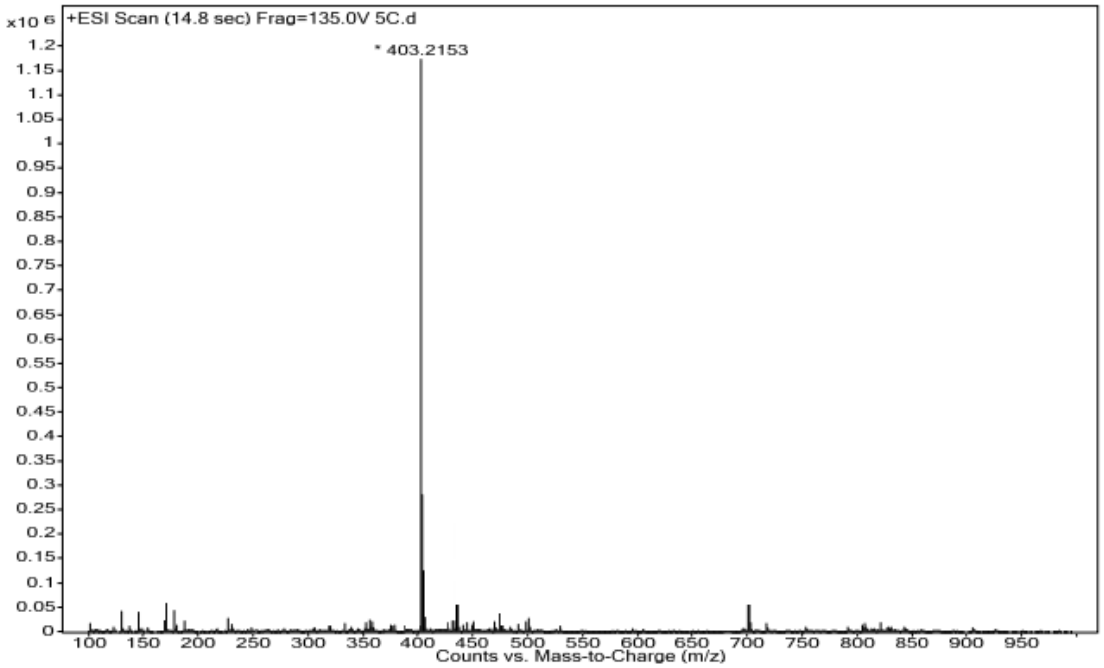

Figure A2.12 Mass spectra of compound **5a3**

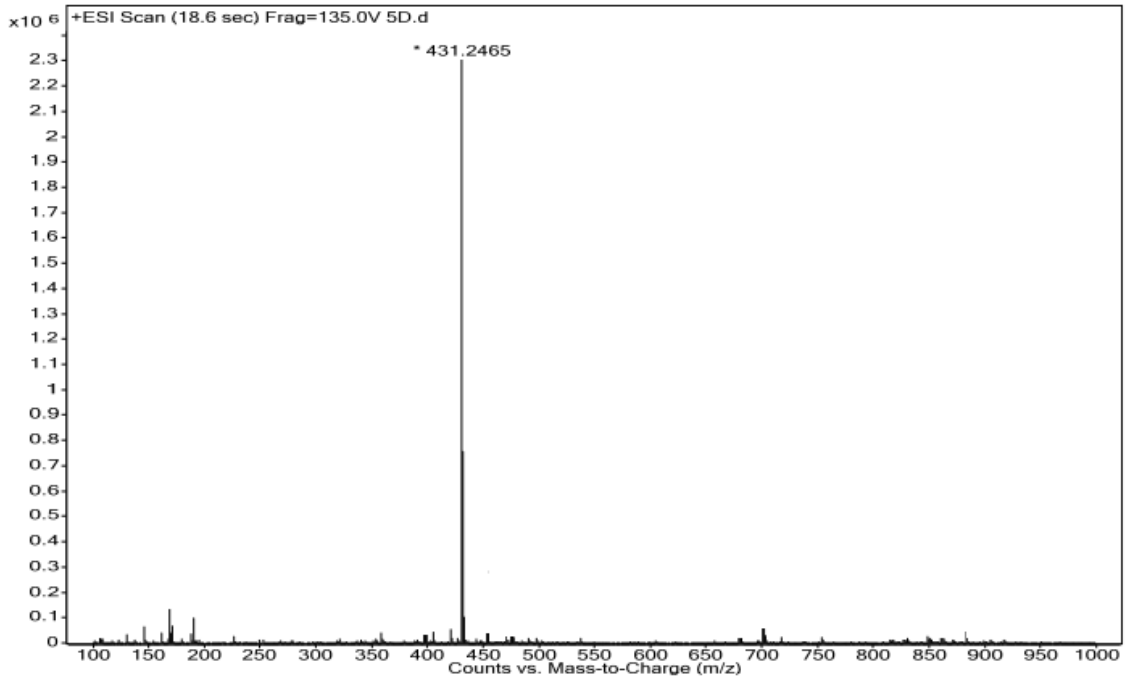

Figure A2.13 Mass spectra of compound **5a4**

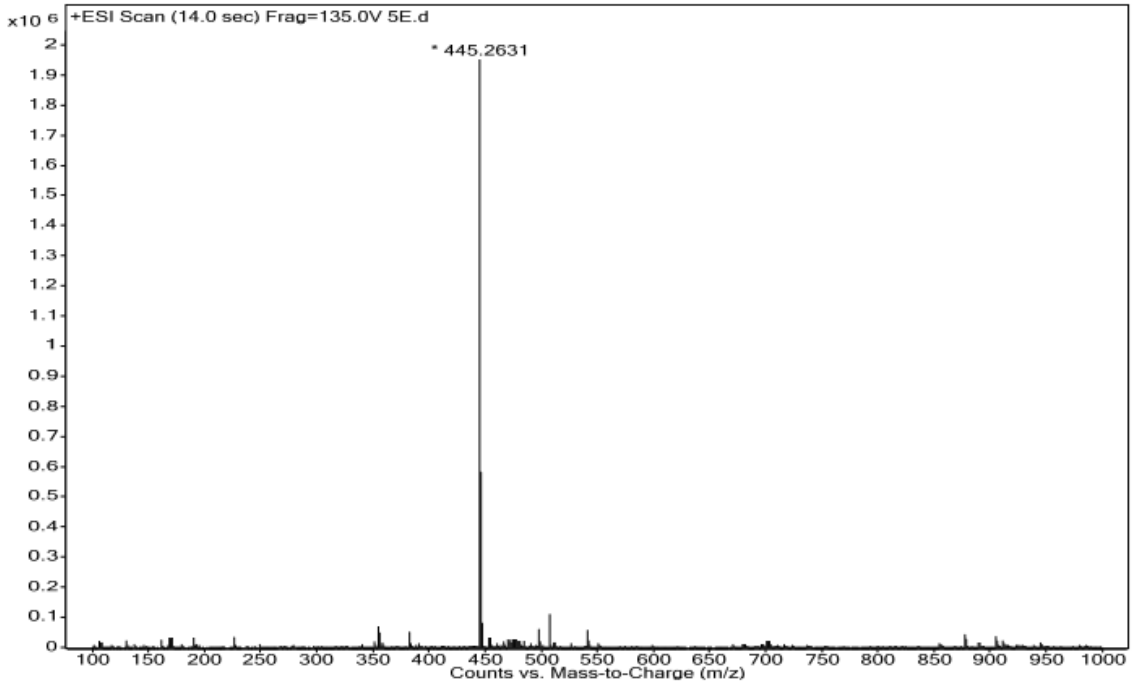

Figure A2.14 Mass spectra of compound **5a5**

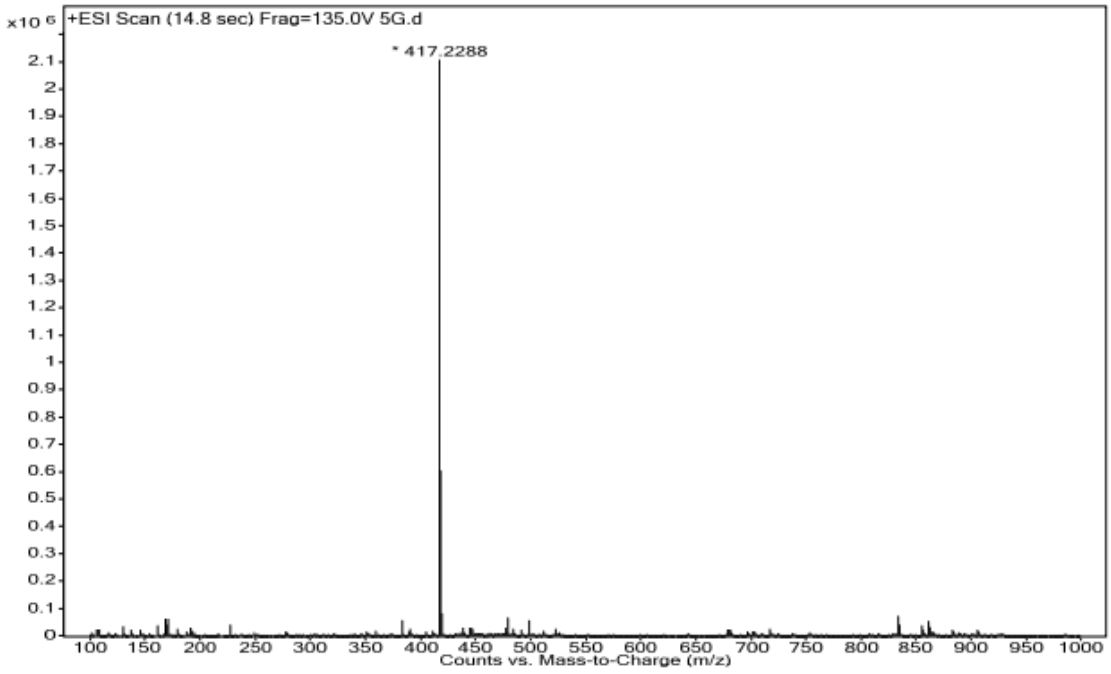

Figure A2.15 Mass spectra of compound **5a6**

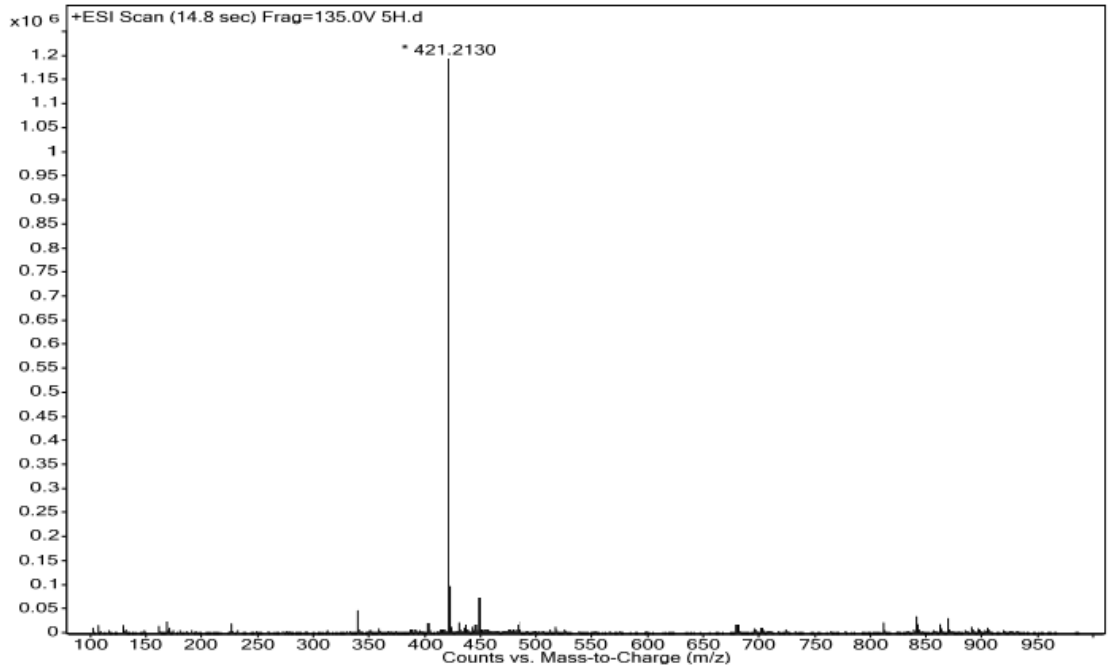

Figure A2.16 Mass spectra of compound **5a7**

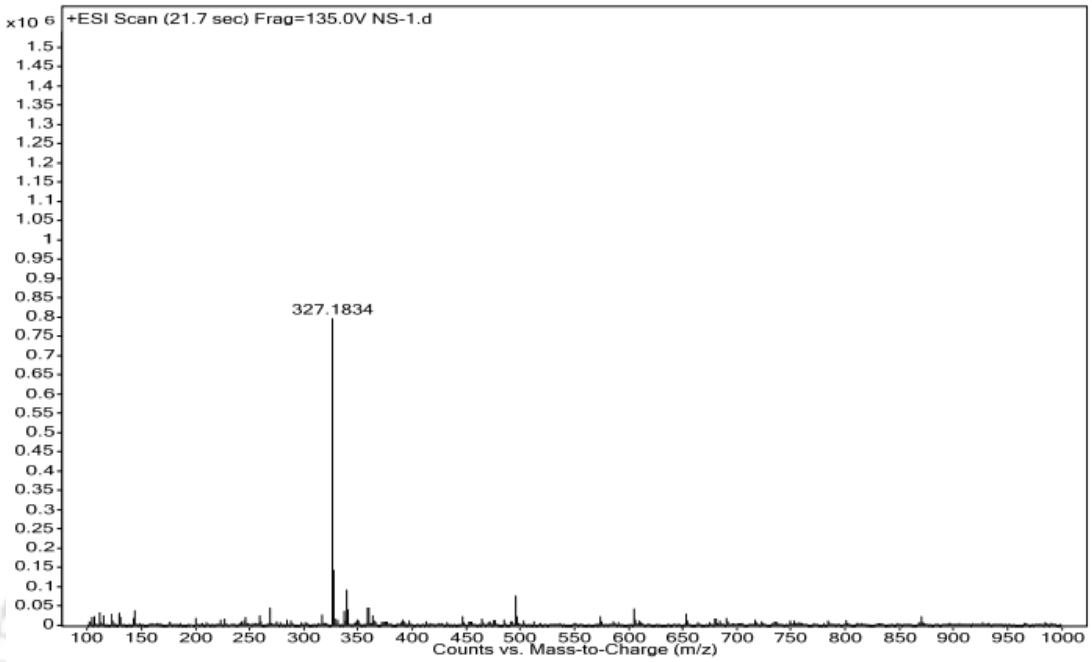

Figure A2.17 Mass spectra of compound **6a1** or **C1**

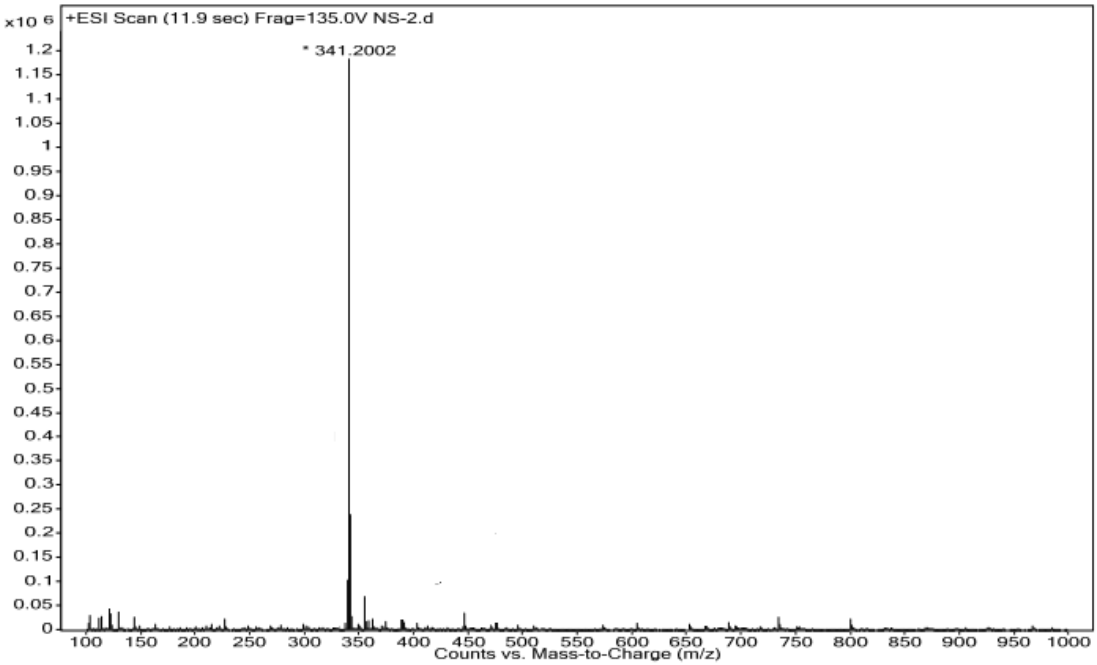

Figure A2.18 Mass spectra of compound **6a2** or **C2**

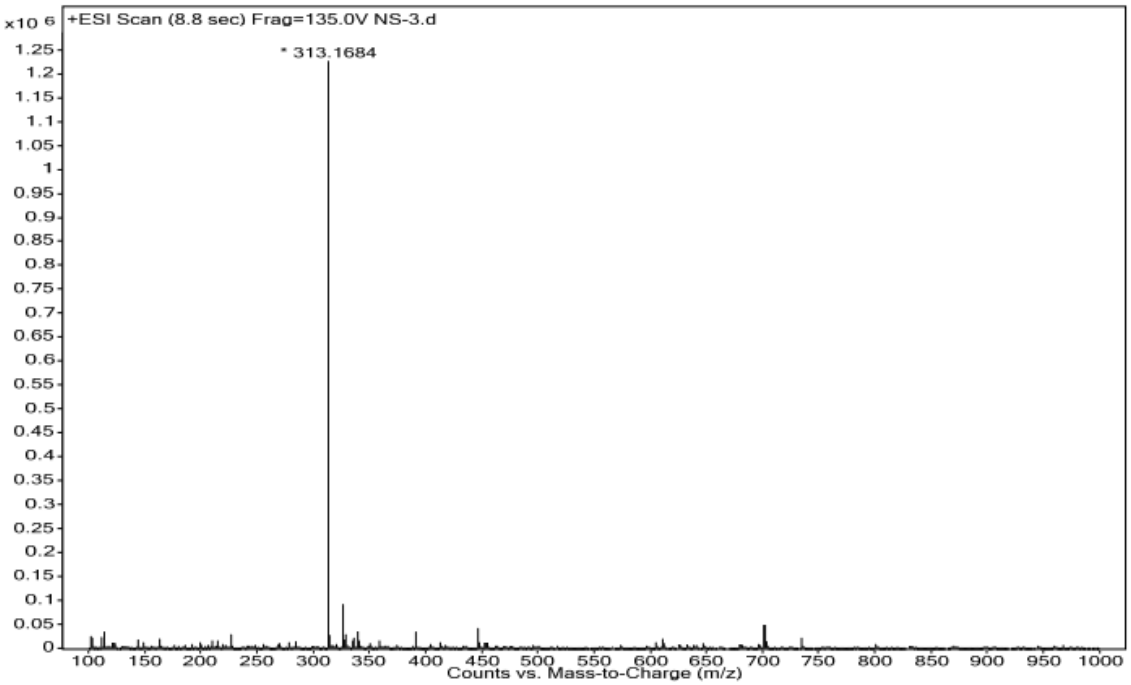

Figure A2.19 Mass spectra of compound **6a3** or **C3**

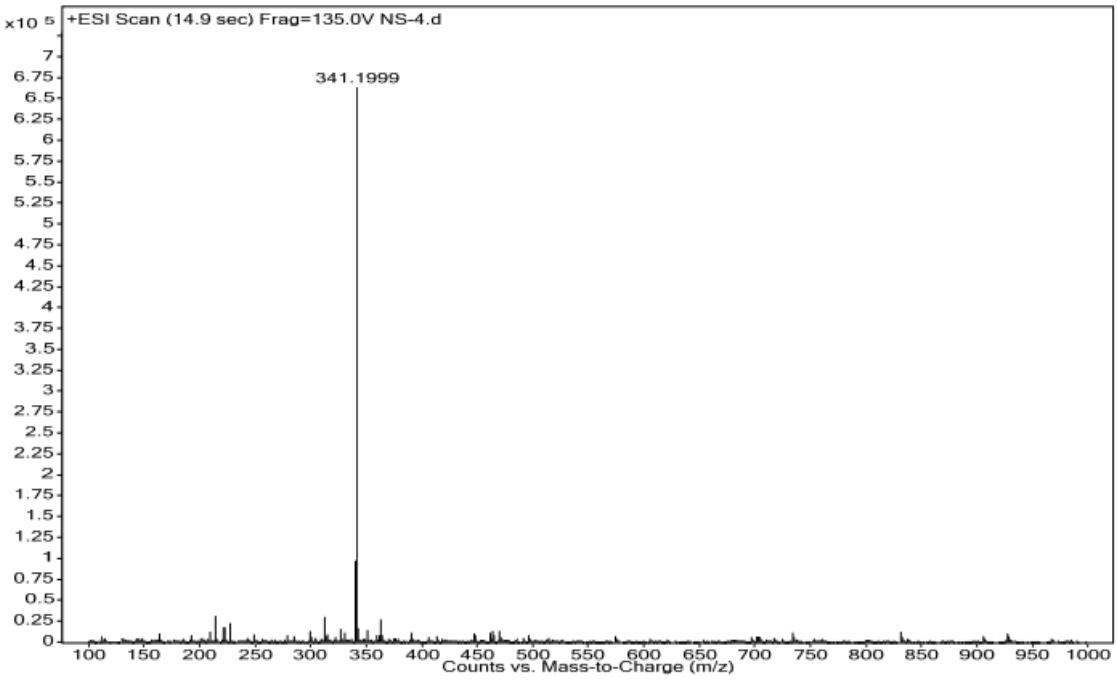

Figure A2.20 Mass spectra of compound **6a4** or **C4**

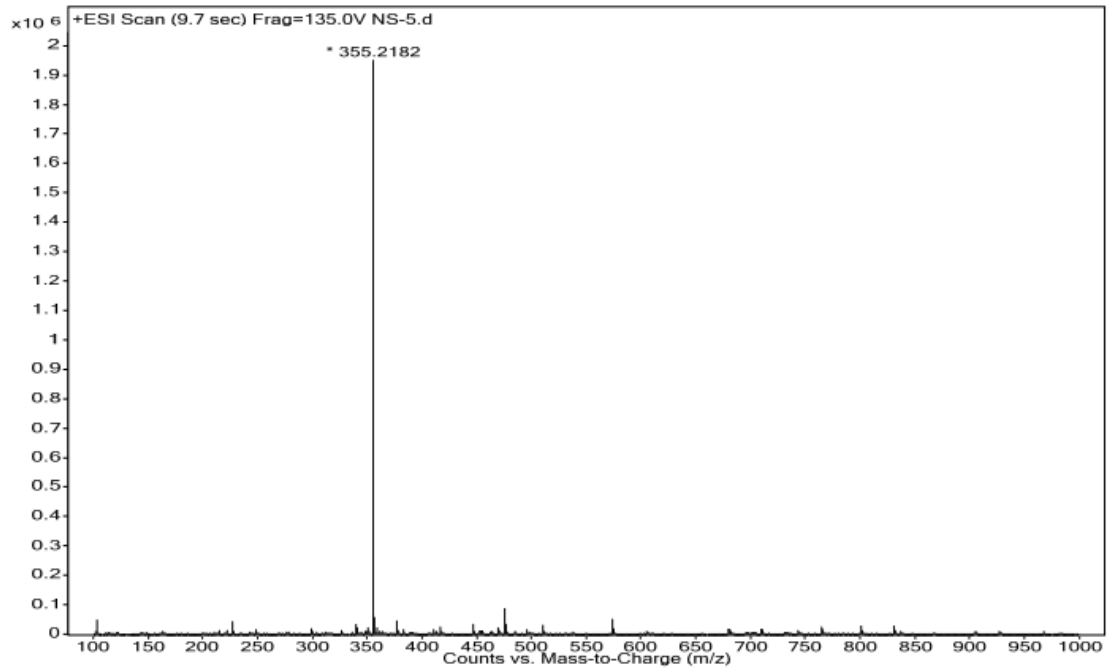

Figure A2.21 Mass spectra of compound **6a5** or **C5**

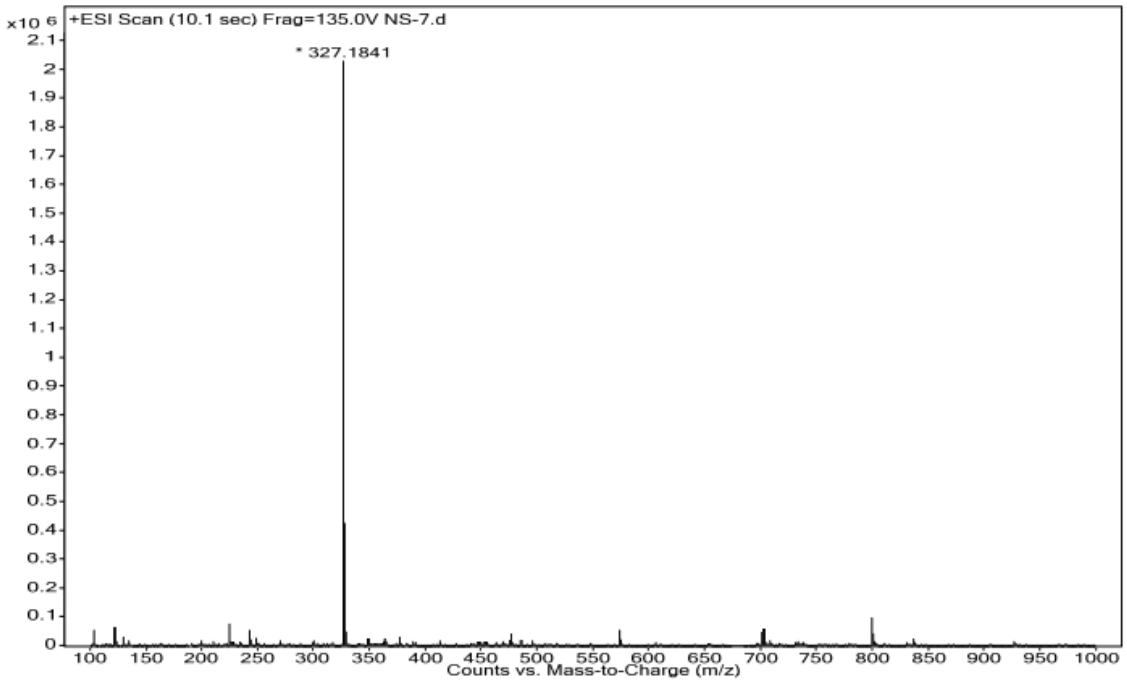

Figure A2.22 Mass spectra of compound **6a6** or **C7**

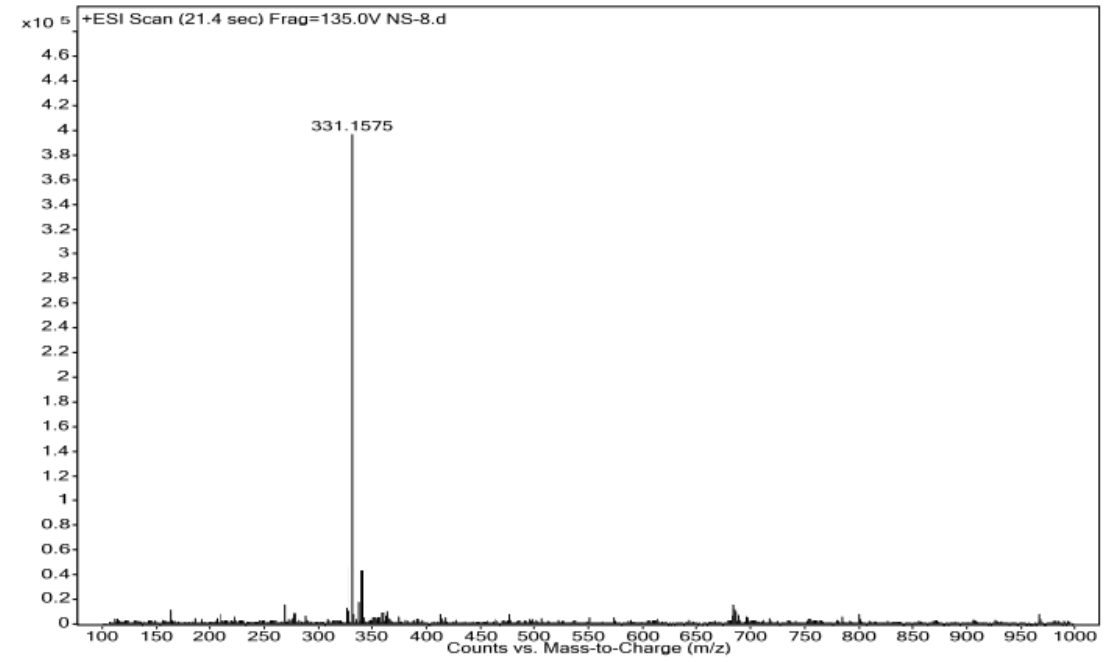

Figure A2.23 Mass spectra of compound **6a7** or **C8**

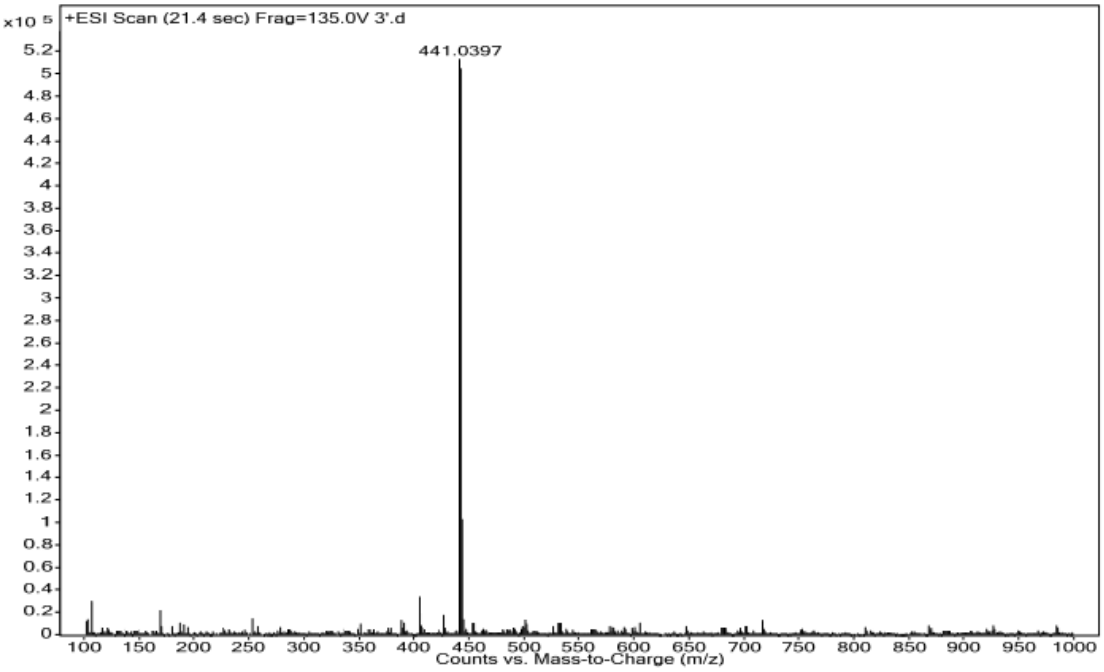

Figure A2.24 Mass spectra of compound **3b1**

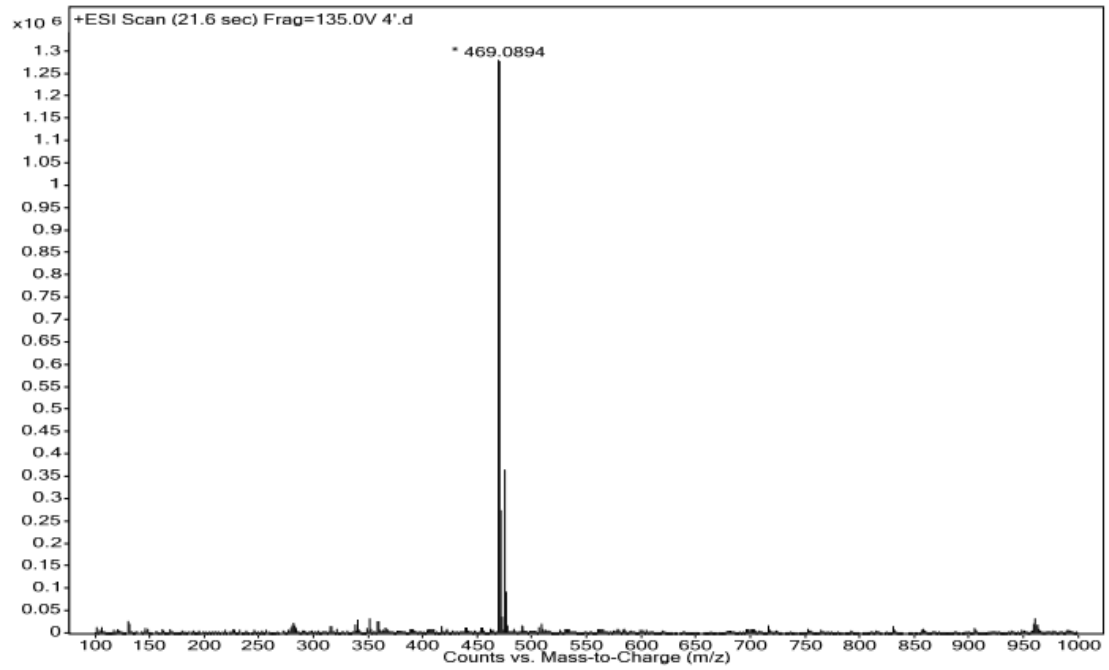

Figure A2.25 Mass spectra of compound **4b1**

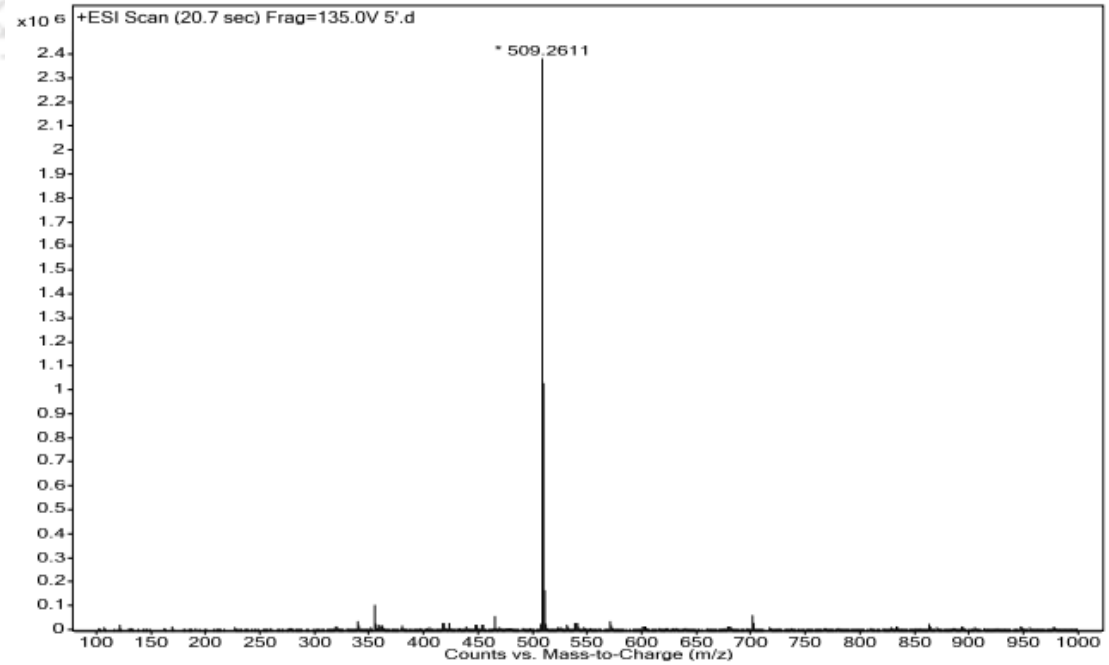

Figure S2.26 Mass spectra of compound **5b1**

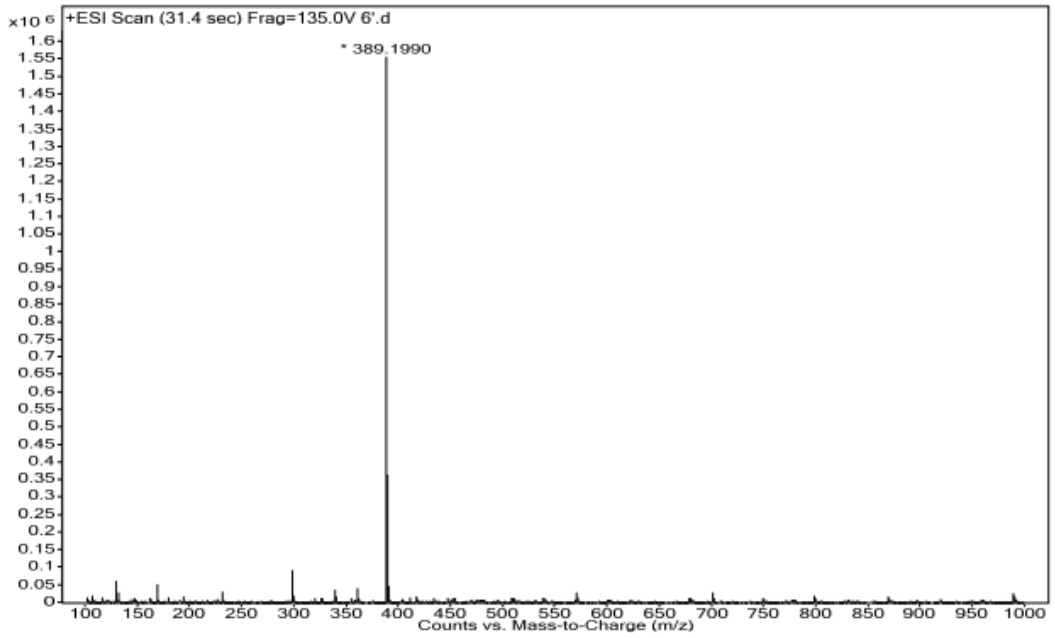

Figure A2.27 Mass spectra of compound **6b1**

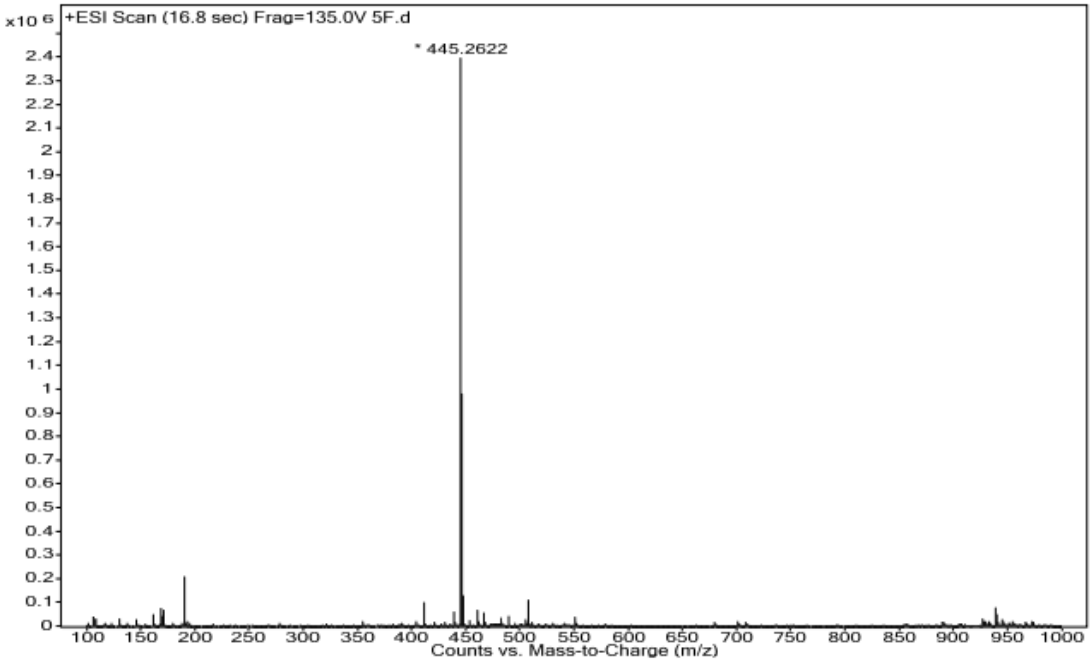

Figure A2.28 Mass spectra of compound **7b2**

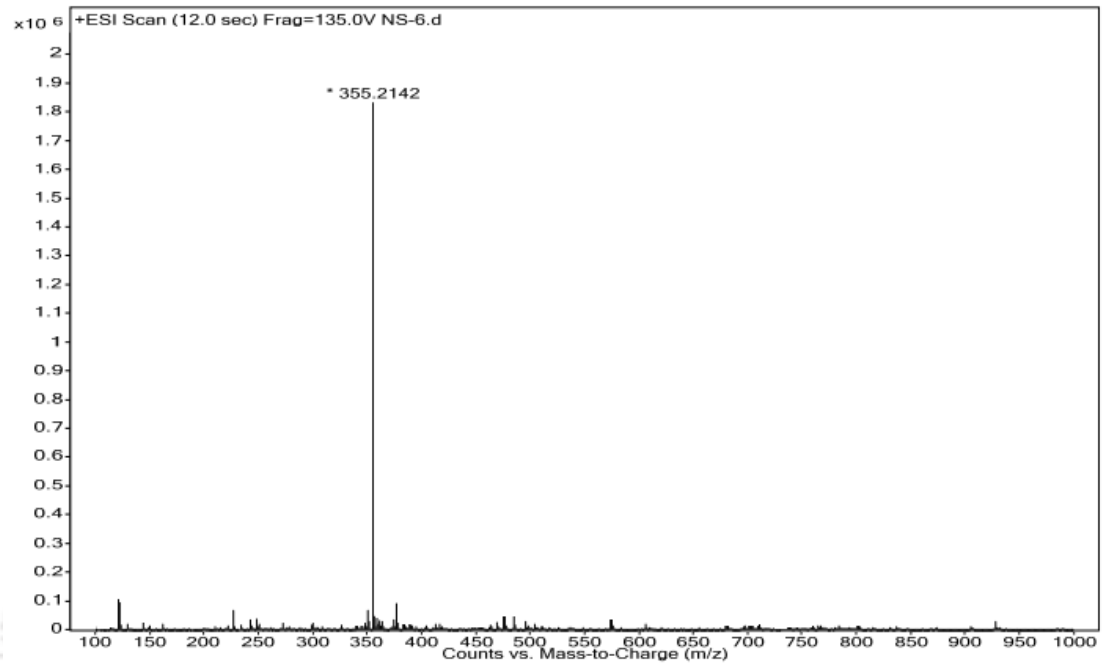

Figure A2.29 Mass spectra of compound **8b2** or **C6**

Appendix-III

Sequencing data of purified clones (PDE9A, PDE5A and PDE4D)

```
Query  35   TCGAGGCCC---TGCGG-AAGCC-GACCTTTGACGTCTGGCTTTGGGAGCCCAATGAG-A  88
            ||||||  ||   ||||| ||||| ||||||||||||||||||||||||||||||||| |
Sbjct  17   TCGAGGGCCCCTTGCGGGAAGCCCGACCTTTGACGTCTGGCTTTGGGAGCCCAATGAGCA  76

Query  89   TGCTGAGCTGCCTGGAGCACATGTACCACGACCTCGGGCTGGTCAGGGACTTCAGCATCA  148
            ||||||||||||||||||||||||||||||||||||||||||||||||||||||||||||
Sbjct  77   TGCTGAGCTGCCTGGAGCACATGTACCACGACCTCGGGCTGGTCAGGGACTTCAGCATCA  136

Query  149  ACCCTGTCACCCTCAGGAGGTGGCTGTTCTGCGTCCACGACAACTACAGAAACAACCCCT  208
            ||||||||||||||||||||||||||||||||||||||||||||||||||||||||||||
Sbjct  137  ACCCTGTCACCCTCAGGAGGTGGCTGTTCTGCGTCCACGACAACTACAGAAACAACCCCT  196

Query  209  TCCACAACTTCCGGCACTGCTTCTGCGTGGCCCAGATGATGTACAGCATGGTCTGGCTCT  268
            ||||||||||||||||||||||||||||||||||||||||||||||||||||||||||||
Sbjct  197  TCCACAACTTCCGGCACTGCTTCTGCGTGGCCCAGATGATGTACAGCATGGTCTGGCTCT  256

Query  269  GCAGTCTCCAGGAGAAGTTCTCACAAACGGATATCCTGATCCTAATGACAGCGGCCATCT  328
            ||||||||||||||||||||||||||||||||||||||||||||||||||||||||||||
Sbjct  257  GCAGTCTCCAGGAGAAGTTCTCACAAACGGATATCCTGATCCTAATGACAGCGGCCATCT  316

Query  329  GCCACGATCTGGACCATCCCGGCTACAACAACACGTACCAGATCAATGCCCGCACAGAGC  388
            ||||||||||||||||||||||||||||||||||||||||||||||||||||||||||||
Sbjct  317  GCCACGATCTGGACCATCCCGGCTACAACAACACGTACCAGATCAATGCCCGCACAGAGC  376

Query  389  TGGCGGTCCGCTACAATGACATCTCACCGCTGGAGAACCACCACTGCGCCGTGGCCTTCC  448
            ||||||||||||||||||||||||||||||||||||||||||||||||||||||||||||
Sbjct  377  TGGCGGTCCGCTACAATGACATCTCACCGCTGGAGAACCACCACTGCGCCGTGGCCTTCC  436

Query  449  AGATCCTCGCCGAGCCTGAGTGCAACATCTTCTCCAACATCCCACCTGATGGGTTCAAGC  508
            ||||||||||||||||||||||||||||||||||||||||||||||||||||||||||||
Sbjct  437  AGATCCTCGCCGAGCCTGAGTGCAACATCTTCTCCAACATCCCACCTGATGGGTTCAAGC  496

Query  509  AGATCCGACAGGGAATGATCACATTAATCTTGGCCACTGACATGGCAAGACATGCAGAAA  568
            ||||||||||||||||||||||||||||||||||||||||||||||||||||||||||||
Sbjct  497  AGATCCGACAGGGAATGATCACATTAATCTTGGCCACTGACATGGCAAGACATGCAGAAA  556

Query  569  TTATGGATTCTTTCAAAGAGAAAATGGAGAATTTTGACTACAGCAACGAGGAGCACATGA  628
            ||||||||||||||||||||||||||||||||||||||||||||||||||||||||||||
Sbjct  557  TTATGGATTCTTTCAAAGAGAAAATGGAGAATTTTGACTACAGCAACGAGGAGCACATGA  616

Query  629  CCCTGCTGAAGATGATTTTGATAAAATGCTGTGATATCTCTAACGAGGTCCGTCCAATGG  688
            ||||||||||||||||||||||||||||||||||||||||||||||||||||||||||||
Sbjct  617  CCCTGCTGAAGATGATTTTGATAAAATGCTGTGATATCTCTAACGAGGTCCGTCCAATGG  676
```

Figure A3.1 Sequencing result of PDE9A clone with His tag at N-terminal site

```
Query  38   TGGTGCCATCTGCCCA-GACCCTTAAAATTACTGACTTTAGCTTCAGTGACTTTGAGCTG  96
            ||||||||||||||| ||||||||||||||||||||||||||||||||||||||||||||
Sbjct  29   TGGTGCCATCTGCCCAAGACCCTTAAAATTACTGACTTTAGCTTCAGTGACTTTGAGCTG  88

Query  97   TCTGATCTGGAAACAGCACTGTGTACAATTCGGATGTTTACTGACCTCAACCTTGTGCAG  156
            ||||||||||||||||||||||||||||||||||||||||||||||||||||||||||||
Sbjct  89   TCTGATCTGGAAACAGCACTGTGTACAATTCGGATGTTTACTGACCTCAACCTTGTGCAG  148

Query  157  AACTTCCGGATGAAACATGAGGTTCTTTGCAGATGGATTTTAAGTGTTAAGAAGAATTAT  216
            ||||||| ||||||||||||||||||||||||||||||||||||||||||||||||||||
Sbjct  149  AACTTCCAGATGAAACATGAGGTTCTTTGCAGATGGATTTTAAGTGTTAAGAAGAATTAT  208

Query  217  CGGAAGAATGTTGCCTATCATAATTGGAGACATGCCTTTAATACAGCTCAGTGCATGTTT  276
            ||||||||||||||||||||||||||||||||||||||||||||||||||||||||||||
Sbjct  209  CGGAAGAATGTTGCCTATCATAATTGGAGACATGCCTTTAATACAGCTCAGTGCATGTTT  268

Query  277  GCTGCTCTAAAAGCAGGCAAAATTCAGAACAAGCTGACTGACCTGGAGATACTTGCATTG  336
            ||||||||||||||||||||||||||||||||||||||||||||||||||||||||||||
Sbjct  269  GCTGCTCTAAAAGCAGGCAAAATTCAGAACAAGCTGACTGACCTGGAGATACTTGCATTG  328

Query  337  CTGATTGCTGCACTAAGCCACGATTTGGATCACCGTGGTGTGAATAACTCTTACATACAG  396
            ||||||||||||||||||||||||||||||||||||||||||||||||||||||||||||
Sbjct  329  CTGATTGCTGCACTAAGCCACGATTTGGATCACCGTGGTGTGAATAACTCTTACATACAG  388

Query  397  CGAAGTGAACATCCACTTGCCCAGCTTTACTGCCATTCAATCATGGAACACCATCATTTT  456
            ||||||||||||||||||||||||||||||||||||||||||||||||||||||||||||
Sbjct  389  CGAAGTGAACATCCACTTGCCCAGCTTTACTGCCATTCAATCATGGAACACCATCATTTT  448

Query  457  GACCAGTGCCTGATGATTCTTAATAGTCCAGGCAATCAGATTCTCAGTGGCCTCTCCATT  516
            ||||||||||||||||||||||||||||||||||||||||||||||||||||||||||||
Sbjct  449  GACCAGTGCCTGATGATTCTTAATAGTCCAGGCAATCAGATTCTCAGTGGCCTCTCCATT  508

Query  517  GAAGAATATAAGACCACGTTGAAAATAATCAAGCAAGCTATTTTAGCTACAGACCTAGCA  576
            ||||||||||||||||||||||||||||||||||||||||||||||||||||||||||||
Sbjct  509  GAAGAATATAAGACCACGTTGAAAATAATCAAGCAAGCTATTTTAGCTACAGACCTAGCA  568

Query  577  CTGTACATTAAGAGGCGAGGAGAATTTTTTGAACTTATAAGAAAAAATCAATTCAATTTG  636
            ||||||||||||||||||||||||||||||||||||||||||||||||||||||||||||
Sbjct  569  CTGTACATTAAGAGGCGAGGAGAATTTTTTGAACTTATAAGAAAAAATCAATTCAATTTG  628

Query  637  GAAGATCCTCATCAAAAGGAGTTGTTTTTGGCAATGCTGATGACAGCTTGTGATCTTTCT  696
            ||||||||||||||||||||||||||||||||||||||||||||||||||||||||||||
Sbjct  629  GAAGATCCTCATCAAAAGGAGTTGTTTTTGGCAATGCTGATGACAGCTTGTGATCTTTCT  688
```

Figure A3.2 Sequencing result of PDE5A clone with His tag at N-terminal site

```
Query  29   AACTAGAAGATG-TGAACAAATGGGG--TCTTCATGTTTTCAGAATAGCAGAGTTGTCTG  85
            || ||||||||| ||||||||||||  ||||||||||||||||||||||||||||||||
Sbjct  8    AAATAGAAGATGGTGAACAAATGGGGGTTCTTCATGTTTTCAGAATAGCAGAGTTGTCTG  67

Query  86   GTAACCGGCCCTTGACTGTTATCATGCACACCATTTTTCAGGAACGGGATTTATTAAAAA  145
            ||||||||||||||||||||||||||||||||||||||||||||||||||||||||||||
Sbjct  68   GTAACCGGCCCTTGACTGTTATCATGCACACCATTTTTCAGGAACGGGATTTATTAAAAA  127

Query  146  CATTTAAAATTCCAGTAGATACTTTAATTACATATCTTATGACTCTCGAAGACCATTACC  205
            ||||||||||||||||||||||||||||||||||||||||||||||||||||||||||||
Sbjct  128  CATTTAAAATTCCAGTAGATACTTTAATTACATATCTTATGACTCTCGAAGACCATTACC  187

Query  206  ATGCTGATGTGGCCTATCACAACAATATCCATGCTGCAGATGTTGTCCAGTCTACTCATG  265
            ||||||||||||||||||||||||||||||||||||||||||||||||||||||||||||
Sbjct  188  ATGCTGATGTGGCCTATCACAACAATATCCATGCTGCAGATGTTGTCCAGTCTACTCATG  247

Query  266  TGCTATTATCTACACCTGCTTTGGAGGCTGTGTTTACAGATTTGGAGATTCTTGCAGCAA  325
            ||||||||||||||||||||||||||||||||||||||||||||||||||||||||||||
Sbjct  248  TGCTATTATCTACACCTGCTTTGGAGGCTGTGTTTACAGATTTGGAGATTCTTGCAGCAA  307

Query  326  TTTTTGCCAGTGCAATACATGATGTAGATCATCCTGGTGTGTCCAATCAATTTCTGATCA  385
            |||||||||||||||||||||||||||||||||||| ||||||||||||||||||||||
Sbjct  308  TTTTTGCCAGTGCAATACATGATGTAGATCATCCTGGTGTGTTCAATCAATTTCTGATCA  367

Query  386  ATACAAACTCTGAACTTGCCTTGATGTACAATGATTCCTCAGTCTTAGAGAACCATCATT  445
            ||||||||||||||||||||||||||||||||||||||||||||||||||||||||||||
Sbjct  368  ATACAAACTCTGAACTTGCCTTGATGTACAATGATTCCTCAGTCTTAGAGAACCATCATT  427

Query  446  TGGCTGTGGGCTTTAAATTGCTTCAGGAAGAAAACTGTGACATTTTCCAGAATTTGACCA  505
            ||||||||||||||||||||||||||||||||||||||||||||||||||||||||||||
Sbjct  428  TGGCTGTGGGCTTTAAATTGCTTCAGGAAGAAAACTGTGACATTTTCCAGAATTTGACCA  487

Query  506  AAAAACAAAGACAATCTTTAAGGAAAATGGTCATTGACATCGTACTTGCAACAGATATGT  565
            ||||||||||||||||||||||||||||||||||||||||||||||||||||||||||||
Sbjct  488  AAAAACAAAGACAATCTTTAAGGAAAATGGTCATTGACATCGTACTTGCAACAGATATGT  547

Query  566  CAAAACACATGAATCTACTGGCTGATTTGAAGACTATGGTTGAAACTAAGAAAGTGACAA  625
            ||||||||||||||||||||||||||||||||||||||||||||||||||||||||||||
Sbjct  548  CAAAACACATGAATCTACTGGCTGATTTGAAGACTATGGTTGAAACTAAGAAAGTGACAA  607

Query  626  GCTCTGGAGTTCTTCTTCTTGATAATTATTCCGATAGGATTCAGGTTCTTCAGAATATGG  685
            ||||||||||||||||||||||||||||||||||||||||||||||||||||||||||||
Sbjct  608  GCTCTGGAGTTCTTCTTCTTGATAATTATTCCGATAGGATTCAGGTTCTTCAGAATATGG  667
```

Figure A3.3 Sequencing result of PDE4D clone with His tag at N-terminal site